

**IMPACTS OF ANTHROPOGENIC ACTIVITIES ON  
SOIL AND WATER QUALITY OF KOLO-CREEK,  
NIGER DELTA, NIGERIA**

**BY**

**AJAYI, OLUMIDE, (B.Sc. Ilorin, M.Sc. South America University)**

**REG: 20184139088**

**A THESIS SUBMITTED TO THE POSTGRADUATE SCHOOL  
FEDERAL UNIVERSITY OF TECHNOLOGY OWERRI**

**IN PARTIAL FULFILMENT OF THE REQUIREMENTS FOR  
THE AWARD OF THE DEGREE OF DOCTOR OF  
PHILOSOPHY (PhD) IN ENVIRONMENTAL GEOLOGY**

**NOVEMBER, 2024**

## CERTIFICATION

This is to certify that Mr. Olumide Ajayi of the Department of Geology, Federal University of Technology, Owerri, Nigeria, completed the project "Impacts of anthropogenic activities on Soil and Water resources of Kolo Creek, Niger Delta, Nigeria."



Prof. O. C. Okeke  
*Principal Supervisor*

22-08-2024

Date



Prof. C.N. Okereke  
*Co-Supervisor*

02/11/2024

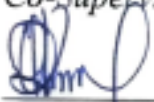
Date



Dr. Y.E. Obioha  
*Co-Supervisor*

02/11/2024

Date



Dr. D.O. Ikoro  
*HOD, Geology*

02/11/24

Date

Prof. Mrs. C. E Ogukwe  
*Dean, School of Physical Science*

\_\_\_\_\_  
Date

Prof. Mrs. J. N. Nwosu  
*Dean, Postgraduate School*

\_\_\_\_\_  
Date



Prof. T.KS. Abam  
*External Supervisor*

5-11-2024

Date

## **DEDICATION**

This project is dedicated to God, whose divine guidance, strength, and wisdom have been my foundation throughout this journey. May this work bring glory to His name and serve as a reflection of His grace in my life.

## ACKNOWLEDGEMENTS

I give all glory and gratitude to God for His kindness, heavenly inspiration, and for granting me safety throughout my time at FUTO. I owe a profound debt of thanks to the late Professor C. A. Ahirakwem, who guided me before his passing. His leadership and unwavering dedication were instrumental in shaping my work. I also extend my heartfelt gratitude to Prof. O.C. Okeke, who became my primary supervisor and made invaluable contributions to this project.

Special thanks are due to my co-supervisors, Prof. C.N. Okereke and Dr. Y.E. Obioha, for their insightful guidance. I would also like to express my appreciation to my H.O.D. and the Deans of the Faculty of Science and Postgraduate Studies for their support.

I am deeply grateful to Professor S. O. Onyekuru for his tireless efforts throughout my academic journey. My sincere thanks go to all the instructors of the Geology Department, especially Dr. S. I. Ibeneme and Professor A.I. Opara, for their expert counsel and kind support.

I acknowledge the invaluable contributions of the non-academic staff, whose names are too numerous to mention here, yet their efforts are deeply appreciated. I also thank my sponsors and mentors, Mr. and Mrs. Ajayi, as well as my in-laws, Mr. and Mrs. Aderemi Agbegende, for their unwavering support and encouragement.

My colleagues and friends at the Department of Geology and Postgraduate School at FUTO are also recognized for the memorable moments we shared, which helped us grow as better individuals and students.

I offer special thanks to John Poopola, the late Professor C. A. Ahirakwem's personal assistant, whose support was indispensable to this work. My heartfelt appreciation also goes to my friend, a computer specialist at FUTO, OBZ Ventures, for his constant technical support throughout the program.

For spiritual guidance and prayers, I express my thanks to the entire congregation of the Celestial Church of Christ, Ancient of Days Parish, Port Harcourt.

I am immensely grateful to my family, friends, and supporters outside the university for their constant encouragement, particularly Mr. Oluwambe Emeyinola, Mr. Aderemi Agbegende, Mr. Fatai Agbegende, and Mrs. Ajayi Temitope (my wife). Finally, I extend my deepest thanks to my wonderful children, Daniel, Raphael, Ezekiel, and Esther, for their enduring support and attention throughout this study.

## TABLE OF CONTENTS

Title page	i
Certification	ii
Dedication	iii
Acknowledgement	iv
Abstract	vii
Table of contents	vi
Lists of figures/ charts	vii
Lists of tables	viii

### CHAPTER ONE: INTRODUCTION

1.1	Background Information	1
1.2	Problem Statement	5
1.3	Objectives	5
1.4	Justification of Study	6
1.5	Scope of Study	6

### CHAPTER TWO: LITERATURE REVIEW

2.1	Previous works	7
-----	----------------	---

### CHAPTER THREE: MATERIALS AND METHODS

3.1	Materials	10
3.2	Methodology	11
3.3	Description of the study area	12
3.3.1	Physiographic and Drainage	13
3.3.2	Climate and Vegetation	14
3.3.3	The Study Area's Geology and Hydrology	15
3.4	Field Data Collection and Sample Analysis	18
3.5	Laboratory Analysis of Soil and Water samples	22
3.5.1	Determination of Soil Electrical Conductivity	22
3.5.2	Nitrate determination	23

3.5.3	Sulphate determination	23
3.5.4	pH Determinations	24
3.5.5	Temperature Determination	24
3.5.6	The process of calculating total dissolved solids (TDS)	24
3.5.7	Determination of Turbidity	24
3.5.8	Determination of Total Hardness	25
3.5.9	Determination of Metal Ion Concentrations in Water Samples	25
3.5.10	Determination of Petroleum Compounds	26
3.5.11	Determination of Geotechnical Properties of Soils	26
3.5.12	Laboratory Testing of Soil Samples	27
3.5.13	Determination of the Soil Samples' Grain Size Distribution	28
3.6	Data Analysis	28
3.7	Geochemical Models	29
3.7.1	Pollution Index	29
3.7.2	Ratio of Sodium Adsorption	30
3.7.3	Groundwater pollution index (PIG)	31
3.7.4	Geo-accumulation	32
3.7.5	Contamination Factor	33
3.7.6	Pollution load index	33
3.7.7	Water quality index (WQI)	34
3.8	Human health risk assessment (HHRA)	34

## **CHAPTER FOUR: RESULTS AND DISCUSSION**

4.1	Results	36
4.2	Discussion	160
4.2.1	Dry and Wet Season Surface Water Samples' Physical and Biochemical Properties	161
4.3	Physical and Bio-Chemical Characteristics of Ground Water Samples	178
4.3.1	Geochemical Models	184
4.4	Physicochemical Characteristics of Soil	196
4.4.1	Geotechnical Characteristics of soil Samples	206
4.4.2	Porosity and Permeability	207
4.4.3	Distribution of Soil Particle Sizes/Consistency Limits	207

## **CHAPTER FIVE: CONCLUSION AND RECOMMENDATIONS**

5.1	Conclusion	209
5.2	Recommendations	211
5.3	Contribution to Knowledge	214

<b>REFERENCES</b>	216
-------------------	-----

## LIST OF TABLES

<b>Tables</b>	<b>Page</b>
3.1: Showing all materials, ranging from the field tools, laboratory tools, reagents, And Software used.	13
3.2: Soil sample ID and Coordinates of the study area	21
3.3: Ground water sample ID and Coordinates of the study area	21
3.4: Surface water sample ID and Coordinates of the study area	22
3.5 Equations used for water quality indices calculation	31
3.6: PIG Assessment Components	32
3.7: Classification of Geo-Accumulation Index (Muller, 1969)	33
4.1a: Physiochemical Properties of Kolo Creek Surface Water (Wet Season)	37
4.1b: Physiochemical Properties of Kolo Creek Surface Water (Dry Season)	38
4.2a: Physiochemical Properties of Kolo Creek Groundwater (Wet Season)	39
4.2b: Physiochemical Properties of Kolo Creek Ground Water (Dry Season)	40
4.3a: Physiochemical Properties of Kolo Creek Soil (Wet Season)	41
4.3b: Physiochemical Properties of Kolo Creek Soil (Dry Season)	42
4.4a: Geotechnical Parameters of soils	43
4.4b Factor loadings of various parameters derived from principal component extraction method for surface water	43
4.5: Correlation matrix of the various parameters in the studied surface water	44
4.6a: Surface Water Pollution index (PI)	45
4.6b: Summary of CF, PLI & WQI for surface water parameters	45
4.7: Values of SAR, KP, Na, MH & SSP for surface water parameters	45
4.8: Classification criteria for surface water WQI	46
4.9: SAR-based irrigation suitability classification criteria for surface water	46
4.10: %Na for surface water quality criteria for irrigation	46
4.11: MH for surface water quality criteria for irrigation	46
4.12: KR Surface water quality criteria for irrigation	46
4.13: SSP Surface water quality criteria for irrigation	46
4.14: Hazard quotient and hazard indexes in the surface water sample (ingestion) for adults	47
4.15: Hazard quotient and hazard indexes in the surface water sample (ingestion) for children	47

<b>Tables</b>	<b>Page</b>
4.16: Carcinogenic risk of heavy metals in the surface water sample (ingestion)	47
4.17: Elevation and some key Aquifer Parameters	48
4.18: Factor loadings of various parameters derived from the principal component extraction method	48
4.19: Correlation matrix of the various parameters in studied groundwater	49
4.20: Summary of CF, PLI, WQI and PIG (Ground Water)	50
4.21: Values of SAR, KR, Na, MH and SSP (Ground Water)	50
4.22: Classification criteria for groundwater WQI	50
4.23: PIG Classification	50
4.24: SAR -Based Irrigation Suitability Classification Criteria	51
4.25: %Na-Groundwater Quality Criteria for irrigation	51
4.26: MH-Groundwater Classification Criteria for irrigation	51
4.27: KR-Groundwater Classification Criteria for irrigation	51
4.28: SSP-Groundwater Classification Criteria for irrigation	51
4.29: Hazard quotient and Hazard indexes of heavy metal in the groundwater samples (Ingestion) adult	51
4.30: Hazard quotient and Hazard indexes of heavy metal in the ground water samples (Ingestion) children	52
4.31: Carcinogenic risk of heavy metals in the groundwater samples (Ingestion) -Adults and Children	52
4.32: Soils Contamination Factors	52
4.33: Geo-accumulation index of heavy metals in soils of Kolo creek	52
4.34 Factor loadings of various parameters derived from the principal component extraction method	53
4.35: Correlation matrix of the various parameters in soils of the study area.	54
4.36: Hazard quotient and Hazard indexes of heavy metal in the soil samples (Dermal)-Adult	55
4.37: Carcinogenic risk of heavy metals in the Soil samples (Dermal) -Adult and Children	55
4.38: Hazard quotient and Hazard indexes of heavy metal in the soil samples (Dermal)-Children	55
4.39: Hazard quotient and Hazard indexes of heavy metal in the Soil samples (Ingestion)-Adult	56
4.40: Carcinogenic risk of heavy metals in the Soil samples (Ingestion) Adult and Children	56
4.41: Atterberg Soil Plasticity Classification	56

## LIST OF FIGURES/CHARTS

<b>Figures</b>	<b>Page</b>
3.1: Workflow of the Study	11
3.2: Location map of the study area	13
3.3 Geologic map of the Niger Delta and environs	16
3.4: Geological map of the study area	17
4.1a: Variogram of pH in Kolo Creek Surface Water	57
4.1b: Seasonal Variations of pH in Kolo Creek Surface Water	57
4.1c: Spatial distribution of pH in Kolo Creek Surface water	58
4.1d: 3D view of pH in Kolo Creek Surface water	58
4.2a Variogram of Electrical Conductivity in Kolo Creek Surface water	59
4.2b: Seasonal Variations of Elect.Conductivity in Kolo Creek Surface water.	59
4.2c: Variogram of TDS in Kolo Creek Surface water	60
4.2d: Seasonal Variations of TDS in Kolo Creek Surface water.	60
4.3a Variogram of Total Hardness in Kolo Creek Surface water	61
4.3b Seasonal Variations of Total Hardness in Kolo Creek Surface water.	61
4.4a Variogram of Chlorides in Kolo Creek Surface water	62
4.4b Seasonal Variations of Chloride in Kolo Creek Surface water.	62
4.5a: Variogram of Calcium in Kolo Creek Surface water	63
4.5b Seasonal Variations of Calcium in Kolo Creek Surface water	63
4.5c: Spatial Distribution of Calcium in Kolo Creek Surface water	64
4.5d: 3D view of Calcium in Kolo Creek Surface water	64
4.6a: Variogram of Magnesium in Kolo Creek Surface water	65
4.6b Seasonal Variations of Magnesium in Kolo Creek Surface water.	65
4.6c: Spatial Distribution of Magnesium in Kolo Creek Surface water	66
4.6d: 3D view of Magnesium in Kolo Creek Surface water	66
4.7a: Variogram of Sodium in Kolo Creek Surface water	67
4.7b Seasonal Variation of Sodium in Kolo Creek Surface water.	67
4.7c: Spatial Distribution of Sodium in Kolo Creek Surface water	68
4.7d: 3D view of Sodium in Kolo Creek Surface water	68
4.8a: Variogram of Potassium in Kolo Creek Surface water	69
4.8b Seasonal Variation of Potassium in Kolo Creek Surface water.	69
4.8c: Spatial Distribution of Potassium in Kolo Creek Surface water	70
4.8d: 3D view of Potassium in Kolo Creek Surface water	70

<b>Figures</b>	<b>Page</b>
4.9a: Variogram of Bicarbonate in Kolo Creek Surface water	71
4.9b Seasonal Variation of Bicarbonate in Kolo Creek Surface water.	71
4.9c: Spatial Distribution of Bicarbonate in Kolo Creek Surface water	72
4.9d: 3D view of Bicarbonate in Kolo Creek Surface water	72
4.10a: Variogram of Sulphate in Kolo Creek Surface water	73
4.10b Seasonal Variation of Sulphate in Kolo Creek Surface water.	73
4.10c: Spatial Distribution of Sulphate in Kolo Creek Surface water	74
4.10d: 3D view of Sulphahte in Kolo Creek Surface water	74
4.11a: Variogram of Nitrates in Kolo Creek Surface water	75
4.11b Seasonal Variation of Nitrate in Kolo Creek Surface water.	75
4.11c: Spatial Distribution of Nitrate in Kolo Creek Surface water	76
4.11d: 3D view of Nitrate in Kolo Creek Surface water	76
4.12a: Variogram of Total Petroleum Hydrocarbon in Kolo Creek Surface water	77
4.12b: Seasonal Variations of Total Petroleum Hydrocarbon in Kolo Creek Surface water	77
4.12c: Spatial Distribution of TPH in Kolo Creek Surface water	78
4.12d: 3D view of TPH in Kolo Creek Surface water	78
4.13a: Variogram of PAH in Kolo Creek Surface water	79
4.13b: Seasonal Variation of PAH in Kolo Creek Surface water	79
4.13c: Spatial Distribution of PAH in Kolo Creek Surface water	80
4.13d: 3D view of PAH in Kolo Creek Surface water	80
4.14a: Variogram of Betex in Kolo Creek Surface water	81
4.14b Seasonal Variations of Betex in Kolo Creek Surface water.	81
4.14c: Spatial Distribution of Betex in Kolo Creek Surface water	82
4.14d: 3D view of Betex in Kolo Creek Surface water	82
4.15a: Spatial Distribution of Iron in Kolo Creek Surface water	83
4.15b: Variogram of Iron in Kolo Creek Surface water	83
4.15c: 3D view of Iron in Kolo Creek Surface water	84
4.16a: Spatial Distribution of Copper in Kolo Creek Surface water	84
4.17a: Spatial Distribution of Zinc in Kolo Creek Surface water	85
4.17b: Variogram of Nitrates in Kolo Creek Surface water	85
4.17c: 3D view of Zinc in Kolo Creek Surface water	86
4.18a: Spatial Distribution of Cadmium in Kolo Creek Surface water	86
4.18b: Variogram of Nitrates in Kolo Creek Surface water	87

<b>Figures</b>	<b>Page</b>
4.18c: 3D view of Cadmium in Kolo Creek Surface water	87
4.19a: Spatial Distribution of Lead in Kolo Creek Surface water	88
4.19b: Variogram of Lead in Kolo Creek Surface water	88
4.19c: 3D view of Lead in Kolo Creek Surface water	89
4.20a: Spatial Distribution of Mercury in Kolo Creek Surface water	89
4.20b: Variogram of Mercury in Kolo Creek Surface water	90
4.20c: 3D view of Mercury in Kolo Creek Surface water	90
4.21: Station Variations of Heavy metals in Kolo Creek surface water	91
4.22: Principal component plot in rotated space	91
4.23: Dendrogram of Kolo Creek Surface Water Parameters	92
4.24: Wilcox diagram of the study area Surface water	92
4.25 Piper Diagram Showing the major Cations and Anions	93
4.26: Durov Diagram Showing the major Cations and Anions	93
4.27: Schoeller Diagram Showing the major Cations and Anions	94
4.28: Stiff Diagrams	94
4.29a: Variogram of pH in Kolo Creek Groundwater	95
4.29b: Seasonal Variation of pH in Kolo Creek Groundwater	95
4.29c: Spatial Distribution of pH in Kolo Creek groundwater	96
4.29d: 3D view of pH in Kolo Creek groundwater	96
4.30a: Variogram of Electrical Conductivity in Kolo Creek Groundwater	97
4.30b: Variogram of TDS in Kolo Creek Groundwater	97
4.30c: Seasonal Variation of E. Conductivity in Kolo Creek Groundwater	97
4.30d: Seasonal Variation of TDS in Kolo Creek Groundwater	98
4.31a: Variogram of total hardness in Kolo Creek Groundwater	98
4.31b: Seasonal Variations of Total Hardness in Kolo Creek groundwater	99
4.32a: Variogram of Chloride in Kolo Creek Groundwater	99
4.32b: Seasonal Variations of Chloride in Kolo Creek groundwater	100
4.32c: Spatial Distribution of Chloride in Kolo Creek groundwater	100
4.32d: 3D view of Chloride in Kolo Creek groundwater	101
4.33a: Variogram of Total Petroleum Hydrocarbon for Groundwater	101
4.33b: Seasonal Variations of TPH in Kolo Creek groundwater	102
4.33c: Spatial Distribution of TPH in Kolo Creek groundwater	102
4.33d: 3D view of TPH in Kolo Creek groundwater	103

<b>Figures</b>	<b>Page</b>
4.34a: Variogram of PAH for Groundwater	103
4.34b: Seasonal Variations of PAH in Kolo Creek groundwater	104
4.34c: Spatial Distribution of PAH in Kolo Creek groundwater	104
4.34d: 3D view of PAH in Kolo Creek groundwater	105
4.35a: Variograms of Betex for groundwater	105
4.35b: Seasonal Variations of Betex in groundwater	106
4.35c: Spatial Distribution of Betex in Kolo Creek groundwater	106
4.35d: 3D view of Betex in Kolo Creek groundwater	107
4.36a: Spatial Distribution of Calcium in Kolo Creek groundwater	107
4.36b: Station Variations of Calcium for groundwater	108
4.36c: 3D view of Calcium in Kolo Creek groundwater	108
4.37a: Variogram of Magnesium for groundwater	109
4.37b: Spatial Distribution of Magnesium in Kolo Creek groundwater	109
4.37c: 3D view of Magnesium in Kolo Creek groundwater	110
4.38a: Spatial Distribution of Sodium in Kolo Creek groundwater	110
4.38b: Variogram of Sodium for groundwater	111
4.38c: 3D view of Sodium in Kolo Creek groundwater	111
4.39: Mean Variations of Major Cations for groundwater	112
4.40a: Variogram of Bicarbonate for groundwater	112
4.40b: Seasonal Variations of Bicarbonate in Kolo Creek groundwater	113
4.40c: Spatial Distribution of Bicarbonate in Kolo Creek groundwater	113
4.40d: 3D view of Bicarbonate in Kolo Creek groundwater	114
4.41a: Mean Variations of Sulphate for groundwater	114
4.41b: Seasonal Variations of Sulphate in Kolo Creek groundwater	115
4.41c: Spatial Distribution of Sulphate in Kolo Creek groundwater	115
4.41d: 3D view of Sulphate in Kolo Creek groundwater	116
4.42a: Mean Variations of Nitrate for groundwater	116
4.42b: Seasonal Variations of Nitrate in Kolo Creek groundwater	117
4.42c: Spatial Distribution of Nitrate in Kolo Creek groundwater	117
4.42d: 3D view of Nitrate in Kolo Creek groundwater	118
4.43: Showing Piper Diagrams of Station S1-S10 for groundwater	118
4.44 Piper Diagram Showing the major Cations and Anions	119
4.45 Durov Diagram Showing the major Cations and Anions	119

<b>Figures</b>	<b>Page</b>
4.46 Schoeller Diagram Showing the major Cations and Anions	120
4.47a: Spatial Distribution of Iron in Kolo Creek groundwater	121
4.47b: 3D view of Iron in Kolo Creek groundwater	121
4.47c: Variogram of Iron for groundwater	122
4.48a: Spatial Distribution of Copper in Kolo Creek groundwater	122
4.48b: 3D view of Copper in Kolo Creek groundwater	123
4.48c: Variogram of Zinc for groundwater	123
4.49a: Variogram of Zinc for groundwater	124
4.49b: Spatial Distribution of Zinc in Kolo Creek groundwater	124
4.49c: 3D view of Zinc in Kolo Creek groundwater	125
4.50a: Spatial Distribution of Lead in Kolo Creek groundwater	125
4.50b: Variogram of Zinc for groundwater	126
4.50c: 3D view of Lead in Kolo Creek groundwater	126
4.51: Elevation, water table, aquifer thickness and transmissivity variations in groundwater	127
4.52: Elevation Plot Showing Groundwater Flow Direction.	127
4.53: Principal component plot in rotated space	128
4.54: Dendrogram of ground water parameters of the study area	128
4.55: Wilcox diagram of ground water parameters of the study area.	129
4.56a: Station Variations of pH in Kolo Creek soil	129
4.56b: Seasonal Variations of pH in Kolo Creek Soil	130
4.57a: Station Variations of E. Conductivity in Kolo Creek Soil	130
4.57b: Seasonal Variations of E. Conductivity in Kolo Creek Soil	131
4.57c: Spatial Variations of E. Conductivity in Kolo Creek Soil	131
4.57d: 3D view of Electrical Conductivity in Kolo Creek Soils	132
4.58a: Station Variations of Chloride in Kolo Creek Soil	132
4.58b: Seasonal Variations of Chlorides in Kolo Creek Soils	133
4.59a: Station Variations of TPH in Kolo Creek Soil	133
4.59b: Seasonal Variations of TPH in Kolo Creek Soil	134
4.59c: Spatial Variations of TPH in Kolo Creek Soil	134
4.59d: 3D View of TPH in Kolo Creek Soils	135
4.60a: Station Variations of PAH in Kolo Creek soil	135
4.60b: Seasonal Variations of PAH in Kolo Creek Soil	136

<b>Figures</b>	<b>Page</b>
4.60c: Spatial Distribution of PAH in Kolo Creek Soil	136
4.60d: 3D View of PAH in Kolo Creek Soils	137
4.61a: Station Variations of Betex in Kolo Creek Soil	137
4.61b: Seasonal Variations of Betex in Kolo Creek Soil	138
4.61c: Spatial Distribution of Betex in Kolo Creek Soil	138
4.61d: 3D View of Betex in Kolo Creek Soil	139
4.62a: Station Variations of Calcium in Kolo Creek Soil	139
4.62b: Seasonal Variations of Calcium in Kolo Creek Soil	140
4.63a: Station Variations of Magnesium in Kolo Creek Soil	140
4.63b: Seasonal Variations of magnesium in Kolo Creek Soil	141
4.64a: Station Variations of Sodium in Kolo Creek Soil	141
4.64b: Seasonal Variations of Sodium in Kolo Creek Soil	142
4.65a: Station Variations of Potassium in Kolo Creek Soil	142
4.65b: Seasonal Variations of Potassium in Kolo Creek Soil	143
4.66a: Station Variations of Bicarbonate in Kolo Creek Soil	143
4.66b: Seasonal Variations of Bicarbonates in Kolo Creek Soils	144
4.67a: Station Variations of Sulphate in Kolo Creek Soil	144
4.67b: Seasonal Variations of Sulphates in Kolo Creek Soils	145
4.68a: Station Variations of Nitrate in Kolo Creek Soil	145
4.68b: Seasonal Variations of Nitrates in Kolo Creek Soils	146
4.69a: Spatial Distribution of Iron in Kolo Creek Soil	146
4.69b: 3D View of Calcium in Kolo Creek Soil	147
4.70a: Spatial Distribution Copper in Kolo Creek Soil	147
4.70b: 3D View of Copper in Kolo Creek Soil	148
4.71a: Spatial Distribution map of Zinc in Kolo Creek Soil	148
4.71b: 3D View map of Zinc in Kolo Creek Soil	149
4.72a: Spatial Distribution map of Cadmium in Kolo Creek Soil	149
4.72b: 3D View map of Cadmium Kolo Creek Soil	150
4.73a: Spatial Distribution map of Lead in Kolo Creek Soil	150
4.73b: 3D View map of Lead in Kolo Creek Soil	151
4.74a: Spatial Distribution map of Mercury in Kolo Creek Soil	151
4.74b: 3D view map of Mercury in Kolo Creek Soil	152
4.75: Seasonal Variations of Heavy Metals in Kolo Creek Soils	152

<b>Figures</b>	<b>Page</b>
4.76: Principal component plot in rotated space soil Parameters	153
4.77: Dendogram of soil parameters of the study area	153
4.78: Soil Permeability, Porosity and Consistency Chart.	154
4.79: Plots of the 10 subsoil samples from Kolo-Creek and environs on modified Cassagrande Plasticity chart (ASTM D2487)	154
4.80: Typical soil particle size distribution of the Study area	155-159

## ABSTRACT

This study evaluates the impact of anthropogenic activities on soil and water resources in Kolo Creek, Niger Delta, Nigeria. Hydrocarbon exploration, illegal refining, and waste disposal have significantly disrupted environmental balance, necessitating site-specific assessments and pollution evaluation for effective mitigation. Soil, surface water, and groundwater samples were collected from ten georeferenced locations, with groundwater extracted from six meters' depth. Heavy metals ( $\text{Fe}^{2+}$ ,  $\text{Pb}^{2+}$ ,  $\text{Cd}^{2+}$ ,  $\text{Cr}^{3+}$ ,  $\text{Cu}^{2+}$ ,  $\text{Zn}^{2+}$ ) were analyzed using atomic absorption spectrophotometry (AAS), while total petroleum hydrocarbons (TPH), polycyclic aromatic hydrocarbons (PAH), and benzene, toluene, ethylbenzene, and xylene (BTEX) were measured via gas chromatography-flame ionization detection (GC-FID). Geotechnical properties (Atterberg limits, porosity, permeability) were assessed per ASTM (1975) and British Standards (BS 1377). Results indicate that apart from low pH (acidic conditions), most surface and groundwater parameters comply with WHO drinking water standards, except  $\text{Fe}^{2+}$  (125.82 mg/L),  $\text{Hg}^{2+}$  (1.05 mg/L), TPH, PAH, and BTEX, which exceed permissible limits. Multivariate statistical analysis identified six (6) principal components, while hierarchical cluster analysis (HCA) revealed two distinct pollution sources. Correlation analysis confirmed strong interrelations among contaminants, implying a common pollution origin for soil, surface water, and groundwater. Contamination factor analysis classifies  $\text{Fe}^{2+}$  (9.1) as highly contaminated in surface water, while  $\text{Ca}^{2+}$  (2.88) and  $\text{Fe}^{2+}$  (125.82) in groundwater indicate moderate to extreme contamination. Water quality index (WQI) results confirm that 100% of water samples are unfit for drinking, irrigation, or industrial use. Additionally, pollution index of groundwater (PIG >2.5) suggests severe contamination. However, irrigation suitability tests indicate that surface water meets agricultural standards based on Sodium Absorption Ratio (SAR) values. Heavy metal contamination in soil, particularly  $\text{Fe}^{2+}$  (18.97),  $\text{Al}^{3+}$  (1.02),  $\text{Hg}^{2+}$  (1.05), and  $\text{Cd}^{2+}$  (1.28), poses significant environmental risks. Geo-accumulation index (Igeo) classifies soil as moderately polluted by  $\text{Cd}^{2+}$  and heavily polluted by  $\text{Fe}^{2+}$  and  $\text{Hg}^{2+}$ . Furthermore, carcinogenic risk (CR) assessment shows that average CR values exceed  $10^{-6}$  ( $>10^{-6}$ ) for both adults and children, indicating a potential cancer risk. Alarmingly, children face a threefold higher cancer risk than adults. Hydrocarbon contamination has altered soil geotechnical properties, evidenced by lower permeability and plasticity index (5–9%), classifying it as low-plastic, partially cohesive silt. However, this modification suggests that affected soils could be reused for engineering applications.

*Keywords:* Hydrocarbon, Heavy Metals, Pollution, Contaminants, Illegal Refining, Atterberg Limits

# CHAPTER ONE

## INTRODUCTION

### 1.1 BACKGROUND INFORMATION

The term "anthropogenic activities" refers to human activities that take place on Earth's surface and involve different environmental elements (Ajayi & Okeke, 2024). These activities can significantly impact the quality of soils, water, and air in the environment, either directly or indirectly. Environmental contamination is the after-effect of these actions and may eventually result in pollution (Seiyaboh & Izah, as cited in Ajayi & Okeke, 2024). In this twenty-first century, environmental contamination remains one of the most significant challenges faced by humanity due to rapid industrialization, development projects, and urbanization (Peng *et al.*, 2023). Various economic activities, including industrial, agricultural, and improper waste management practices across different sectors, contribute substantially to this environmental threat (Peng *et al.*, 2023).

Soils are unique elements in the Earth system as they serve as the interface between the atmosphere, hydrosphere, terrestrial biosphere, and solid earth. The types of soil and vegetation that cover the landscape are crucial in controlling the hydrologic cycle, particularly in determining how much water infiltrates into the ground compared to the amount that flows over the surface. Among the major geo-environmental and geotechnical challenges faced by emerging nations like Nigeria are heavy metal-induced soil pollution, crude oil spills, and the overuse of fertilizers on farmlands. Liquid crude oil spills have the potential to seep into the ground, contaminating groundwater, altering the physico-chemical characteristics of the soil, and harming plant life (Obeta & Eze-Uzomaka, 2013).

Sikakwe, Ephraim, Nganje, Ntekim & Amah (2015) explain that mining operations affect land and water habitats in several ways, including changes to hydro-geological systems, soil contamination, and surface water pollution. The behavior and properties of soil engineering are altered as a result of these changes, which have significant impacts on both planned and existing constructions that rely on the affected soils for

stability. This may lead to structural or functional failure of structures, especially if pollution causes the soil to become more flexible, lose its ability to support weight, settle more quickly, or obstruct water or other liquids from draining. This could result in the abandonment of contaminated soil sites, a reduction in the scope of planned works, or an increase in project costs (Akinwumi *et al.*, 2014).

One of the biggest environmental issues of the modern era is the leakage of pollutants and effluents into water bodies, a problem that affects people worldwide. While natural sources also contribute to environmental contamination, human activities are the primary cause of increased pollution levels in ecosystems. Water pollution occurs when large volumes of substances are intentionally added to a body of water, making it unfit for human use (Edori & Odoemelam, 2022). Water is essential for all living organisms. Different types of water resources are categorized as solid (ice), gaseous (vapor), and liquid. "The three categories of surface water resources are fresh water, salt water (also called estuarine water), and brackish water (salt and freshwater interphase), categorized based on their origins" (Enaregha *et al.*, 2022; Ajayi & Okeke, 2024).

The availability of water is crucial for life to exist in all environments. Beyond drinking, surface water is the most extensively utilized water resource. In developing nations such as Nigeria, surface water resources are used for transportation, fishing, and providing water for domestic activities like cooking, washing, and bathing, particularly in rural areas along the coast. Most residential uses and drinking are supplied by freshwater resources (Seiyaboh & Izah, 2019).

Contaminated groundwater can pose a serious risk to human health, particularly by causing waterborne diseases. Additionally, the quality of groundwater directly affects agricultural production and crop yield. Therefore, groundwater is an essential natural resource for both agricultural and domestic uses (Okoroh & Ibuot, 2022). Groundwater is increasingly relied upon as a growing source of water for residential, commercial, and industrial purposes (Akakuru *et al.*, 2021).

"Rivers have been severely contaminated, making the water unsuitable for beneficial use" (Ezekiel *et al.*, as cited in Ajayi & Okeke, 2024). Ajayi & Okeke (2024) highlight

that "water is a vital resource for human existence; in a healthy adult, it makes up 73% of fat-free body weight, and in non-obese individuals, it makes up 60% of body weight." Despite covering 75% of the world, only 1% of water is pure enough for human consumption. Polluted water has several adverse impacts: (a) reduces available supply, (b) stifles economic growth at local, regional, and national levels, (c) presents known and unknown public health hazards, (d) restricts recreational activities, and (e) exacerbates already-disturbed natural processes. Adebayo and Tawabini (2012) emphasized that the unsustainable use of new technologies and natural resources, such as petroleum, leads to environmental degradation by exceeding the Earth's carrying capacity. Recent studies continue to support this perspective. For instance, Osman *et al.*, (2023) discuss how energy derived from fossil fuels contributes significantly to global climate change, accounting for more than 75% of global greenhouse gas emissions. The concept of ecological overshoot illustrates how human demands can exceed the Earth's regenerative capacity, leading to resource depletion and environmental degradation. This underscores the importance of sustainable resource use to maintain ecological balance.

One example of such technology is "the use of complex drilling fluids with toxic chemical components that jeopardize the health of oil workers as well as marine fauna and flora (the drilling fluid-smearred cuttings are often disposed of)" (Adebayo & Tawabini, 2012). Furthermore, the extensive use of large tankers for transporting petroleum products around the globe negatively impacts marine environments. Residents depend on surface and groundwater systems for their water supply, but these sources are highly vulnerable to contamination from anthropogenic activities such as industrial discharge, agricultural runoff, and urbanization, as well as natural processes like climate variability. Recent studies have applied advanced methods like GIS-based DRASTIC models and intrinsic vulnerability assessments to identify at-risk areas and improve groundwater management. These approaches provide valuable insights for mitigating pollution and ensuring sustainable water resources (Hussein, 2021; Canora & Sdao, 2022; Kazakis *et al.*, 2021). Regular evaluations of water quality and pollution

risks are essential for determining the present and intended use-value of water resources. Advanced monitoring and modeling techniques, such as GIS-based frameworks and dynamic assessments, are becoming increasingly important for understanding water quality trends and developing effective management strategies (Zessner, 2021).

Water pollution is influenced by the use of water, the presence of specific compounds, and their effects on ecosystems and human health. Even substances that may not initially appear as pollutants can interact with the environment in ways that disrupt water utility and ecological balance. The impact often depends on the context of water reuse and environmental factors.

Surface water resources in the Niger Delta, particularly in Bayelsa state, are contaminated by human wastes such as sewage from pier toilet systems, wastes from slaughterhouses, processed food wastes, oil palm waste, and solid wastes from household items like leftover pesticide cans, detergents, and marketing wastes. Ajayi & Okeke (2024) note that "scrap metal is a significant waste stream that is not dumped directly into the sea and is a significant industry in the Niger Delta." This involves collecting, sorting, and selling scrap metals for later use by the steel and iron ore industries. After rainfall, additional waste streams may flow through drainage systems (Ajayi & Okeke, 2024).

"Other human activities that take place in waterways include dredging, which involves both automated and manual techniques, and the construction of bridges to facilitate road building" (Ajayi & Okeke, 2024). In the coastal areas of Nigeria, particularly Bayelsa state, goods are regularly transported by water. However, waterways may become contaminated if sustainable practices are not followed. Flooding is another major source of contamination in waterways. When flooding occurs along riverbanks, debris from nearby areas often enters the water and is carried downstream. "Depending on the nature of the debris that the water transports, some of it ends up as suspended or deposited soil during the process" (Ajayi & Okeke, as cited in Seiyaboh & Jackson, 2017).

## **1.2 PROBLEM STATEMENT**

The physical and biochemical properties of soils and water supplies in the study area are constantly being altered due to activities both within and outside the region. These include farming, fishing, improper waste disposal, illegal crude oil refining, petroleum hydrocarbon exploration, exploitation, and agricultural practices. "These activities have the potential to degrade the status and utility of natural resources by introducing harmful elements, such as heavy metals, into the environment" (Okoroh & Ibuot, 2022).

## **1.3 OBJECTIVES OF THE STUDY**

### **Main Objective:**

To investigate the effects of human activities on the water and soil resources of Kolo Creek.

### **Specific Objectives:**

1. To determine the concentrations of petroleum hydrocarbons in the study area's soils, surface waters, and groundwater. This includes measuring the levels of benzene, toluene, ethylbenzene, xylene (BTEX), total petroleum hydrocarbons (TPH), and polycyclic aromatic hydrocarbons (PAH).
2. To evaluate the outcomes of these activities, as well as the level of regulatory compliance, and their impact on the geotechnical properties of the soils in the study area.
3. To assess the danger levels of heavy metals and other physicochemical characteristics in the soil, surface water, and groundwater samples from the study area, and determine the risks they pose to the environment and public health.
4. To develop maps and geochemical models for the study area.
5. To establish a database and create maps depicting the spatial distribution and concentration of contaminants in the research area, along with the sample locations.

## 1.4 JUSTIFICATION OF THE STUDY

The justification for this study can be viewed from several perspectives:

- **Environmental Importance:** Kolo Creek, located in the Niger Delta, is rich in biodiversity and vital ecosystems but has suffered significant degradation due to anthropogenic activities.
- **Human Health and Livelihoods:** The surrounding communities rely on Kolo Creek's natural resources for agriculture, fishing, and drinking water. Therefore, this study addresses an urgent public health concern.
- **Geotechnical and Engineering Significance:** From a geotechnical perspective, the study assesses how hydrocarbon pollution affects soil properties, including porosity, permeability, and Atterberg limits.
- **Policy and Remediation:** There is a clear policy gap in the enforcement of environmental regulations in the Niger Delta. This study aims to provide evidence-based data that can be used to influence policies on environmental protection, regulation of industrial activities, and remediation efforts.

## 1.5 Scope of Study

This study assesses the impact of human activities on the soils and water quality of Kolo Creek using geochemical, physicochemical, and geotechnical techniques. The research covers various aspects, including geochemical mapping, sample collection, laboratory analysis, and result interpretation in relation to environmental impact, water quality, and health risk standards. Data obtained were compared with the World Health Organization (WHO) guidelines. The study was conducted over one year, capturing seasonal variations during both the rainy and dry seasons.

## CHAPTER TWO

### LITERATURE REVIEW

#### 2.1 PREVIOUS WORKS

Nigeria, like many emerging and developed nations, has long faced environmental challenges. The environment, defined as "the sum of all external influences and conditions impacting an organism's, individual's, or community's life and development" (Hussein, 2021), plays a crucial role in sustaining life. However, human activities contribute to the release of toxic substances and pollutants, endangering both ecosystems and public health. Environmental pollution, characterized by the introduction of harmful substances that disrupt ecological balance, has significant adverse effects on living organisms (Zessner, 2021; Hussein, 2021). Recent research by George *et al.*, (2021) highlighted soil contamination with heavy metals and petroleum hydrocarbons in crude oil-polluted regions, particularly in the Okpare-Olomu area of the Niger Delta. Their study revealed high contamination levels, especially in total petroleum hydrocarbons (TPH) and toxic metals, which serve as key indicators of environmental degradation.

In a study of Kolo Creek, which receives effluent discharges from industrial and human activities, Inengite, Oforika, and Osuji (2010) conducted a four-season assessment (Dry, Late Dry, Rainy, and Late Rainy). Their findings, based on geo-accumulation indices, indicated that the creek was highly contaminated with iron (Fe) rather than lead (Pb), chromium (Cr), or nickel (Ni). The mean concentrations of the heavy metals were as follows: Fe (12.45 mg/L), Pb (0.03 mg/L), Cr (0.02 mg/L), and Ni (0.01 mg/L). Pb and Cr showed the strongest positive correlation, while Fe and Ni exhibited the strongest negative correlation. When compared to the Nigeria Midstream and Downstream Petroleum Regulatory Authority (NMDPRA) intervention values (Pb: 0.05 mg/L, Cr: 0.05 mg/L, Ni: 0.05 mg/L), the results confirmed that Kolo Creek was free of Pb, Cr, and Ni pollution.

Similarly, Ogamba, Ebere, and Izah (2017) evaluated the physicochemical quality of Kolo Creek's soil and concluded that human activities have significantly influenced soil

composition. Their study found high concentrations of nutrients, including cations such as calcium ( $\text{Ca}^{2+}$ : 45.6 mg/kg), magnesium ( $\text{Mg}^{2+}$ : 28.3 mg/kg), potassium ( $\text{K}^+$ : 12.4 mg/kg), and sodium ( $\text{Na}^+$ : 10.2 mg/kg), as well as anions such as nitrate ( $\text{NO}_3^-$ : 8.7 mg/kg), phosphate ( $\text{PO}_4^{3-}$ : 5.3 mg/kg), and sulfate ( $\text{SO}_4^{2-}$ : 6.8 mg/kg). These findings suggest the impact of runoff and anthropogenic activities on the waterway.

Ebue and Bariweni (2019) reported that Kolo Creek water was biologically polluted but physicochemically potable for domestic use. Their study found a mean *E. coli* level of  $39.83 \pm 2.93$  CFU, with pH values averaging  $7.23 \pm 0.37$  during the dry season and  $6.78 \pm 0.18$  during the wet season. Dissolved oxygen (DO) levels were  $7.58 \pm 1.00$  mg/L in the dry season and  $9.29 \pm 2.67$  mg/L in the wet season. Other physicochemical parameters included total dissolved solids (TDS:  $120 \pm 15$  mg/L), electrical conductivity (EC:  $250 \pm 30$   $\mu\text{S}/\text{cm}$ ), and turbidity ( $5.2 \pm 0.8$  NTU). When assessed using the water quality index, the creek was classified as medium (Class III) and deemed unsuitable for direct consumption.

Seiyaboh and Jackson (2017) highlighted alarming hydrocarbon contamination in Kolo Creek's soil. Their findings showed that hydrocarbon content ranged from 0.14–3.79 mg/kg, while total petroleum hydrocarbons (TPH) varied between 0.08–2.41 mg/kg. Apart from pH, magnesium, and potassium, surface water and soil in Imirigi were found to be slightly impacted by anthropogenic activities. This study underscores the persistent threat of hydrocarbon pollution in the Niger Delta region.

Several studies have examined the effects of petroleum hydrocarbons on soil and water resources in the Niger Delta. Okonofua, Babalola, and Ojuri (2019) observed that in the Ologbo field, Niger Delta, TPH was undetectable beyond a vertical depth of 460m. However, subsurface imaging revealed that TPH concentrations in the study area exceeded the WHO-recommended limits (50–100 mg/kg). Similarly, Nwankwo, Ekeocha, and Ikoro (2015) investigated the impact of an oil spill in Akinima, Rivers State, on soil quality. Heavy metal analysis from contaminated sites was compared to control samples and the Nigeria Midstream and Downstream Petroleum Regulatory

Authority (NMDPRA) target values. The pH of contaminated samples ranged from 4.8 to 6.97, whereas control samples had pH values between 6.82 and 6.99, with TPH below detectable limits. Compared to uncontaminated soil, polluted samples exhibited higher levels of heavy metals and TPH. The average pH of the contaminated soil was within the acidic range, and TPH values exceeded regulatory limits.

Nwankwoala and Omofuophu (2020) employed a risk-based modeling technique to assess the environmental impact of an oil spill at Bonny Terminal, using soil as the medium. Their study evaluated the potential health risks, estimated the volume of the spill, identified pollutants, and analyzed contamination levels. Groundwater and soil samples were collected both near the spill site and in neighboring villages to assess the extent of pollution. Nwankwoala and Mzaga (2017) further examined soil composition, grain size distribution, contaminant concentration, migration pathways, and the environmental effects of hydrocarbon pollution in a section of the Eastern Niger Delta's Central Swamp Depobelt. Their findings indicated that the predominant soil type ranged from fine gravel to fine silty sands, with permeability values between  $1.36$  and  $1.58 \times 10^{-4}$  m/sec. While heavy metal concentrations remained within acceptable limits, contaminated sites exhibited higher Atterberg limits compared to control sites, indicating alterations in soil properties due to pollution.

Despite numerous studies in the region, limited research has focused on Kolo Creek, specifically regarding the combined effects of oil spills, illegal refining, and gas flaring. This study addresses that gap by providing comprehensive data on soil and water contamination and associated human health risks. By integrating findings from previous research, this work aims to contribute to a deeper understanding of the environmental and health impacts of hydrocarbon pollution in the Niger Delta, with a particular focus on Kolo Creek.

## CHAPTER THREE

### MATERIALS AND METHODS

#### 3.1 Materials

The materials used in this research work are presented in table 3.1 below:

Table 3.1: Lists all of the components, including the chemicals, software, field and laboratory instruments, and other items.

S/N	FIELD TOOLS	LABORATORY TOOLS	REAGENTS	SOFTWARES USED
1	Topographic map	pH meter	Sabour and Dextrose Agar	Microsoft office, Surfer 11 and ArcGis
2	Global positioning system (e trex GPS)	Glass ware	Nutrient agar	
3	Light hand auger	Hanna Hi 83200 photometer	Distilled Water	
4		Burette	Mineral Salts Agar (medium)	
5		Cornical flask	Nitric acid	
6		Pipettes	Perchloric acid	
7		Atomic Absorption Spectrophotometer	Sulphuric acid	
8		Crucibles	Air oxidant gas	
9		Incubator	Acetylene gas	
10		Autoclave	E.D.TA	
11		Burnsen burner	Sodium hydroxide	
12		Petric dishes	Solochrome	
13		Test tubes	Moedant Black	
14			FAS	
15			Feroin indicator	
16			Phosphoric acid	
17			Potassium dichromate	
18			Nessler reagent	
19			Barium chloride	
20			Hydrochloric acid	
21			Sodium acetate	
22			Buffer 7.0, 4.0, and 9.0	
23			Potassium Chloride Solution	

### 3.2 Methodology

This study underwent a series of workflow and quality control processes; figure 3.1 below presents a step-by-step account of how this project was carried out.

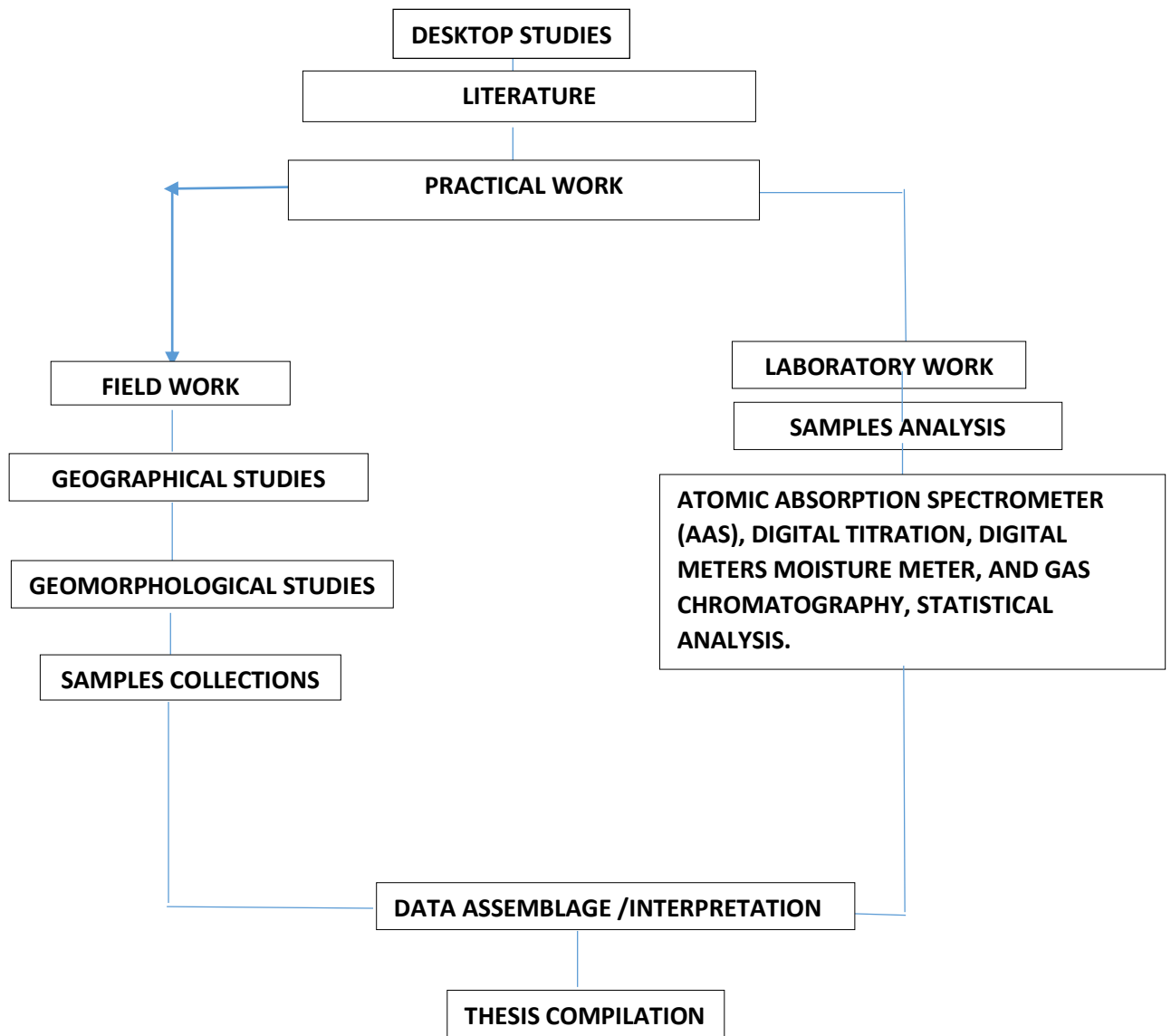


Fig 3.1: Workflow

### **3.3 Description of the study area**

Kolo Creek and its surroundings form a non-tidal freshwater zone that has undergone significant industrialization and urbanization due to the oil and gas infrastructure in the region (Inengite, Oforka, & Osuji, 2010; Ajayi & Okeke, 2024). The creek originates in Okarki, Engenni, Rivers State, and flows through the Ogbia Local Government Area of Bayelsa State, Nigeria, eventually serving as a tributary of the Orashi River (Ajayi & Okeke, 2024). Geographically, it lies between longitudes  $6^{\circ}18'0''$  and  $6^{\circ}36'0''$  East and latitudes  $4^{\circ}48'0''$  and  $5^{\circ}6'0''$  North (Figure 3.2).

Kolo Creek extends approximately 85 km, covering an area of 1,625 square kilometers, with an elevation ranging from 10 to 7 meters (Eli, 2012). The creek passes through about 21 communities, including Okarki, Otegue II, Ibelebiri, Oruma/Yibama, Otuasega, Imiringi, Emeyal 1 and 2, Kolo 1, 2, and 3, Otuegila, Otakeme, Otuabagi, Ewoma/Otuabi, Otuogidi, Ogbia Town, Otuabo/Abobiri, Ekpenkiri, Akakumama, and Bukiri (Gobo, Amangabara, & Etiga, 2013). These communities rely on the creek for various domestic, agricultural, and economic activities.

The primary human activities along the creek include open defecation, floodplain farming, sand mining, illicit crude oil refining, and oil palm and cassava processing. These activities significantly impact the quality of soil, streams, and water resources (Ayotunde & Bariweni, 2018; Izonfuo & Bariweni, 2001). The combination of industrialization, urbanization, and these anthropogenic activities has led to environmental degradation, making Kolo Creek a critical area for studying the effects of pollution on freshwater ecosystems.

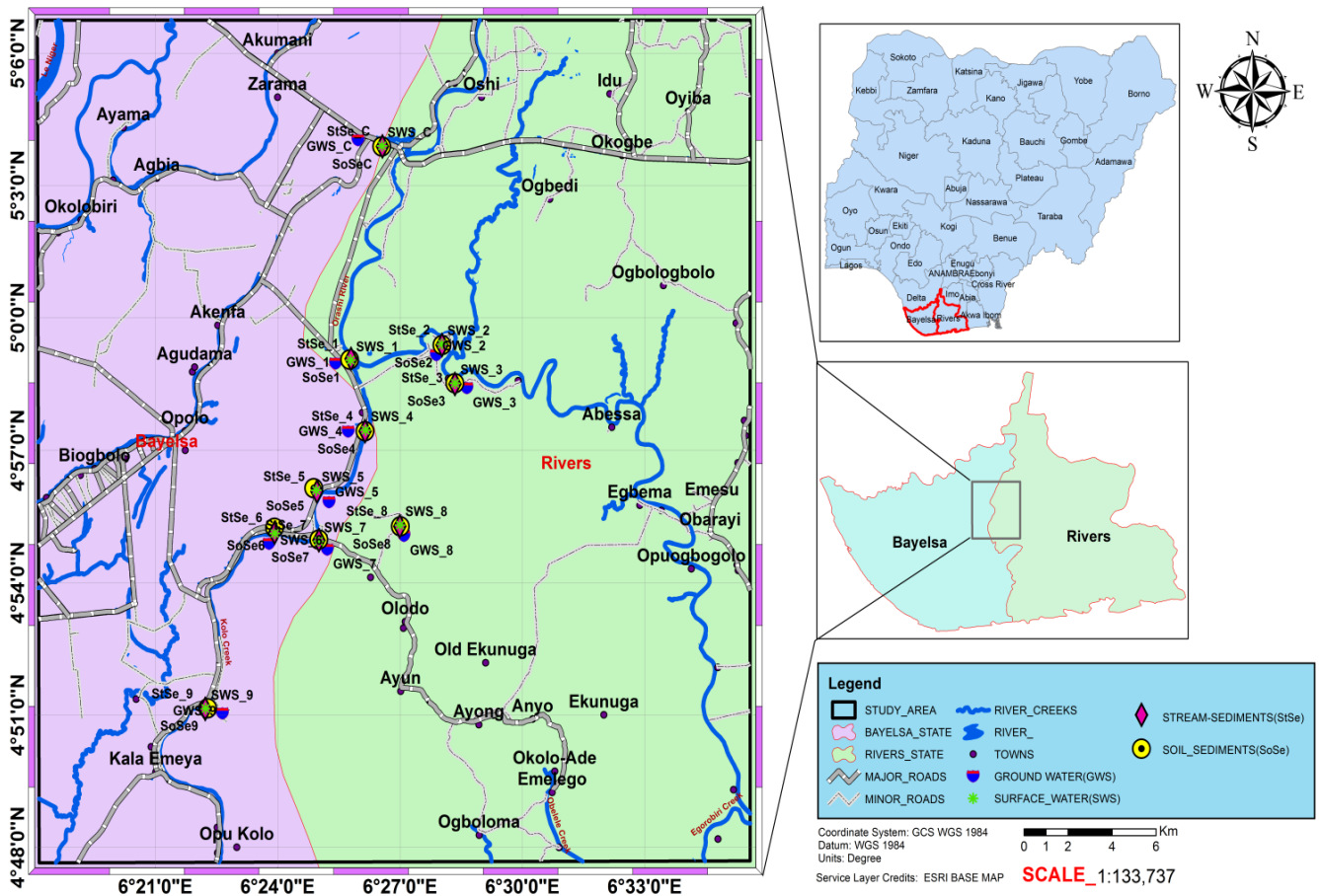


Figure 3.2: Location Map

### 3.3.1 Physiographic and Drainage

The meandering paths of the Kolo Creek and Elebele systems have likely contributed to the formation of silted river belt soils in the area. These soils are predominantly peaty clay and waterlogged, remaining submerged for extended periods due to the region's low-lying floodplains, which reach a maximum elevation of eight meters above sea level. This unique geomorphological setting creates a dynamic and ecologically sensitive environment.

Kolo Creek, a key water and material sink in the study area, serves as a distributary of the Orashi River and is the origin of the area's name (Ezekwe & Utong, 2017; Ajayi & Okeke, 2024). The Elebele/Ekuruba stream runs through the center of the wetlands, while Kolo Creek flanks the study area, forming a critical hydrological network (Ajayi

& Okeke, 2024). During the dry season (November to April), Kolo Creek acts as the primary discharge channel for the wetlands, playing a vital role in maintaining the hydrological balance of the region.

In addition to these natural watercourses, the study area features a variety of other water bodies, including lakes, ponds, borrow pits, and small channels. These features drain into either the Elebele/Ekuruba stream or Kolo Creek, further influencing the area's hydrology and sediment dynamics (Ajayi & Okeke, 2024). The interplay between natural and anthropogenic water systems underscores the complexity of the region's environmental challenges and highlights the need for sustainable management practices.

### **3.3.2 Climate and Vegetation**

Ajayi & Okeke (2024) noted that the Kolo Creek region is characterized by tropical rainforests and freshwater marshes, which experience regular flooding throughout the year, particularly from May to November. The region's defining features include seasonal floods, continuously swampy marsh forest vegetation, and frequent freshwater inundation. These ecological conditions create a unique and dynamic environment that supports diverse flora and fauna.

The two predominant soil types in the study area are young, shallow, poorly drained inceptisol Aquepts and acid sulfate soils (Sulpha-quepts). These soils are typically waterlogged and support vegetation dominated by raffia palms, which thrive in the freshwater marsh environment (Elmi et al., 2004; Ajayi & Okeke, 2024). The combination of these soil types and vegetation contributes to the region's ecological richness and hydrological complexity.

According to Köppen's climate classification, the area falls under the tropical wet (Af) climate zone, characterized by consistently high temperatures and significant annual precipitation. The average temperature remains above 18°C, while annual rainfall exceeds 1,500 mm. Although rainfall occurs throughout the year, there is a slight decrease in precipitation in August, as well as between December and February. Temperature variations within the year remain minimal, typically staying below 30°C

(Dupuis & Ucan-Marin, 2015). Nighttime temperatures average 22°C, while daytime highs can reach 32°C. This stable, warm, and humid climate supports the region's lush vegetation and contributes to its high biodiversity.

### **3.3.3 The Study Area's Geology and Hydrology**

#### **Regional Geology of the Niger Delta**

The research area is located in southern Nigeria's Niger Delta Basin, a geologically significant region formed at the continental margin of West Africa. The Niger Delta lies at the juncture where the Equatorial coast, moving eastward, shifts southward toward the Equator. According to Whiteman (2012), the Benue Trough developed as a failed arm of a rift triple junction between the African and South American continents, ultimately leading to the opening of the South Atlantic Ocean and the formation of the Niger Delta.

#### **Geological Evolution of the Niger Delta**

Kolo Creek is part of the Niger Delta Basin, which serves as a primary hub for onshore petroleum operations. The basin is bounded by:

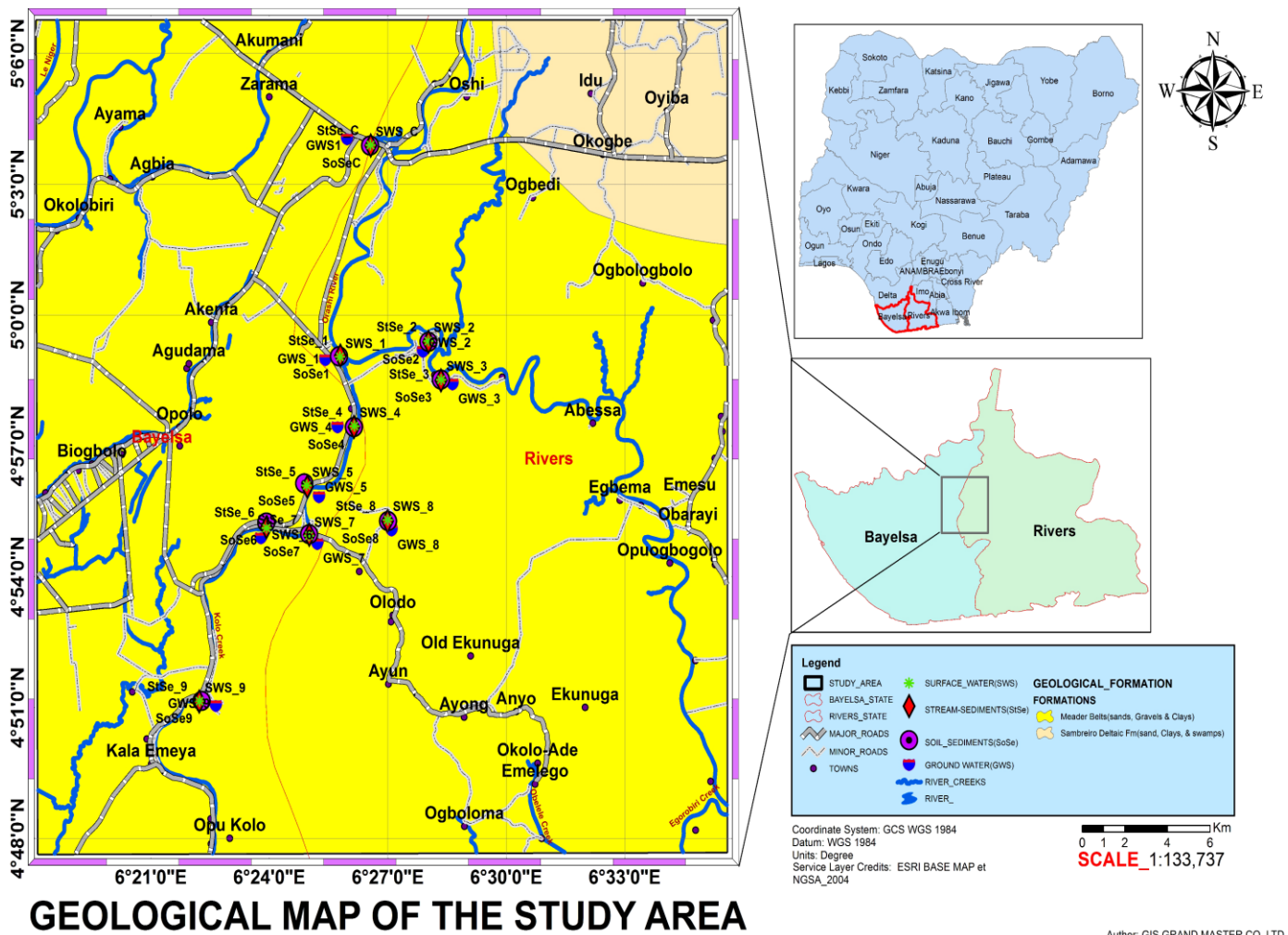
- The Cretaceous Abakaliki High to the northeast,
- The Gulf of Guinea to the south, and
- The Calabar Flank, a hinge line enclosing the Precambrian basement rocks, to the east-southeast (Olobaniyi & Owoyemi, 2004).

The Niger Delta originated during the Aptian–Albian period, following the breakup of the supercontinent Gondwana. It was shaped by a triple junction rift system that developed during the Late Jurassic, leading to the separation of South America and Africa (Fig. 3.3).

Following the Paleocene transgression, the Eocene sedimentary cycle marked the beginning of modern Niger Delta expansion. Hospers (1965) suggested that delta formation commenced over the African continental margin in the Middle to Late Eocene. As the delta continued to grow, it developed rollover anticlines, shale diapirs, and growth faults, which play crucial roles in hydrocarbon accumulation.



share the same general characteristics as the subsurface units and are the surface lateral equivalents of the subsurface units.



**GEOLOGICAL MAP OF THE STUDY AREA**

Figure 3.4: Geologic Map of the Study Area.

“With notable ground water storage and recharging of more than  $6.63 \times 10^8$  m<sup>3</sup> yearly, the Benin formation is the water-bearing unit in the examined area” (Oteze, 1981). Boreholes supply Bayelsa's municipal water demands, streams, and rivers that access the aquifer system. As a result, the aquifer may be susceptible to harmful pollutant penetration.

“These aquifers have been divided into three main zones: a transition zone with a mix of marine and continental materials, a coastal zone with a preponderance of marine deposits, and a northern bordering zone with shallow aquifers containing mostly

continental deposits” (Etu-Efeotor & Akpokodje, 1990). Following this divide, a notable trend in aquifer properties has been noted. Four clearly defined aquifers in the upper 305 meters, ranging in thickness to more than 120 meters, were their summary of the hydrostratigraphic units of the Benin Formation (Fig: 3.4).

These aquifers ranged in conditions from semi-confined to confine at depths, starting from unconfined at the surface. An interval made up of a complicated aquifer system shown to be non-uniform, discontinuous, and diverse by the very discontinuous shale strata that divide the aquifers.

### **3.4 Field Data Collection and Sample Analysis**

#### **Topographic and Geological Survey**

The Nigeria Geological Survey Department in Bayelsa provided topographic and geologic maps for the study. Key features related to geology, hydrology, and geomorphology were identified. A preliminary site visit was conducted to assess pollutant sources and potential receptors in the research area. For efficient planning of soil, water, and environmental monitoring, field observations were integrated with topographic and geological maps, ensuring accurate identification of land features.

#### **Sampling Strategy and Procedures**

Sampling was conducted in 2021 to capture variations across two seasons:

- Wet Season (March, April, May)
- Dry Season (October, November, December)

#### **Soil Sampling**

Soil samples were collected from strategic locations, including hydrocarbon-polluted residential, commercial, and industrial areas.

- A total of 20 soil samples were collected, including:
  - 18 samples from polluted areas

- 2 samples from Mbiama (1 km away from the polluted zone, serving as control)
- Soil samples were obtained at depths of 0.5 m, 1.0 m, and 1.5 m using a hand auger.
- Each sample (~1 kg) was placed in sterile polythene bags and transported to GETAMME LABORATORIES NIGERIA LTD, Port Harcourt, for analysis.
- Soil samples were air-dried at room temperature, crushed, and sieved through a 2 mm mesh screen before analysis.

### **Surface Water Sampling**

- 10 surface water samples were collected from geo-referenced sites along Kolo Creek.
- Sampling depth: 10 cm below the water surface.
- Sterile polypropylene containers, pre-rinsed with acidified water, were used for sample collection.
- To prevent air contact, the samples were corked underwater immediately upon collection.
- Storage: Samples were refrigerated at 4°C until analysis.

### **Groundwater Sampling**

- 10 boreholes (Bh1 to Bh9 and BhCtr) were drilled at geo-referenced locations:
  - Okarki, Igovia, Ikodu, Otegwe, Otuasega, Oruma, Obedum, Odan, Imiringi, and Mbiama.
- Boreholes were drilled to a depth of 6 meters.
- Environmental samples were collected at 0-1 m and every 1 m down to 6 m.
- Samples were kept cold and transported for laboratory examination.

### **Analytical Parameters**

#### **Water Quality Parameters (23 total)**

1. Total Petroleum Hydrocarbons (TPH)
2. Polycyclic Aromatic Hydrocarbons (PAH)
3. BTEX (Benzene, Toluene, Ethylbenzene, Xylene)

4. pH
5. Temperature
6. Conductivity
7. Turbidity
8. Total Hardness
9. Total Dissolved Solids (TDS)
10. Nitrate ( $\text{NO}_3^-$ )
11. Sulphate ( $\text{SO}_4^{2-}$ )
12. Metallic Ions:
  - Calcium ( $\text{Ca}^{2+}$ )
  - Sodium ( $\text{Na}^+$ )
  - Magnesium ( $\text{Mg}^{2+}$ )
  - Potassium ( $\text{K}^+$ )
  - Chromium ( $\text{Cr}^{2+}$ )
  - Lead ( $\text{Pb}^+$ )
  - Zinc ( $\text{Zn}^{2+}$ )
  - Mercury ( $\text{Hg}^+$ )
  - Iron ( $\text{Fe}^{2+}$ )
  - Copper ( $\text{Cu}^{2+}$ )
  - Aluminum ( $\text{Al}^{2+}$ )
  - Cadmium ( $\text{Cd}^{2+}$ )

Soil Quality Parameters (23 total)

1. Total Petroleum Hydrocarbons (TPH)
2. Polycyclic Aromatic Hydrocarbons (PAH)
3. BTEX (Benzene, Toluene, Ethylbenzene, Xylene)
4. pH
5. Conductivity
6. Total Hardness
7. Total Dissolved Solids (TDS)

8. Nitrate ( $\text{NO}_3^-$ )
9. Sulphate ( $\text{SO}_4^{2-}$ )
10. Metallic Ions (*same as for water analysis*)

### Geotechnical Parameters

1. Permeability
2. Porosity
3. Liquid Limit
4. Plastic Limit
5. Plasticity Index

### Location of Sampling Points

Sampling points for soil, surface water, and groundwater investigations were strategically selected and geo-referenced along Kolo Creek. (Refer to Tables 3.2, 3.3, 3.4, and 3.5 for details.)

Table 3.2: Soils Sample ID and Coordinates

S/N	SAMPLE_ID	LATITUDE	LONGITUDE
1	SoSe1	4.9842	6.4295
2	SoSe2	4.9897	6.4672
3	SoSe3	4.9753	6.4725
4	SoSe4	4.9572	6.4358
5	SoSe5	4.9357	6.4148
6	SoSe6	4.9207	6.3988
7	SoSe7	4.9163	6.4169
8	SoSe8	4.9213	6.4502
9	SoSe9	4.8525	6.3715
10	SoSeC	5.0648	6.4426

Table 3.3: Ground Water Sample ID and Coordinates

S/N	SAMPLE_ID	LATITUDE	LONGITUDE
1	GWS_C	5.0671	6.4329
2	GWS_1	4.9828	6.4237
3	GWS_2	4.986	6.4649
4	GWS_3	4.9735	6.4774
5	GWS_4	4.9571	6.4289
6	GWS_5	4.9304	6.421
7	GWS_6	4.9147	6.3965
8	GWS_7	4.9125	6.4203

9	GWS_8	4.9176	6.4516
10	GWS_9	4.8506	6.3775

Table 3.4: Surface Water Sample ID and Coordinates

S/N	SAMPLE_ID	LATITUDE	LONGITUDE
1	SWS_C	5.0648	6.4428
2	SWS_1	4.9845	6.43
3	SWS_2	4.9897	6.4672
4	SWS_3	4.9751	6.4725
5	SWS_4	4.9572	6.4358
6	SWS_5	4.9344	6.4161
7	SWS_6	4.9189	6.3988
8	SWS_7	4.916	6.4169
9	SWS_8	4.9213	6.4499
10	SWS_9	4.8523	6.3704

### 3.5 Laboratory Analysis of Soil and Water samples

Pollutant concentrations are measured and conventional procedures were used to assess physicochemical parameters such as pH, nitrate, sulphates, total hardness (TH), salinity, and electrical conductivity (EC) using the Atomic Absorption Spectrophotometer (AAS). Using a Ho riba model U-10  $\mu$  meter, two physicochemical parameters that were detected in situ were temperature and pH.

#### 3.5.1 Determination of Soil Electrical Conductivity

A conductivity meter was used to electrometrically measure the soil samples' electrical conductivity. Several times, the meter was being calibrated with a 0.01 M potassium chloride (KCl) standard solution, the electrode was cleaned with distilled water. At 25°C, the standard reference solution has an electrical conductivity of 1,413  $\mu$ S/cm. To achieve a 1:1 soil to water ratio, a 50 ml beaker, weigh out roughly 20 g of air-dried soil that has been crushed and sieved through a 2-mm mesh size sieve. After adding 20 milliliters of distilled water, stir the mixture occasionally with a glass rod and let it rest for 30 minutes.

The electrical conductivity was measured by inserting the conductivity meter's electrode into the partially settled suspension or supernatant. Care was taken to prevent stirring the suspension during the measurement process, and the electrodes were periodically rinsed with distilled water in between readings before being wiped dry with fresh tissue or filter paper.

### **3.5.2 Nitrate determination**

The Na-acetate Extraction Method was used to measure the nitrate in the soil: Around 5.0 g of soil were transferred into a shaking bottle, shaken for a minute, filtered, and mixed with 20 ml of extracting solution (100 g Na acetate + 30 ml of diluted 99.58% acetic acid to make one liter) and 1/4 teaspoon (or around 0.25 g) of activated carbon. Transferring a 1 ml aliquot of the soil extract into a sample vial and mixing it were the steps in the test method. After swiftly adding 0.5 ml of the brucine reagent (2.5 g brucine sulfate in 100 ml glacial acetic acid), 2 ml of sulfuric acid was added. After mixing this solution for roughly 30 seconds, it was to stand for five minutes. The solution was re-mixed and continuously stirred for approximately 30 seconds before 2 milliliters of distilled water were added. Water was then added to the solution until the sample vial's 10 ml mark was reached. Vials were allowed to stand and cool naturally for approximately fifteen minutes, allowing the test solution to take on a brownish hue. The HACH DR 890 colorimeter was used to measure the absorbance at 400 nm indicating the amount of ppm nitrate ( $\text{NO}_3^-$ ).

### **3.5.3 Sulphate determination**

Procedure for Extraction and Testing: The  $\text{KH}_2\text{PO}_4$  Extraction Method was used to perform the extraction. A 25 ml extraction solution ( $\text{KH}_2\text{PO}_4$  solution with 500 ppm) was added to roughly 5 g of dirt that had been air dried, sieved, and weighed into a centrifuge tube with a mesh size of 2 mm. The soil solution was shaken for thirty minutes on a mechanical shaker before the suspension was filtered through whatman filter paper. 10 milliliters of the sample aliquot were pipetted into a 25 milliliter volumetric flask, and distilled water was added to the full mark to raise the capacity.

Then, 1 milliliter of a gelatin-BaCl<sub>2</sub> reagent (0.6 grams of gelatin in 200 milliliters of hot distilled water plus 2 grams of chilled solution) was added, thoroughly mixing the mixture, following a 30-minute standing period (during which the test solution precipitated to a white color), a HACH DR 890 colorimeter was used to measure the content at 420 nm.

#### **3.5.4 pH Determinations**

The PYE UNICAm pH meter or digital pH meter (model P. 107) provided by Hach USA, phosphate buffer of 4.0 borate buffer pH = 9.18, Glass electrodes made of platinum and silver were used to measure the pH of the water samples.

#### **3.5.5 Temperature Determination**

The temperatures of the creek water were taken immediately before collection of the samples using a mercury in glass thermometer (range 0<sup>0</sup> -100<sup>0</sup> c) supplied by Philips CO.

#### **3.5.6 The process of calculating total dissolved solids (TDS)**

A 100mls of the water sample filtered through What-man No 42 filter paper was vaporised in a weighed 250ml evaporating dish. The difference in weight constitutes the TDS. The value got was multiplied by a factor of 10 to express it in mg/l or ppm.

#### **3.5.7 Determination of Turbidity**

Formazin Turbidity Scale was used for turbidity measurements. The scale was calibrated with known concentrations of formazin. Distilled water was used to zero the instrument. 25mls of the water sample was taken in 25ml cell holder, inserted into the instrument and the turbidity read directly in Formazin Turbidity Unit (FTU).

### **3.5.8 Determination of Total Hardness**

Calculation of the hardness from the individual concentrations of each hardness producing cation remains the generally accepted method. These concentrations were converted to the equivalent CaCO<sub>3</sub> concentration and the resulting CaCO<sub>3</sub> concentrations totalled. Total Hardness = (ppm Ca x 2.496) + (ppm Mg x 4.115). Atomic absorption spectrophotometer (model ISO-7 ZEEMAN) was used in determining ppm calcium, iron and magnesium.

### **3.5.9 Determination of Metal Ion Concentrations in Water Samples**

The concentrations of metallic ions in water samples were measured using Atomic Absorption Spectroscopy (AAS). For calibration, four standard solutions were prepared at concentrations of 5.00 ppm, 7.50 ppm, 10.00 ppm, and 15.00 ppm, specific to each metal ion analyzed. Deionized water served as a blank, and preparation methods for stock solutions, including sodium thiosulfate, bi-iodate, manganese, and potassium fluoride solutions.

### **Sample Preparation and Pretreatment**

To prepare water samples for analysis, wet digestion with concentrated nitric acid (HNO<sub>3</sub>) was used as a pretreatment for measuring ions such as Na<sup>+</sup>, K<sup>+</sup>, Ca<sup>2+</sup>, and Mg<sup>2+</sup>. In this process, a 100 ml water sample in an Erlenmeyer flask was acidified with HNO<sub>3</sub> and heated on a water bath until fully evaporated. After adding 25 ml of concentrated HNO<sub>3</sub> and heating almost to boiling, the solution was allowed to evaporate to a smaller volume, with caution taken to avoid spattering. This wet ashing process continued with repeated HNO<sub>3</sub> additions until a white residue formed, which was cooled, dissolved in concentrated hydrochloric acid (HCl), and filtered. The solution was neutralized with concentrated ammonia and diluted to 50 ml in a volumetric flask.

For heavy metal sample preparation, the water sample pH was adjusted to 4.0 using 3 ml of concentrated HNO<sub>3</sub>. A 100 ml sample was measured in a conical flask, combined with 5 ml of concentrated HCl, and heated for 15 minutes. After cooling, the solution

was filtered through a sintered glass or porcelain filter and diluted to 100 ml in a volumetric flask with redistilled water.

### **AAS Analysis**

The pre-treated water samples were directly aspirated into the air-acetylene and nitrous oxide flame of the AAS, following a warm-up of the hollow cathode lamp for 30 minutes. The absorbance readings, measured directly from the calibrated graph in the AAS, indicated concentrations in ppm (or mg/L). Standards and samples were aspirated in sequence, with deionized water used as a blank. By comparing sample absorbance values with the standards, metal ion concentrations were directly determined and displayed on the spectrophotometer screen.

#### **3.5.10 Determination of Petroleum Compounds**

Due to their hazardous properties and adverse effects on human health, key pollutants of concern—BTEX (Benzene, Toluene, Ethylbenzene, and Xylenes), PAHs (Polycyclic Aromatic Hydrocarbons), and Total Petroleum Hydrocarbons (TPH)—were analyzed in soil, surface water, and groundwater samples from the study area. Chemical analyses were conducted in accordance with established regulatory standards. The separation and identification of petroleum hydrocarbons in the samples were performed using gas chromatography equipped with an Agilent 6890N Flame Ionization Detector (GC-FID).

#### **3.5.11 Determination of Geotechnical Properties of Soils**

##### **Atterberg Limits**

The Atterberg limits were determined using soil particles smaller than 0.425 mm. These limits define the boundaries between different states of consistency in fine-grained soils:

- **Plastic Limit (WP):** The water content at which the soil begins to exhibit plastic behavior. This is determined by rolling soil into 3 mm diameter threads, where it crumbles upon further deformation.

- **Liquid Limit (WL):** The water content at which soil in a standard cup, cut by a groove of standard dimensions, flows together after being subjected to 25 standard shocks.

The **Plasticity Index (IP)**, a measure of the range of water contents over which soil exhibits plastic behavior, was calculated as the difference between the liquid limit and the plastic limit ( $IP = WL - WP$ ). Distilled water was used to adjust the soil to the required consistency during the tests. The tests were conducted following the procedures outlined in **BS 1377: Part 2: 1990**.

### 3.5.12 Laboratory Testing of Soil Samples

Soil samples collected from selected boreholes were analyzed in laboratories following **ASTM (1975)** and **British Standards (BS 1377)** guidelines (Koepfinger, Sherr & Cook, 1976). The particle size distribution was determined by passing a known weight of oven-dried soil through an **ASTM sieve No. 200 (0.074 mm)** and shaking the sample using a mechanical shaker until no fines remained.

#### **Particle Size Distribution and Hydraulic Conductivity**

The weight retained on each sieve was measured, and the percentage of material passing through each successive sieve size was calculated based on the initial sample weight. This data was used to plot grain size distribution curves, with the percentage passing plotted against grain size.

Hydraulic conductivity (**K**) of the aquifer materials was estimated using the grain size distribution curves and the **empirical formula by Hazen (1983)**:

$$K=C \cdot (d_{10})^2$$

Where:

- **K** = Hydraulic conductivity (cm/s)
- **C** = Constant (Freeze and Cherry, 1979)
- **d<sub>10</sub>** = Effective diameter (mm), defined as the grain size at which 10% of the total sample weight comprises smaller grains.

This method was applied specifically for homogeneous sandy soils to determine their permeability characteristics.

### **3.5.13 Determination of the Soil Samples' Grain Size Distribution**

The size of the grains is an important property of unconsolidated materials. The amount of pore spaces that can contain water and the ease of water transmission through the material are determined by the distribution of grain sizes. By passing the material through nested sieves with varying mesh sizes, the grain size distribution of the soils was determined. Using a hydrometer, the silt and clay fractions were determined. In order to conduct this analysis, the soil was completely suspended in a water column and allowed to settle to the bottom of the column without being disturbed. The density of the water-soil suspension was determined using a hydrometer as a function of time. The distribution of particle sizes was inferred since different sized particles settle at different speeds. The particle size distribution curve was used to illustrate the study of grain size result.

Two types of laboratory analyses were conducted on the soil samples. This study used the sieve analysis (particle size distribution) technique for the first time. To get a sense of the lithology and estimate the permeability of the recovered contaminated soils, basic sieve properties were assessed.

## **3.6 Data Analysis**

Data on soils, groundwater, and surface water are analyzed using principle components analysis (PCA), correlation, and hierarchical cluster analysis (HCA). Statistical Analysis Software (SAS) was used to analyze a few geochemical characteristics of Kolo Creek. For the analysis of geochemical data, SAS is a very suitable tool. SAS analyzes data using both the t-test and the ANOVA test. The SAS software uses a t-test that is of the Least Turkey B kind. The LSD is used as an ANOVA test confirming tool. The Kolo-Creek's soils, surface water, and ground water were all examined using the SAS.

The SAS determined the following for surface water, ground water, and soils: (i) whether there was a substantial difference in the mean value of a certain geochemical parameter along the measurement stations, or not (S1–S10) (ii) The seasonal fluctuations in the geochemical parameter mean values. The variance (F) and probability (Pr) of the geochemical parameters are found using the Anova test.

In general, there is a considerable difference in the mean value of the geochemical parameter under discussion when the Pr is smaller than 0.05, we accept the null hypothesis and reject the alternative hypothesis. On the other hand, we accept the alternative and reject the null hypothesis when the Pr is higher than 0.05. Using Diagram's program, the Wilcox diagrams were plotted. The statistical software suite for the social sciences (SPSS) version 17.0 was used to calculate principal components analysis (PCA), Pearson's correlation coefficients, and hierarchical cluster analysis (HCA). The RockWare Aq.QA model 1.1.1[1.1.5.1] was utilized to generate hydro-geochemical evolution charts. The Variogram and geographic distribution of the parameters were created using SURFER 15 software.

### **3.7 Geochemical Models**

#### **3.7.1 Pollution Index**

The concentrations of the primary constituent cations and anions in milligrams per liter (mg/l) were converted to milli-equivalents per liter (meq/l) in order to assess the level of contamination, see equation 3.0 below;

$$\text{Concentrations}(\text{meq/l}) = \frac{\text{Concentrations}(\text{mg/l})}{\text{Equivalent mass}} \text{ (Todd, 1980) ..... (3.0)}$$

Ajayi & Okeke (2024) mentioned that “by evaluating the amounts of pH, total dissolved solids (TDS), total hardness, sulfate, and chloride in milligrams per liter, the pollution index (PI) of the water samples was determined”. This was achieved by applying the subsequent method: “The total dissolved solids (TDS), pH, total alkalinity, total hardness, sulfate, and chloride were taken into account while calculating the pollution

index (PI) of the water samples from Kolo Creek” (Horton, 1965; Ajayi & Okeke, 2024). Equation (3.1) was used to determine the PI.

$$PI = \sqrt{\frac{\left(\frac{\max C_{ij}}{L_{ij}}\right)^2}{2} + \frac{\left(\frac{\text{mean} C_{ij}}{L_{ij}}\right)^2}{2}} \dots\dots\dots (3.1)$$

where

C<sub>i</sub> =Concentration of chemical parameter

L<sub>ij</sub> = WHO permissible levels

The relative pollution contribution of each item is indicated by the value of (C<sub>ij</sub>/L<sub>ij</sub>). The crucial value is defined as a value of 1.0. Consequently, any number greater than one for (C<sub>ij</sub>/L<sub>ij</sub>) indicates that the water needs to be treated before being used for a particular purpose.

### 3.5.2 Ratio of Sodium Adsorption

The concentrations in meq/l were utilized to compute the sodium adsorptive ratio (SAR) and to create Piper trilinear, Schooler, Durov, and stiff diagrams. Equation (3.2) was used to calculate the SAR (Wilcox, 1955). Additional equations for calculating water quality indices are shown in Table 3.5.

$$SAR = \frac{Na^+}{\sqrt{\frac{Ca^{2+}+Mg^{2+}}{2}}} \dots\dots\dots (3.2)$$

Table 3.5: Formulas utilized in the computation of water quality indices.

Water Quality Indices	Equations	Units	Equation No	References
Sodium Adsorption ratio	$SAR = \frac{Na^+}{\sqrt{\frac{Ca^{2+} + Mg^{2+}}{2}}}$	meq/L	3.3	(Sherrard <i>et al.</i> , 1987)
Percentage sodium (%Na)	$\%Na = \left( \frac{Na^+ + K^+}{Ca^{2+} + Mg^{2+} + Na^+ + K^+} \right) * 100$	%	3.4	Kacmaz and Nakoman (2010)
Magnesium Hazard	$Mg = \left( \frac{Mg^+}{Ca^{2+} + Mg^{2+}} \right) * 100$	%	3.6	(Szabolcs, 1964)
Kelly ratio	$KR = \frac{Na^+}{Ca^{2+} + Mg^{2+}}$	meq/L	3.6	(Kelley, 1963)
Soluble Sodium Percentage	$SSP = \left( \frac{Na^+ + K^+ + 100}{Ca^{2+} + Mg^{2+} + Na^+ + K^+} \right)$	%	3.7	(Richards, 1954)

### 3.7.3 Groundwater pollution index (PIG)

The PIG has been a technique in evaluating the drinking water quality of groundwater. Five phases are taken into consideration when using the PIG, according to (Akakuru *et al.*, 2022). Step I is the estimation of the relative weight (Rw), which is based on a scale of 1 to 5 that represents the importance of each factor in the evaluation of water quality in relation to human health (Table 3.6). In step II, each groundwater quality variable's weight parameter (Wp) is determined with the goal of determining how much each variable contributes overall to the groundwater quality status (Eq. 3.8). The assessment of the status of concentration (Sc) is done in Step III. This was achieved by dividing the water variable content (C) in each sample by the corresponding quality standard limit (Ds) (Eq. 3.9). The PIG was assessed using the (WHO, 2017) criteria in this work. Step IV: multiplies the weight parameter (Wp) by the concentration status (Sc) to determine the overall quality of groundwater (Ow) (Eq. 3.10). The whole Ow values for each sample are added together in Step V (Eq. 3.11)

$$\rho = \frac{Rw}{\sum Rw} \dots\dots\dots (3.8)$$

$$Sc = \frac{C}{Dc} \dots\dots\dots (3.9)$$

$$O_w = w_p * si \dots\dots\dots (3.10)$$

$$\text{Where, } PIG = \sum O_w \dots\dots\dots (3.11)$$

Table 3.6: PIG Assessment Components

Parameters	Rw	Wp	Summation	WHO(2017)
PH	3	0.076923	39	8.8
EC	3	0.076923	39	1400
TDS	3	0.076923	39	100
HC03	3	0.076923	39	500
N03	5	0.128205	39	50
S04	5	0.128205	39	400
Cl	4	0.102564	39	400
Na	4	0.102564	39	200
Ca	1	0.025641	39	200
K	2	0.051282	39	70
Mg	2	0.051282	39	150
Fe	4	0.102564	39	0.1
Summation	39			

### 3.7.4 Geo-accumulation

Numerous researches have made extensive use of these indicator (Chinemelu & Okeke, 2019), the geo-accumulation Index (Igeo) was proposed by (Muller, 1969). Using this technique, the concentration of heavy metals in a system is compared to levels that existed before industrialization. The method is frequently used to evaluate soil pollution with heavy metals. The geo-accumulation index was computed as follows, see equation 3.12:

$$I_{geo} = \log_2 (C_n / 1.5B_n) \dots\dots\dots (3.12)$$

B<sub>n</sub> is the element's geochemical background value in the soil, and C<sub>n</sub> is the element's measured concentration at a specific location (Chinemelu & Okeke, 2019). In order to minimize the potential consequences of potentially variable background values resulting from varying lithology, the constant 1.5 was utilized in the Igeo equation. Based on their

values, the geo-accumulation index has been split into seven enrichment classes, which are as follows:

**Table 3.7 Classification of Geo-accumulation Index** (Muller, 1969)

Index class	Igeo value	Level of contamination Classification
0	$I_{geo} < 0$	Uncontaminated
1	$0 < I_{geo} < 1$	Uncontaminated to Moderately contaminated
2	$1 < I_{geo} < 2$	Moderately contaminated
3	$2 < I_{geo} < 3$	Moderately to Heavily(Strongly) contaminated
4	$3 < I_{geo} < 4$	Heavily(Strongly) contaminated
5	$4 < I_{geo} < 5$	Heavily(Strongly) to extremely contaminated
6	$I_{geo} > 5$	Extremely Contaminated

### 3.7.5 Contamination Factor

The degree of heavy metal contamination in soils is evaluated using the contamination factor in respect to background concentrations. By dividing the concentration of each metal in the soil or soils by the background value, the CF was computed as shown in equation 3.13 below:

$$CF = C_s / C_n \dots\dots\dots(3.13)$$

Where  $C_s$  and  $C_n$  stand for the element concentration in the sample and the background concentration, respectively, and CF stands for the contamination factor of the element of interest. In this investigation, the WHO averages were utilized. Four categories are used: No or low contamination ( $CF < 1$ ), moderate contamination ( $CF < 3$ ), significant contamination ( $CF < 6$ ), and very high contamination ( $CF \leq CF, 6$ ).

### 3.7.6 Pollution load index

The PLI was determined by equation 3.14 (Hakanson, 1980).

$$PLI = \sqrt[n]{CF_1 * CF_2 * CF_3 * CF_4 * \dots * CF_n} \dots\dots\dots (3.14)$$

CF stands for contamination factor, and n for element number.

### 3.7.7 Water quality index (WQI)

The WQI was determined using the weighted arithmetic index equation. Each parameter's satisfied score scale (qi) was calculated by dividing the groundwater pattern's pattern attention (Ci) by the corresponding style (Si). Next, the outcome is multiplied by 100 (Akakuru *et al.*, 2022; Akakuru & Akudinobi, 2018; Gopinath *et al.*, 2019).

$$q_i = \frac{C_i}{S_i} * 100 \quad \dots\dots\dots (3.15)$$

The relative weight (Wi) was obtained by comparing the value to the WHO standard (Si) of the comparison boundary.

$$W_i = \frac{1}{S_i} \quad \dots\dots\dots (3.16)$$

$$WQI = \sum q_i w_i \quad \dots\dots\dots (3.17)$$

where wi is the unit ith parameter's weight and qi is the quality ith parameter.

### 3.8 Human health risk assessment (HHRA)

It deals with the potential harm to a population's health that can result from exposure to PAHs. It is separated between risk assessments that are carcinogenic and those that are not; the USEPA carried out the former. The following procedures, which were adopted from (Okafor, Omokpariola, Igbokwe, Theodore and Chukwu, 2022) were used to determine the HHRA for the 10 water samples (surface and subsurface) that were analyzed. The equations utilized were Chronic Daily Intake by Dermal (CDI<sub>der</sub>, 18) and Chronic Daily Intake by Ingestion (CDI<sub>ing</sub>, equation 3.18).

$$CDI_{der} = \frac{CS * SA * AF * |ABS| * ETEF * ED * CF}{BW * AT} \quad \dots\dots\dots (3.18)$$

$$CDI_{ing} = \frac{CS * IR * EF * ED * CF}{BW * AT} \quad \dots\dots\dots (3.19)$$

where: “AF is water adherence (adults and children: 0.2 mgcm<sup>-2</sup>), CS is concentration of the constituent of interest, ET is exposure time (adult during bathing, cooking, washing, and other domestic activities: 3 h/event, children during bathing, playing, and

other domestic activities, 2 h/event), and ABS is the fraction of the constituent absorbed through the skin (0.13)” (Okafor *et al.*, 2022). “The data provided by Okafor *et al.* (2022) includes exposure frequency (EF) of 350 days, exposure duration (ED) of 48.9 years and 6 years for adults and children, conversion factor (CF) of 1.00E-06, body weight (BW) of 70 kg and 15 kg for adults and children, average time (AT) of  $70 \times 365$  for carcinogens, and exposed skin area in cm<sup>2</sup> (SA) (Okafor *et al.*, 2022).

$$\text{Risk}_{\text{total}} = \text{Risk}_{\text{der}} + \text{Risk}_{\text{ing}} = (\text{CDI}_{\text{der}} + \text{CDI}_{\text{ing}}) \times \text{CSF} \quad \dots\dots\dots(3.20)$$

Where: Risk is the very small possibility that a person will develop cancer over their lifetime. CSF stands for cancer slope factor, expressed in mg/kg/day. Equation 20 offers the risk evaluation that is not carcinogenic:

$$\text{HI} = \text{HQ}_{\text{der}} + \text{HQ}_{\text{ing}} = \left( \frac{\text{CDI}_{\text{der}}}{\text{RfD}} + \frac{\text{CDI}_{\text{ing}}}{\text{RfD}} \right) \quad \dots\dots\dots(3.21)$$

where the hazard index, or HI, indicates the probability of suffering a health consequence. HQ stands for Hazard Quotient. The definition of a reference dose is mg/kg/day.

## **CHAPTER FOUR**

### **RESULTS AND DISCUSSION**

#### **4.1 RESULTS**

Tables 4.1, 4.2, 4.3, and 4.4 present the findings of the physical and geochemical properties of soil, ground water, surface water, and their geotechnical qualities.

**Table 4.1a:** Kolo Creek Surface Water's Physicochemical Characteristics (Wet Season)

Sampling Station	Units	S1	S2	S3	S4	S5	S6	S7	S8	S9	S10	Total Mean	Minimum	Maximum	WHO 2017
Coordinates	Latitude	5.0648	4.9845	4.9897	4.9751	4.9572	4.9344	4.9189	4.916	4.9213	4.8523				
	Longitude	6.4428	6.43	6.4672	6.4725	6.4358	6.4161	6.3988	6.4169	6.4499	6.3704				
TPH	mg/L	542.33	460.67	447.33	316.67	394.33	468.17	296.33	113.67	120.17	43.27	320.29	43.27	542.33	0.3
PAH	mg/L	34.40	58.00	35.00	30.40	0.00	56.00	0.00	0.00	0.00	0.00	21.38	0.00	58.00	0.2
Betex	mg/L	37.00	36.67	28.00	36.00	44.67	19.67	51.33	47.33	54.67	0.00	35.53	0.00	54.67	1.5
pH	N/A	5.87	5.70	5.84	5.81	5.76	5.80	5.72	5.78	5.76	6.77	5.88	5.70	6.77	8.2– 8.8
Total Hardness	mg/l	36.5	33.5	34.3	33.92	26.5	23.36	35	35.92	35.5	19.5	31.85	19.50	36.50	400
TDS	mg/l	144.45	112.2	93.2	86.5	96.7	94.5	84.5	86.4	80.7	66.9	94.605	66.90	144.45	1500
Turbidity	NTU	22.45	22.7	24.7	25.5	22.2	23.4	26.22	29	27.6	14.3	23.807	14.30	29.00	10
Conductivity	µS/cm	15.00	13.00	13.67	13.61	13.00	16.30	13.33	13.40	11.33	12.17	13.36	11.33	16.30	1400
Sodium	mg/l	9.40	12.13	13.60	15.80	19.40	16.13	15.27	14.47	14.90	23.63	15.47	9.40	23.63	200
Calcium	mg/l	11.33	7.13	11.63	11.53	11.57	10.67	10.97	12.27	10.00	8.67	10.58	7.13	12.27	200
Magnesium	mg/l	8.63	11.07	9.93	10.40	9.97	10.53	10.37	9.67	10.07	7.63	9.83	7.63	11.07	150
Potassium	mg/l	6.47	6.03	5.58	5.92	6.31	6.12	6.17	5.94	6.26	5.87	6.07	5.58	6.47	50-70
Bicarbonate	mg/l	9.93	9.07	8.77	8.87	7.83	7.80	8.73	9.10	9.10	6.13	8.53	6.13	9.93	500
Chloride	mg/l	9.65	9.62	9.36	8.69	10.10	9.50	10.00	9.45	10.96	7.15	9.45	7.15	10.96	400
Sulphate	mg/l	54.43	51.33	53.07	50.90	42.87	43.33	44.80	39.63	43.30	31.26	45.49	31.26	54.43	400
Nitrate	mg/l	6.87	8.17	7.27	7.83	7.80	8.00	8.00	7.60	7.60	6.77	7.59	6.77	8.17	50
Iron	mg/l	1.77	1.97	1.47	0.80	3.73	1.47	2.60	2.00	1.23	0.60	1.76	0.60	3.73	<0.1
Lead	mg/l	0.04	0.02	0.04	0.03	0.05	0.04	0.05	0.03	0.04	0.00	0.03	0.00	0.05	0.01
Copper	mg/l	0.72	0.68	0.64	0.75	0.89	0.73	0.59	0.70	0.65	0.02	0.63	0.02	0.89	2
Cadmium	mg/l	0.33	0.29	0.26	0.34	0.30	0.32	0.30	0.29	0.29	0.00	0.27	0.00	0.34	0.003
Zinc	mg/l	2.80	3.53	3.07	3.10	3.57	2.80	2.93	3.10	2.37	2.97	3.02	2.37	3.57	5
Mercury	mg/l	0.11	0.23	0.19	0.20	0.24	0.18	0.20	0.27	0.22	0.18	0.20	0.11	0.27	0.006
Aluminium	mg/l	0.00	0.01	0.00	0.00	0.01	0.00	0.01	0.01	0.00	0.00	0.01	0.00	0.01	0.10max

**Table 4.1b: Kolo Creek Surface Water's Physicochemical Characteristics (Dry Season)**

Sampling Station	Units	S1	S2	S3	S4	S5	S6	S7	S8	S9	S10	Total Mean	Minimum	Maximum	WHO 4th edition
Coordinates	Latitude	5.0648	4.9845	4.9897	4.9751	4.9572	4.9344	4.9189	4.916	4.9213	4.8523				
	Longitude	6.4428	6.43	6.4672	6.4725	6.4358	6.4161	6.3988	6.4169	6.4499	6.3704				
TPH	mg/L	395.00	328.67	358.00	307.17	292.33	362.83	269.33	153.00	123.03	12.00	260.14	12.00	395.00	0.3
PAH	mg/L	66.00	46.00	64.00	84.23	0.00	35.00	33.83	0.00	0.00	0.00	32.91	0.00	84.23	0.2
Betex	mg/L	25.73	19.27	12.97	30.07	22.23	24.93	22.90	16.70	11.30	3.33	18.94	3.33	30.07	1.5
pH	N/A	5.99	5.88	5.96	5.88	5.88	5.87	5.82	5.83	5.82	6.48	5.94	5.82	6.48	8.2– 8.8
Total Hardness	mg/l	37.37	33.75	37.37	34.93	26.5	23.78	35.82	35.92	33.55	19.5	31.85	19.50	37.37	400
TDS	mg/l	147.42	114.18	92.43	86.72	98.88	92.48	86.83	85.15	83	68.6	95.57	68.60	147.42	1500
Turbidity	NTU	25.17	24.67	26.27	24.9	23.92	24.9	27.62	29.43	31.62	15.4	26.94	15.40	31.62	10
Elet. Conductivity	µS/cm	9.33	16.33	26.00	20.00	16.00	15.33	17.33	17.67	18.67	14.00	17.07	9.33	26.00	1400
Sodium	mg/l	8.67	8.70	8.27	8.13	8.37	8.23	8.53	7.90	8.43	6.90	8.21	6.90	8.70	200
Calcium	mg/l	11.77	10.90	11.67	11.50	11.80	11.03	11.10	12.03	10.43	8.60	11.08	8.60	12.03	200
Magnesium	mg/l	9.23	11.13	10.07	10.90	10.53	10.63	10.60	10.17	10.17	7.97	10.14	7.97	11.13	150
Potassium	mg/l	6.57	5.98	6.10	5.88	6.48	6.37	6.30	6.06	6.27	5.72	6.17	5.72	6.57	50-70
Bicarbonate	mg/l	6.50	8.97	9.23	9.47	8.27	8.27	9.17	9.40	9.67	6.40	8.53	6.40	9.67	500
Chloride	mg/l	16.43	16.30	16.13	15.77	16.93	16.53	16.70	16.33	17.40	8.33	15.69	8.33	17.40	400
Sulphate	mg/l	76.43	70.33	73.33	73.50	64.57	65.33	66.33	63.17	66.23	52.63	67.19	52.63	76.43	400
Nitrate	mg/l	3.57	3.53	3.17	3.13	3.37	3.27	3.50	3.63	3.13	1.53	3.18	1.53	3.63	50
Iron	mg/l	1.00	0.70	0.93	0.90	1.40	0.90	1.27	0.70	0.97	0.33	0.91	0.33	1.40	<0.1
Lead	mg/l	0.03	0.03	0.03	0.03	0.05	0.04	0.04	0.03	0.03	0.00	0.03	0.00	0.05	0.01
Copper	mg/l	0.73	0.68	0.67	0.71	0.82	0.74	0.65	0.77	0.64	0.00	0.64	0.00	0.82	2
Cadmium	mg/l	0.35	0.31	0.31	0.37	0.32	0.37	0.32	0.30	0.28	0.00	0.29	0.00	0.37	0.003
Zinc	mg/l	2.24	3.19	1.98	2.66	2.63	2.21	2.37	2.30	2.47	0.40	2.24	0.40	3.19	5
Mercury	mg/l	0.17	0.22	0.23	0.18	0.24	0.21	0.16	0.15	0.21	0.00	0.18	0.00	0.24	0.006
Aluminium	mg/l	0.00	0.00	0.00	0.00	0.00	0.00	0.00	0.00	0.00	0.00	0.00	0.00	0.00	0.10max

**Table 4.2a: Kolo Creek Groundwater's Physicochemical Characteristics (Wet Season)**

Station	Units	S1	S2	S3	S4	S5	S6	S7	S8	S9	S10	Total Mean	Minimum	Maximum	WHO 2017
Coordinates	Latitude	5.0648	4.9845	4.9897	4.9751	4.9572	4.9344	4.9189	4.916	4.9213	4.8523				
Parameters	Longitude	6.4428	6.43	6.4672	6.4725	6.4358	6.4161	6.3988	6.4169	6.4499	6.3704				
TPH	mg/L	135.67	156.80	126.33	119.33	120.67	108.67	131.33	82.67	76.00	15.00	107.25	15.00	156.80	0.3
PAH	mg/L	3.20	3.23	2.50	0.50	0.40	0.01	0.01	0.00	0.00	0.00	0.99	0.00	3.23	0.2
Betex	mg/L	2.92	3.67	3.28	2.05	2.00	2.10	2.72	1.84	1.26	0.26	2.21	0.26	3.67	1.5
PH	N/A	6.27	6.57	6.53	6.50	6.27	6.77	6.40	6.77	6.27	7.20	6.55	6.27	7.20	6.5– 8.5
Temperature	OC	26.07	25.70	26.23	25.73	25.60	26.17	26.60	26.07	26.47	27.30	26.19	25.60	27.30	28
Conductivity	µS/cm	94.00	177.43	131.83	137.33	129.63	169.43	145.23	150.37	68.53	31.17	123.50	31.17	177.43	500
Total Hardness	mg/l	60.00	100.67	90.67	76.67	82.33	86.67	97.67	84.67	89.00	30.67	79.90	30.67	100.67	500
TDS	mg/l	101.03	98.43	79.00	66.73	160.33	68.37	175.03	127.00	88.23	46.27	101.04	46.27	175.03	500
Sodium	mg/l	79.77	76.43	66.80	73.67	51.17	70.20	58.97	78.80	73.90	57.70	68.74	51.17	79.77	200
Calcium	mg/l	24.37	16.83	16.10	16.00	16.40	23.87	25.30	24.67	24.97	10.70	19.92	10.70	25.30	75
Magnesium	mg/l	4.80	3.77	2.67	2.07	1.32	1.43	6.37	1.57	0.87	0.82	2.57	0.82	6.37	50
Potassium	mg/l	22.17	21.00	21.18	19.05	17.43	15.90	19.17	21.53	22.47	16.00	19.59	15.90	22.47	200
Bicarbonate	mg/l	46.00	39.00	16.13	16.73	19.73	21.43	16.67	11.40	10.75	10.90	20.88	10.75	46.00	200
Chloride	mg/l	41.83	34.40	18.57	20.50	30.30	15.03	30.23	43.40	35.50	15.17	28.49	15.03	43.40	250
Sulphate	mg/l	106.03	95.10	113.90	104.33	85.83	94.73	108.03	114.70	104.57	102.33	102.96	85.83	114.70	250
Nitrate	mg/l	3.73	3.83	3.37	3.23	2.40	2.93	2.13	2.20	2.43	1.23	2.75	1.23	3.83	50
Iron	mg/l	50.23	53.17	45.33	28.11	36.24	29.55	30.14	25.88	38.26	27.06	36.40	25.88	53.17	0.3
Lead	mg/l	0.02	0.01	0.01	0.01	0.01	0.01	0.01	0.01	0.01	0.00	0.01	0.00	0.02	0.01
Copper	mg/l	0.73	0.40	0.33	0.80	0.23	0.57	0.07	0.43	0.63	0.10	0.43	0.07	0.80	2
Cadmium	mg/l	0.00	0.00	0.00	0.00	0.00	0.00	0.00	0.00	0.00	0.00	0.00	0.00	0.00	0.05
Chromium	mg/l	0.00	0.00	0.00	0.00	0.00	0.00	0.00	0.00	0.00	0.00	0.00	0.00	0.00	0.05
Zinc	mg/l	1.17	0.79	1.01	1.30	1.15	0.93	0.88	1.18	1.11	0.20	0.97	0.20	1.30	3

**Table 4.2b: Kolo Creek Groundwater's Physicochemical Characteristics (Dry Season)**

Station	Units	S1	S2	S3	S4	S5	S6	S7	S8	S9	S10	Total Mean	Minimum	Maximum	WHO 2017
Coordinates	Latitude	5.0648	4.9845	4.9897	4.9751	4.9572	4.9344	4.9189	4.916	4.9213	4.8523				
Parameters	Longitude	6.4428	6.43	6.4672	6.4725	6.4358	6.4161	6.3988	6.4169	6.4499	6.3704				
TPH	mg/L	137.67	128.00	137.67	113.67	129.67	107.00	125.67	93.00	73.33	15.33	106.10	15.33	137.67	0.3
PAH	mg/L	4.03	4.27	2.37	1.57	1.00	0.01	0.00	0.00	0.00	0.00	1.33	0.00	4.27	0.2
Betex	mg/L	3.42	3.83	3.42	2.42	2.00	1.75	1.75	1.59	1.34	0.00	2.15	0.00	3.83	1.5
PH	N/A	6.03	6.40	6.33	6.23	6.00	6.53	6.40	6.50	6.60	7.20	6.42	6.00	7.20	6.5– 8.5
Temperature	0C	26.57	25.90	26.50	26.27	26.07	25.93	27.43	26.17	26.63	27.43	26.49	25.90	27.43	28
Conductivity	µS/cm	90.00	155.93	132.17	117.00	186.37	77.00	150.57	156.03	124.53	94.40	128.40	77.00	186.37	500
Total Hardness	mg/l	60.57	118.40	107.73	101.33	115.00	56.00	117.93	83.20	86.27	78.83	92.53	56.00	118.40	500
TDS	mg/l	112.97	117.70	113.80	112.87	110.87	117.67	119.07	113.67	119.00	117.47	115.51	110.87	119.07	500
Sodium	mg/l	78.63	79.40	71.30	41.03	87.27	34.73	80.57	64.87	59.80	47.00	64.46	34.73	87.27	200
Calcium	mg/l	28.33	21.57	19.97	22.63	24.07	25.57	20.20	18.80	18.00	16.83	21.60	16.83	28.33	75
Magnisium	mg/l	5.13	4.90	2.66	2.90	2.62	3.80	3.67	3.03	3.03	2.30	3.40	2.30	5.13	50
Potassium	mg/l	19.77	16.87	19.64	15.03	15.88	16.53	11.47	19.73	16.57	17.43	16.89	11.47	19.77	200
Bicarbonate	mg/l	45.70	44.70	44.13	44.40	45.87	33.93	34.43	33.87	32.33	31.57	39.09	31.57	45.87	200
Chloride	mg/l	35.03	37.50	32.40	35.63	33.20	44.40	34.60	44.33	33.67	33.90	36.47	32.40	44.40	250
Sulphate	mg/l	156.57	141.85	115.27	105.40	115.00	130.33	123.73	142.63	137.87	111.00	127.97	105.40	156.57	250
Nitrate	mg/l	4.57	4.53	2.00	2.00	2.47	2.67	2.14	1.50	1.51	1.24	2.46	1.24	4.57	50
Iron	mg/l	53.46	45.17	38.75	41.67	41.52	36.24	33.27	24.87	33.47	29.04	37.75	24.87	53.46	0.3
Lead	mg/l	0.01	0.01	0.00	0.01	0.01	0.03	0.01	0.00	0.01	0.00	0.01	0.00	0.03	0.01
Copper	mg/l	0.60	0.33	0.53	0.67	0.40	0.60	0.10	0.30	0.57	0.17	0.43	0.10	0.67	2
Cadmium	mg/l	0.00	0.00	0.00	0.00	0.00	0.00	0.00	0.00	0.00	0.00	0.00	0.00	0.00	0.05
Chromium	mg/l	0.00	0.00	0.00	0.00	0.00	0.00	0.00	0.00	0.00	0.00	0.00	0.00	0.00	0.05
Zinc	mg/l	1.22	0.76	0.99	1.40	1.05	0.90	0.92	1.01	1.08	0.20	0.95	0.20	1.40	3

**Table 4.3a** Kolo Creek Soil Physicochemical Characteristics (Wet Season)

Sampling Station	Units	S1	S2	S3	S4	S5	S6	S7	S8	S9	S10	Total Mean	Minimum	Maximum	FME	
															Standard	
Coordinates	Latitude	5.0648	4.9845	4.9897	4.9751	4.9572	4.9344	4.9189	4.916	4.9213	4.8523					
	Longitude	6.4428	6.43	6.4672	6.4725	6.4358	6.4161	6.3988	6.4169	6.4499	6.3704					
TPH	mg/kg	195.00	128.67	158.00	107.17	192.33	162.83	169.33	153.00	123.03	12.00	140.14	12.00	195.00	50	
PAH	mg/kg	57.77	43.53	47.23	34.23	0.00	42.83	33.83	0.00	0.00	0.00	25.94	0.00	57.77	1	
Betex	mg/kg	12.67	18.63	10.40	10.57	21.33	24.93	12.27	10.33	12.73	3.33	13.72	3.33	24.93	0.2	
PH	N/A	5.99	5.88	5.96	5.88	5.88	5.87	5.82	5.83	5.82	6.48	5.94	5.82	6.48	6.5	
Conductivity	µS/cm	59.33	56.33	46.00	50.00	56.00	45.33	47.33	57.67	48.67	34.00	50.07	34.00	59.33	100	
Sodium	mg/kg	48.67	38.70	38.27	38.13	48.37	48.23	38.53	47.90	48.43	46.90	44.21	38.13	48.67	NS	
Calcium	mg/kg	11.77	10.90	11.67	11.50	11.80	11.03	11.10	12.03	10.43	8.60	11.08	8.60	12.03	200	
Magnesium	mg/kg	9.23	11.13	10.07	10.90	10.53	10.63	10.60	10.17	10.17	7.97	10.14	7.97	11.13	100	
Potassium	mg/kg	6.57	5.98	6.10	5.88	6.48	6.37	6.30	6.06	6.27	5.72	6.17	5.72	6.57	>100	
Bicarbonate	mg/kg	26.50	28.97	29.23	29.47	38.27	38.27	29.17	29.40	29.67	26.40	30.53	26.40	38.27	30	
Chloride	mg/kg	16.43	16.30	16.13	15.77	16.93	16.53	16.70	16.33	17.40	18.33	16.69	15.77	18.33	250	
Sulphate	mg/kg	76.43	70.33	73.33	73.50	64.57	65.33	66.33	63.17	66.23	52.63	67.19	52.63	76.43	100	
Nitrate	mg/kg	13.57	13.53	13.17	13.13	23.37	23.27	13.50	13.63	23.13	21.53	17.18	13.13	23.37	205	
Iron	mg/kg	214.00	210.70	212.93	213.90	217.40	213.90	211.27	219.70	214.97	26.93	195.57	26.93	219.70	1	
Lead	mg/kg	0.03	0.03	0.03	0.03	0.05	0.04	0.04	0.03	0.03	0.00	0.03	0.00	0.05	0.05	
Copper	mg/kg	0.73	0.68	0.67	0.71	0.82	0.74	0.65	0.77	0.64	0.00	0.64	0.00	0.82	2	
Cadmium	mg/kg	0.35	0.31	0.31	0.37	0.32	0.37	0.32	0.30	0.28	0.00	0.29	0.00	0.37	0.1	
Zinc	mg/kg	2.24	3.19	1.98	2.66	2.63	2.21	2.37	2.30	2.47	0.40	2.24	0.40	3.19	5	
Mercury	mg/kg	0.17	0.22	0.23	0.18	0.24	0.21	0.16	0.15	0.21	0.00	0.18	0.00	0.24	0.001	
Aluminum	mg/kg	0.00	0.00	0.00	0.00	0.00	0.00	0.00	0.00	0.00	0.00	0.00	0.00	0.00	<0.01	

**Table 4.3b:** Kolo Creek Soil Physicochemical Characteristics (Dry Season)

Sampling Station	Units	S1	S2	S3	S4	S5	S6	S7	S8	S9	S10	Total Mean	Minimum	Maximum	FME	
															Standard	
Coordinates	Latitude	5.0648	4.9845	4.9897	4.9751	4.9572	4.9344	4.9189	4.916	4.9213	4.8523					
	Longitude	6.4428	6.43	6.4672	6.4725	6.4358	6.4161	6.3988	6.4169	6.4499	6.3704					
TPH	mg/kg	142.33	160.67	147.33	116.67	114.33	128.17	136.33	113.67	120.17	43.27	122.29	43.27	160.67	50	
PAH	mg/kg	40.27	44.23	46.93	30.40	0.00	25.67	23.00	0.00	0.00	0.00	21.05	0.00	46.93	1	
Betex	mg/kg	20.00	21.00	18.67	14.33	14.67	19.67	21.33	17.00	16.67	0.00	16.33	0.00	21.33	0.2	
pH	N/A	5.87	5.70	5.84	5.81	5.76	5.80	5.72	5.78	5.76	6.77	5.88	5.70	6.77	6.5	
Conductivity	µS/cm	74.50	52.00	63.67	63.61	43.00	56.33	44.33	53.00	51.33	52.17	55.39	43.00	74.50	100	
Sodium	mg/kg	49.40	12.13	13.60	15.80	19.40	16.13	15.27	14.47	14.90	23.63	19.47	12.13	49.40	NS	
Calcium	mg/kg	11.33	7.13	11.63	11.53	11.57	10.67	10.97	12.27	10.00	8.67	10.58	7.13	12.27	200	
Magnesium	mg/kg	8.63	11.07	9.93	10.40	9.97	10.53	10.37	9.67	10.07	7.63	9.83	7.63	11.07	100	
Potassium	mg/kg	6.47	6.03	5.58	5.92	6.31	6.12	6.17	5.94	6.26	5.87	6.07	5.58	6.47	>100	
Bicarbonate	mg/kg	29.93	29.07	28.77	28.87	27.83	37.80	38.73	29.10	19.10	26.13	29.53	19.10	38.73	30	
Chloride	mg/kg	19.65	17.62	16.36	18.69	13.10	15.50	21.00	17.45	14.96	17.15	17.15	13.10	21.00	250	
Sulphate	mg/kg	54.43	51.33	53.07	50.90	42.87	43.33	44.80	39.63	43.30	31.26	45.49	31.26	54.43	100	
Nitrate	mg/kg	16.87	18.17	17.27	17.83	17.80	18.00	18.00	17.60	17.60	16.77	17.59	16.77	18.17	205	
Iron	mg/kg	216.77	117.97	211.47	210.80	223.73	216.47	219.60	122.00	221.23	28.60	178.86	28.60	223.73	1	
Lead	mg/kg	0.04	0.02	0.04	0.03	0.05	0.04	0.05	0.03	0.04	0.00	0.03	0.00	0.05	0.05	
Copper	mg/kg	0.72	0.68	0.64	0.71	0.82	0.73	0.59	0.80	0.63	0.00	0.63	0.00	0.82	2	
Cadmium	mg/kg	0.33	0.29	0.26	0.34	0.30	0.32	0.30	0.29	0.29	0.00	0.27	0.00	0.34	0.1	
Zinc	mg/kg	2.80	3.53	3.07	3.10	3.57	2.80	2.93	3.10	2.37	2.97	3.02	2.37	3.57	5	
Mercury	mg/kg	0.11	0.23	0.19	0.20	0.24	0.18	0.20	0.27	0.22	0.18	0.20	0.11	0.27	0.001	
Aluminium	mg/kg	0.00	0.00	0.00	0.00	0.00	0.00	0.00	0.00	0.00	0.00	0.00	0.00	0.00	<0.01	

**Table 4.4a: GEOTECHNICAL PARAMETERS**

SUMMARY RESULTS OF GEOTECHNICAL PARAMETER								
SITE NAME	SAMPLE ID	Moisture Content	Moisture Content	PERMEABILITY K x 10 <sup>-4</sup> (m/sec)	POROSITY %	ATTERBERG LIMITS (%)		
		Dry Season	Wet Season			LL	PL	PI
OKARKI	S1	25.5	32.5	1.4	1.29	25	17	8
IKODU	S2	25.2	30	1.3	1.34	28	23	5
IGOVIA	S3	24.9	28.2	1.3	1.31	24	18	6
OTEGWE	S4	25	27.5	1.3	1.28	24	15	9
OTUASEGA	S5	14.4	23.7	1.4	1.37	35	27	8
ORUMA	S6	17.8	23	1.3	1.27	30	21	9
OBEDUM	S7	15.1	23.9	1.4	1.34	32	25	7
ODAN	S8	12	21.1	1.3	1.29	36	29	7
IMIRINGI	S9	13	24.2	1.2	1.28	33	26	7
MBIAMA	S10(CRL)	14.4	22.8	2.2	1.86	28	17	11
Average		18.73	25.69	1.41	1.363	29.5	21.8	7.7
Maximum		25.5	32.5	2.2	1.86	36	29	11
Minimum		12	21.1	1.2	1.27	24	15	5

Table 4.4b Factor loadings of various parameters derived from the principal component extraction method for surface water.

Parameters	Communalities	Component				
		1	2	3	4	5
Copper	.875	<b>.955</b>				
Chromium	.707	<b>.950</b>				
pH	.872	<b>-.924</b>				
Lead	.549	<b>.852</b>				
Magnisium	.813	<b>.765</b>			.363	
TPH	.754	<b>.674</b>		<b>.562</b>		
Bicarbonate	.774	<b>.653</b>			.372	-.307
Betex	.876	<b>.644</b>	<b>.560</b>			-.350
Mercury	.927	<b>.618</b>		-.421		.419
Calcium	.926	<b>.538</b>			-.355	
Sulphate	.953	.305	<b>-.907</b>			
Nitrate	.832		<b>.903</b>			
Sodium	.813		<b>.865</b>			.305
Chloride	.584	.368	<b>-.815</b>			
Aluminium	.935		<b>.692</b>			
Iron	.778	<b>.522</b>	<b>.663</b>			
E.Conductivity	.949		<b>-.622</b>	-.407	.337	
Zinc	.838	<b>.571</b>	<b>.574</b>			.372
DS	.764	<b>.496</b>		<b>.727</b>		
PAH	.865	.326	-.409	<b>.514</b>	<b>.496</b>	.331
Potassium	.892	<b>.475</b>			<b>-.658</b>	
Cadmium	.853			.427	.380	<b>-.625</b>
<b>Eigenvalues</b>		7.591	5.500	2.016	1.666	1.355
<b>Variance (%)</b>		34.506	25.002	9.165	7.573	6.160
<b>Cumulative var. (%)</b>		34.506	59.508	68.674	76.247	82.407

Bold values indicate significant contributor (loadings greater than 0.4 (+ or -))

**Table 4.5:** Surface water study's correlation matrix for the different parameters

	TPH	PAH	Betex	pH	Hardness	DS	Turbidity	E.C	Na	Ca	Mg	K	HC03	Cl	S04	N03	Fe	Pb	Cu	Cd	Cr	Zn	Hg	Al	
TPH	1	<b>.635**</b>	.297	<b>-.519*</b>	.266	<b>.715**</b>	.071	.058	-.075	.217	.402	.292	.257	.038	.231	.295	.395	<b>.536*</b>	<b>.613**</b>	.222	<b>.629**</b>	<b>.455*</b>	.197	.089	
PAH		1	-.076	-.185	.301	<b>.486*</b>	.030	.322	-.316	.049	.366	-.011	.133	.265	<b>.543*</b>	-.142	-.200	.001	.277	.225	<b>.451*</b>	.088	.034	-.230	
Betex			1	<b>.688**</b>	<b>.467*</b>	.214	.378	-.382	.254	.232	.348	.220	.405	-.256	-.299	<b>.641**</b>	<b>.681**</b>	<b>.610**</b>	<b>.540*</b>	.355	<b>.521*</b>	<b>.492*</b>	.437	<b>.601**</b>	
pH				1	<b>-.621**</b>	-.318	<b>-.775**</b>	-.114	.209	-.419	<b>-.798**</b>	-.322	<b>-.724**</b>	-.272	-.210	-.286	-.491*	<b>-.790**</b>	<b>-.887**</b>	-.272	<b>-.869**</b>	-.443	-.511*	-.339	
Hardness					1	.413	<b>.734**</b>	.193	-.323	.435	.392	.162	<b>.703**</b>	.329	.406	.070	.102	.363	<b>.545*</b>	.431	<b>.623**</b>	.247	.294	.095	
DS						1	.091	-.185	-.291	.211	.082	<b>.544*</b>	.110	.202	.386	.039	.185	.292	<b>.474*</b>	.158	<b>.499*</b>	.246	.038	-.003	
Turbidity							1	.301	-.348	<b>.556*</b>	<b>.627**</b>	.291	<b>.726**</b>	<b>.553*</b>	.385	-.044	.096	<b>.563**</b>	<b>.697**</b>	.177	<b>.727**</b>	.183	<b>.485*</b>	.054	
E.C								1	<b>.467*</b>	.259	.322	-.073	<b>.485*</b>	<b>.518*</b>	<b>.524*</b>	<b>-.483*</b>	-.257	.061	.165	.183	.225	-.214	.065	-.298	
Na									1	-.200	-.267	-.222	-.338	<b>-.718**</b>	<b>-.852**</b>	<b>.788**</b>	.426	-.051	-.199	-.019	-.321	<b>.547*</b>	.307	.388	
Ca										1	.235	.259	.324	.410	.349	-.120	.140	<b>.624**</b>	<b>.620**</b>	-	<b>.600**</b>	.113	.273	-.135	
Mg											1	.130	<b>.593**</b>	<b>.481*</b>	.390	.022	.179	<b>.578**</b>	<b>.729**</b>	.187	<b>.766**</b>	.405	<b>.574**</b>	.154	
K												1	.075	<b>.468*</b>	.295	-.116	.263	<b>.530*</b>	<b>.490*</b>	.067	<b>.498*</b>	.036	.195	-.015	
HC03													1	.304	.267	.086	.140	<b>.469*</b>	<b>.593**</b>	.275	<b>.630**</b>	.310	.336	.070	
Cl														1	<b>.877**</b>	-	<b>.739**</b>	-.305	.286	.429	-	<b>.509*</b>	-.202	.192	-.381
S04															1	<b>.777**</b>	-.408	.134	.347	.006	<b>.478*</b>	-.311	-.055	<b>-.460*</b>	
N03																1	<b>.614**</b>	.245	.170	.240	.072	<b>.699**</b>	.375	<b>.553*</b>	
Fe																	1	<b>.589**</b>	.435	.087	.277	<b>.577**</b>	.411	<b>.804**</b>	
Pb																		1	<b>.816**</b>	.153	<b>.773**</b>	.396	.474*	.187	
Cu																			1	.011	<b>.942**</b>	<b>.498*</b>	.590**	.173	
Cd																				1	.213	.122	-.190	.095	
Cr																					1	.395	<b>.513*</b>	.064	

\*\* Correlation is significant at the 0.01 level (2-tailed).

\* Correlation is significant at the 0.05 level (2-tailed).

Bold =Relationship

**Table 4.6a: Surface Water Pollution index (PI)**

Parameters	S1	S2	S3	S4	S5	S6	S7	S8	S9	S10
PH	0.65	0.69	0.67	0.71	0.72	0.73	0.73	0.73	0.72	0.78
TDS	0.10	0.08	0.06	0.06	0.07	0.06	0.06	0.06	0.06	0.05
HC03	0.05	0.04	0.05	0.05	0.06	0.03	0.05	0.04	0.03	0.02
S04	0.06	0.06	0.04	0.07	0.04	0.05	0.04	0.05	0.05	0.03
Cl-	0.08	0.07	0.10	0.10	0.09	0.10	0.08	0.06	0.08	0.02
<b>Average</b>	0.19	0.19	0.18	0.20	0.20	0.19	0.19	0.19	0.19	0.18
<b>Total</b>	0.94	0.94	0.92	0.99	0.98	0.97	0.96	0.93	0.94	0.90
<b>PI</b>	0.65	0.69	0.67	0.71	0.72	0.73	0.73	0.73	0.72	0.78

**Table 4.6b: CF and WQI (Surface water)**

	Contamination Factor								WQI
	Na	Ca	Mg	HC03	Cl	S04	N03	Fe	
S1	0.043	0.078	0.092	0.013	0.041	0.191	0.071	10	2839.7
S2	0.044	0.073	0.111	0.018	0.041	0.176	0.071	7	14251.5
S3	0.041	0.078	0.101	0.018	0.04	0.183	0.063	9.333	12224.7
S4	0.041	0.077	0.109	0.019	0.039	0.184	0.063	9	13147.6
S5	0.042	0.079	0.105	0.017	0.042	0.161	0.067	14	13101.1
S6	0.041	0.074	0.106	0.017	0.041	0.163	0.065	9	11437.3
S7	0.043	0.074	0.106	0.018	0.042	0.166	0.07	12.667	10499.4
S8	0.04	0.08	0.102	0.019	0.041	0.158	0.073	7	7848.6
S9	0.042	0.07	0.102	0.019	0.044	0.166	0.063	9.667	10559.3
S10	0.035	0.057	0.08	0.013	0.021	0.132	0.031	3.333	9164.2
Total mean	0.0412	0.074	0.1014	0.0171	0.0392	0.168	0.0637	9.1	

**Table 4.7: Values of SAR, KR, Na, MH and SSP (Surface Water)**

	SAR (meq/l)	KR (meq/l)	Na%	MH (%)	SSP
	1.17	2.349602	74.6	15.33865	0.5963094
	1.5	3.000378	78.4	18.50359	0.6469486
	1.58	3.150685	80.1	11.76904	0.6278251
	0.8	1.607259	68.7	11.34613	0.50288
	1.64	3.270456	79.4	9.806371	0.672161
	0.59	1.182881	63.6	12.92996	0.4307743
	1.69	3.375698	79.4	15.36313	0.6951395
	1.49	2.970992	79.5	13.89313	0.6094582
	1.42	2.843265	78.4	14.42155	0.6139763
	1.23	2.45662	77.1	12.02091	0.5624427
Mean	1.311	2.6207836	75.92	13.539246	0.5957915
STD	0.3668621	0.7291004	5.5161984	2.5092524	0.0794695

Table 4.8: Classification criteria for Surface water WQI

WQI Values	Water Quality Status	Sample No	Percentage (%)	No of Samples	Possible usage
<50	Excellent				Drinking, Irrigation and Industrial
50-100	Good				Drinking, Irrigation and Industrial
100-200	Poor				Irrigation and Industrial
200-300	Very Poor				Irrigation
>300	Unsuitable for drinking	S1-S10	100	10	Proper treatment required before usage

Table 4.9: SAR -Based Irrigation suitability Classification Criteria for Surface water

Sodium Hazard	Zone	Sample No	Sample %	Class of water
<10	Z1	S1-S10	100	Excellent
10-18	Z2			Good
18-26	Z3			Permissible
>26	Z4			Unsuitable

Table 4.10: %Na-Surface water quality Criteria for irrigation

Sodium Hazard	Zone	Sample No	Sample %	Class of water
<20	Z1			Excellent
20-40	Z2			Good
40-60	Z3			Permissible
60-80	Z4	S1-S10	100	Doubtful
>80	Z5			Unsuitable

Table 4.11: MH-Surface water Classification Criteria for irrigation

MH range	Zone	Sample No	Sample %	Class of water
<50	Z1	S1-S10	100	Safe
>50	Z2			Unsafe

Table 4.12: KR-Surface water Classification Criteria for irrigation

KR Range	Zone	Sample No	Sample %	Class of water
<1	Z1			Suitable
>1	Z2	S1-S10	100	Unsuitable

Table 4.13: SSP-Surface water Classification Criteria for irrigation

SSP Range	Zone	Sample No	Sample %	Class of water
<50	Z1	S1-S10	100	Safe
>50	Z2			Unsafe

Table 4.14: Hazard quotient and Hazard indexes of heavy metal in the Surface water samples (Ingestion)

HQ(ADULT)								HI	
Location	Iron	Lead	Copper	Cadmium	Chromium	zinc	Mercury	Aluminum	
S1	0.05541	0.021185	0.397021	0.002152	2.52E-05	0.204914	0.003346	1.15E-05	0.684065
S2	0.061683	0.011555	0.371407	0.001888	2.42E-05	0.258582	0.007318	1.9E-05	0.712478
S3	0.046001	0.025037	0.353111	0.001691	1.87E-05	0.22443	0.005855	1.43E-05	0.656157
S4	0.025092	0.015407	0.413488	0.002261	2.31E-05	0.226869	0.006273	1.31E-05	0.689426
S5	0.117094	0.026962	0.490331	0.001998	9.88E-06	0.261022	0.007527	2.02E-05	0.904964
S6	0.046001	0.021185	0.400681	0.00213	1.76E-05	0.204914	0.005646	1.19E-05	0.680585
S7	0.081548	0.028888	0.325667	0.001976	3.4E-05	0.214672	0.006273	1.9E-05	0.659077
S8	0.062729	0.019259	0.382385	0.001888	1.21E-05	0.226869	0.008573	4.4E-05	0.701759
S9	0.038683	0.025037	0.3586	0.00191	2.2E-05	0.173201	0.0069	1.07E-05	0.604364
S10	0.018819	0	0.010978	0	1.43E-05	0.217112	0.00575	1.43E-05	0.252686

Table 4.15: Hazard quotient and Hazard indexes of heavy metal in the surface water samples (Ingestion)

HQ(CHILDREN)								HI	
Location	Iron	Lead	Copper	Cadmium	Chromium	zinc	Mercury	Aluminum	
S1	0.131238	0.050175	0.940333	0.005096	5.98E-05	0.485333	0.007924	2.72E-05	1.620187
S2	0.146095	0.027368	0.879667	0.004472	5.72E-05	0.612444	0.017333	3.96E-05	1.687477
S3	0.108952	0.059298	0.836333	0.004004	4.42E-05	0.531556	0.013867	2.97E-05	1.554084
S4	0.059429	0.036491	0.979333	0.005356	5.46E-05	0.537333	0.014857	2.72E-05	1.632881
S5	0.277333	0.06386	1.161333	0.004732	2.34E-05	0.618222	0.017829	4.21E-05	2.143375
S6	0.108952	0.050175	0.949	0.005044	4.16E-05	0.485333	0.013371	2.48E-05	1.611943
S7	0.193143	0.068421	0.771333	0.00468	8.06E-05	0.508444	0.014857	3.96E-05	1.560999
S8	0.148571	0.045614	0.905667	0.004472	2.86E-05	0.537333	0.020305	9.16E-05	1.662082
S9	0.091619	0.059298	0.849333	0.004524	0.000052	0.410222	0.016343	2.23E-05	1.431414
S10	0.044571	0	0.026	0	3.38E-05	0.514222	0.013619	2.97E-05	0.598476

Table 4.16: Carcinogenic risk of heavy metals in the groundwater samples (Ingestion)

Locations	CR (Adult)			CR (Children)		
	Cd	Cr	Pb	Cd	Cr	Pb
S1	0.043749	0.020704	0.006843	0.103619	0.049036	0.016207
S2	0.038392	0.019804	0.003732	0.090931	0.046904	0.00884
S3	0.034374	0.015303	0.008087	0.081415	0.036244	0.019153
S4	0.045981	0.018903	0.004976	0.108905	0.044772	0.011787
S5	0.040624	0.008101	0.008709	0.096217	0.019188	0.020627
S6	0.043303	0.014403	0.006843	0.102561	0.034112	0.016207
S7	0.040178	0.027905	0.009331	0.09516	0.066092	0.0221
S8	0.038392	0.009902	0.006221	0.090931	0.023452	0.014733
S9	0.038839	0.018003	0.008087	0.091988	0.04264	0.019153
S10	0	0.011702		0	0.027716	0
RISK	0.363833	0.164729	0.062828	0.861727	0.390156	0.148807

**Table 4.17: Elevation and some key Acquirer Parameters**

Location	Longitude	Latitude	Elevation (m)	Water depth	Aquifer Thickness (B)	Hydraulic Conductivity (K)	Transmissivity (T)
SWC	6.4400	5.0600	13.11	5.96	16.06	0.51	8.19
SW1	6.4300	4.9800	15.55	6.64	17.11	0.66	11.29
SW2	6.4700	4.9900	13.41	5.84	14.64	0.46	3.81
SW3	6.4700	4.9800	18.59	5.75	10.35	0.36	3.73
SW4	6.4400	4.9600	20.12	6.62	9.57	0.58	5.55
SW5	6.4200	4.9300	14.63	6.73	20.54	0.53	10.89
SW6	6.4000	4.9200	13.41	5.81	13.65	0.44	6.01
SW7	6.4200	4.9200	14.33	6.83	18.42	0.37	6.82
SW8	6.4500	4.9200	19.51	6.63	17.33	0.32	5.55
SW9	6.3700	4.8500	15.55	5.9	18.61	0.45	8.38
Mean			15.821	6.271	15.628	0.468	7.022
Min			13.11	5.75	9.57	0.32	3.73
Max			20.12	6.83	20.54	0.66	11.29
Stdv			2.64	0.45	3.58	0.11	2.64

Table 4.18 Factor loadings of various parameters derived from the principal component extraction method

Parameters	Communalities	Component					
		1	2	3	4	5	6
Betex	.904	<b>.892</b>					
TPH	.926	<b>.862</b>					
Nitrate	.835	<b>.816</b>		-.308			
Iron	.863	<b>.802</b>			-.377		
PAH	.948	<b>.796</b>			<b>-.532</b>		
Magnesium	.710	<b>.648</b>		<b>.458</b>			
Bicarbonate	.708	<b>.638</b>		<b>.492</b>			
Calcium	.784	<b>.582</b>	.347		.395		
Sodium	.685	<b>.478</b>	-.401			<b>.424</b>	
Conductivity	.863	.404	<b>-.730</b>		.403		
Hardness	.852	.399	<b>-.722</b>		.333		
Lead	.806	<b>.432</b>	<b>.571</b>			-.382	
Copper	.686	<b>.430</b>	<b>.527</b>	-.322	.342		
Sulphate	.718	.330		<b>.611</b>		.315	
Chloride	.754	.367	.323	<b>.600</b>			
Potassium	.768			<b>-.532</b>		<b>.506</b>	
Zinc	.861	<b>.553</b>			<b>.644</b>		
TDS	.946	-.377				-.467	<b>.754</b>
Eigenvalues		6.337	2.304	1.993	1.768	1.195	1.022
Variance (%)		35.207	12.798	11.070	9.823	6.639	5.678
Cumulative var. (%)		35.207	48.005	59.075	68.898	75.537	81.215

Bold values indicate significant contributor (loadings greater than 0.4 (+ o-))

**Table 4.19: Correlation matrix of the various parameters in studied groundwater**

	Zinc	Copper	Lead	Iron	TPH	PAH	Betex	Conductivity	Hardness	TDS	Sodium	Calcium	Magnesium	Potassium	Bicarbonate	Chloride	Sulphate	Nitrate
Zinc	1.000	<b>.650<sup>b</sup></b>	.383	.262	<b>.616<sup>b</sup></b>	.166	.451	.298	.249	-.033	.217	<b>.484</b>	.108	.222	.152	.253	.080	.324
Copper		1.000	.437	.315	.279	.251	.255	-.085	-.135	-.178	.096	.379	-.060	.319	.240	.136	.054	.377
Lead			1.000	.342	.393	.101	.243	-.077	-.145	-.126	-.133	<b>.514<sup>b</sup></b>	.336	.018	.136	.322	.046	<b>.437</b>
Iron				1.000	<b>.616<sup>b</sup></b>	<b>.869<sup>a</sup></b>	<b>.717<sup>a</sup></b>	.034	.153	-.377	.296	.282	<b>.454</b>	.268	<b>.598<sup>b</sup></b>	.179	.133	<b>.749<sup>a</sup></b>
TPH					1.000	<b>.579</b>	<b>.887<sup>a</sup></b>	<b>.572</b>	<b>.485</b>	-.189	.407	.401	<b>.544<sup>b</sup></b>	.142	.448	.154	.049	<b>.673<sup>b</sup></b>
PAH						1.000	<b>.818<sup>a</sup></b>	.113	.163	-.247	.397	.166	<b>.505<sup>b</sup></b>	.309	<b>.608<sup>b</sup></b>	.123	.273	<b>.804<sup>a</sup></b>
Betex							1.000	.446	.411	-.274	.407	.327	<b>.579<sup>b</sup></b>	.307	.448	.102	.158	<b>.778<sup>a</sup></b>
Conductivity								1.000	<b>.763<sup>a</sup></b>	-.172	.439	.108	.186	-.097	.230	.053	-.030	.200
Hardness									1.000	-.243	.354	.168	.192	-.206	.311	.156	.021	.094
TDS										1.000	-.213	-.387	-.096	-.207	-.190	-.012	-.061	-.239
Sodium											1.000	.198	.112	.258	.144	-.011	.134	<b>.477</b>
Calcium												1.000	<b>.448</b>	.149	.304	<b>.501<sup>b</sup></b>	.324	.358
Magnesium													1.000	.036	<b>.536<sup>b</sup></b>	.386	<b>.480</b>	<b>.460</b>
Potassium														1.000	-.204	.178	-.077	.312
Bicarbonate															1.000	<b>.477</b>	<b>.440</b>	.326
Chloride																1.000	<b>.454</b>	.033
Sulphate																	1.000	.190
Nitrate																		1.000

Bold values indicate moderate and strong correlations (values greater than 0.4 (+ or -))

<sup>a</sup> Strong correlation

<sup>b</sup> Moderate correlation

**Table 4.20: Summary of CF, PLI , WQI and PIG (Ground Water)**

	Contamination Factor								PLI	WQI	PIG
	Na	Ca	Mg	HC03	Cl	S04	N03	Fe			
S1	0.3932	3.7778	0.1027	0.2285	0.1401	0.6263	0.0913	178.211	1.7848	16868.3	17.58674
S2	0.397	2.8756	0.0979	0.2235	0.15	0.5674	0.0907	150.577	1.3632	14251.5	18.5398
S3	0.3565	2.6622	0.0533	0.2207	0.1296	0.4611	0.04	129.155	0.4695	12224.7	15.83346
S4	0.2052	3.0178	0.0579	0.222	0.1425	0.4216	0.04	138.9	0.4125	13147.6	9.955708
S5	0.4363	3.2089	0.0523	0.2293	0.1328	0.46	0.0493	138.4	0.6698	13101.1	12.71538
S6	0.1737	3.4089	0.0759	0.1697	0.1776	0.5213	0.0533	120.8	0.5396	11437.3	10.48558
S7	0.4028	2.6933	0.0733	0.1722	0.1384	0.4949	0.0429	110.911	0.5343	10499.4	10.70923
S8	0.3243	2.5067	0.0607	0.1693	0.1773	0.5705	0.0301	82.8889	0.3671	7848.6	9.264984
S9	0.299	2.4	0.0607	0.1617	0.1347	0.5515	0.0301	111.555	0.3353	10559.3	13.46427
S10	0.235	2.2444	0.046	0.1578	0.1356	0.444	0.0247	96.811	0.188	9164.2	9.53054
Total mean	0.3223	2.87956	0.06807	0.19547	0.14586	0.51186	0.04924	125.821	0.66641		

**Table 4.21: Values of SAR, KR, Na, MH and SSP (Ground Water)**

	SAR	KR	Na%	MAR	SSP
	0.21	0.412698	42.1	43.96825	0.239146
	0.2	0.394856	40	50.5295	0.236993
	0.19	0.380368	39.8	46.31902	0.228972
	0.18	0.363095	38.5	48.66071	0.223341
	0.19	0.374627	39.9	47.16418	0.225011
	0.19	0.38	40.3	49.07692	0.227022
	0.2	0.393241	40.6	48.84793	0.233577
	0.18	0.355856	38.6	45.7958	0.218494
	0.2	0.409385	41.6	49.35275	0.238905
	0.21	0.416499	43.2	48.08853	0.236382
Mean	0.195	0.3880625	40.46	47.780359	0.2307843
STD	0.0108012	0.0208394	1.4833895	1.963749	0.0072324

**Table 4.22: Classification criteria for groundwater WQI**

WQI Values	Water Quality Status	Sample No	Percentage (%)	No of Samples	Possible usage
<50	Excellent				Drinking, Irrigation and Industrial
50-100	Good				Drinking, Irrigation and Industrial
100-200	Poor				Irrigation and Industrial
200-300	Very Poor				Irrigation
>300	Unsuitable for drinking	S1-S10	100	10	Proper treatment required before usage

**Table 4.23: PIG Classification**

Range	Zone	Sample No	sample %	Groundwater Pollution Degree
<1	Z1			Insignificant Pollution
1-1.5	Z2			Low Pollution
1.5-2.0	Z3			Moderate Pollution
2.0-2.5	Z4			High Pollution
>2.5	Z5	S1-S10	100	Very high Pollution

Sodium Hazard	Zone	Sample No	Sample %	Class of water
<10	Z1	S1-S10	100	Excellent
10-18	Z2			Good
18-26	Z3			Permissible
>26	Z4			Unsuitable

Sodium Hazard	Zone	Sample No	Sample %	Class of water
<20	Z1			Excellent
20-40	Z2	S2,S3,S4 & S5	40%	Good
40-60	Z3	S1,S6.S7,S8,S9& S10	60%	Permissible
60-80	Z4			Doubtful
>80	Z5			Unsuitable

MH range	Zone	Sample No	Sample %	Class of water
<50	Z1	S1, S3--S10	90%	Safe
>50	Z2	S2	10%	Unsafe

KR Range	Zone	Sample No	Sample %	Class of water
<1	Z1	S1-S10	100	Suitable
>1	Z2			Unsuitable

SSP Range	Zone	Sample No	Sample %	Class of water
<50	Z1	S1-S10	100	Safe
>50	Z2			Unsafe

Table 4.29: Hazard quotient and Hazard indexes of heavy metal in the ground water samples (Ingestion).

Location	HQ(Children)								HI
	Fe	Pb	Cu	Cd	Cr	Zn	Hg	Al	
S1	3.731619	0.5942857	0.9533333	0	0	0.202222222	0	0	5.4814603
S2	3.9495238	0.2971429	0.52	0	0	0.137511111	0	0	4.9041778
S3	3.367619	0.5942857	0.4333333	0	0	0.175644444	0	0	4.5708825
S4	2.0879238	0.4457143	1.04	0	0	0.225333333	0	0	3.7989714
S5	2.6921143	0	0.3033333	0	0	0.198755556	0	0	3.1942032
S6	2.1948952	0.1980952	0.7366667	0	0	0.161777778	0	0	3.2914349
S7	2.239219	0.1980952	0.0866667	0	0	0.151955556	0	0	2.6759365
S8	1.9225143	0.1980952	0.5633333	0	0	0.204533333	0	0	2.8884762
S9	2.8421714	0.1485714	0.8233333	0	0	0.1924	0	0	4.0064762
S10	2.010419	0	0.13	0	0	0.034666667	0	0	2.1750857
Average	2.703802	0.2674286	0.559	0	0	0.16848	0	0	3.69871

Table 4.30: Carcinogenic risk of heavy metals in the groundwater samples (Ingestion)

Locations	CR (Adult)			CR (Children)		
	Cd	Cr	Pb	Cd	Cr	Pb
S1	0	0	7.46E-06	0	0	1.768E-05
S2	0	0	3.73E-06	0	0	8.84E-06
S3	0	0	7.46E-06	0	0	1.768E-05
S4	0	0	5.6E-06	0	0	1.326E-05
S5	0	0	0	0	0	0
S6	0	0	2.49E-06	0	0	5.893E-06
S7	0	0	2.49E-06	0	0	5.893E-06
S8	0	0	2.49E-06	0	0	5.893E-06
S9	0	0	1.87E-06	0	0	4.42E-06
S10	0	0	0	0	0	0
Average	0	0	3.36E-06	0	0	7.96E-06

Table 4.32: Soils Contamination Factors

	Contamination Factor (CF=C <sub>s</sub> /C <sub>n</sub> )										CF	
	S1	S2	S3	S4	S5	S6	S7	S8	S9	S10		Mean
Iron (mg/l)	180.4	0.9	1.1	1.1	1.2	0.9	0.8	1.1	0.9	1.2	18.97	Very high Contamination
Lead (mg/l)	0.67	0.8	1.5	0.8	1.7	0.8	1.2	0.7	1.2	0	0.924	Low Contamination
Copper (mg/l)	0.36	0.9	1	1.1	1.2	0.9	0.8	1.3	0.8	0	0.831	Low Contamination
Cadmium (mg/l)	3.4	0.9	1	1.3	0.9	1.1	0.9	1	1	0	1.128	Moderate Contamination
Zinc (mg/l)	0.5	1.3	0.8	1.1	1.1	0.8	1.1	1	0.9	0.7	0.929	Low Contamination
Mercury (mg/l)	1.4	1.6	0.9	0.9	1.3	0.8	0.9	1.2	1	0.4	1.049	Moderate Contamination
Aluminium (mg/l)	0.33	1.4	0.9	0.9	1.2	0.7	1.6	1.7	0.3	1.2	1.02	Moderate Contamination

Table 4.33: GEO-ACCUMULATION INDEX OF HEAVY METALS IN SOILS OF KOLO CREEK

Location/Parameters	S1	S2	S3	S4	S5	S6	S7	S8	S9	S10	Igeo	Pollution Intensity
Iron	6.91	6.82	7	7.08	7.36	7.2	6.91	7.07	6.95	7.25	7.05	Very highly Polluted
Lead	-1.2	-1.6	-1	-1.4	-0.7	-1	-0.7	-1.2	-1	0	-0.99	Unpolluted
Copper	-2.1	-2.1	-2.2	-2.1	-1.9	-2	-2.3	-1.9	-2.2	0	-1.88	Unpolluted
Cadmium	1.18	0.98	0.91	1.25	1.06	1.21	1.05	0.98	0.93	0	0.95	very lightly polluted
Zinc	-1.6	-1.2	-1.6	-1.4	-1.3	-1.6	-1.5	-1.5	-1.6	-2.2	-1.53	Unpolluted
Mercury	6.54	7.24	7.13	6.97	7.31	7.01	6.91	7.15	7.17	5.93	6.94	Very highly Polluted
Aluminum	-2.2	-1.7	-1.9	-2.1	-1.8	-2.2	-1.6	-0.8	-2.7	-2.4	-1.94	Unpolluted

Table 4.34 Factor loadings of various parameters derived from the principal component extraction method

	Communalities	Component				
		1	2	3	4	5
TPH	.820	<b>.865</b>	.244	-.023	.103	-.026
PAH	.838	.393	.299	-.339	<b>.569</b>	-.394
Betex	.882	<b>.793</b>	-.202	.380	.234	-.108
pH	.820	<b>-.880</b>	.170	-.032	.040	.119
E.Conductivity	.846	.379	-.016	-.300	<b>.592</b>	<b>.512</b>
Sodium	.891	-.026	<b>.918</b>	.163	-.099	.104
Calcium	.663	<b>.602</b>	.263	-.164	-.151	.427
Magnesium	.906	<b>.773</b>	-.127	-.019	-.129	<b>-.525</b>
Potassium	.624	<b>.510</b>	.368	.296	-.167	.337
Bicarbonate	.676	.421	.062	<b>.652</b>	.213	-.155
Chloride	.756	-.174	.080	.420	<b>.735</b>	.050
Sulphate	.932	.375	<b>.806</b>	-.186	-.054	-.322
Nitrate	.804	-.105	-.138	<b>.871</b>	-.119	.025
Iron	.864	<b>.892</b>	.192	-.085	-.114	.106
Lead	.871	<b>.877</b>	-.071	.197	-.139	.195
Copper	.928	<b>.952</b>	-.016	-.073	-.099	.070
Zinc	.810	<b>.506</b>	<b>-.677</b>	-.216	.189	.113
Mercury	.712	<b>.617</b>	<b>-.512</b>	-.089	-.239	-.062
Eigenvalues		7.138	2.725	1.993	1.557	1.227
Variance (%)		39.656	15.140	11.073	8.647	6.819
Cumulative var. (%)		39.656	54.796	65.869	74.516	81.335

Bold values indicate significant contributor (loadings greater than 0.4 (+ or -))

**Table 4.35: Correlation matrix of the various parameters in soils of the study area.**

	TPH	PAH	Betex	pH	E.C	Na	Ca	Mg	K	HC03	Cl	S04	N03	Fe	Pb	Cu	Zn	Hg
TPH	1	.500*	.642**	-.672**	.387	.176	.458*	.596**	.608**	.355	-.093	.525*	-.147	.727**	.679**	.795**	.301	.473*
PAH		1	.344	-.241	.342	.070	.099	.306	.070	.141	.105	.511*	-.413	.327	.134	.278	.132	.026
Betex			1	-.769**	.304	-.174	.235	.630**	.378	.547*	.095	.063	.285	.583**	.744**	.708**	.439	.464*
pH				1	-.232	.216	-.419	-.798**	-.322	-.257	.096	-.210	.048	-.779**	-.790**	-.894**	-.443	-.511*
E.C					1	-.019	.327	.008	.123	-.022	.171	.031	-.240	.341	.221	.384	.445*	.094
Na						1	.211	-.151	.428	.124	.056	.722**	.067	.116	-.091	-.017	-.573**	-.419
Ca							1	.235	.259	.237	-.159	.349	-.255	.677**	.624**	.639**	.113	.273
Mg								1	.130	.367	-.226	.390	-.088	.654**	.578**	.725**	.405	.574**
K									1	.233	-.064	.295	.134	.497*	.530*	.469*	.036	.195
HC03										1	.299	.108	.378	.278	.443	.303	.117	.154
Cl											1	-.107	.198	-.227	-.156	-.259	-.117	-.320
S04												1	-.254	.459*	.134	.349	-.311	-.055
N03													1	-.179	.055	-.130	-.162	-.007
Fe														1	.862**	.827**	.287	.388
Pb															1	.797**	.396	.474*
Cu																1	.483*	.602**
Zn																	1	.712**
Hg																		1

\*. Correlation is significant at the 0.05 level (2-tailed).

\*\* . Correlation is significant at the 0.01 level (2-tailed).

Table 4.36: Hazard quotient and Hazard indexes of heavy metal in the soil samples (Dermal)

HQ(ADULT)								HI	
Location	Iron	Lead	Copper	Cadmium	Chromium	zinc	Mercury	Aluminum	
S1	0.000565	2.07E-05	3.31E-05	8.81E-07	0	1.02E-05	7.77E-09	3.63E-07	0.00063
S2	0.000558	2.07E-05	3.08E-05	7.77E-07	0	1.52E-05	1.04E-08	5.96E-07	0.000626
S3	0.000426	1.55E-05	2.99E-05	7.51E-07	0	2.03E-05	1.04E-08	5.44E-07	0.000493
S4	0.00055	2.07E-05	3.22E-05	9.33E-07	0	1.53E-05	8.64E-09	4.92E-07	0.000619
S5	0.00055	1.55E-05	3.72E-05	8.03E-07	0	1.74E-05	7.77E-09	6.22E-07	0.000622
S6	0.000571	2.59E-05	3.36E-05	9.07E-07	0	1.87E-05	7.77E-09	5.18E-07	0.000651
S7	0.000558	2.07E-05	2.81E-05	8.03E-07	0	1.52E-05	1.21E-08	4.66E-07	0.000623
S8	0.000558	2.59E-05	3.58E-05	7.77E-07	0	1.6E-05	1.21E-08	5.44E-07	0.000637
S9	0.000443	1.55E-05	2.9E-05	7.51E-07	0	1.63E-05	4.32E-09	5.7E-07	0.000505
S10	7.19E-05	0	0	0	0	1.46E-05	4.32E-09	2.33E-07	8.68E-05

Table 4.37: Carcinogenic risk of heavy metals in the Soil samples (Dermal)

CR (ADULT)			CR ( CHILDREN)			
Locations	Cd	Cr	Pb	Cd	Cr	Pb
S1	9.25E-06		1.09E-07	4.02E-05		4.72E-07
S2	8.16E-06	0	1.09E-07	3.54E-05	0	4.72E-07
S3	7.89E-06	0	8.16E-08	3.43E-05	0	3.54E-07
S4	9.79E-06	0	1.09E-07	4.25E-05	0	4.72E-07
S5	8.43E-06	0	8.16E-08	3.66E-05	0	3.54E-07
S6	9.52E-06	0	1.36E-07	4.13E-05	0	5.91E-07
S7	8.43E-06	0	1.09E-07	3.66E-05	0	4.72E-07
S8	8.16E-06	0	1.36E-07	3.54E-05	0	5.91E-07
S9	7.89E-06	0	8.16E-08	3.43E-05	0	3.54E-07
S10	0	0	0	0	0	0

Table 4.38: Hazard quotient and Hazard indexes of heavy metal in the Soil samples (Ingestion)

HQ(CHILDREN)							HI	
Location	Iron	Lead	Copper	Cadmium	zinc	Mercury	Aluminum	
S1	4.12E-06	1.53E-07	1.14E-07	6.56E-09	1.13E-07	2.68E-09	0	4.51E-06
S2	3.14E-06	1.15E-07	1E-07	5.76E-09	1.5E-07	4.4E-09	0	3.52E-06
S3	4.06E-06	1.53E-07	9.71E-08	5.16E-09	1.13E-07	4.02E-09	1.91E-11	4.43E-06
S4	4.06E-06	1.15E-07	1.21E-07	6.9E-09	1.29E-07	3.64E-09	0	4.44E-06
S5	4.22E-06	1.91E-07	1.04E-07	6.09E-09	1.38E-07	4.59E-09	0	4.66E-06
S6	4.12E-06	1.53E-07	1.17E-07	6.5E-09	1.12E-07	3.83E-09	1.91E-11	4.51E-06
S7	4.12E-06	1.91E-07	1.04E-07	6.03E-09	1.18E-07	3.44E-09	0	4.54E-06
S8	3.27E-06	1.15E-07	1E-07	5.76E-09	1.21E-07	4.02E-09	1.91E-11	3.61E-06
S9	4.17E-06	1.53E-07	9.71E-08	5.83E-09	1.08E-07	4.21E-09	1.91E-11	4.54E-06
S10	5.31E-07	0	0	0	7.54E-08	1.72E-09	0	6.08E-07

Table 4.39: Hazard quotient and Hazard indexes of heavy metal in the Soil samples (Ingestion)

Location	HQ(ADULT)						HI	
	Iron	Lead	Copper	Cadmium	zinc	Mercury	Aluminum	
S1	1.37E-06	5.09E-08	3.79E-08	2.18E-09	5.13E-10	3.74E-08	0	1.5E-06
S2	1.05E-06	3.82E-08	3.34E-08	1.92E-09	4.9E-10	4.99E-08	0	1.17E-06
S3	1.35E-06	5.09E-08	3.23E-08	1.72E-09	3.79E-10	3.76E-08	6.37E-12	1.47E-06
S4	1.35E-06	3.82E-08	4.01E-08	2.3E-09	4.68E-10	4.28E-08	0	1.48E-06
S5	1.4E-06	6.37E-08	3.45E-08	2.03E-09	2.01E-10	4.61E-08	0	1.55E-06
S6	1.37E-06	5.09E-08	3.9E-08	2.16E-09	3.57E-10	3.73E-08	6.37E-12	1.5E-06
S7	1.37E-06	6.37E-08	3.45E-08	2.01E-09	6.91E-10	3.94E-08	0	1.51E-06
S8	1.09E-06	3.82E-08	3.34E-08	1.92E-09	2.45E-10	4.01E-08	6.37E-12	1.2E-06
S9	1.39E-06	5.09E-08	3.23E-08	1.94E-09	4.46E-10	3.6E-08	6.37E-12	1.51E-06
S10	1.77E-07	0	0	0	2.9E-10	2.51E-08	0	2.02E-07

Table 4.40: Carcinogenic risk of heavy metals in the Soil samples (Ingestion)

Locations	CR (Children)			CR (Adult)		
	Cd	Cr	Pb	Cd	Cr	Pb
S1	7E-09	0	4.55E-12	2.33E-09	0	1.52E-12
S2	6.14E-09	0	3.42E-12	2.04E-09	0	1.14E-12
S3	5.5E-09	0	4.55E-12	1.83E-09	0	1.52E-12
S4	7.36E-09	0	3.42E-12	2.45E-09	0	1.14E-12
S5	6.5E-09	0	5.69E-12	2.16E-09	0	1.89E-12
S6	6.93E-09	0	4.55E-12	2.31E-09	0	1.52E-12
S7	6.43E-09	0	5.69E-12	2.14E-09	0	1.89E-12
S8	6.14E-09	0	3.42E-12	2.04E-09	0	1.14E-12
S9	6.21E-09	0	4.55E-12	2.07E-09	0	1.52E-12
S10	0	0	0	0	0	0

Table 4.41: Atterberg Soil Plasticity Classification (Prakash, 1979)

Plasticity Index(%)	Soil Type	Degree of Plasticity	Degree of Cohensiveness
0	Sand	Non-Plastic	Non- Cohensive
<7	Silt	Low Plastic	Partly Cohensive
7-17	Silt Clay	Medium Plastic	Cohensive
>17	Clay	High Plastic	Cohensive

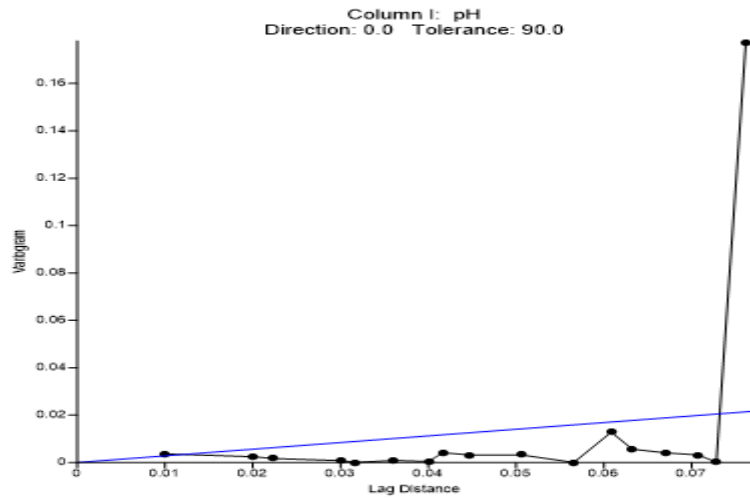


Fig 4.1a: Variogram of pH in Kolo-Creek Surface water.

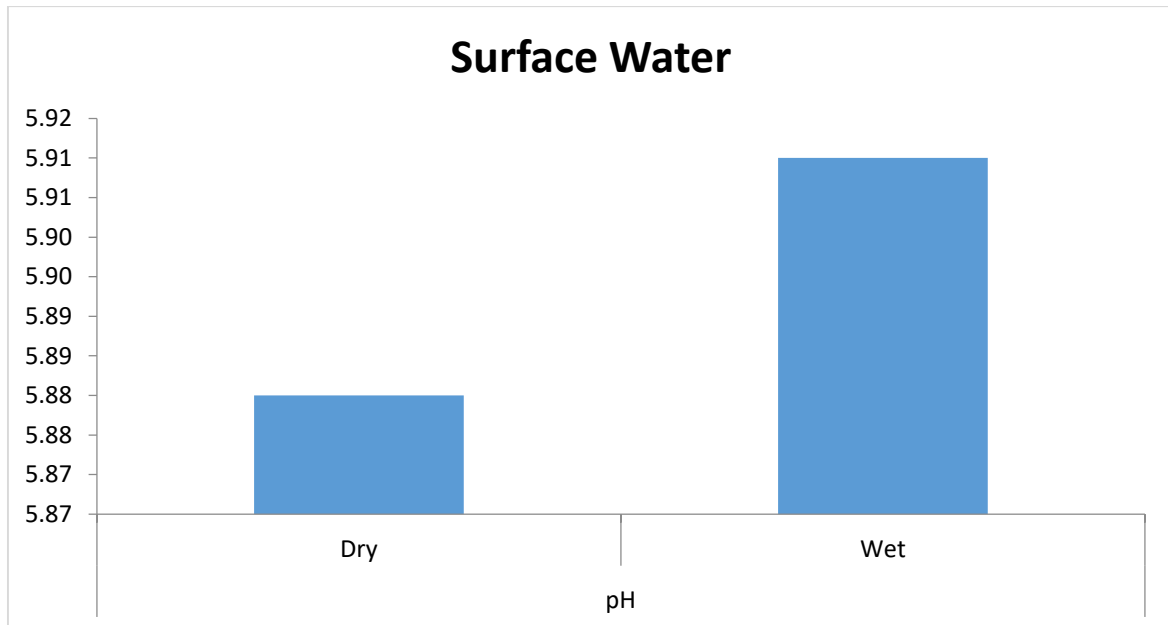


Fig 4.1b: Seasonal Variations of pH in Kolo-Creek Surface water.

Fig 4.1c: pH distribution in surface water at Kolo-Creek

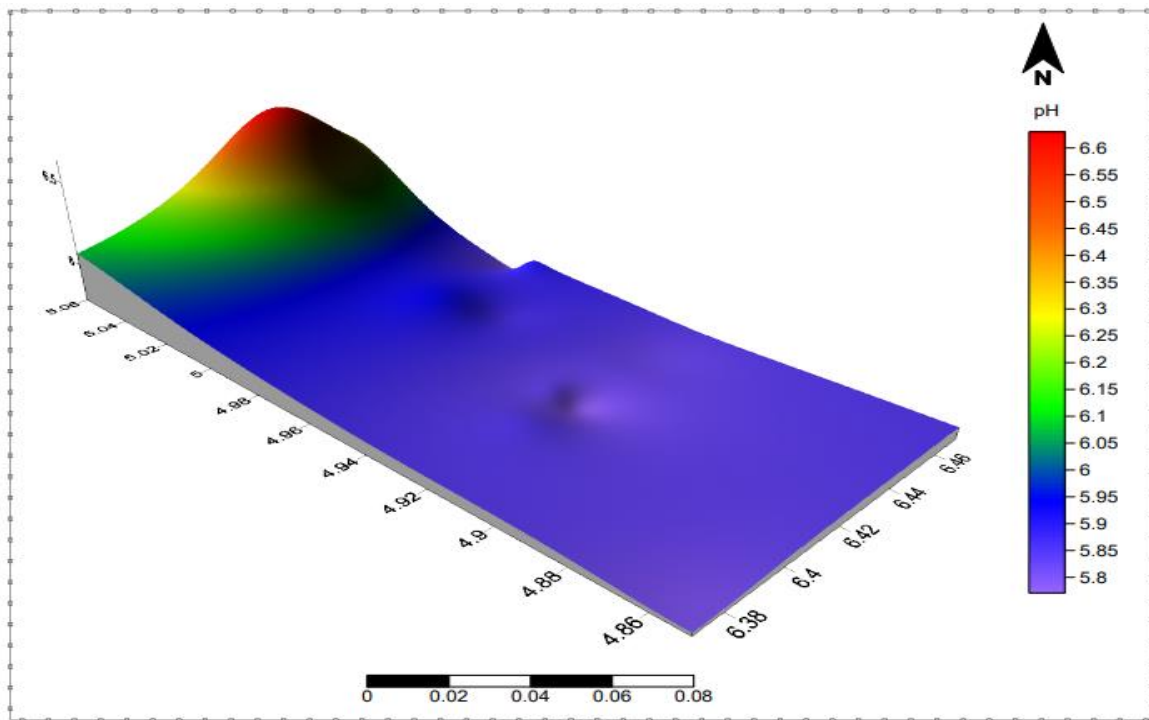


Fig 4.1d: 3D representation of the pH in Kolo-Creek surface water

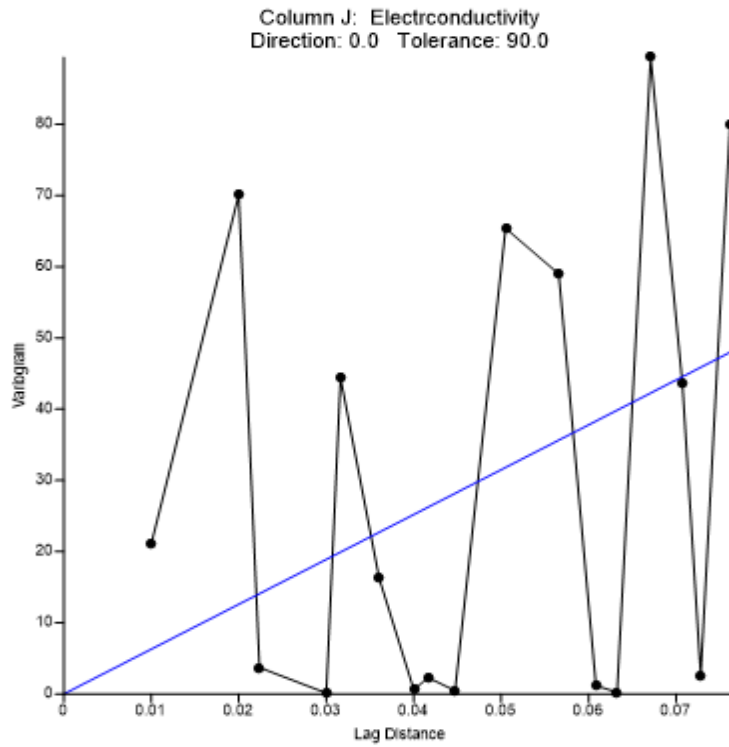


Fig: 4.2a: Variogram of Electrical Conductivity in Kolo Creek Surface water

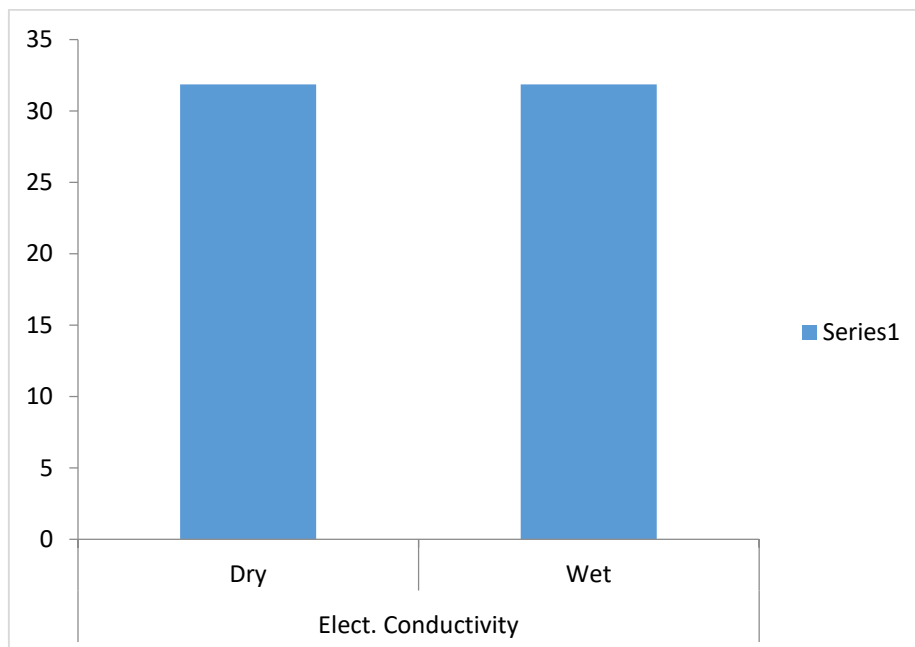


Fig 4.2b: Seasonal Variations of Elect. Cond. in Kolo-Creek Surface water.

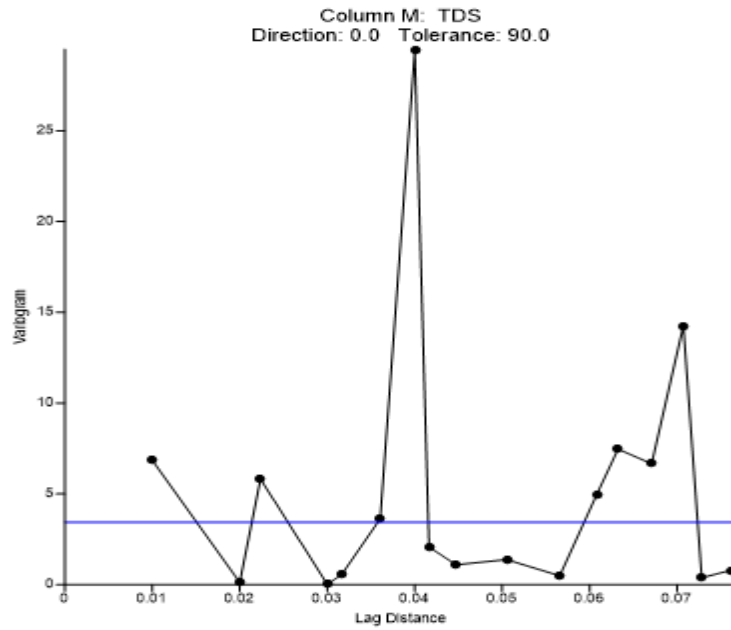


Fig 4.2c: Variogram of TDS in Kolo Creek Surface water

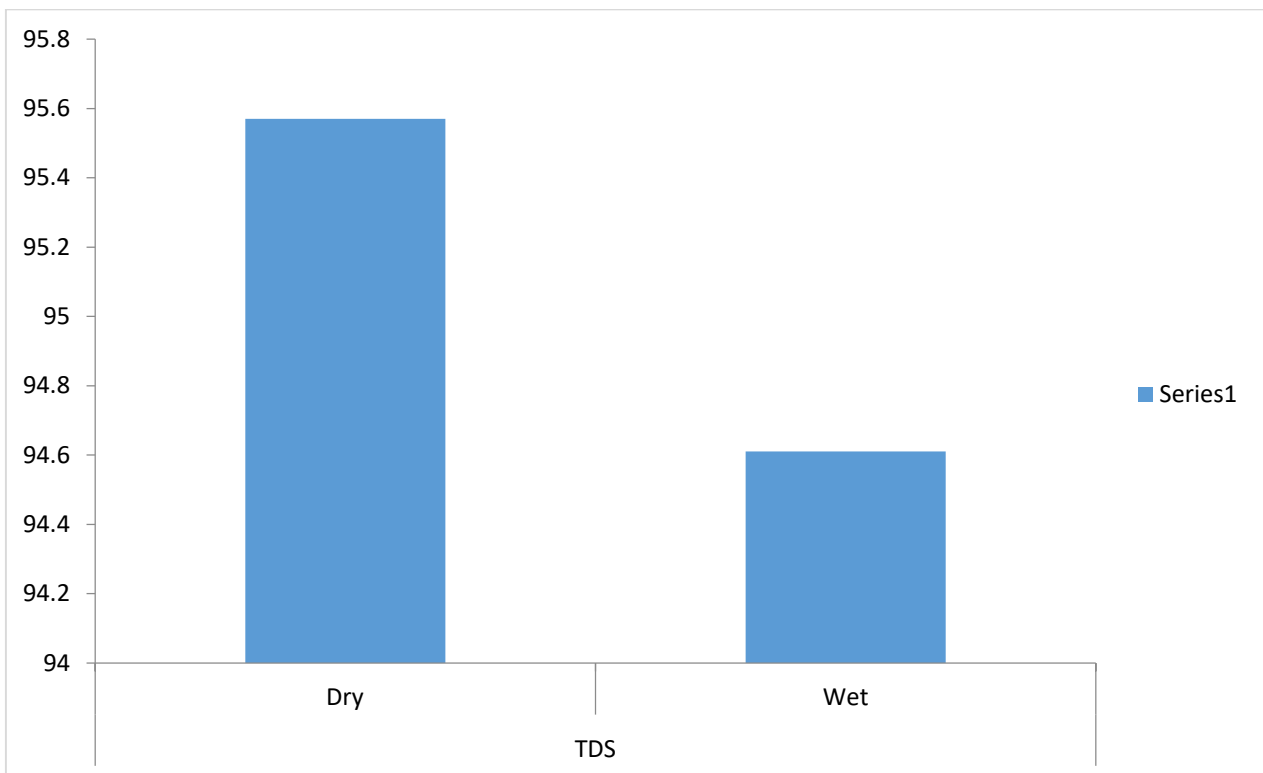


Fig 4.2d: Seasonal Variations of TDS in Kolo Creek Surface water.

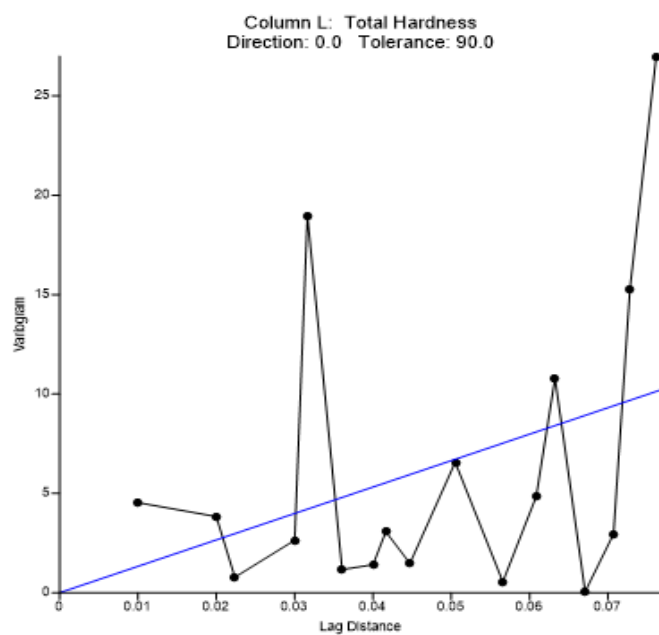


Fig. 4.3a: Variogram of Total Hardness in Kolo Creek Surface Water

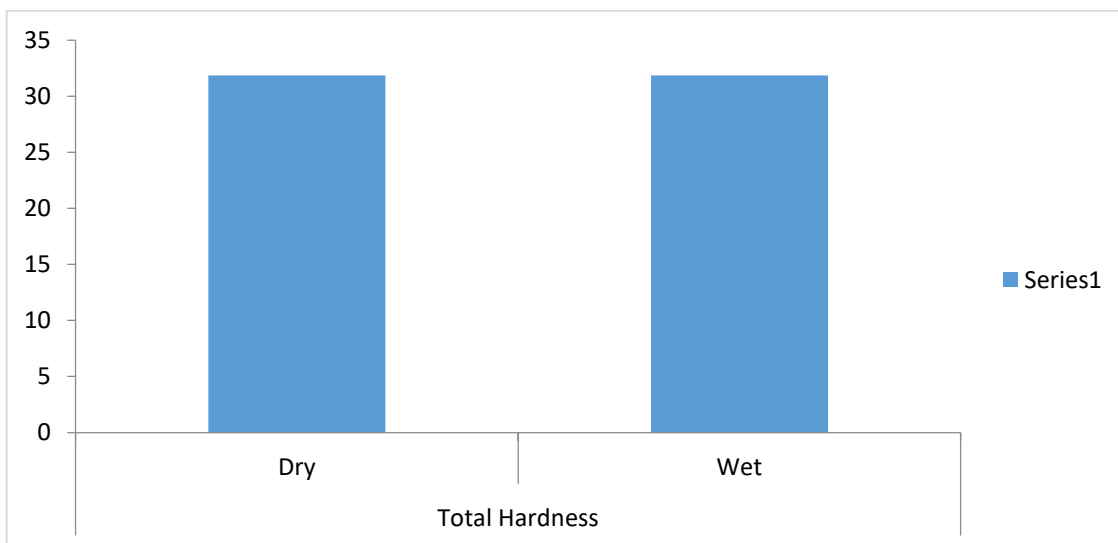


Fig 4.3b: Seasonal Variations of Total Hardness in Kolo Creek Surface water.  
Chloride

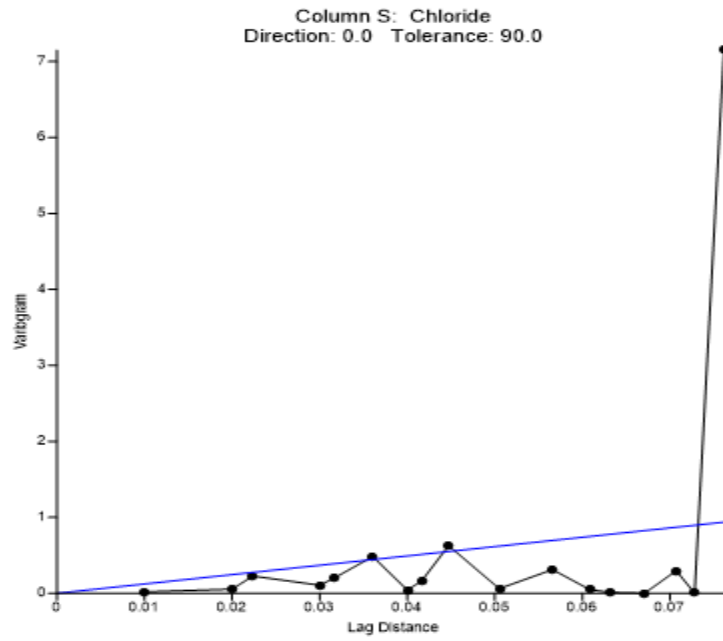


Fig 4.4a: Variogram of Chlorides in Kolo Creek Surface water

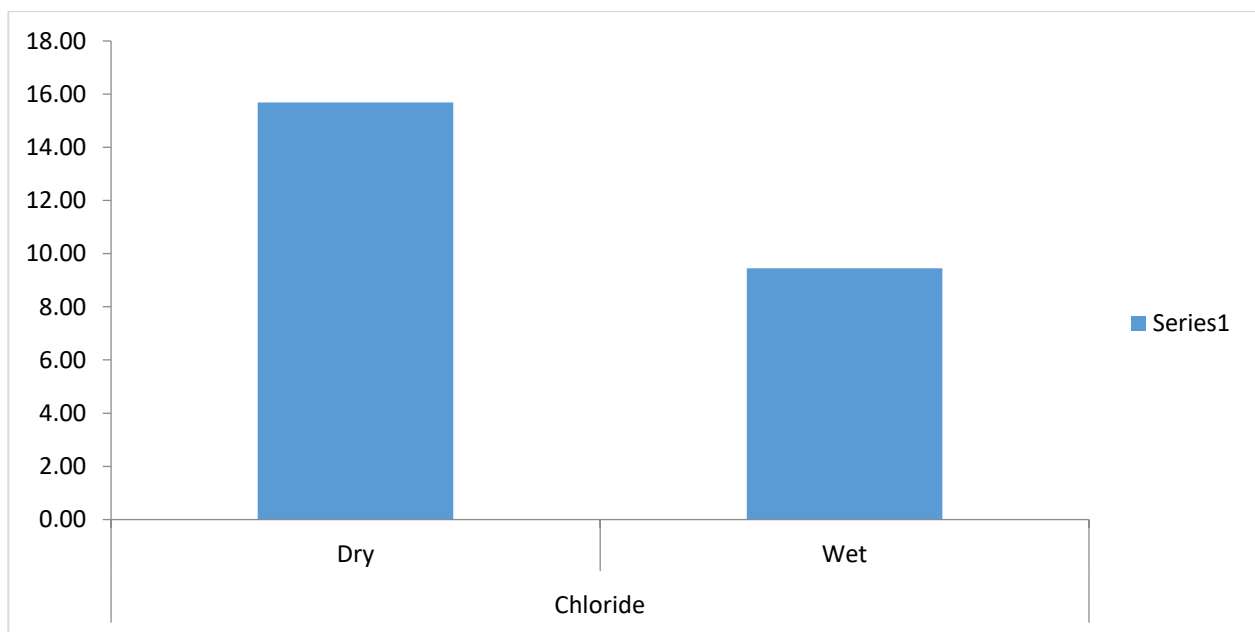


Fig 4.4b: Seasonal Variations of Chloride in Kolo Creek Surface water.

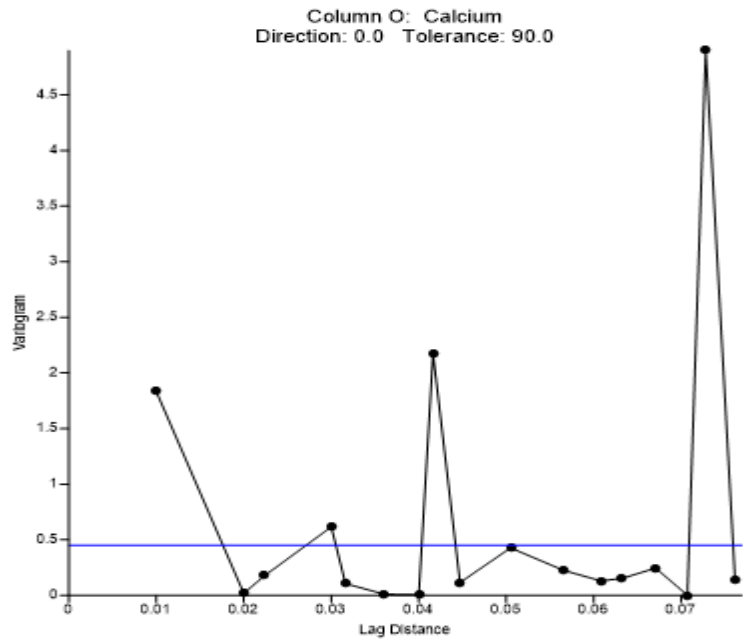


Fig 4.5a: Variogram of Calcium in Kolo Creek Surface water

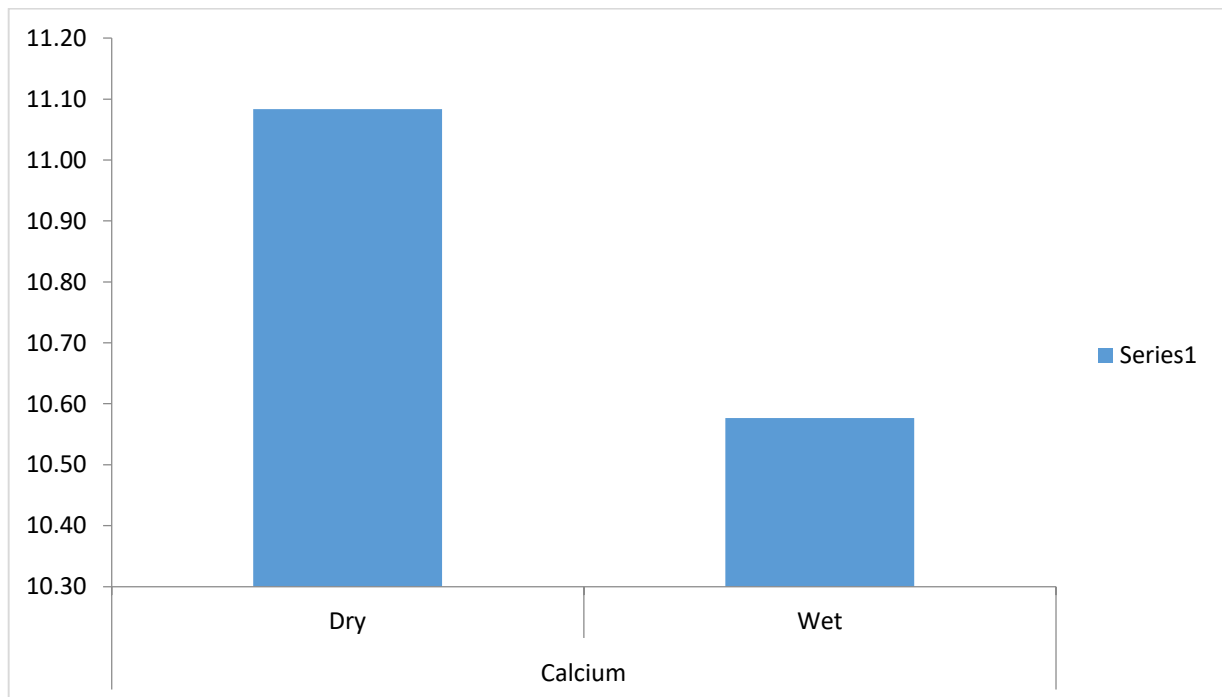


Fig: 4.5b Seasonal Variations of Calcium in Kolo Creek Surface water.

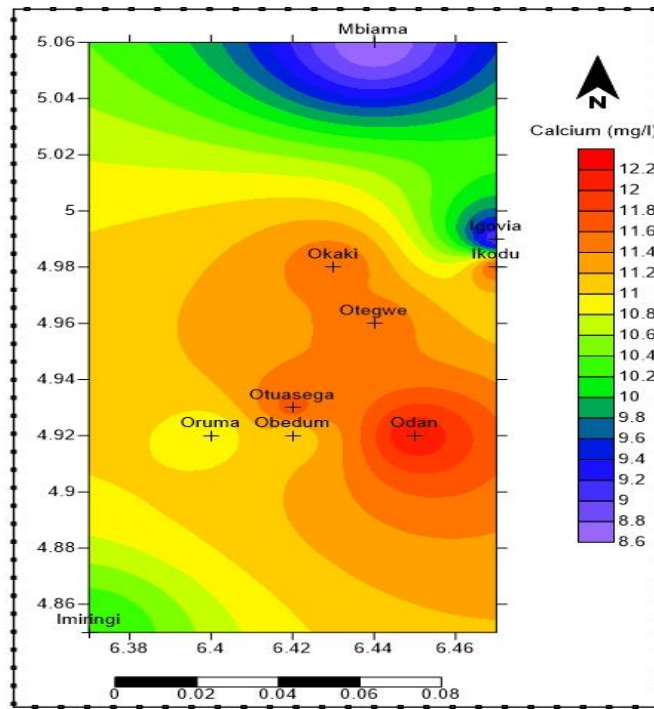


Fig 4.5c: Spatial Distribution of Calcium in Kolo Creek Surface water

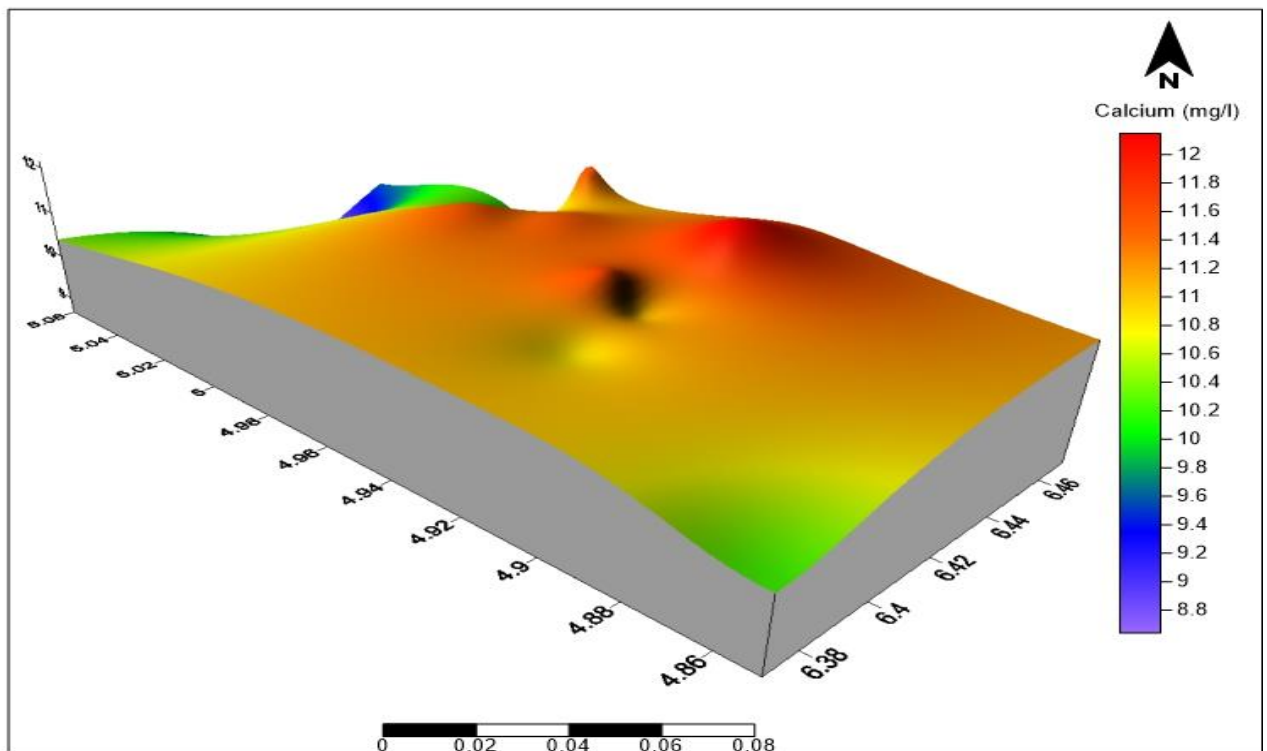


Fig 4.5d: 3D view of Calcium in Kolo Creek Surface water

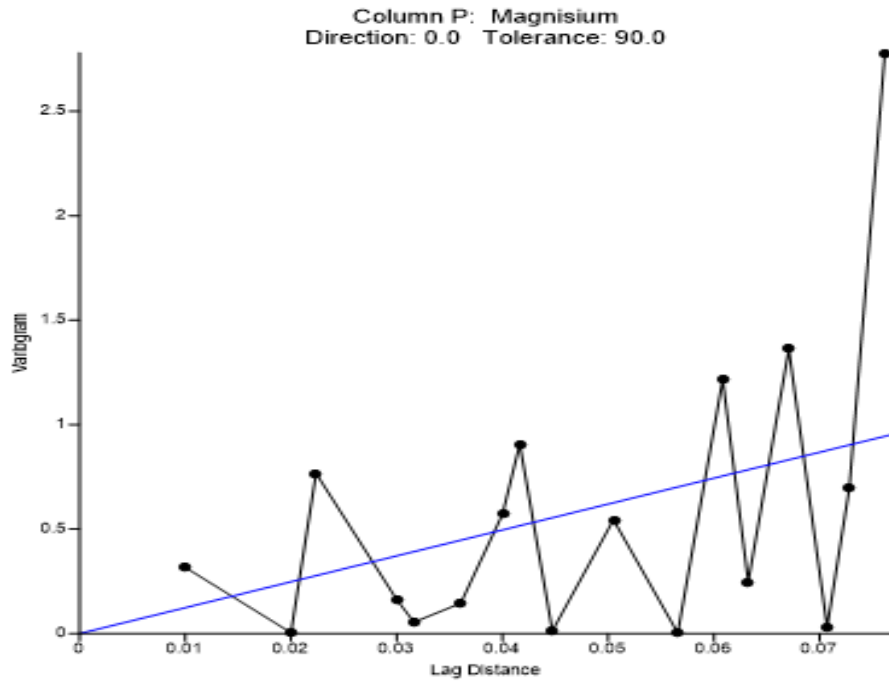


Fig 4.6a: Variogram of Magnesium in Kolo Creek Surface water

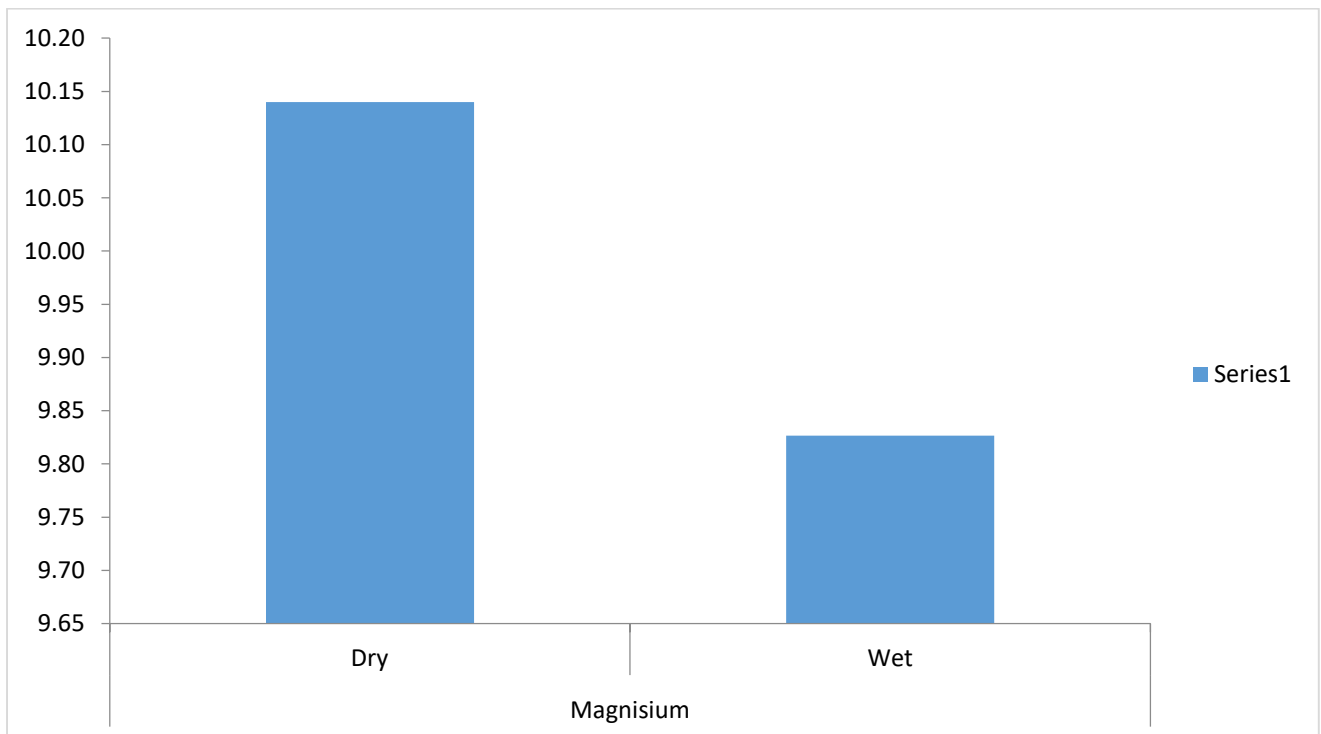


Fig: 4.6b Seasonal Variations of Magnesium in Kolo Creek Surface water.

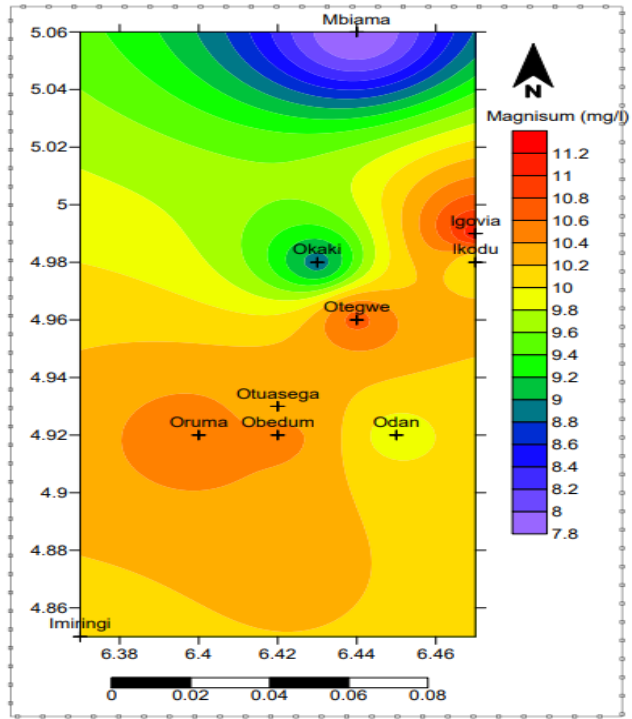


Fig 4.6c: Spatial Distribution of Magnesium in Kolo Creek Surface water

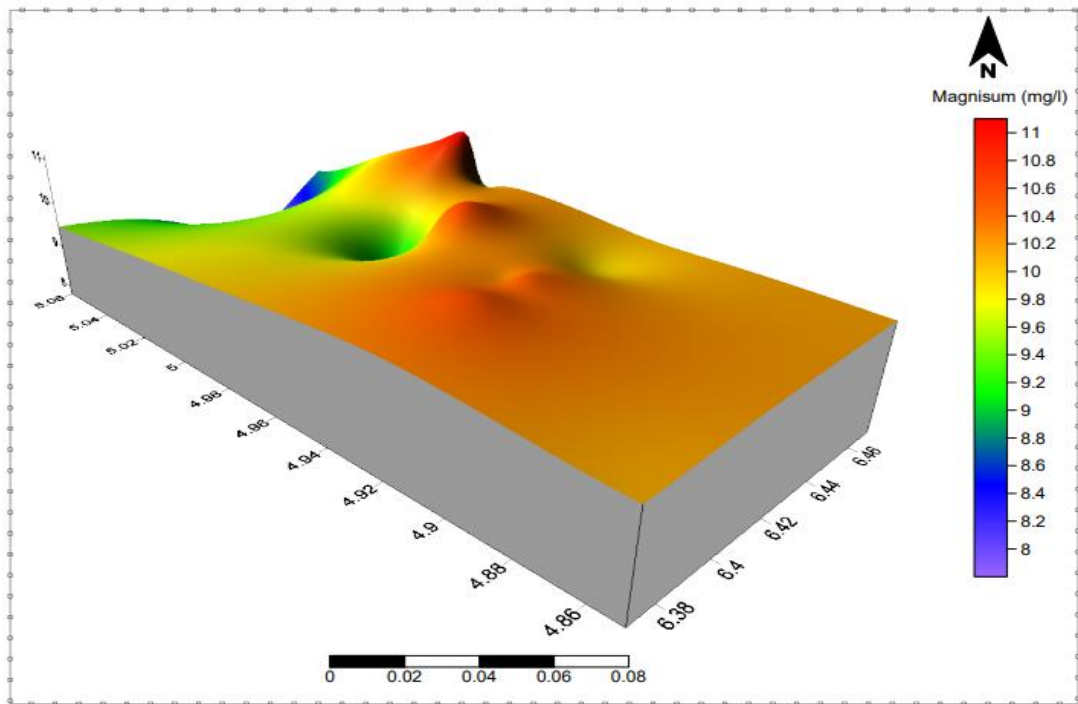


Fig 4.6d: 3D view of Magnesium in Kolo-Creek Surface water

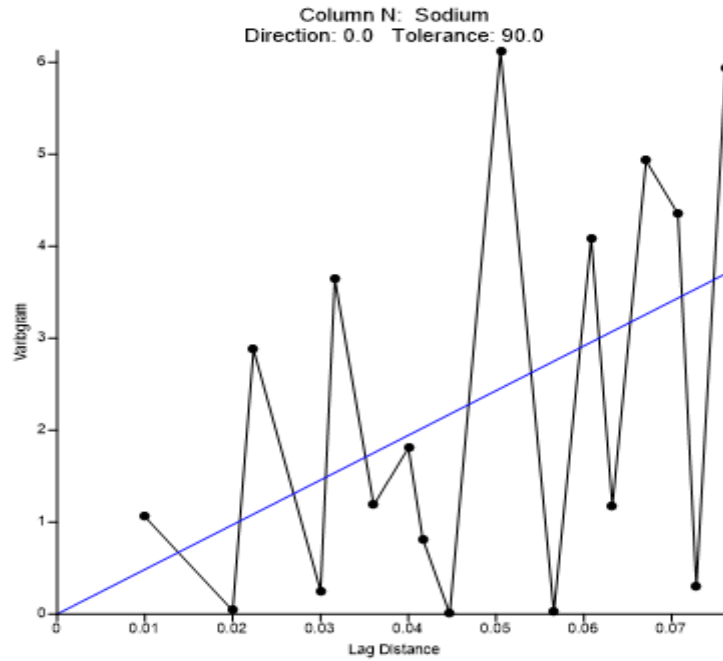


Fig 4.7a: Variogram of Sodium in Kolo Creek Surface water

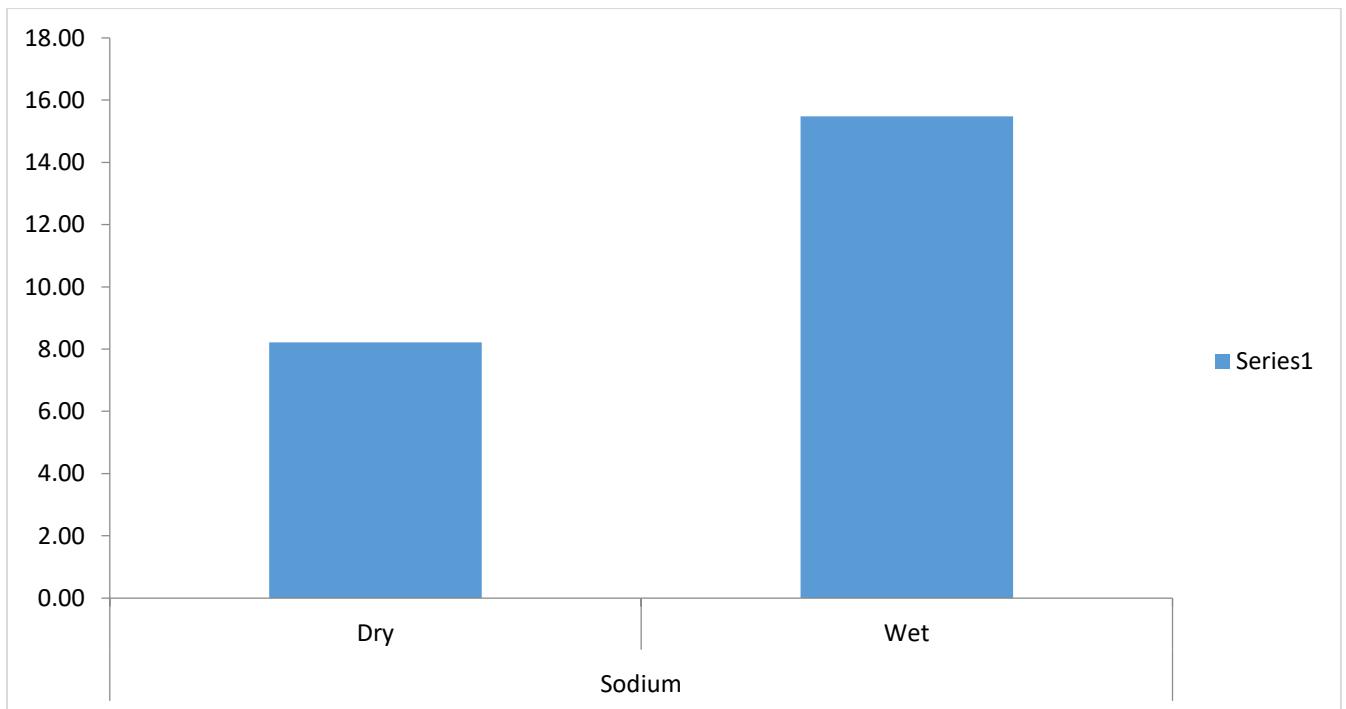


Fig: 4.7b Seasonal Variation of Sodium in Kolo Creek Surface water.

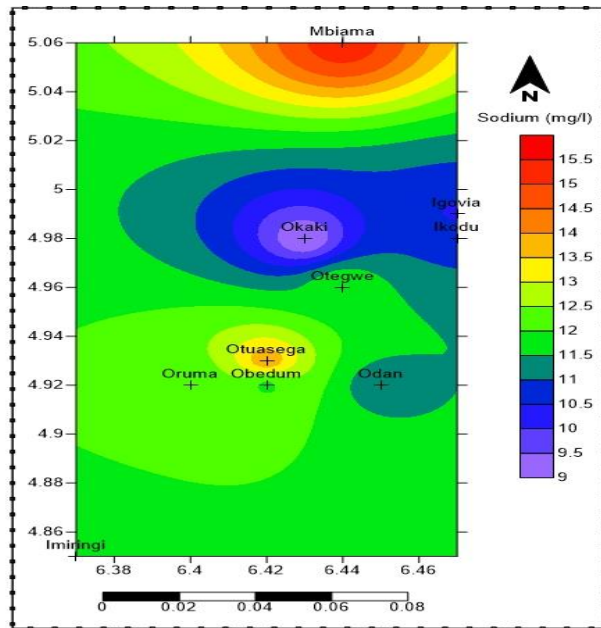


Fig 4.7c: Spatial Distribution of Sodium in Kolo Creek Surface water

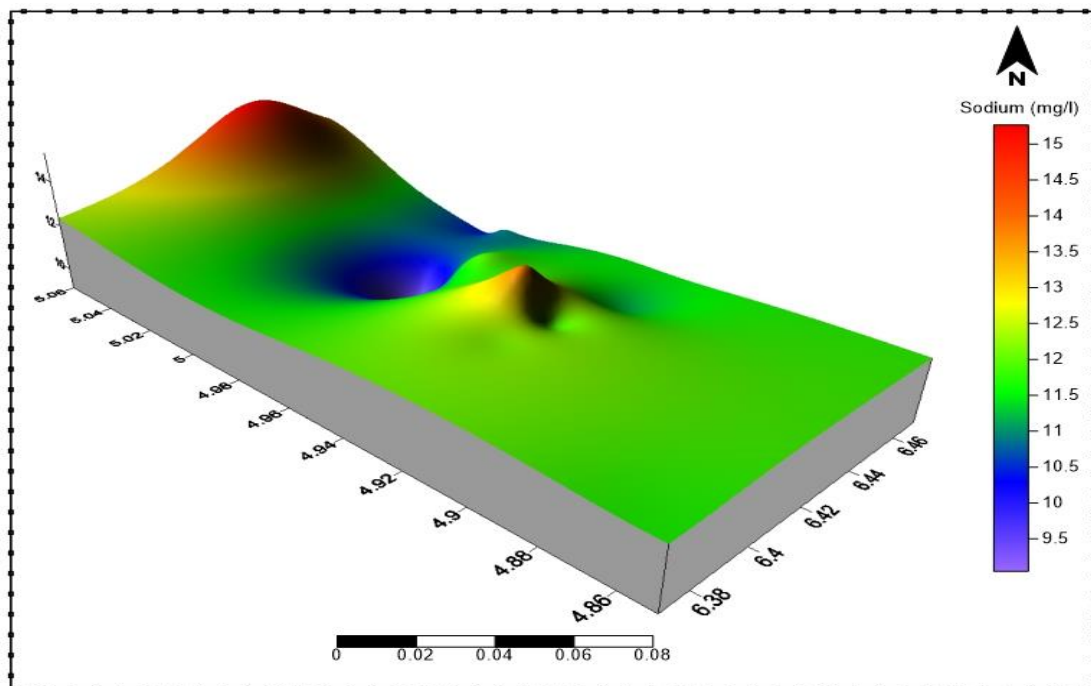


Fig 4.7d: 3D view of Sodium in Kolo Creek Surface water

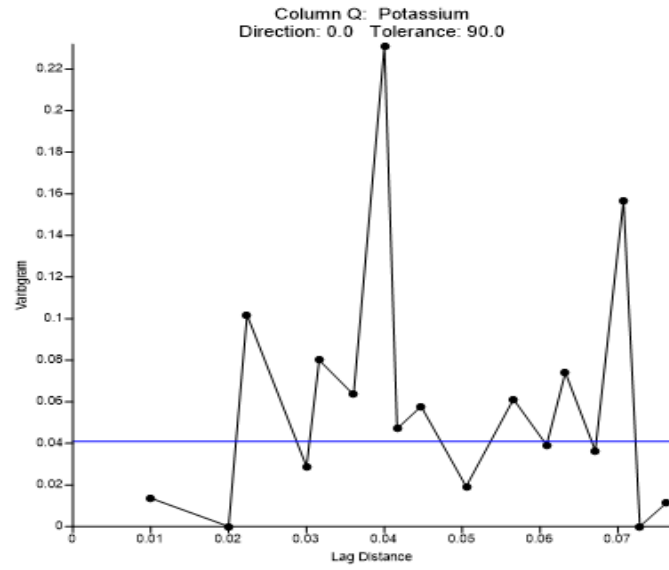


Fig 4.8a: Station Variation of Potassium in Kolo Creek Surface water

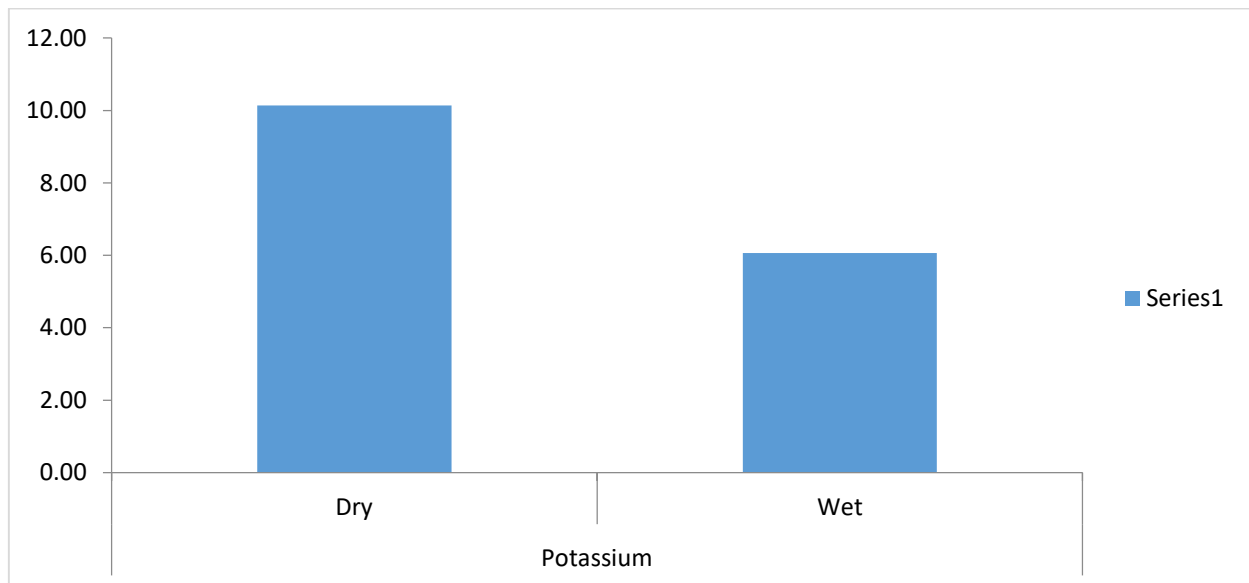


Fig: 4.8b Seasonal Variation of Potassium in Kolo Creek Surface water.

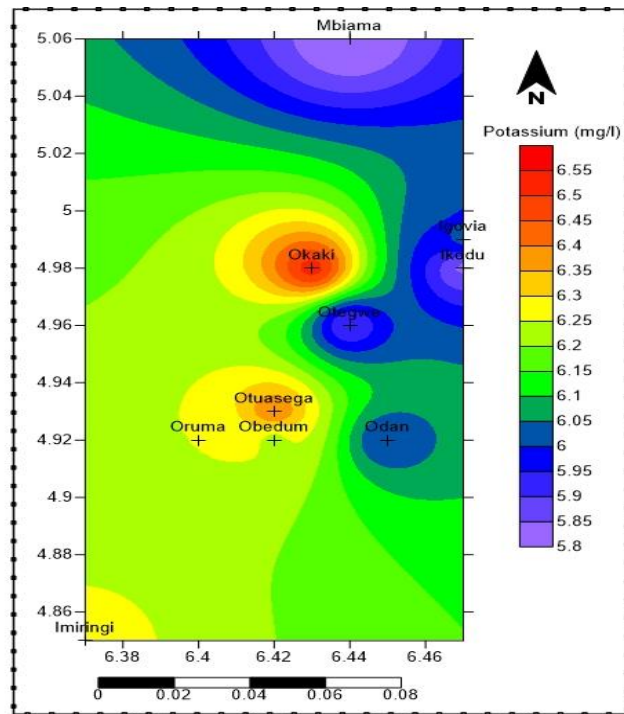


Fig 4.8c: Spatial Distribution of Potassium in Kolo Creek Surface water

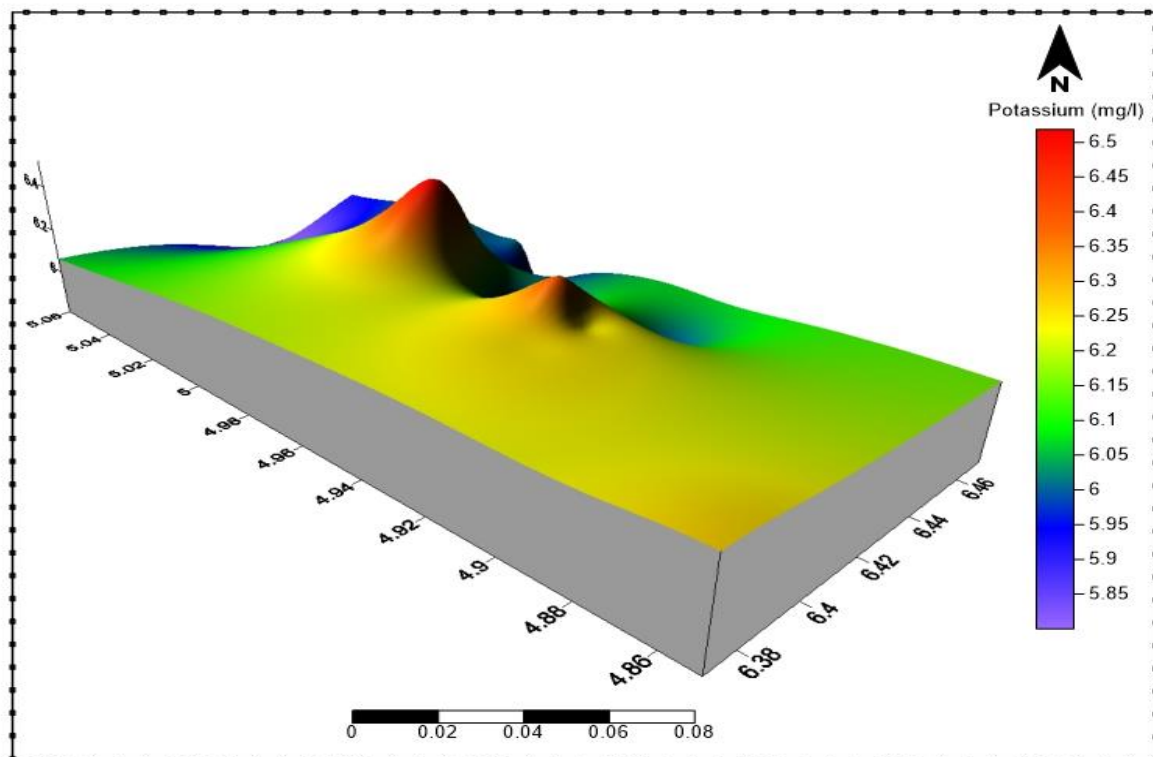


Fig 4.8d: 3D view of Potassium in Kolo Creek Surface water

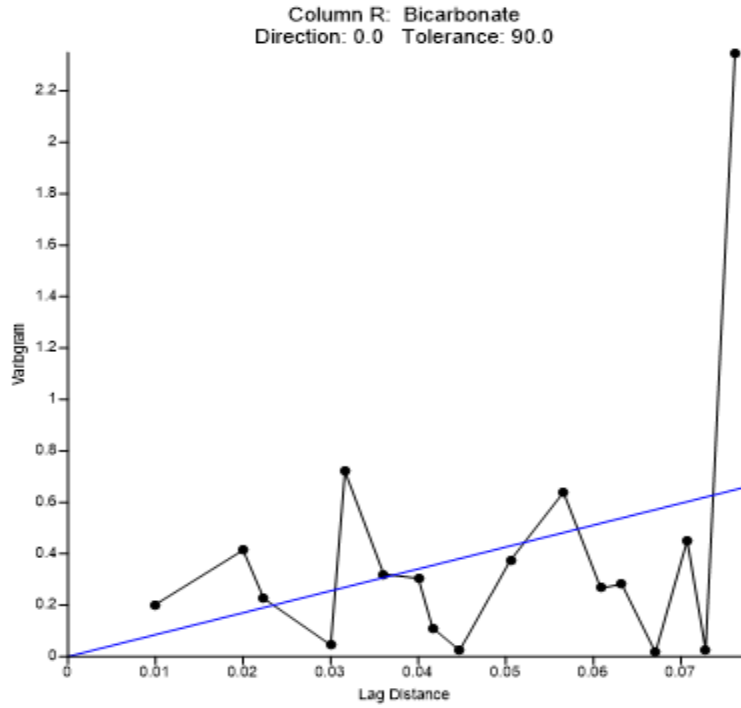


Fig 4.9a: Variogram of Bicarbonate in Kolo Creek Surface water

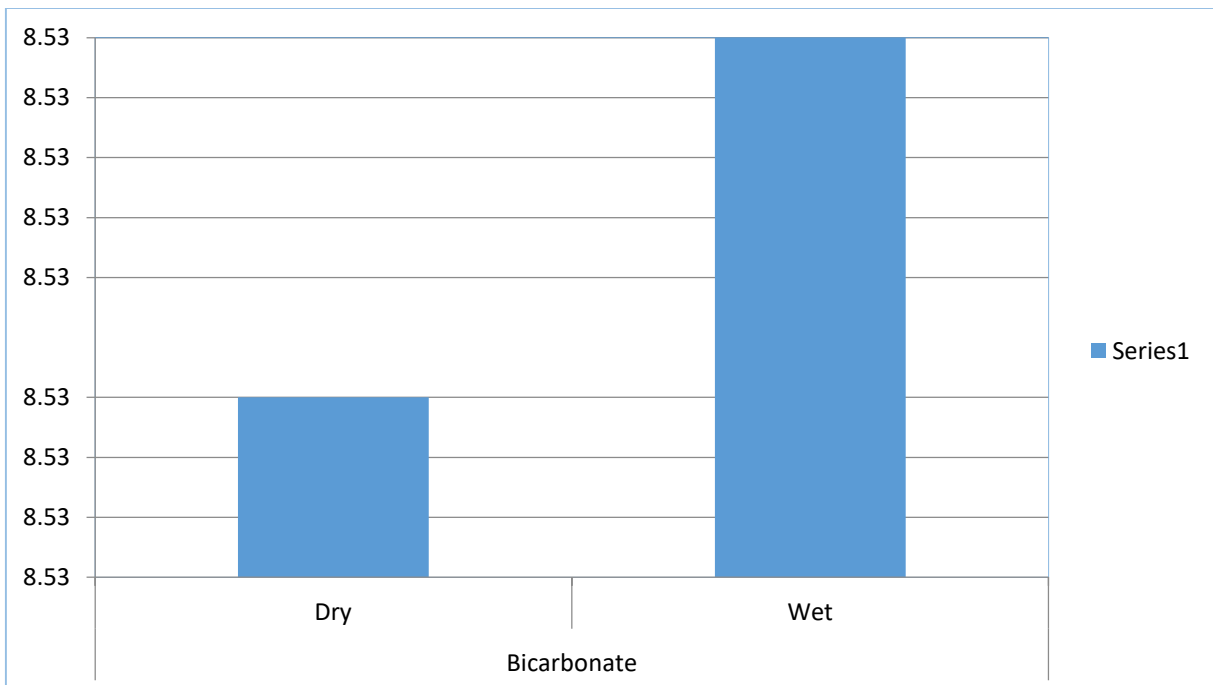


Fig: 4.9b Seasonal Variation of Bicarbonate in Kolo Creek Surface water.

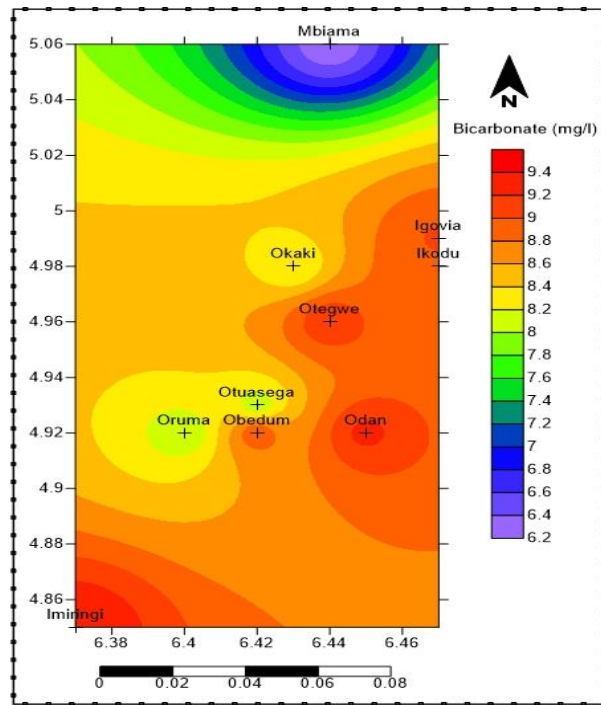


Fig 4.9c: Spatial Distribution of Bicarbonate in Kolo Creek Surface water

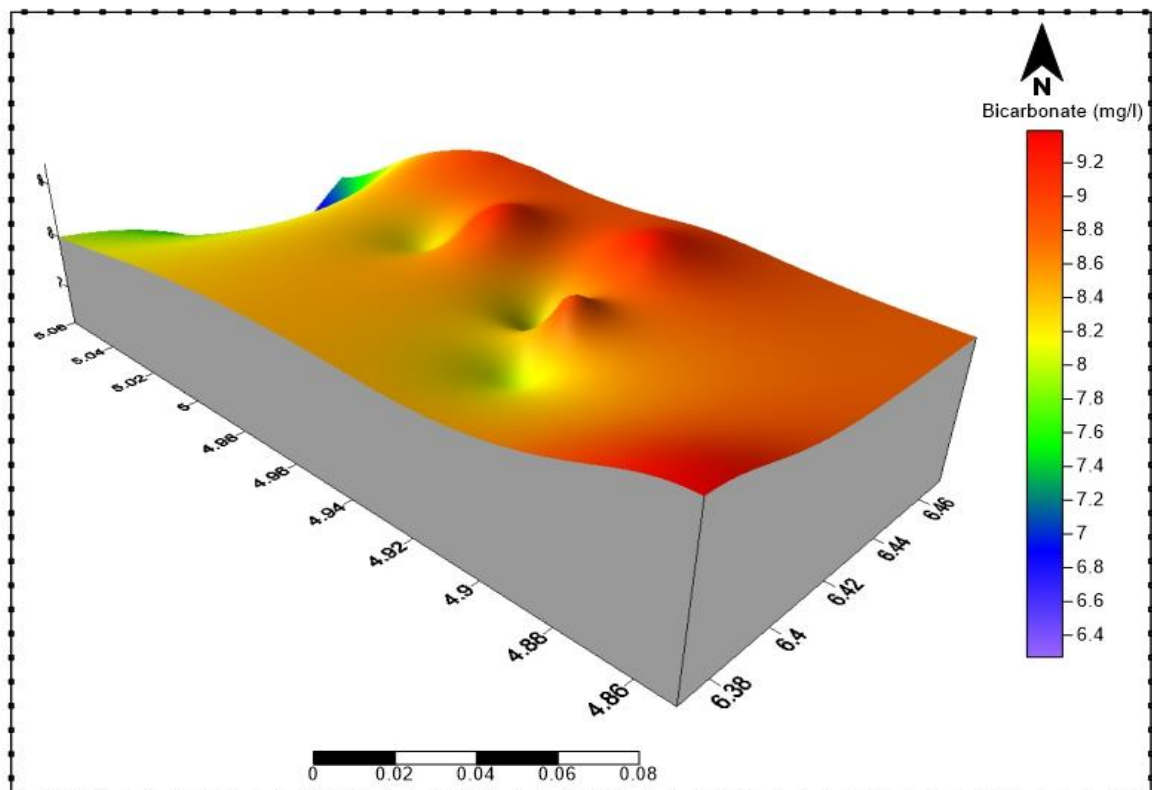
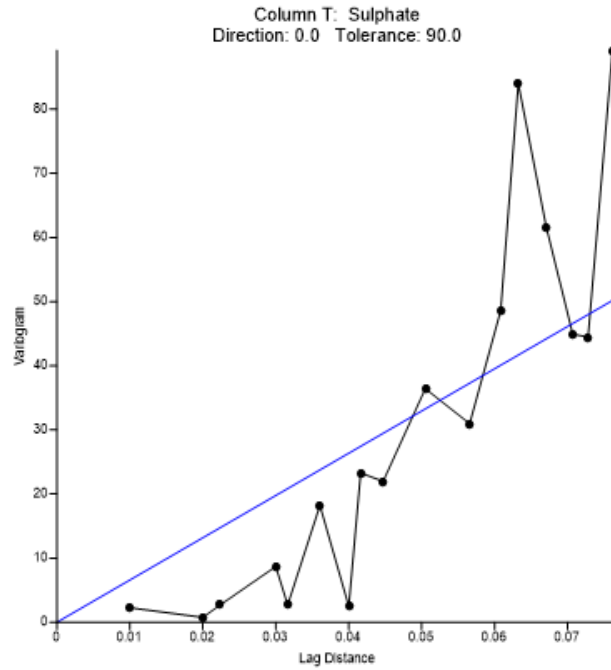
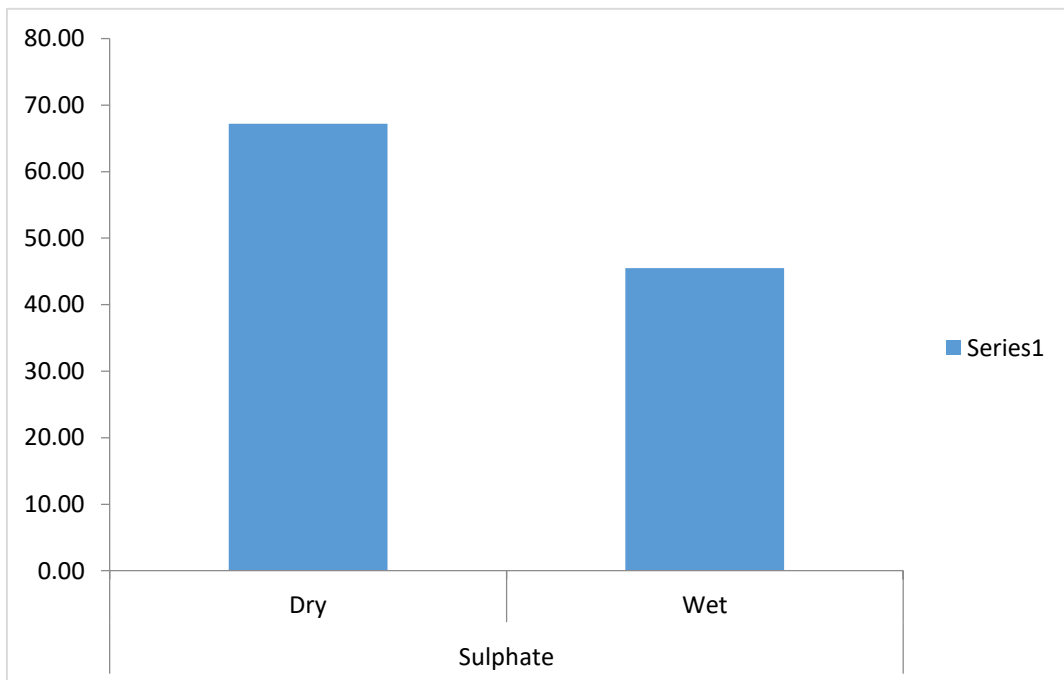


Fig 4.9d: 3D view of Bicarbonate in Kolo Creek Surface water



**Fig 4.10a: Variogram of Sulphate in Kolo Creek Surface water**



**Fig: 4.10b Seasonal Variation of Sulphate in Kolo Creek Surface water.**

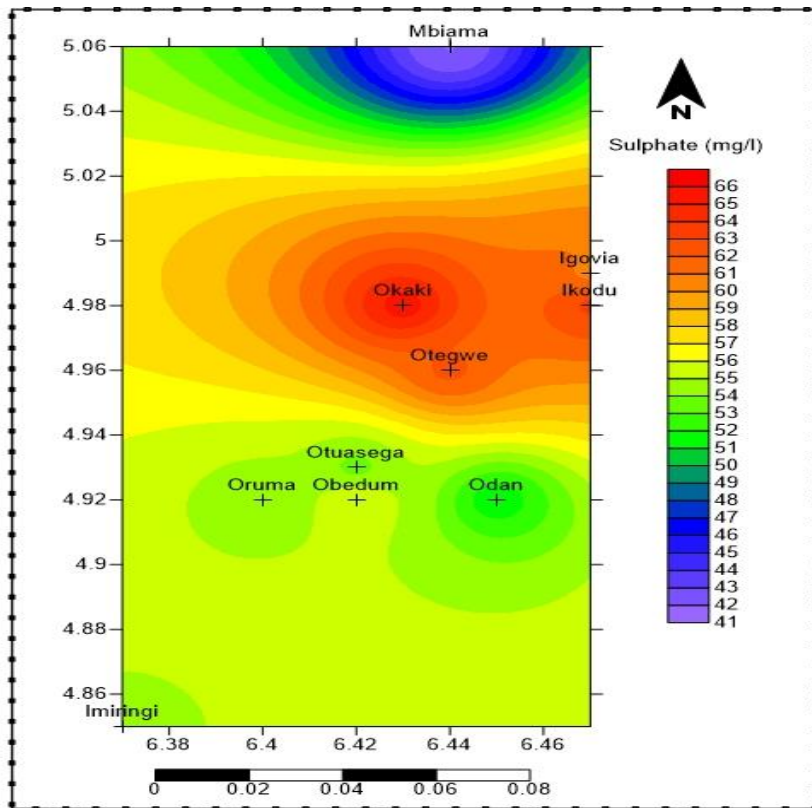


**Fig 4.10c: Spatial Distribution of Sulphate in Kolo Creek Surface water**

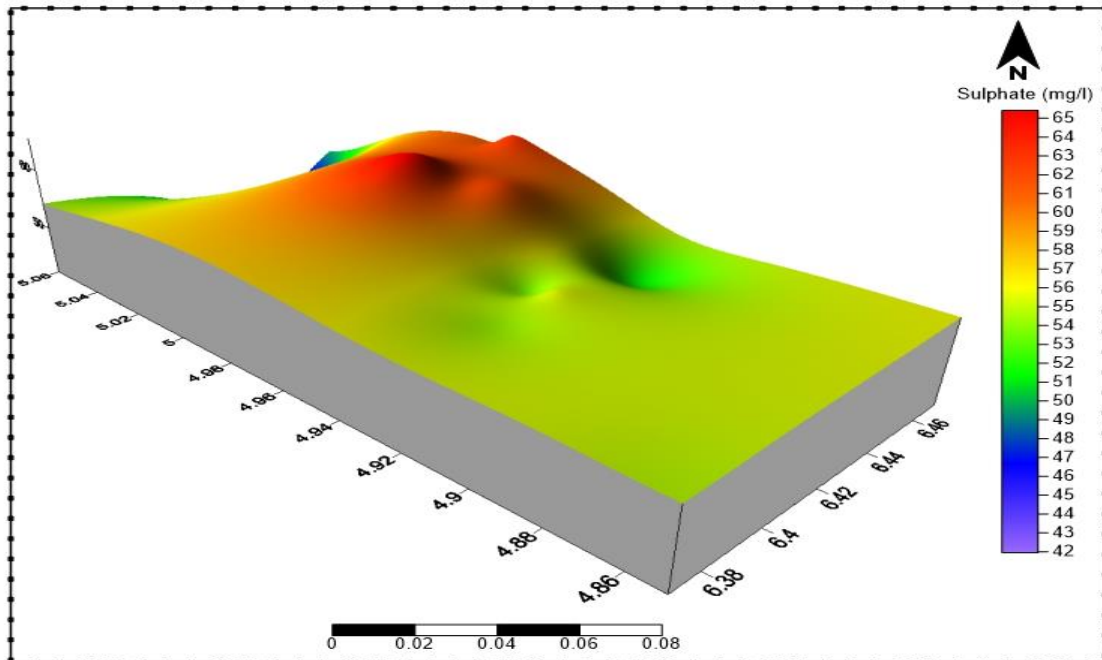


**Fig 4.13d: 3D view of Sulpahte in Kolo Creek Surface water**

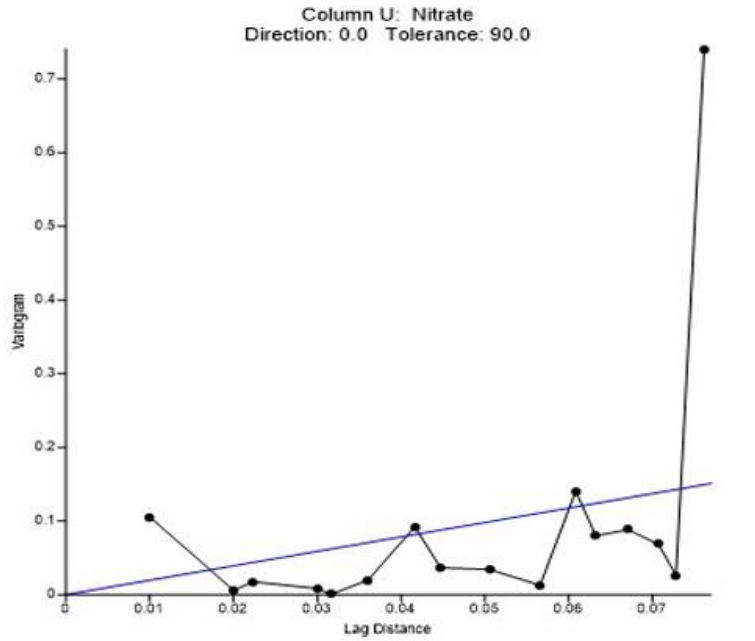


**Fig 4.11a: Variogram of Nitrates in Kolo Creek Surface water**

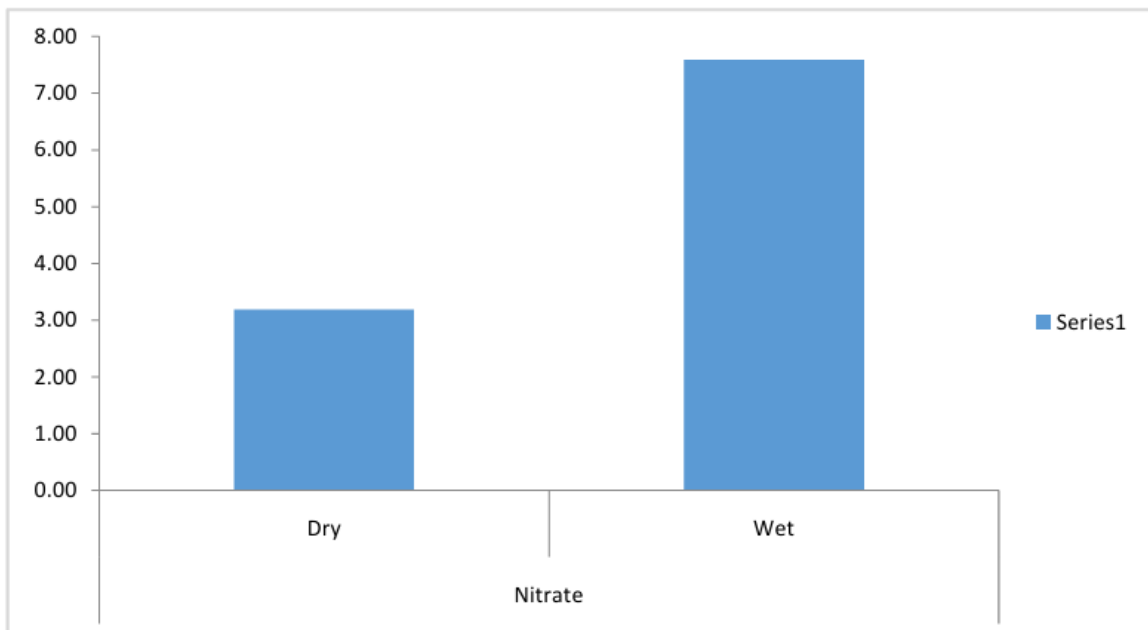


**Fig: 4.11b Seasonal Variation of Nitrate in Kolo Creek Surface water.**

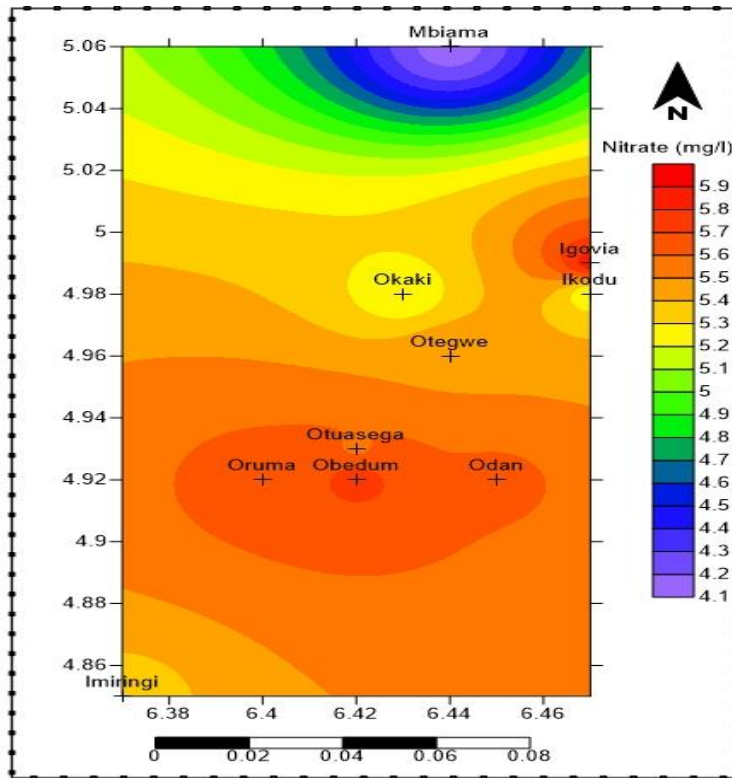


**Fig 4.11c: Spatial Distribution of Nitrate in Kolo Creek Surface water**

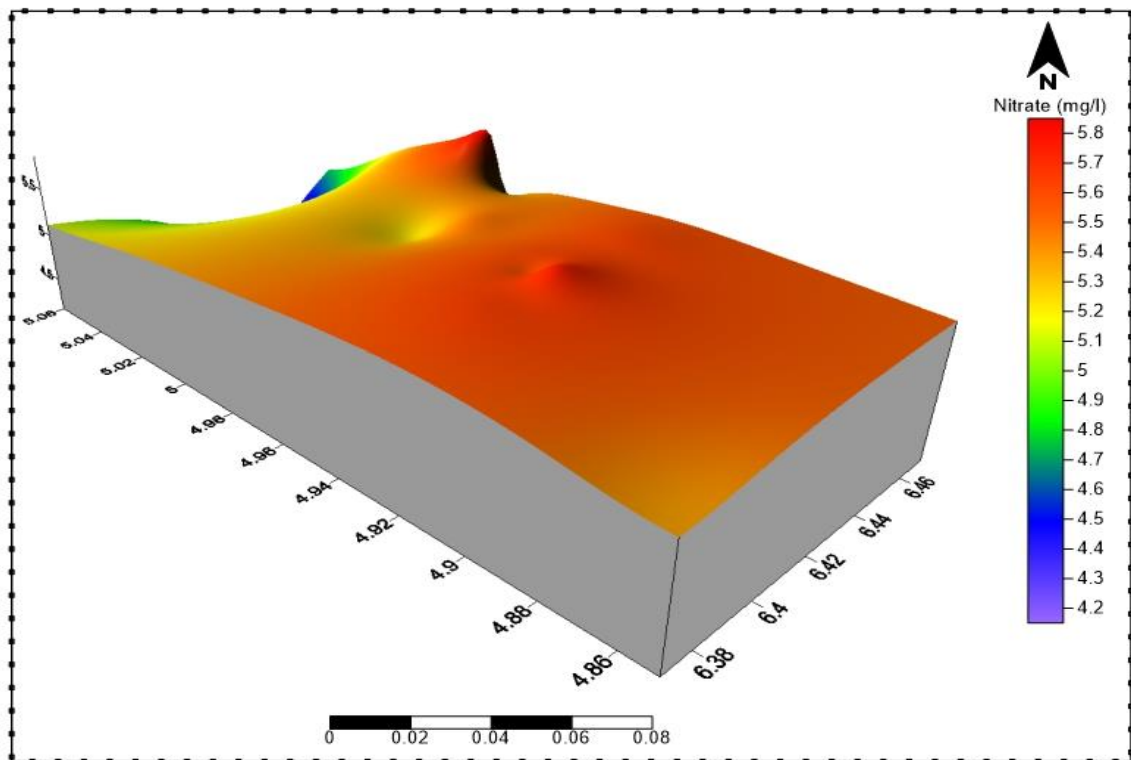


**Fig 4.11d: 3D view of Nitrate in Kolo Creek Surface water**

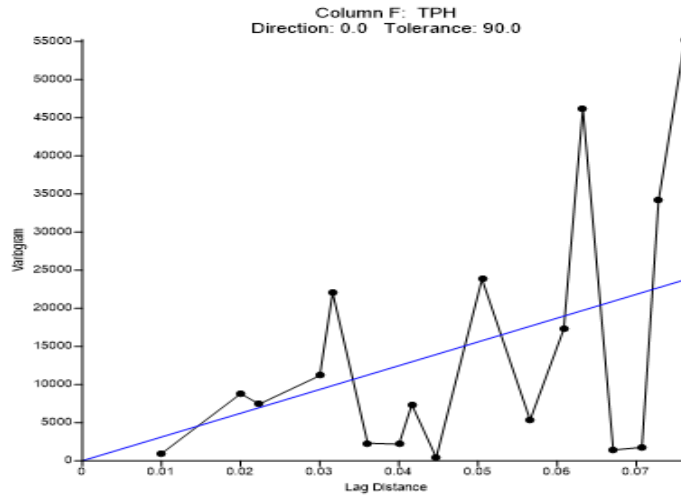


**Fig 4.12a: Variogram of Total Petroleum Hydrocarbon in Kolo Creek Surface water**

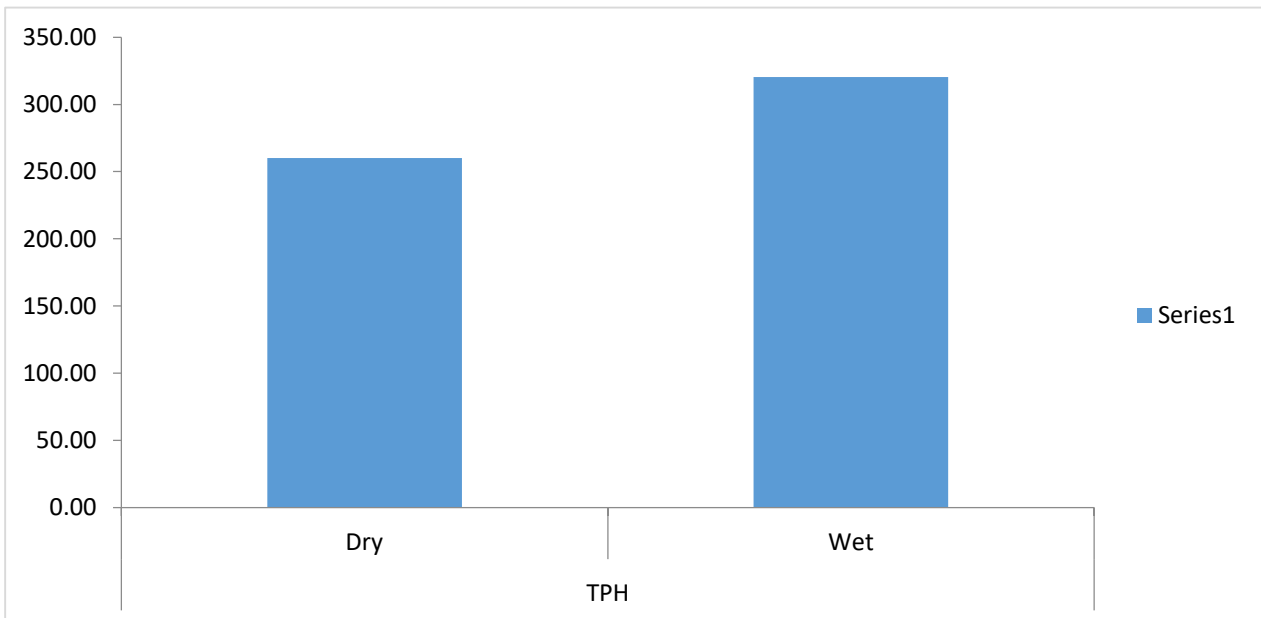


**Fig 4.12b: Seasonal Variations of Total Petroleum Hydrocarbon in Kolo Creek Surface water.**

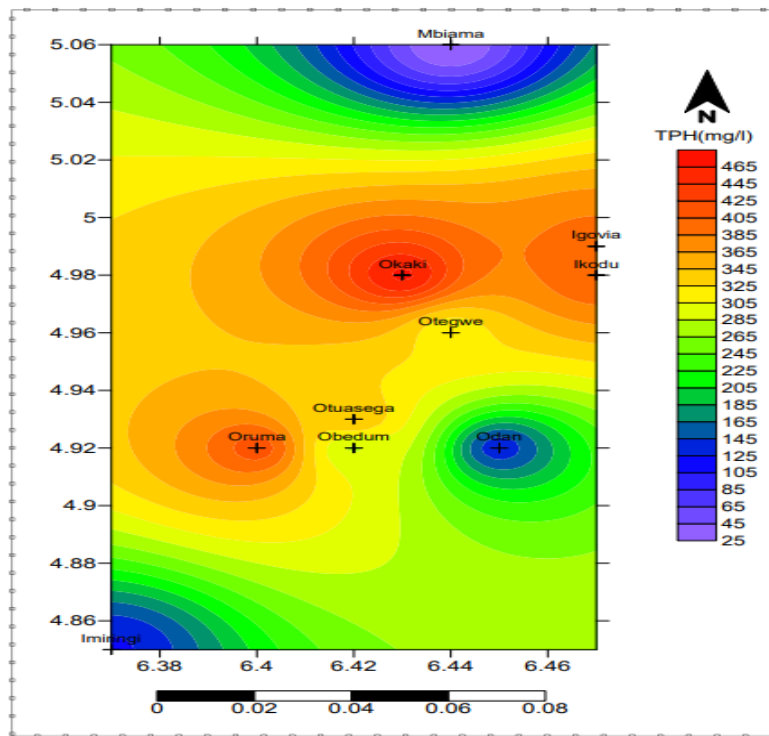


**Fig 4.12c: Spatial Distribution of TPH in Kolo Creek Surface water**

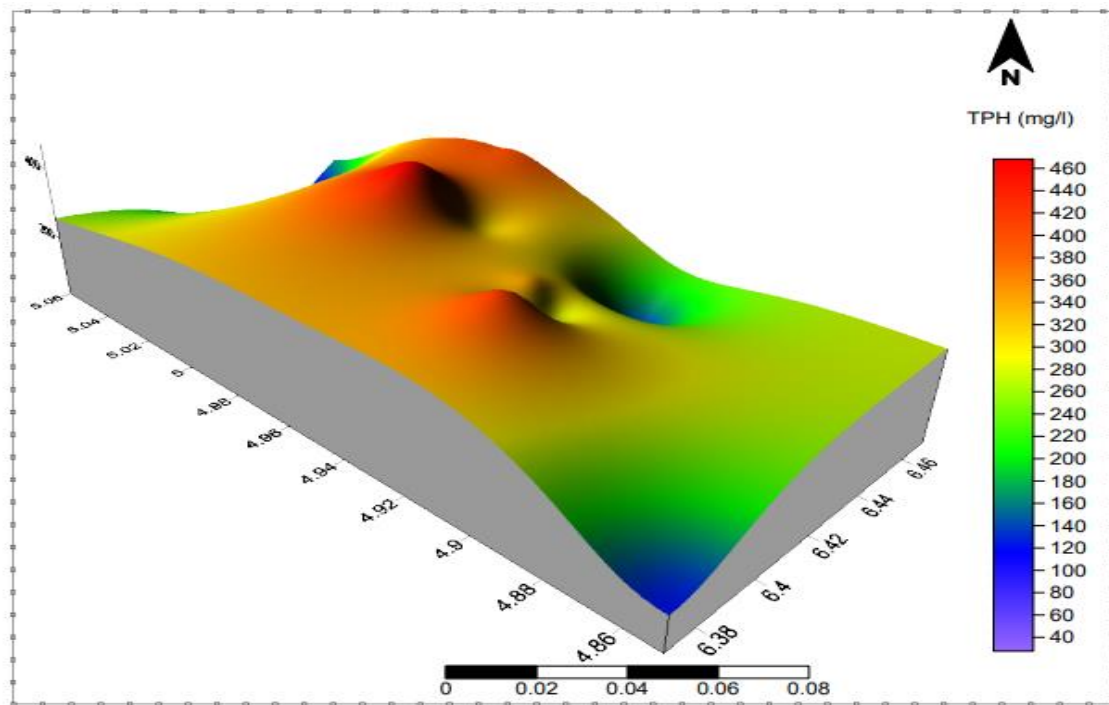


**Fig 4.12d: 3D view of TPH in Kolo Creek Surface water**

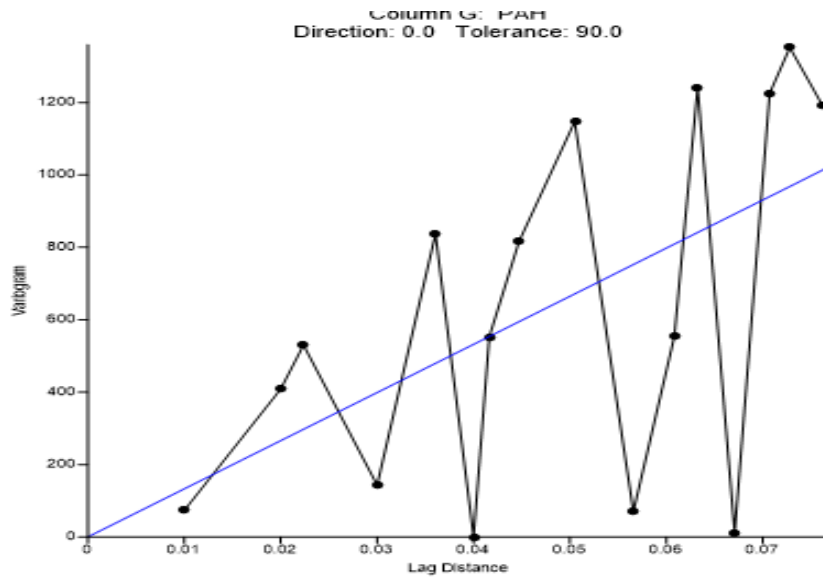


**Fig 4.13a: Variogram of PAH in Kolo Creek Surface water**

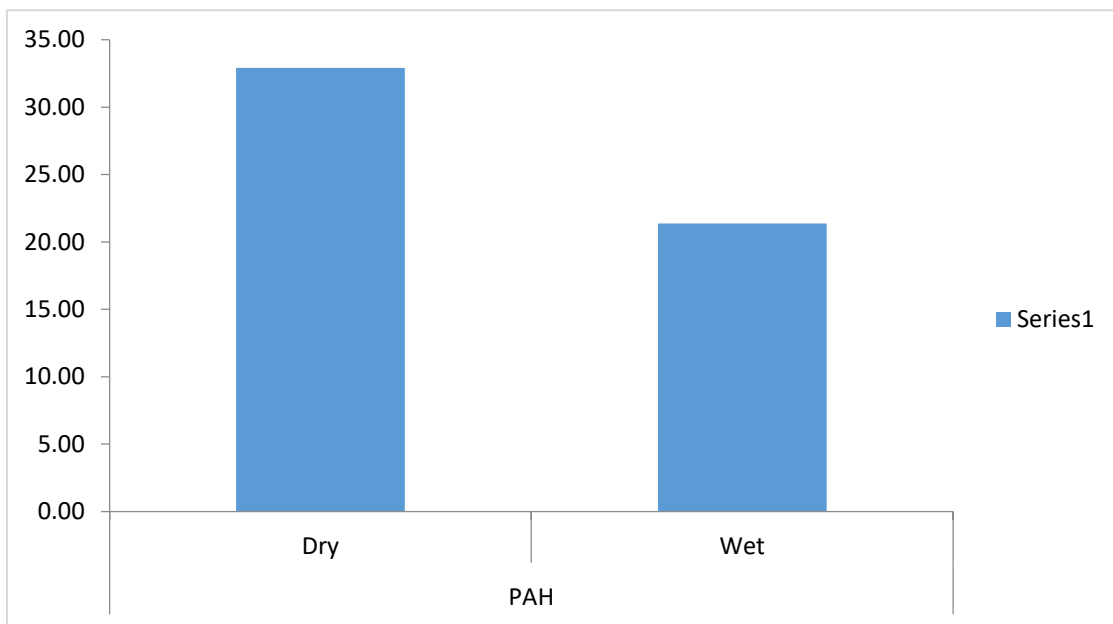


**Fig 4.13b: Seasonal Variation of PAH in Kolo-Creek Surface water**

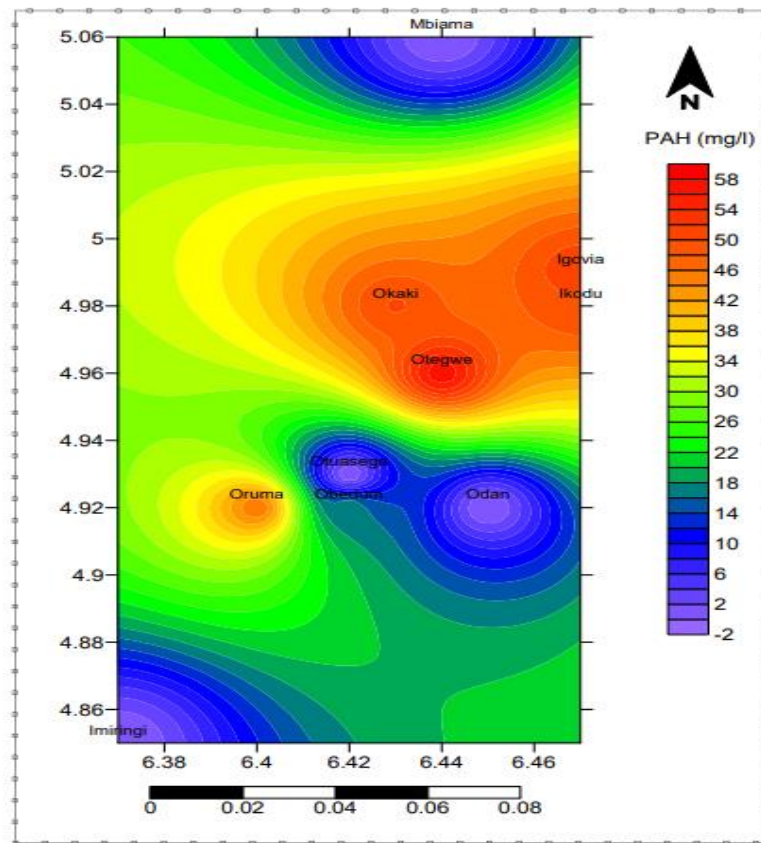


**Fig 4.13c: Spatial Distribution of PAH in Kolo Creek Surface water**

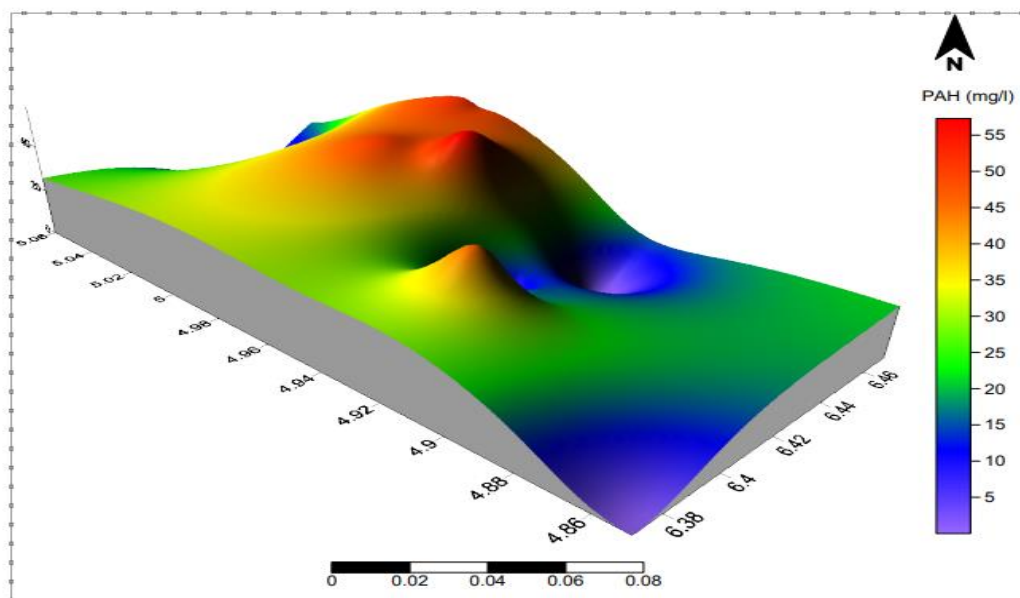


**Fig 4.13d: 3D view of PAH in Kolo Creek Surface water**

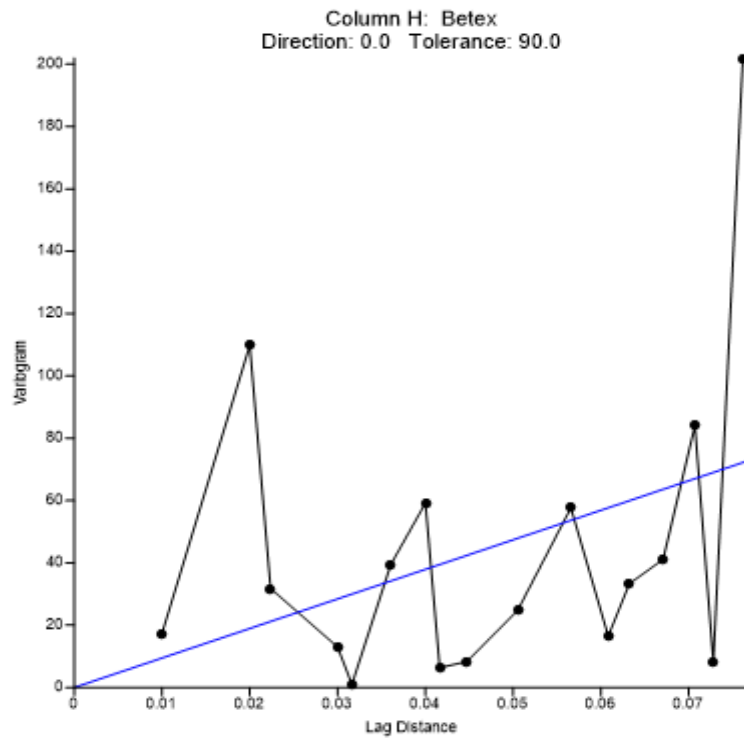


**Fig 4.14a: Variogram of Betex in Kolo Creek Surface water**

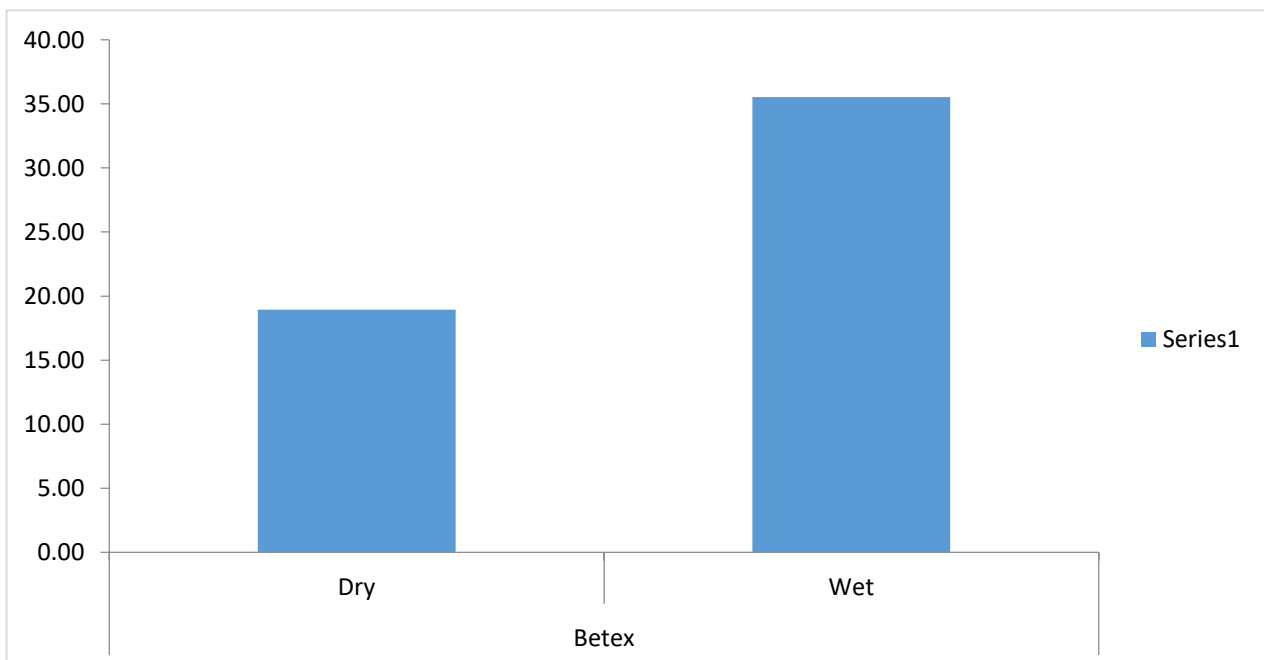


**Fig: 4.14b Seasonal Variations of Betex in Kolo Creek Surface water.**

**Fig 4.14c: Spatial Distribution of Betex in Kolo Creek Surface water**

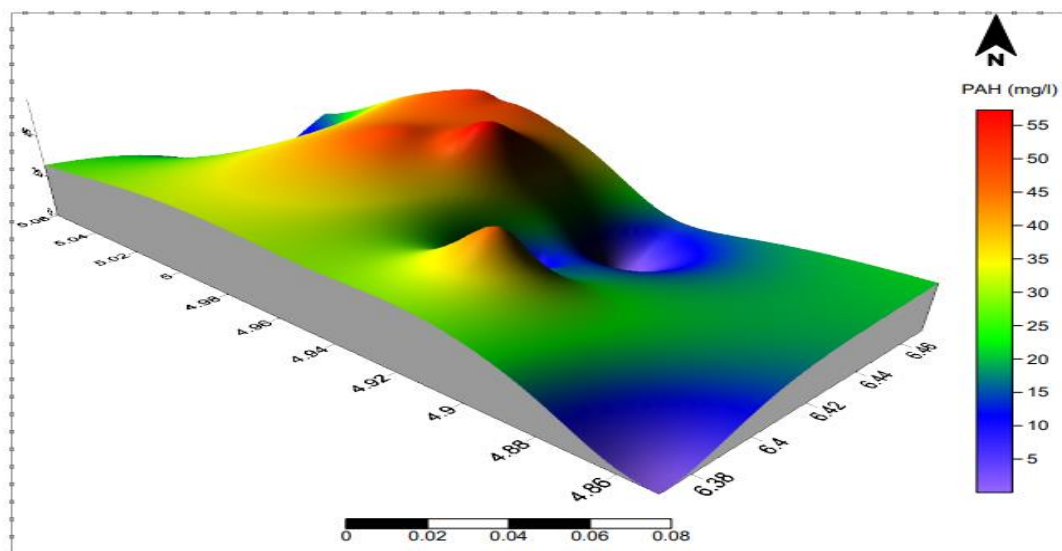


**Fig 4.14d: 3D view of Betex in Kolo Creek Surface water**

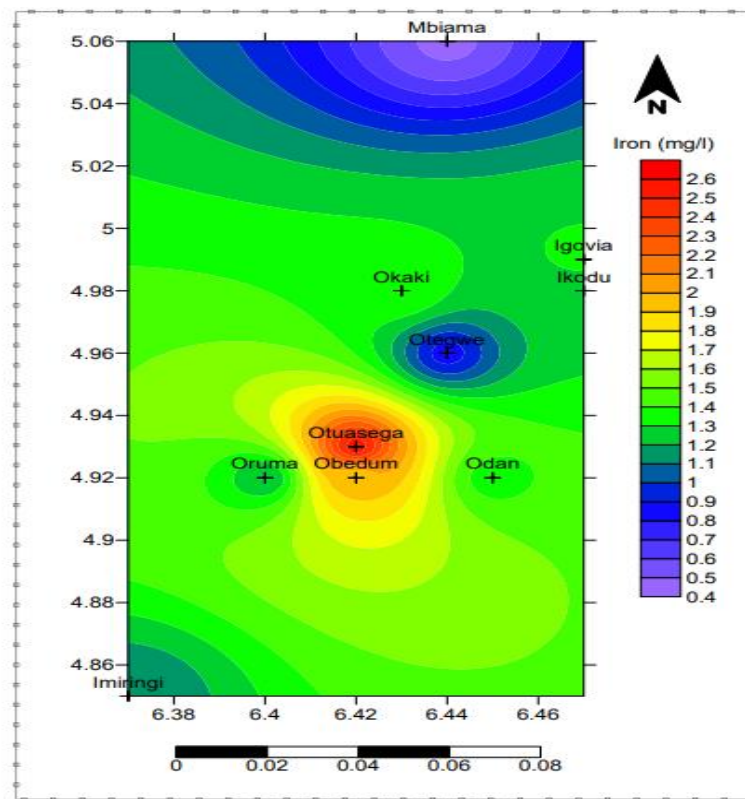


**Fig 4.15a: Spatial Distribution of Iron in Kolo Creek Surface water**

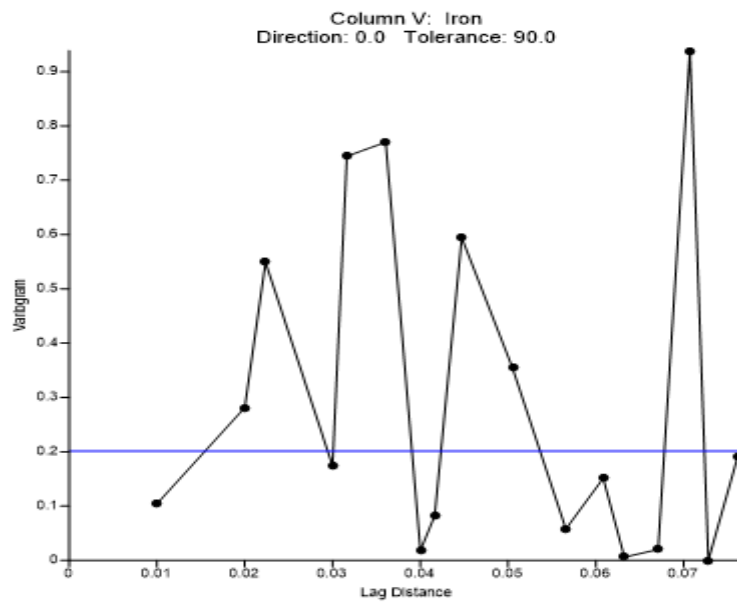


**Fig 4.15b: Variogram of Iron in Kolo Creek Surface water**

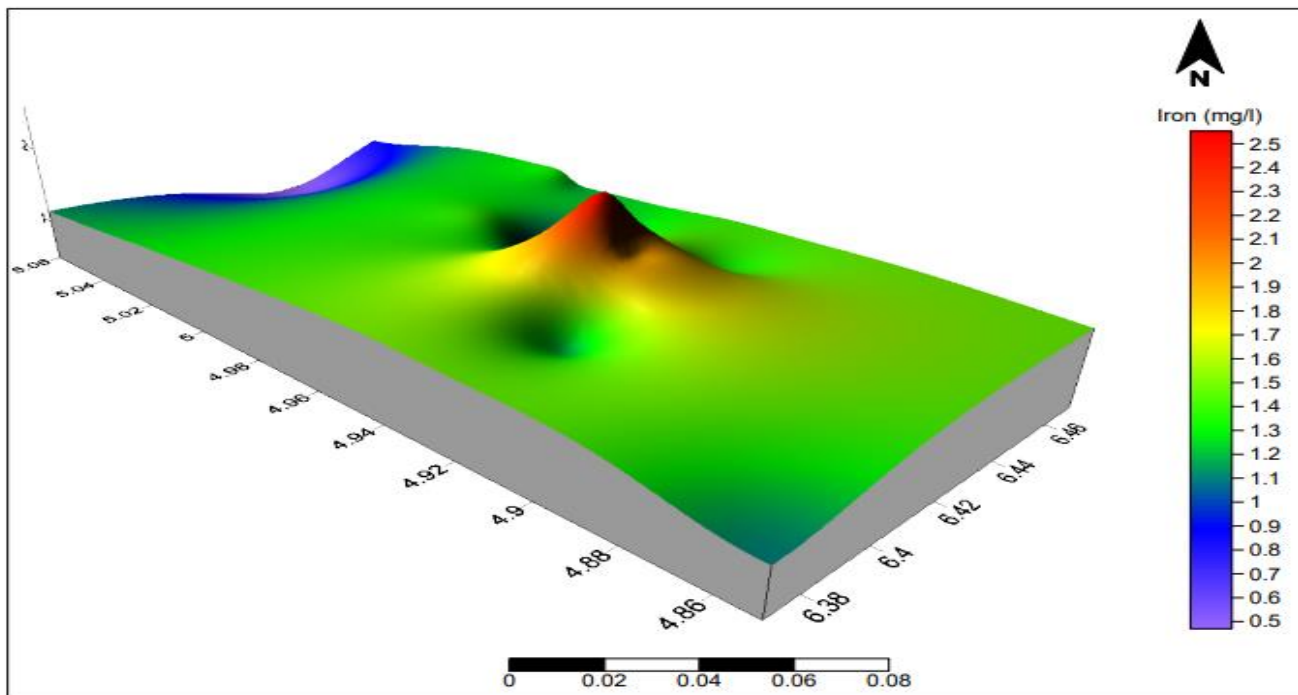


**Fig 4.15c: 3D view of Iron in Kolo Creek Surface water**

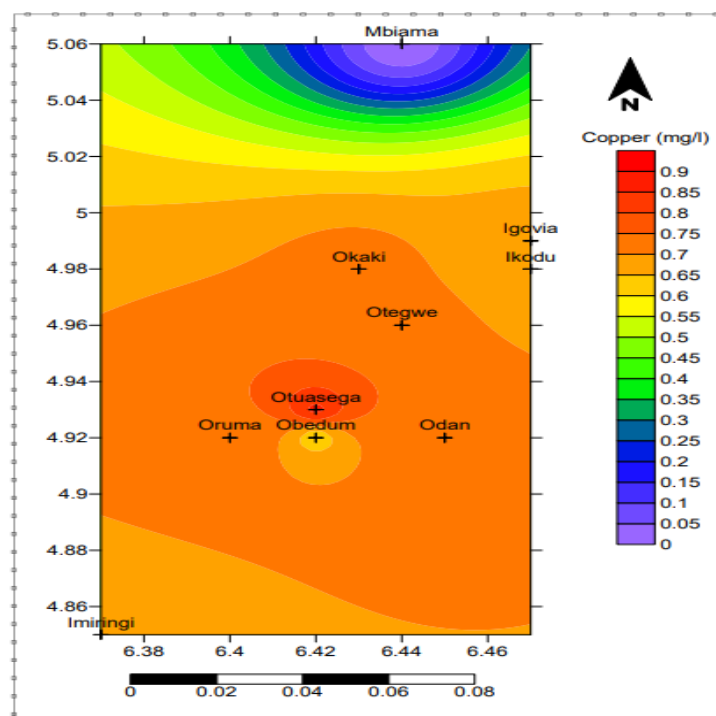


**Fig 4.16a: Spatial Distribution of Copper in Kolo-Creek Surface water**

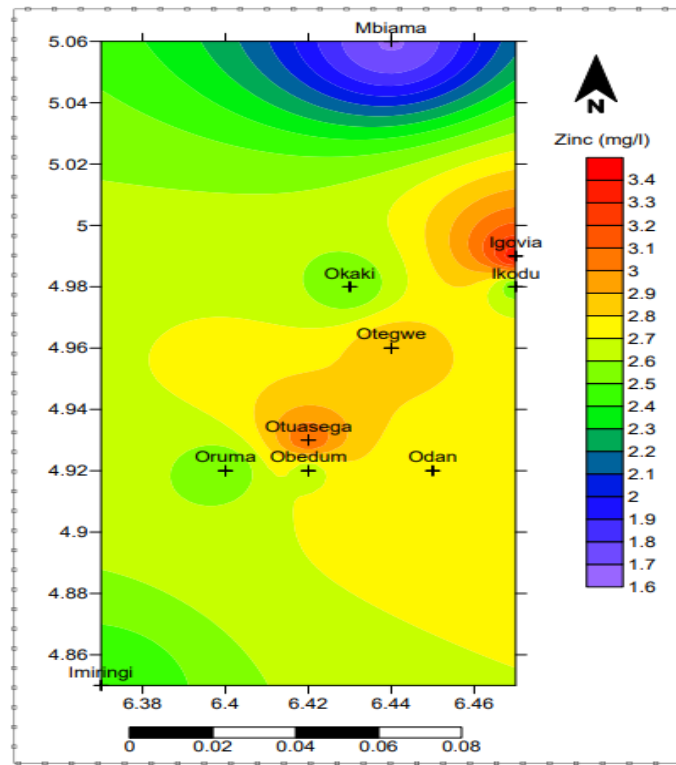


**Fig 4.17a: Spatial Distribution of Zinc in Kolo Creek Surface water**

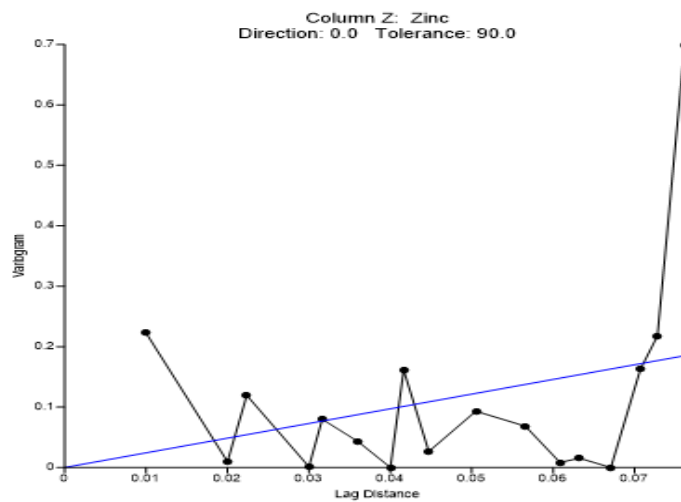


**Fig 4.17b: Variogram of Zinc in Kolo Creek Surface water**

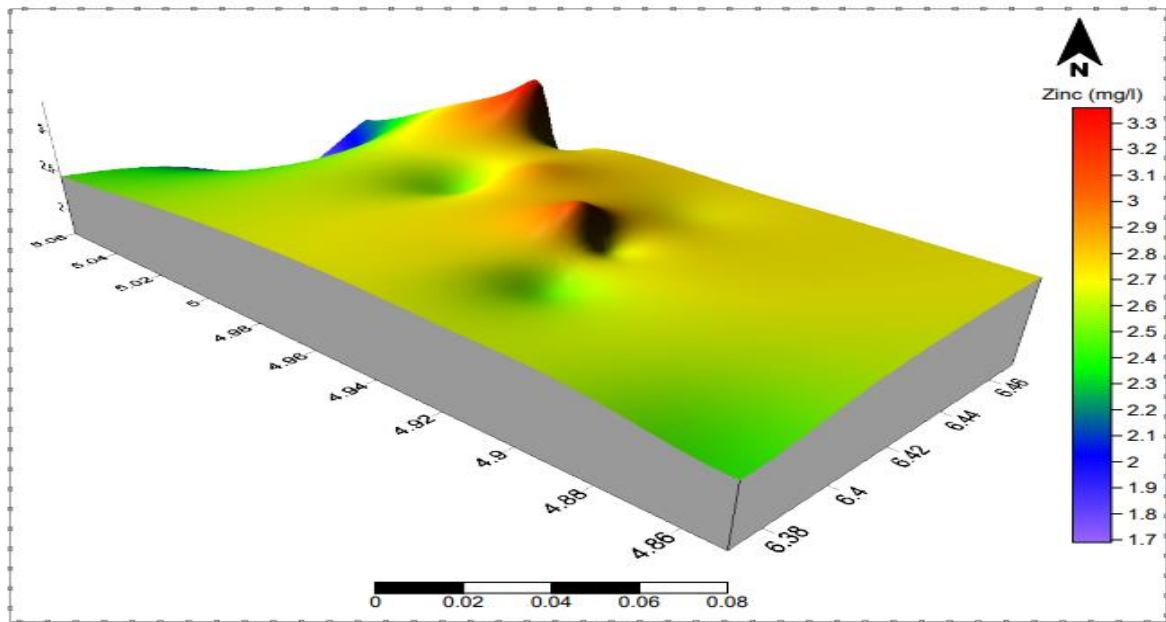


**Fig 4.17c: 3D view of Zinc in Kolo Creek Surface water**

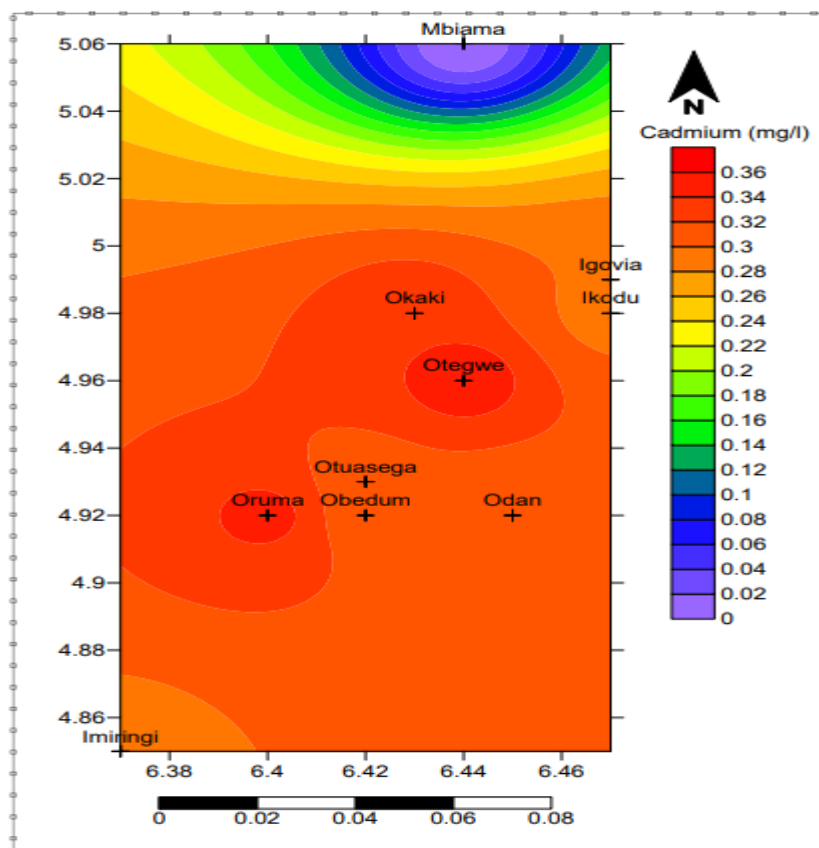


**Fig 4.18a: Spatial Distribution of Cadmium in Kolo Creek Surface water**

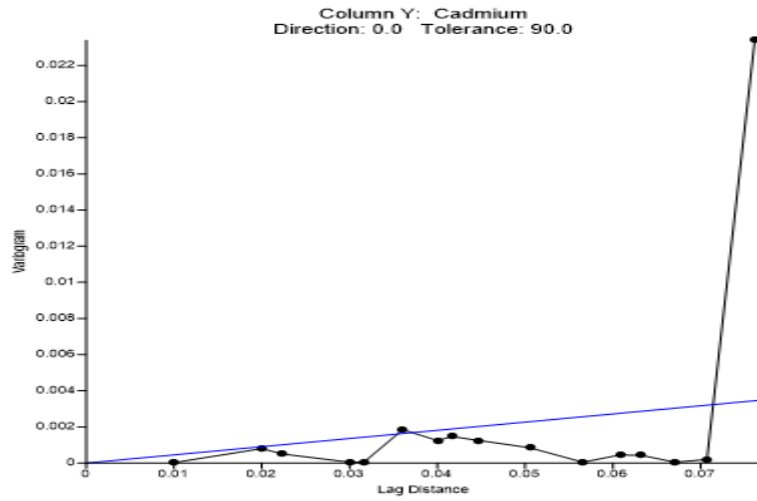


**Fig 4.18b: Variogram of Cadmium in Kolo Creek Surface water**

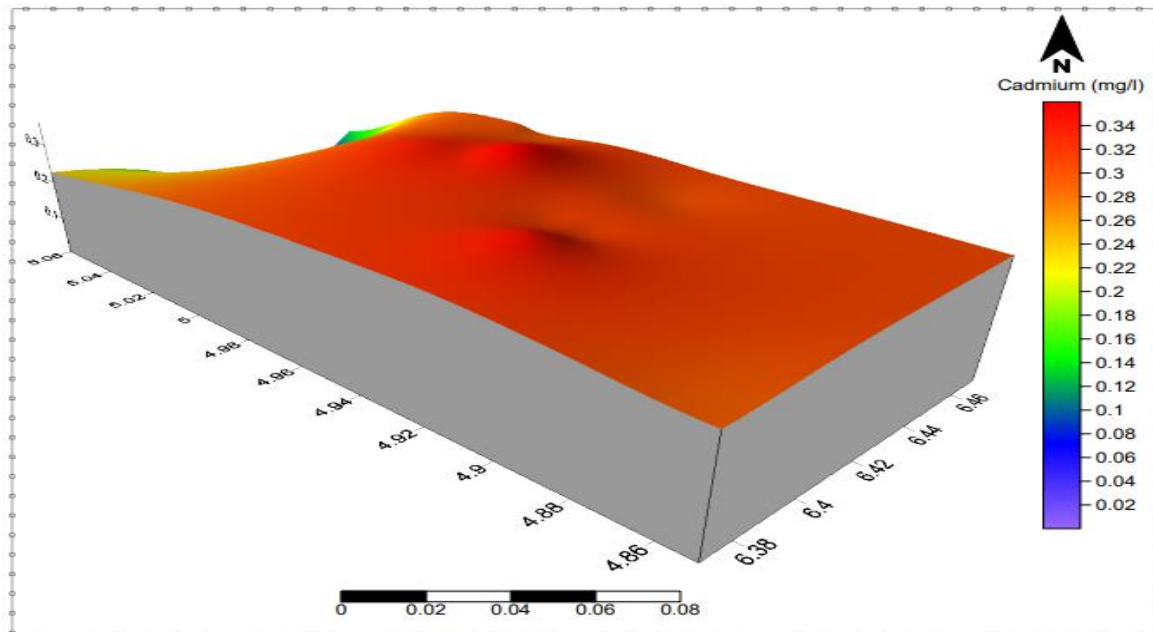


**Fig 4.18c: 3D view of Cadmium in Kolo Creek Surface water**

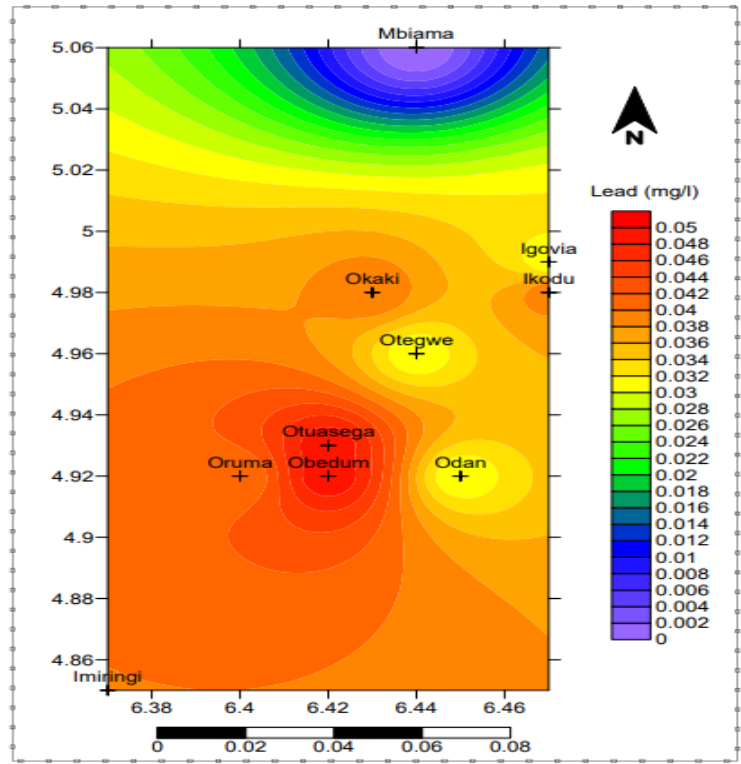


**Fig 4.19a: Spatial Distribution of Lead in Kolo Creek Surface water**

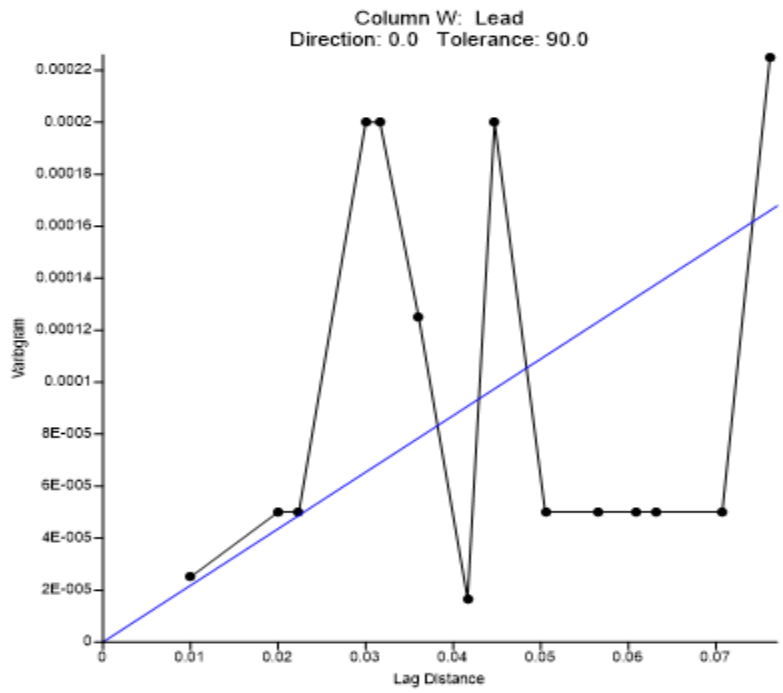


**Fig 4.19b: Variogram of Lead in Kolo Creek Surface water**

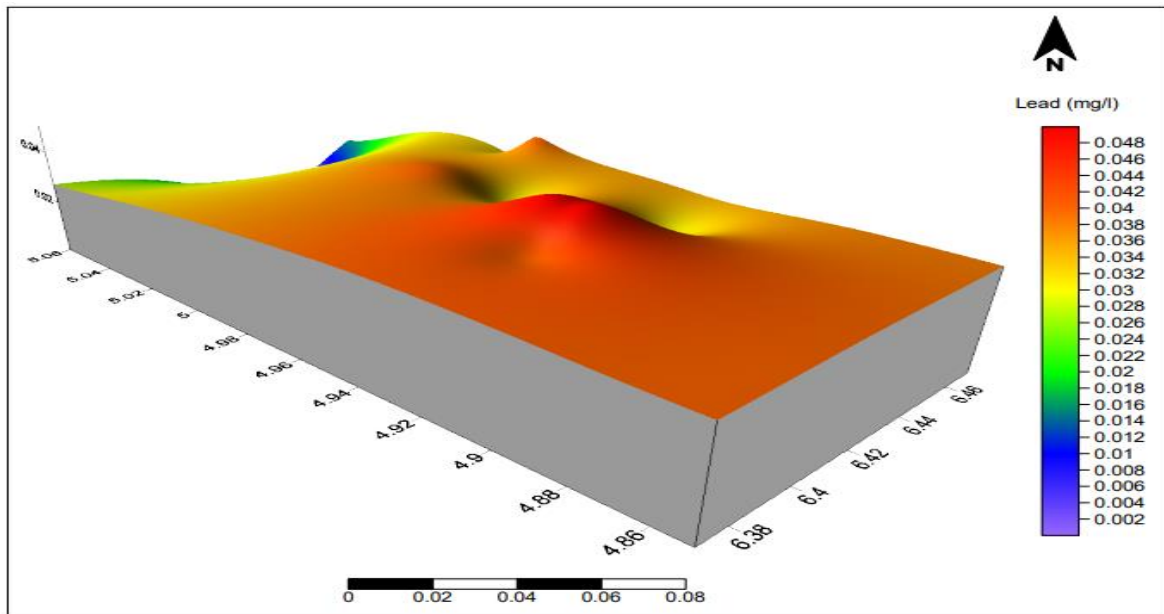


**Fig 4.19c: 3D view of Lead in Kolo Creek Surface water**

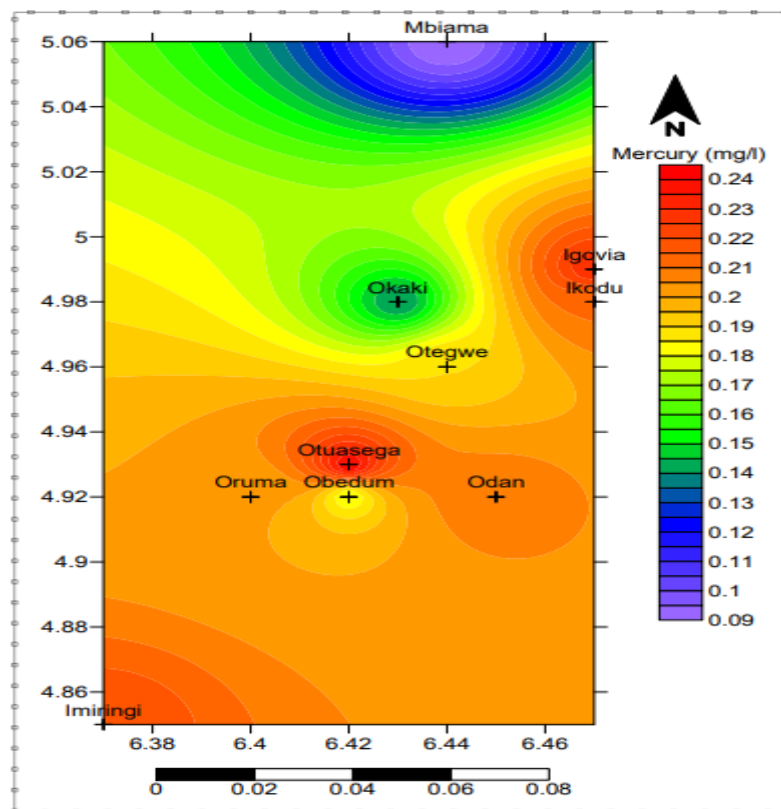


**Fig 4.20a: Spatial Distribution of Mercury in Kolo Creek Surface water**

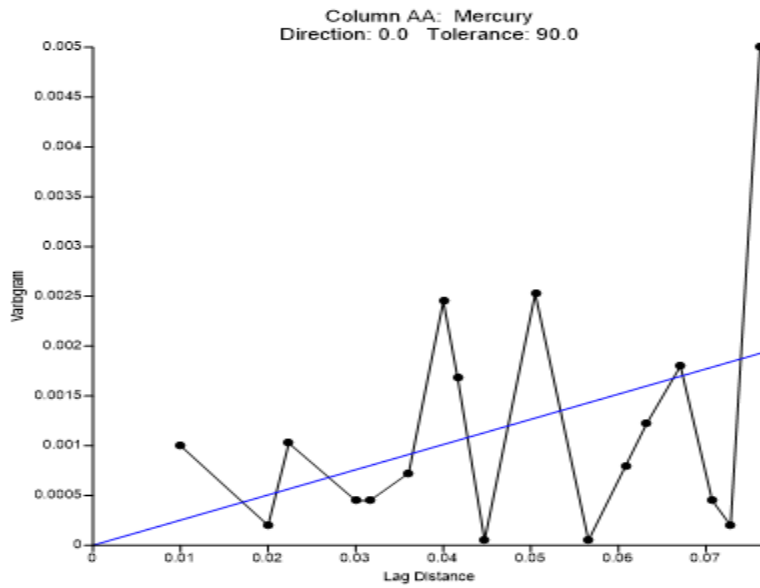


**Fig 4.20b: Variogram of Mercury in Kolo Creek Surface water**

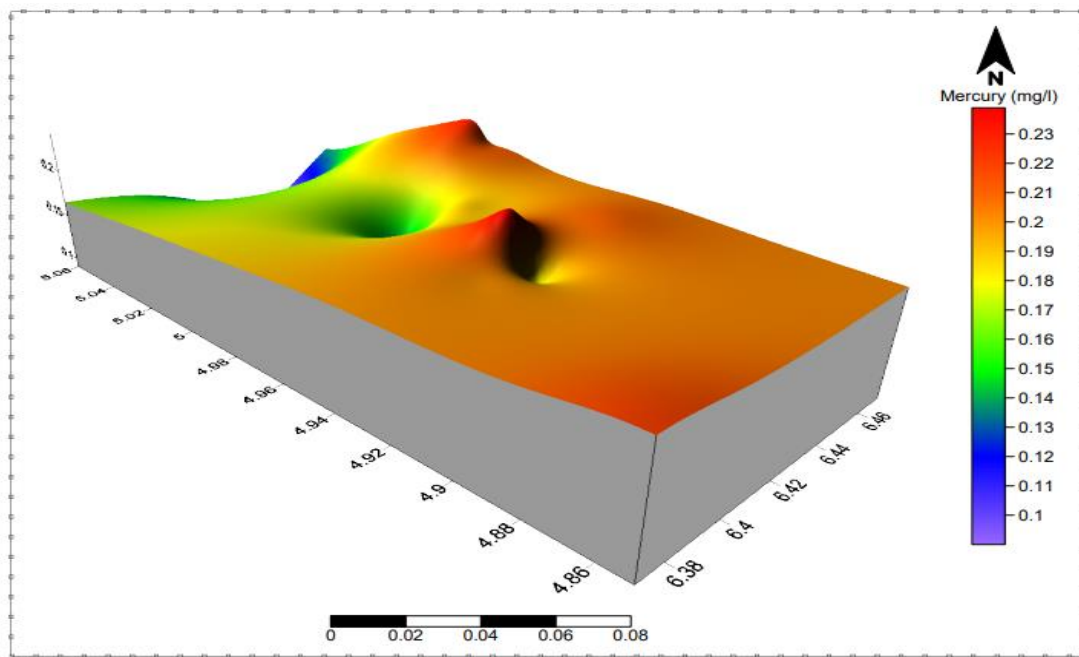


**Fig 4.20c: 3D view of Mercury in Kolo Creek Surface water**

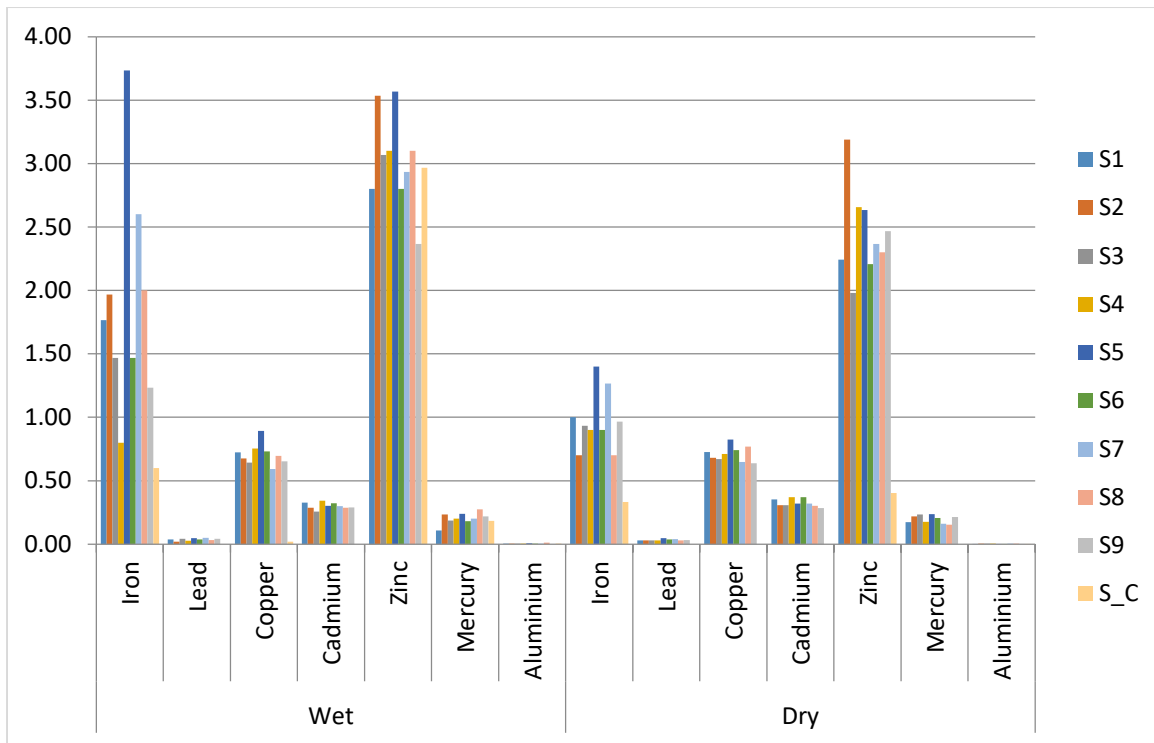


Fig 4.21: Station Variations of Heavy metals in Kolo Creek surface water

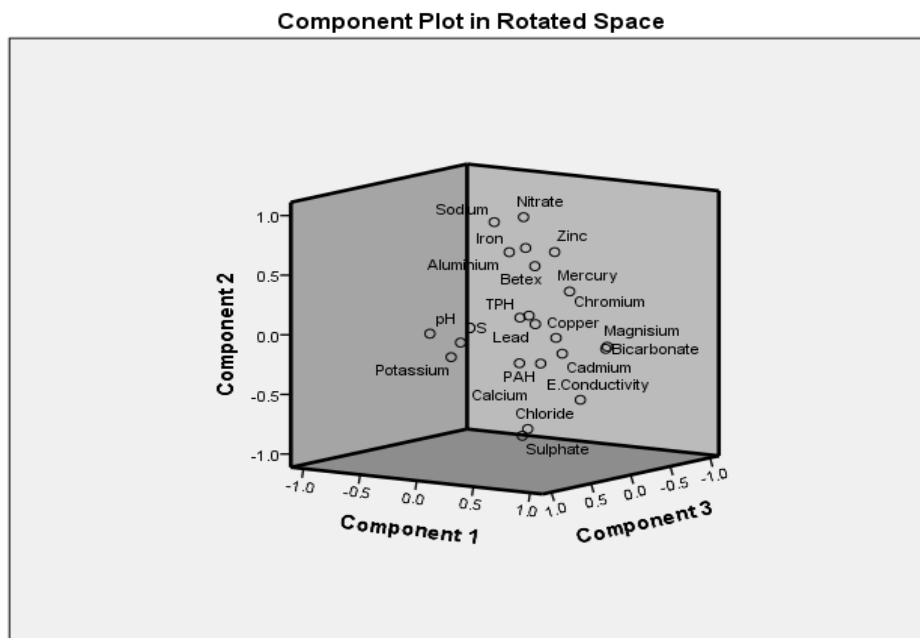


Fig. 4.22: Principal component plot in rotated space

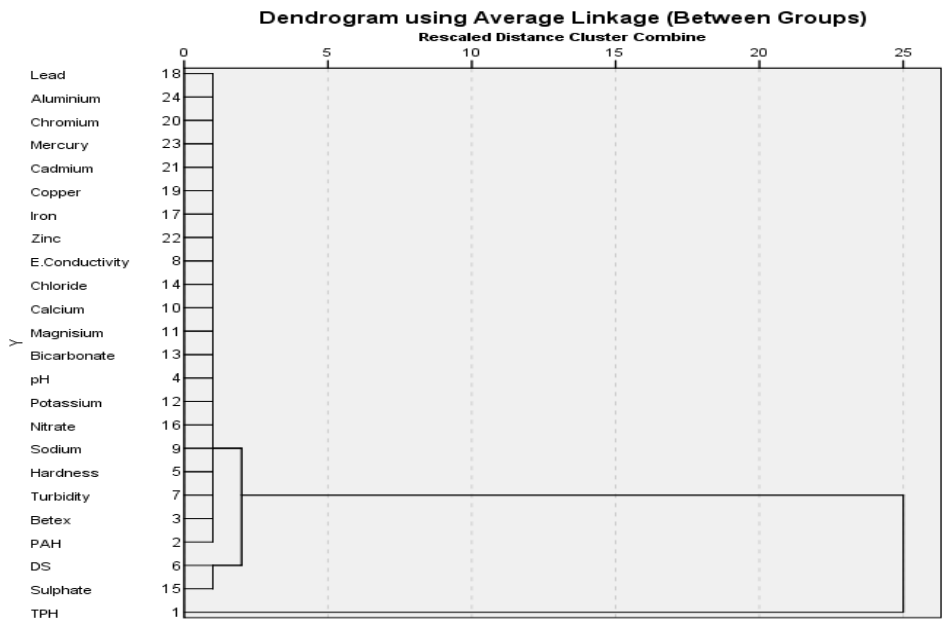


Fig 4.23: Dendrogram of Kolo Creek Surface Water Parameters

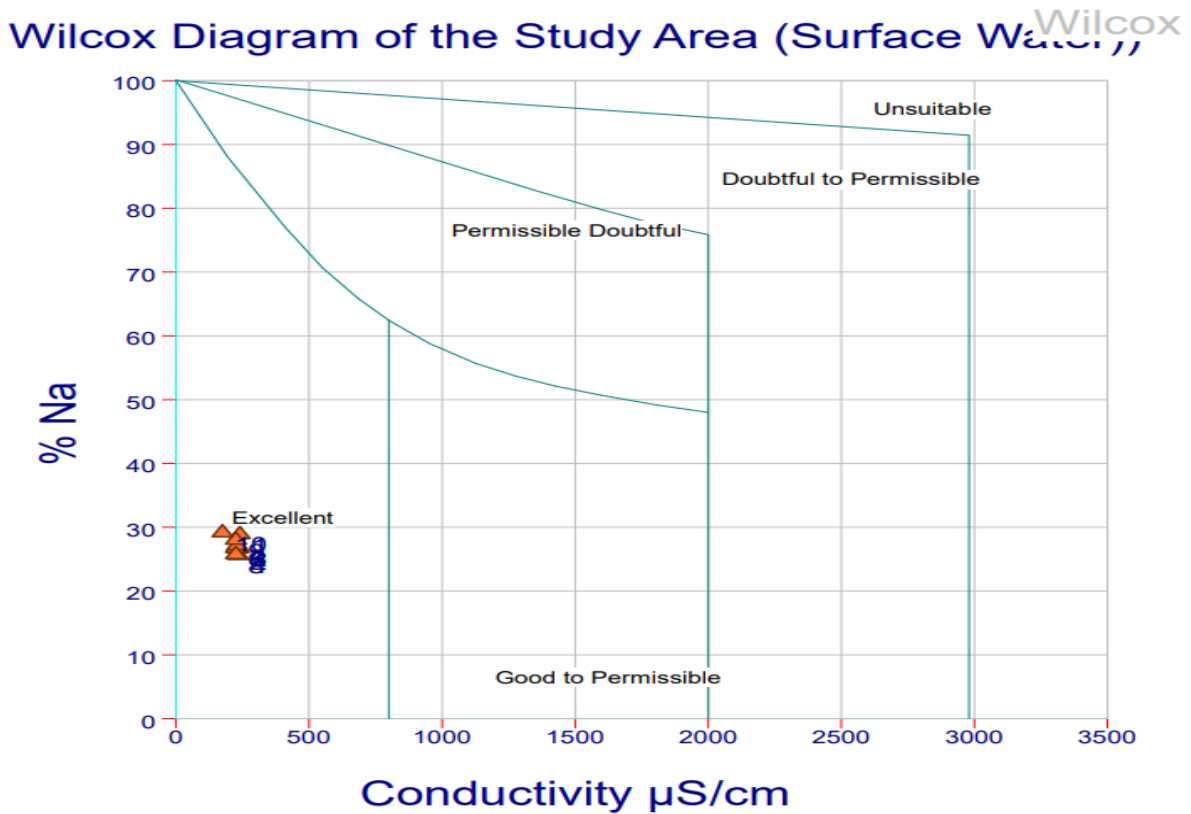
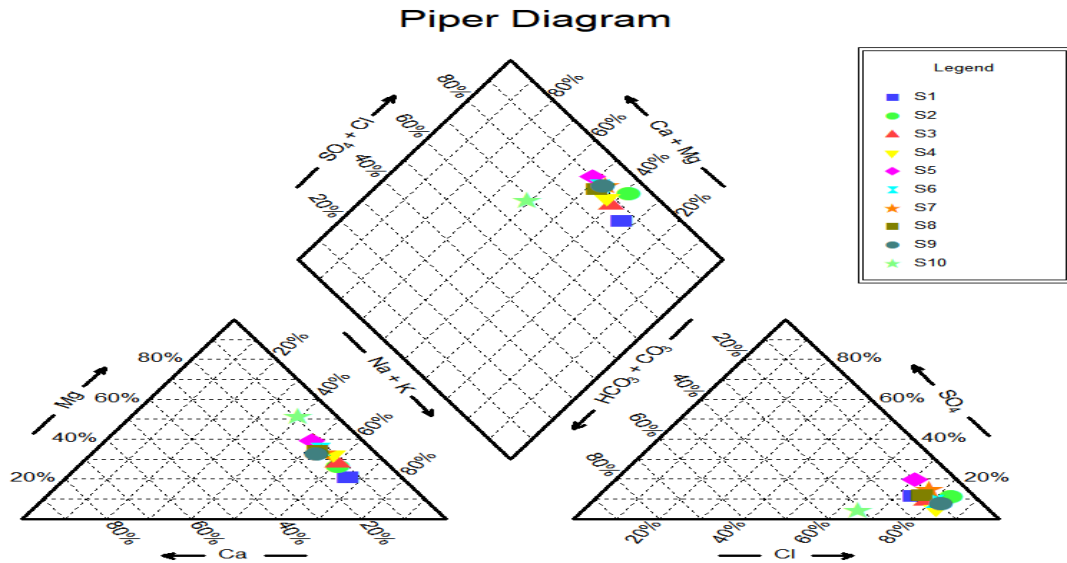
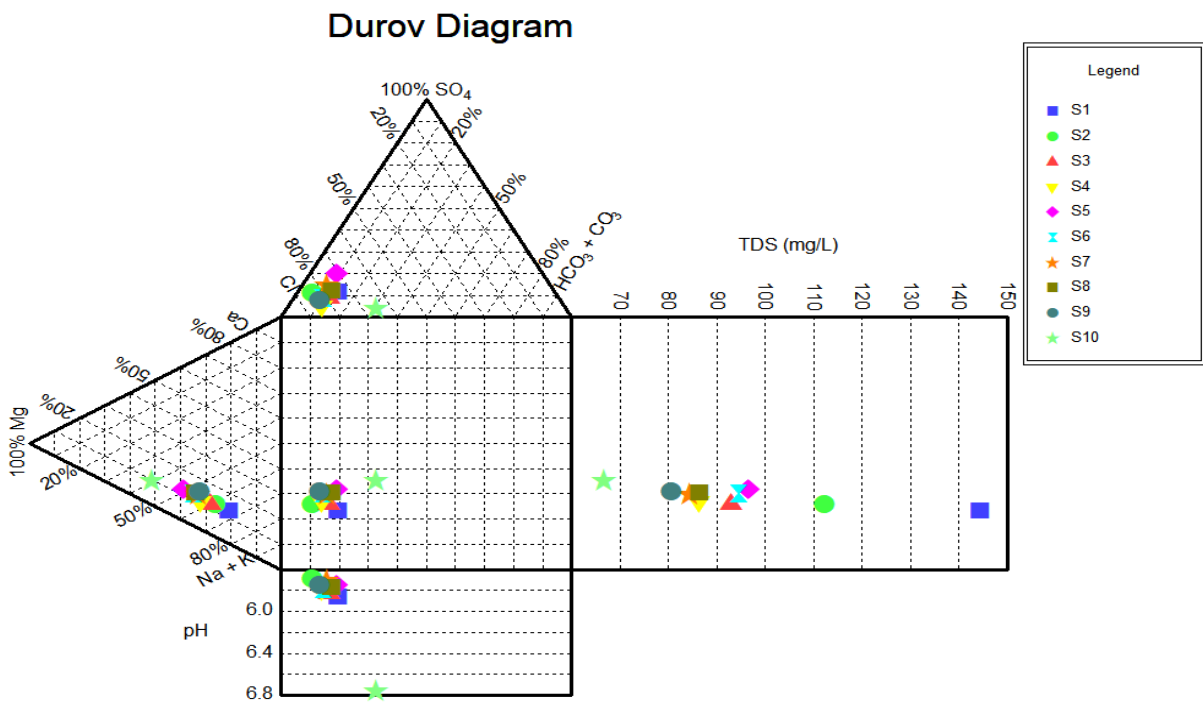


Fig 4.24: Wilcox diagram of the study area Surface water



**Fig 4.25** Piper Diagram Illustrating the Principal Anions and Cations



**Figure 4.26:** Durov Diagram Showing the major Cations and Anions

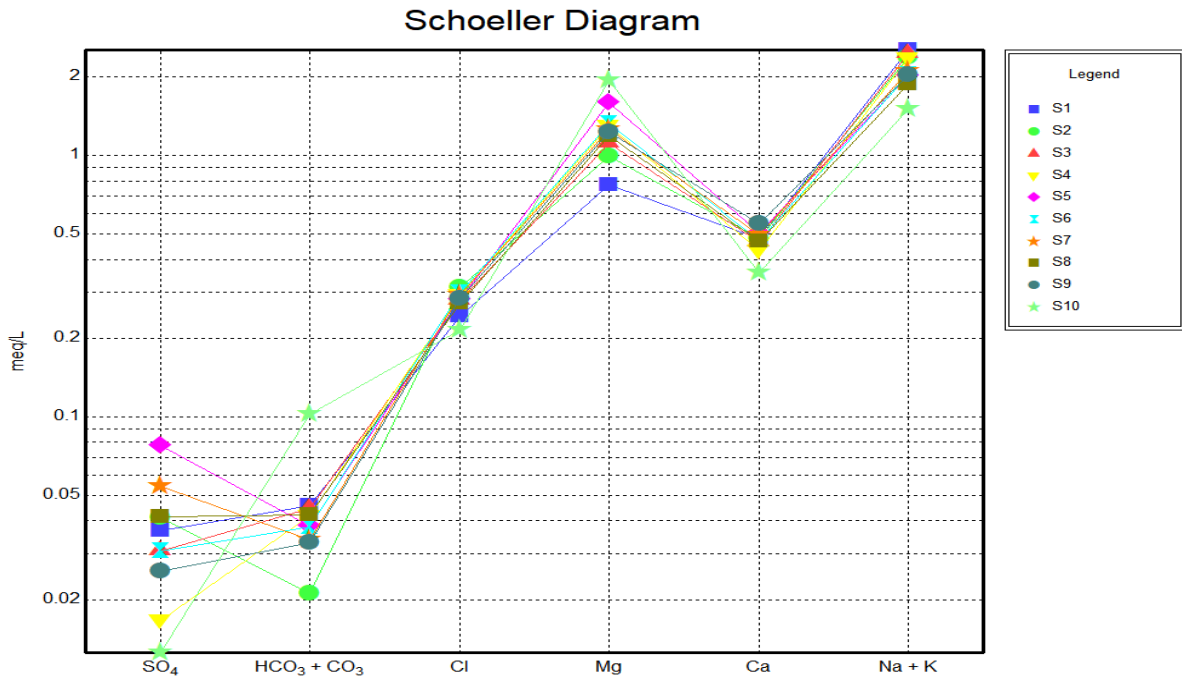


**Figure 4.27: Schoeller Diagram Showing the major Cations and Anions**

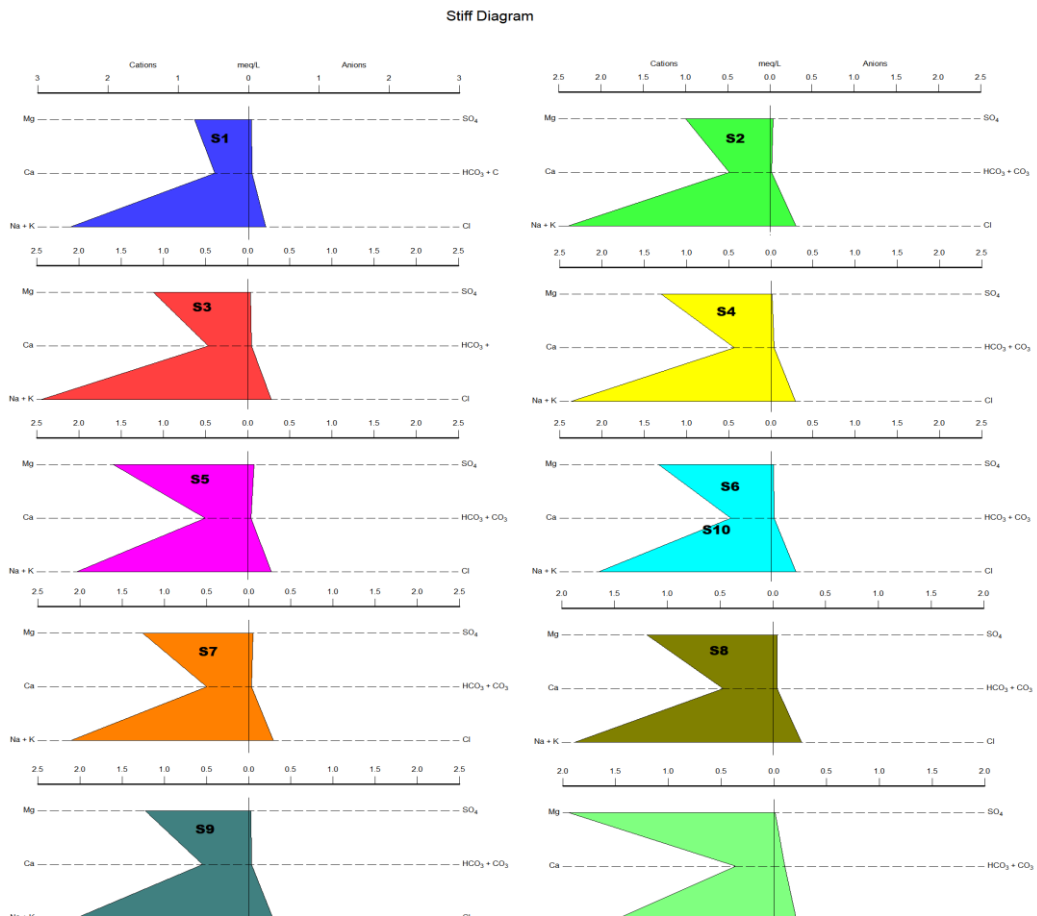


**Figure 4.28: Stiff Diagrams**

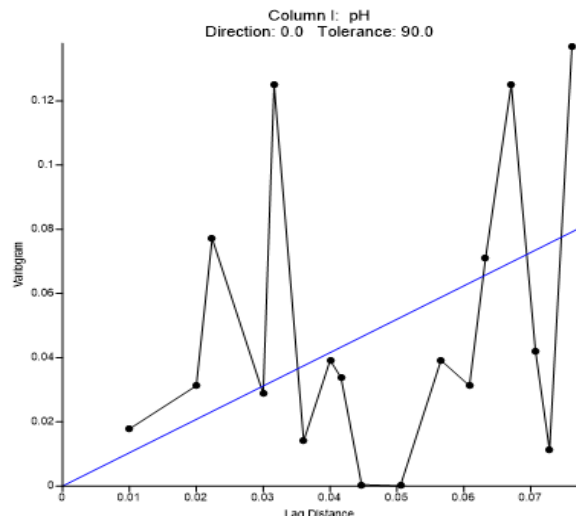


**Figure 4.29a: Variogram of pH in Kolo Creek Groundwater**

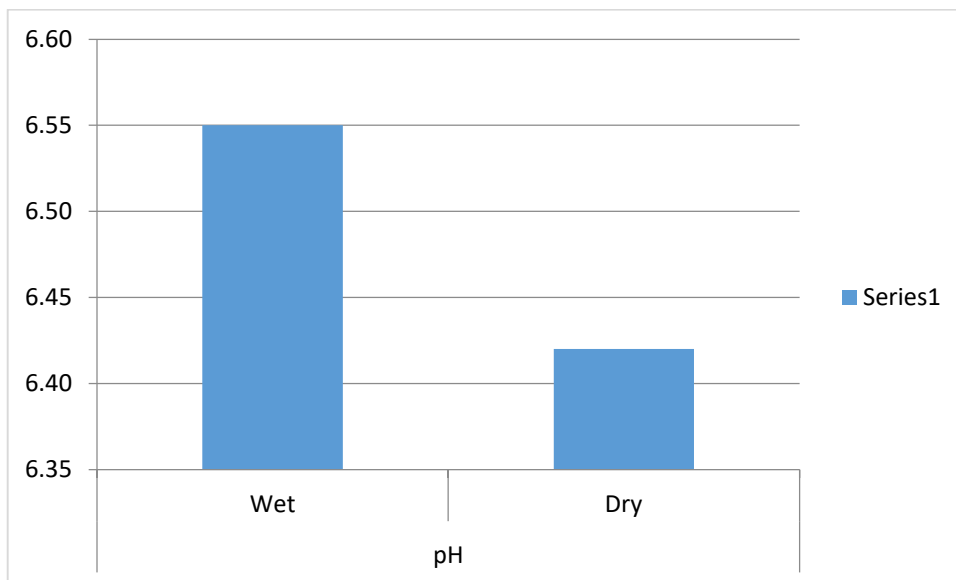


**Figure 4.29b: Seasonal Variation of pH in Kolo Creek Groundwater**

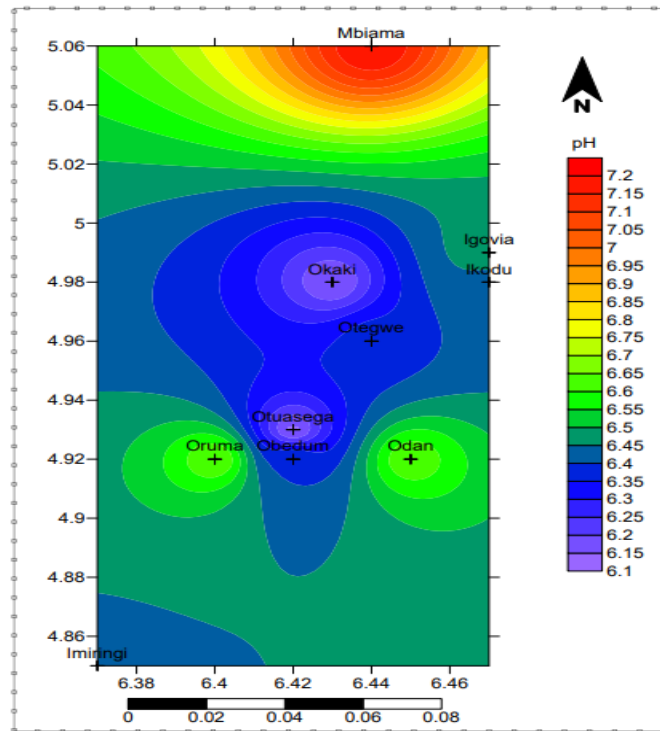


**Fig 4.29c: Spatial Distribution of pH in Kolo Creek groundwater**

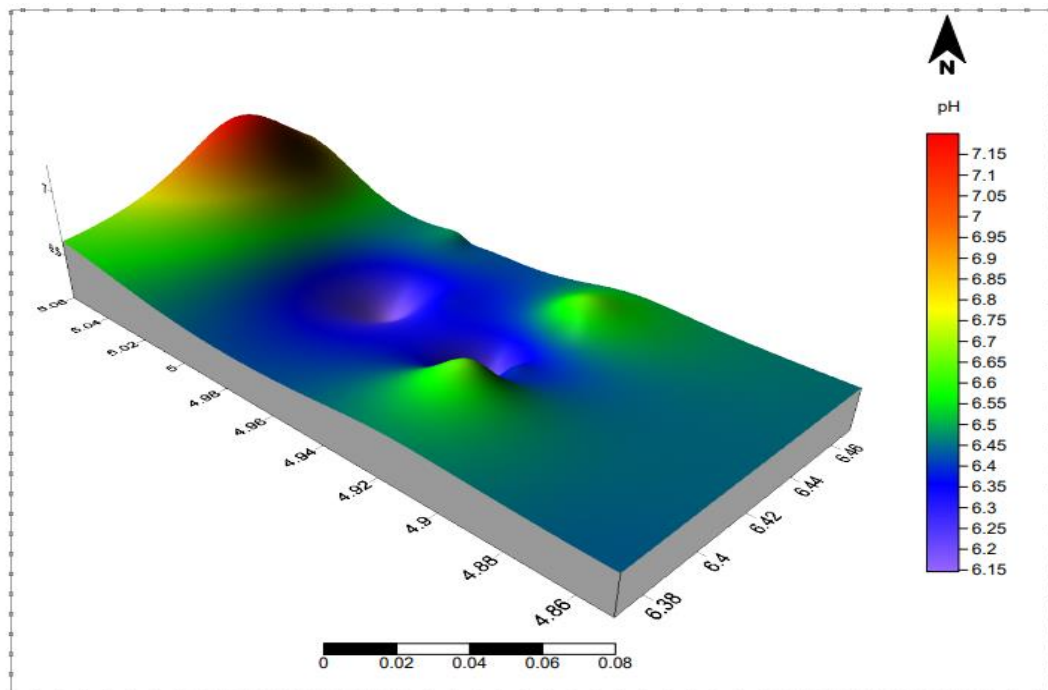


**Fig 4.29d: 3D view of pH in Kolo Creek groundwater**

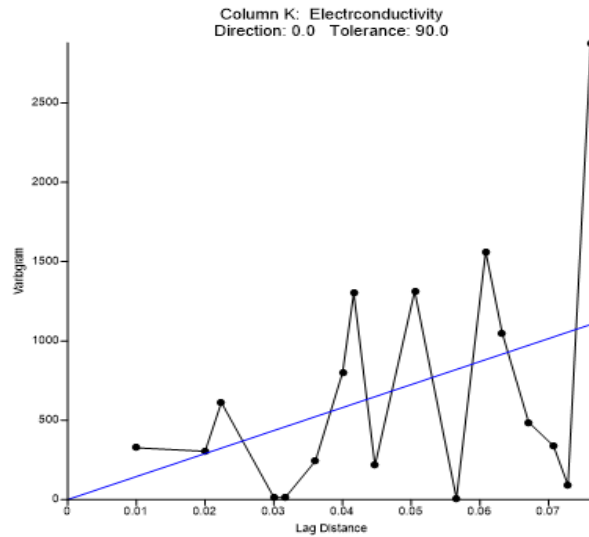


**Fig 4.30a: Station Variation of Electrical Conductivity in Kolo Creek Groundwater**

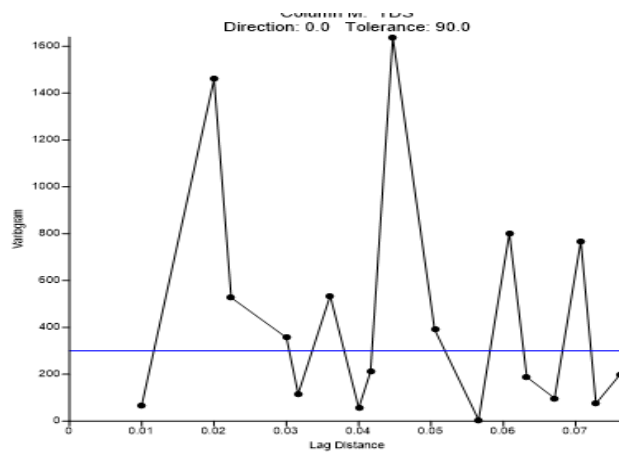


**Fig 4.30b: Station Variation of TDS in Kolo Creek Groundwater**

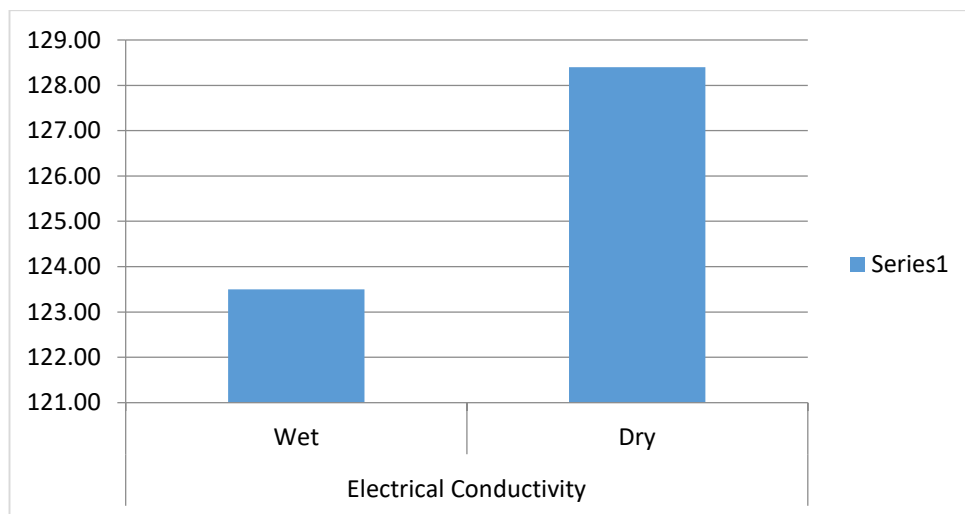


**Figure 4.30c: Seasonal Variation of E. Conductivity in Kolo Creek Groundwater**

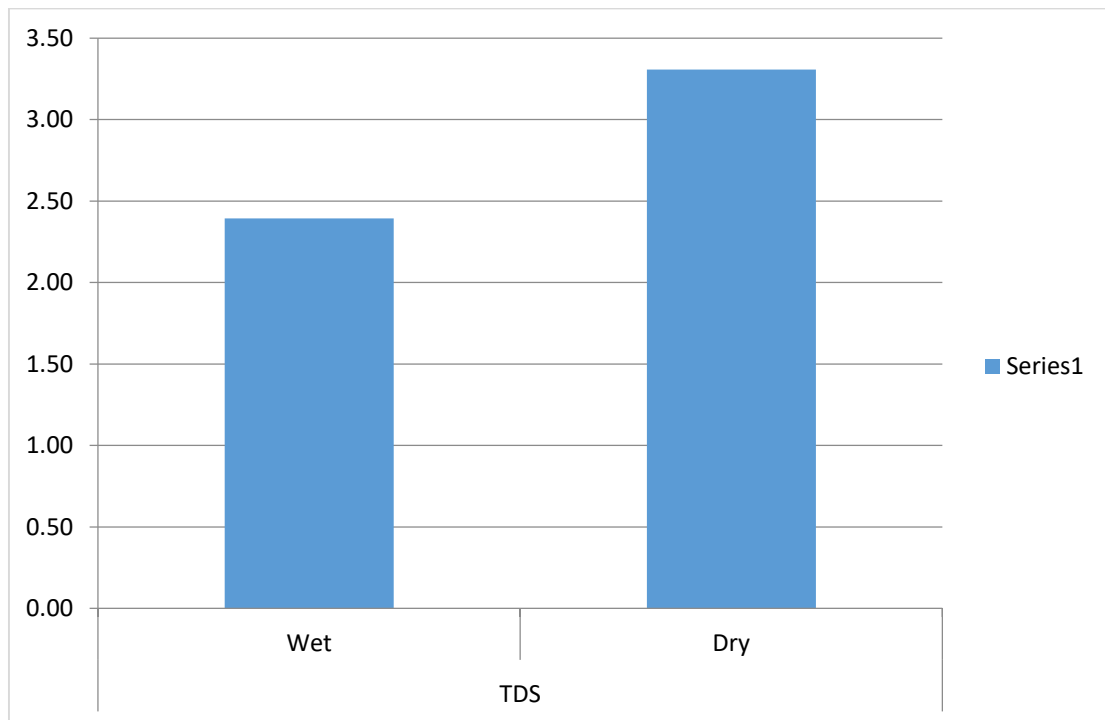


**Figure 4.30d: Seasonal Variation of TDS in Kolo Creek Groundwater Total**

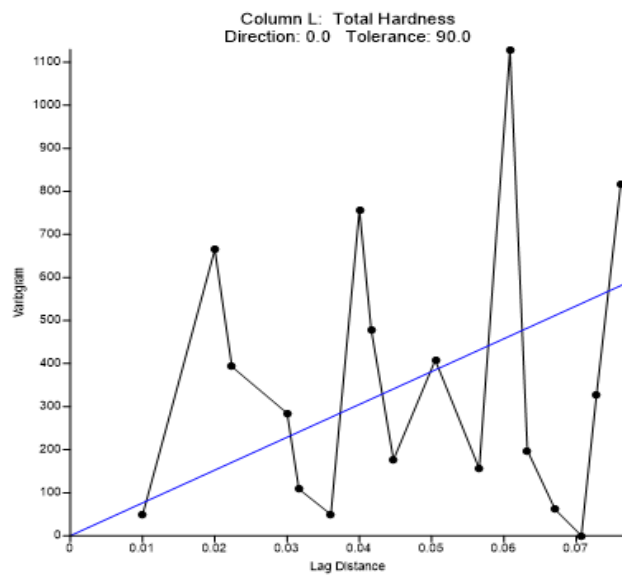


**Fig 4.31a: Station Variation of total hardness in Kolo Creek Groundwater**

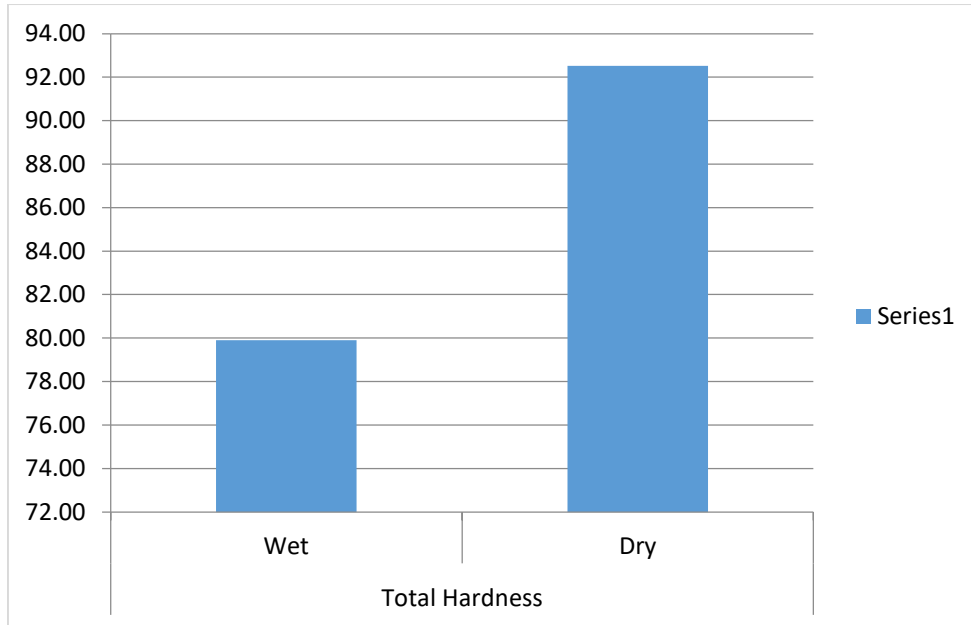


**Fig 4.31b: Seasonal Variations of Total Hardness in Kolo Creek groundwater**

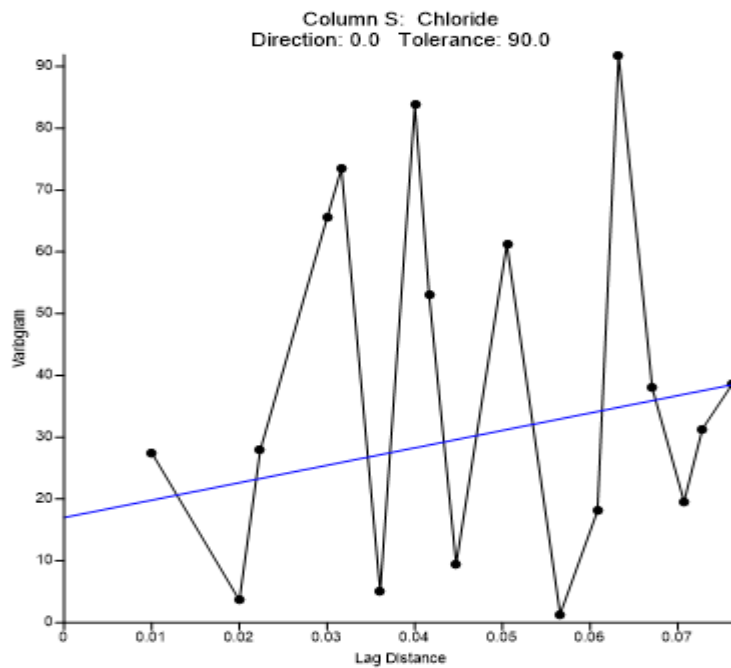


**Fig 4.32a: Station Variation of Chloride in Kolo Creek Groundwater**

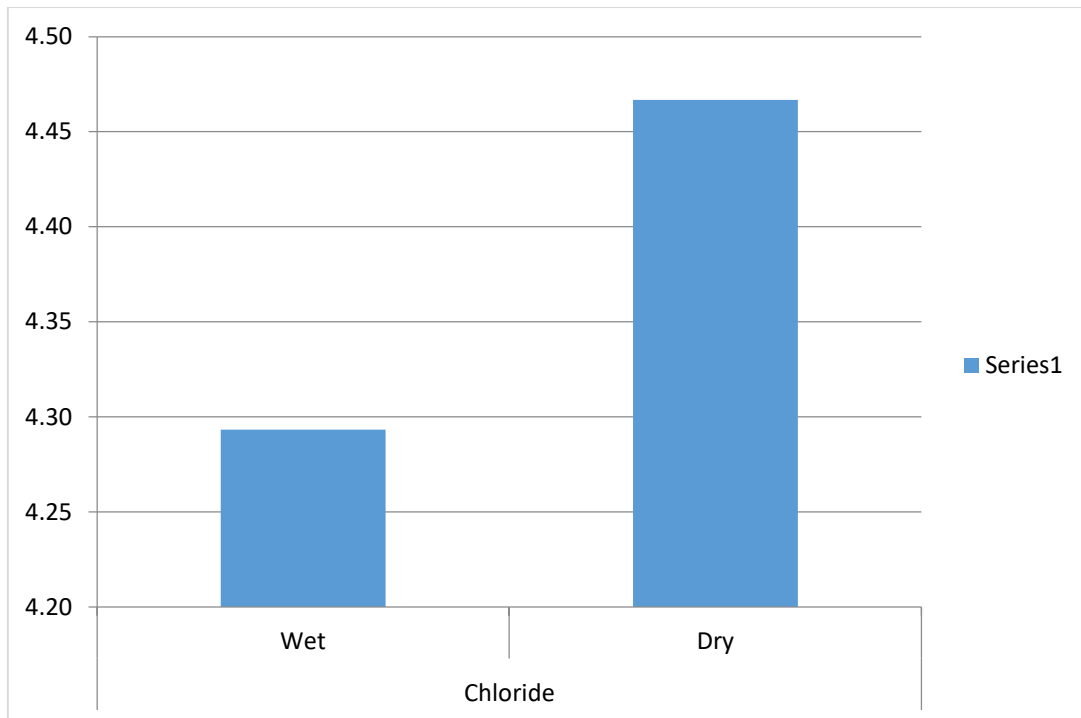


**Fig 4.32b: Seasonal Variations of Chloride in Kolo Creek groundwater**

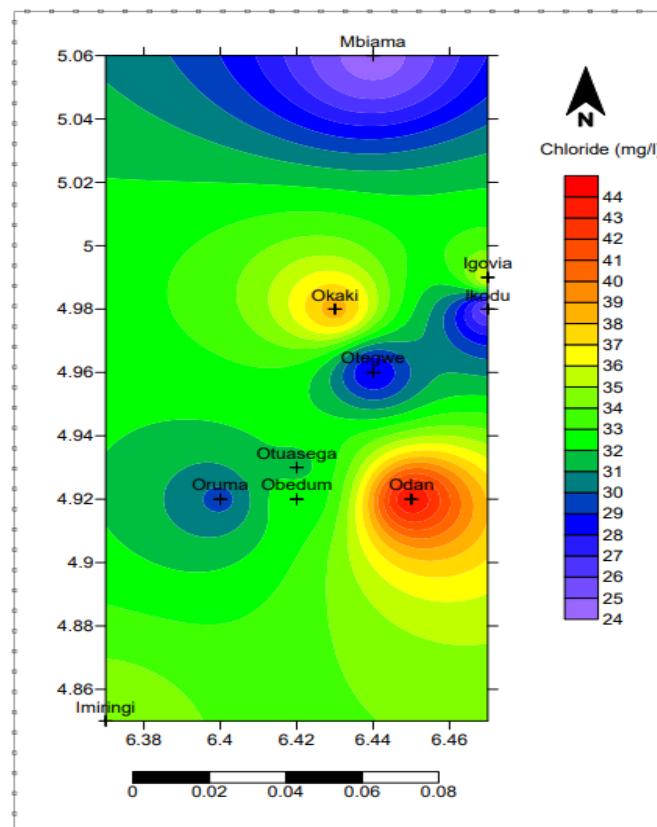


**Fig 4.32c: Spatial Distribution of Chloride in Kolo Creek groundwater**

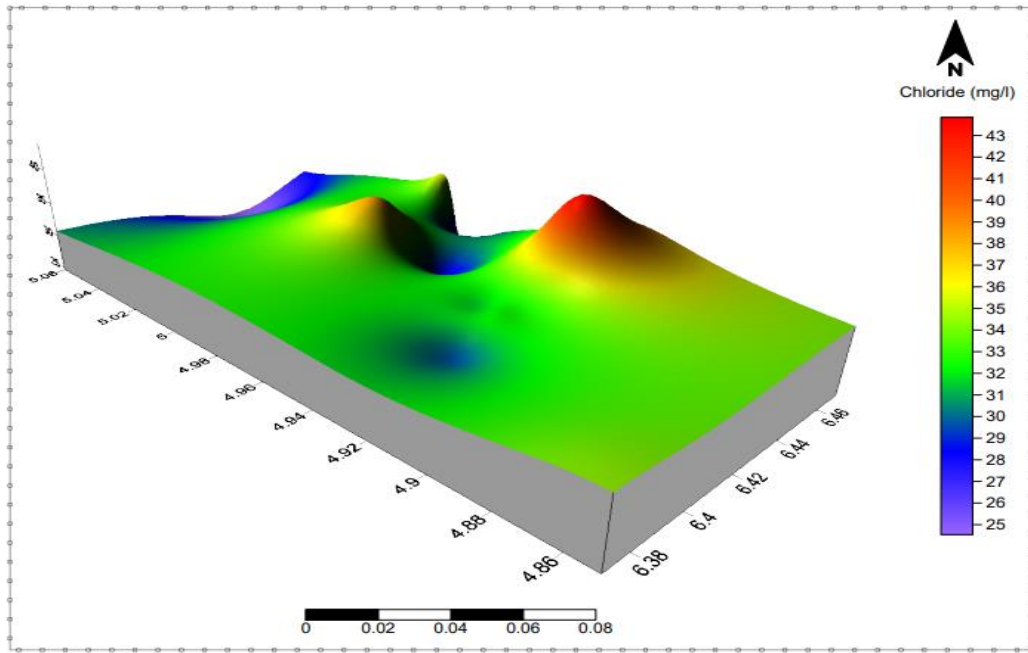


**Fig 4.32d: 3D view of Chloride in Kolo Creek groundwater**

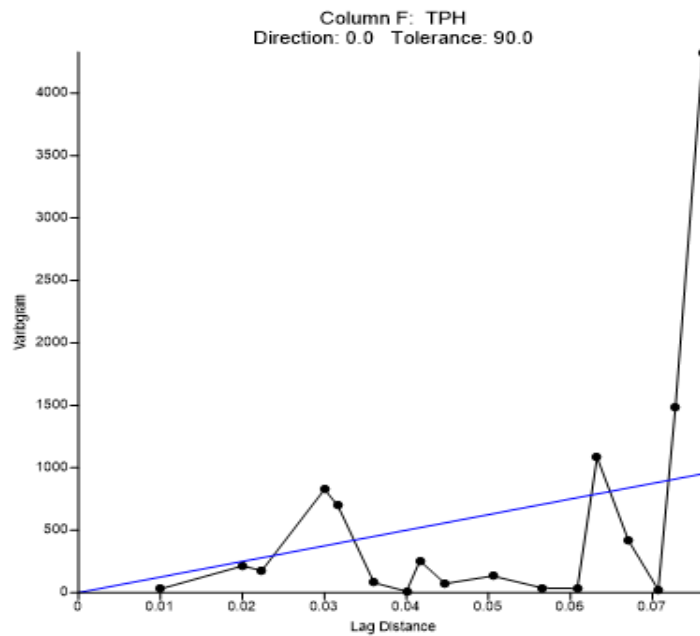


**Fig 4.33a: Station Variation of Total Petroleum Hydrocarbon for Groundwater**

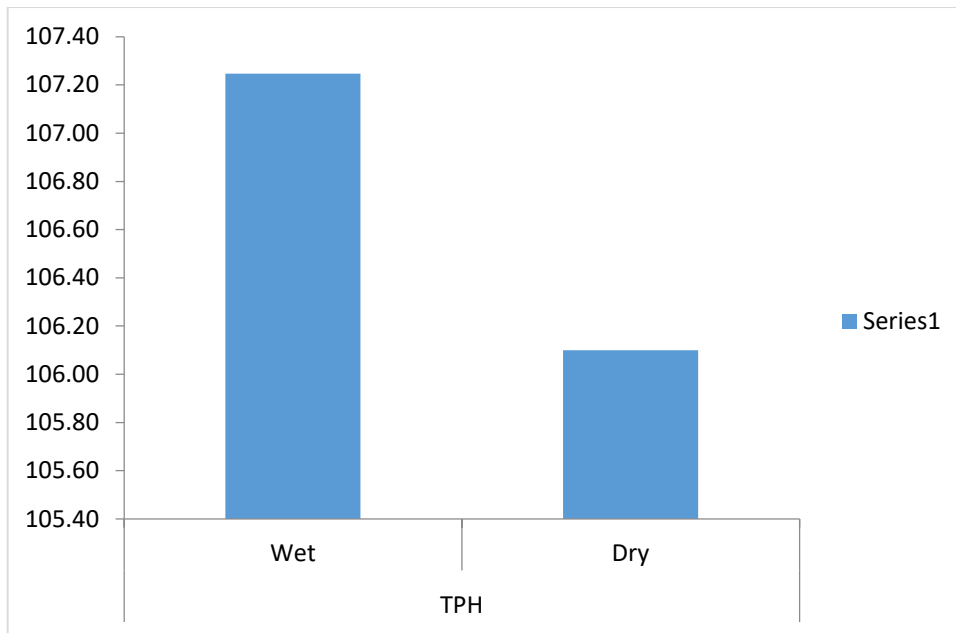


**Fig 4.33b: Seasonal Variations of TPH in Kolo Creek groundwater**

**Fig 4.33c: Spatial Distribution of TPH in Kolo Creek groundwater**

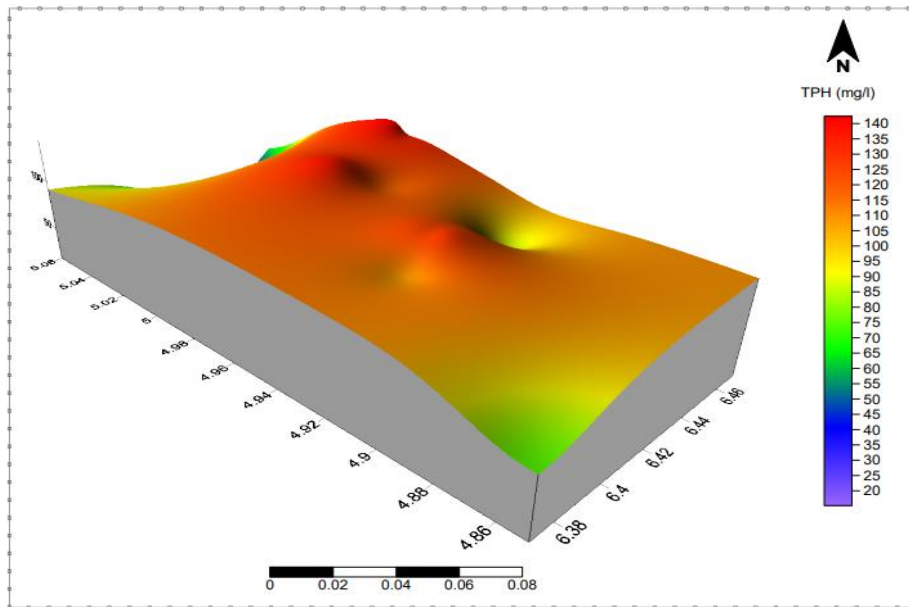


**Fig 4.33d: 3D view of TPH in Kolo Creek groundwater**

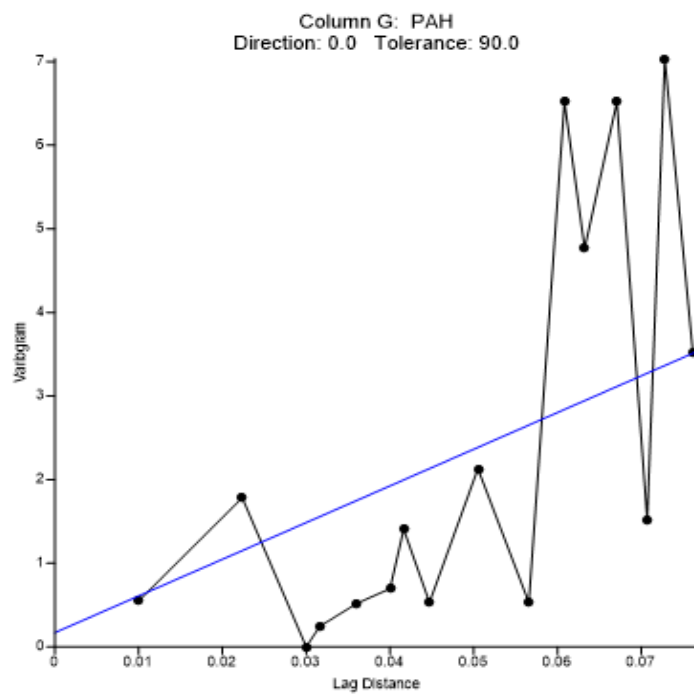


**Fig 4.34a: Station Variation of PAH for Groundwater**

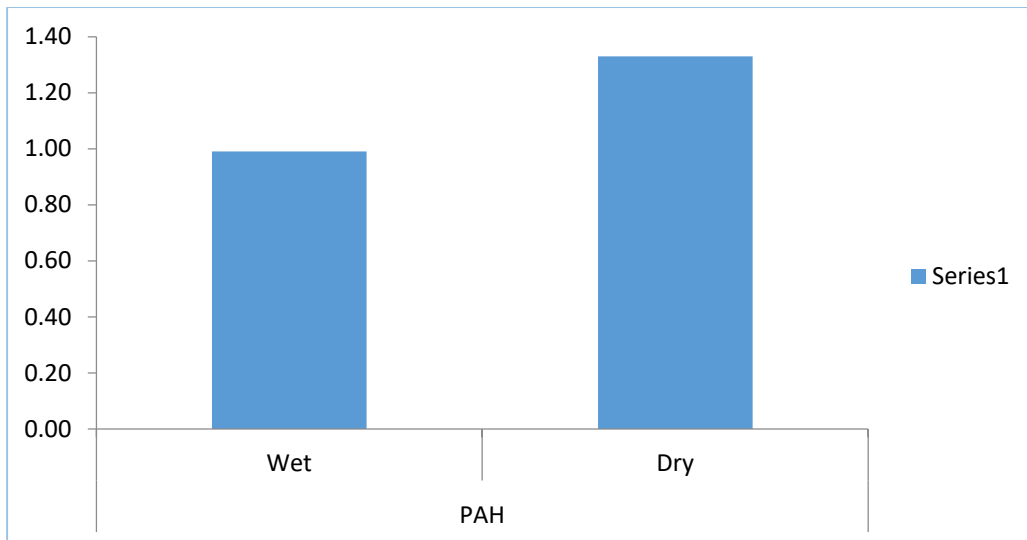


**Fig 4.34b: Seasonal Variations of PAH in Kolo Creek groundwater**

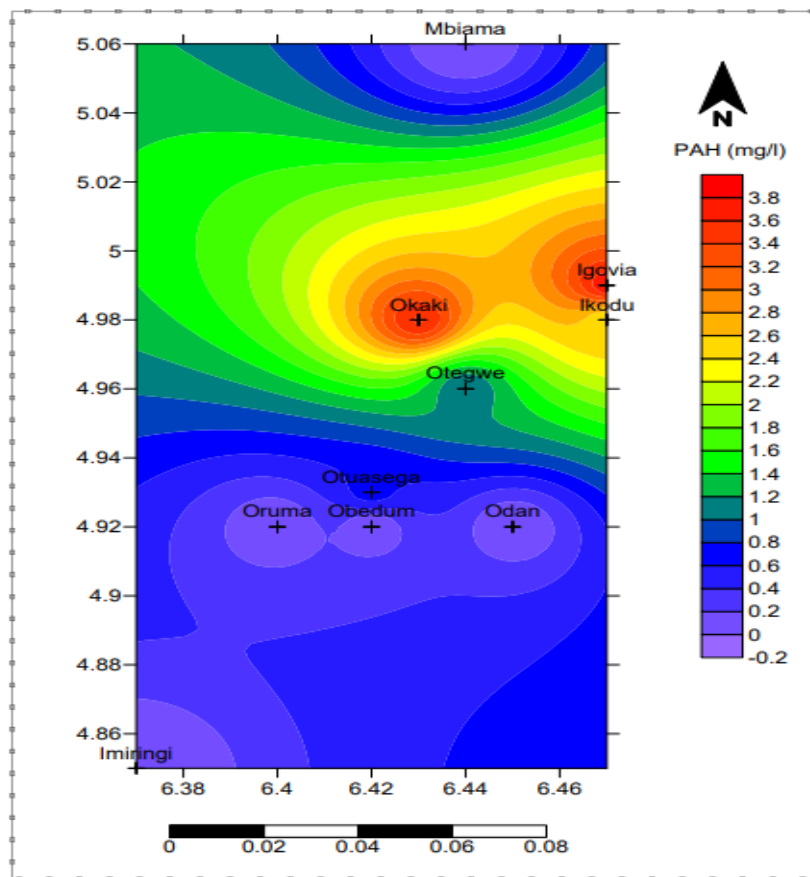


**Fig 4.34c: Spatial Distribution of PAH in Kolo Creek groundwater**

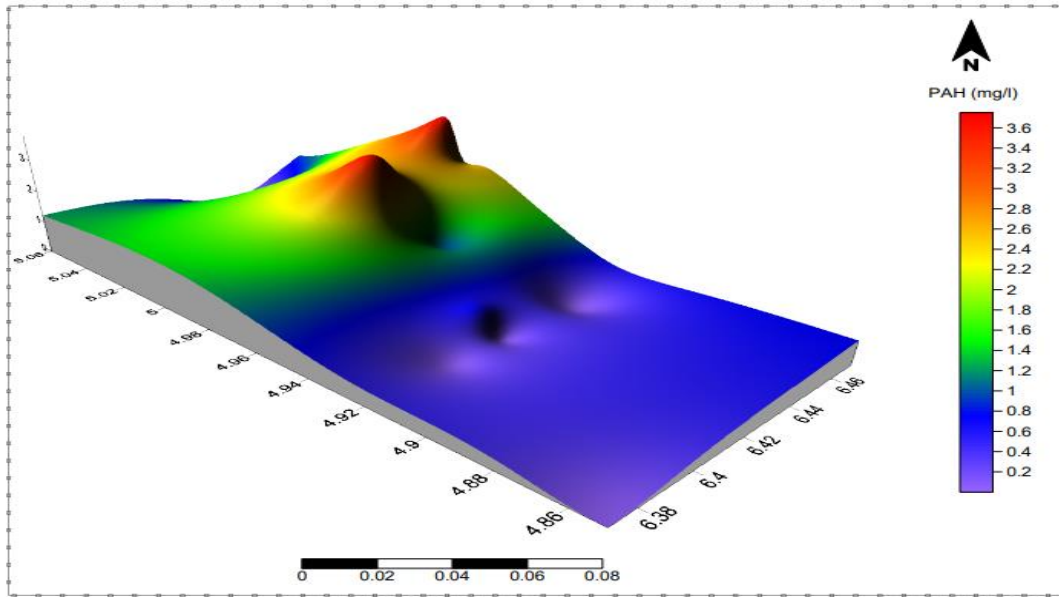


**Fig 4.34d: 3D view of PAH in Kolo Creek groundwater**

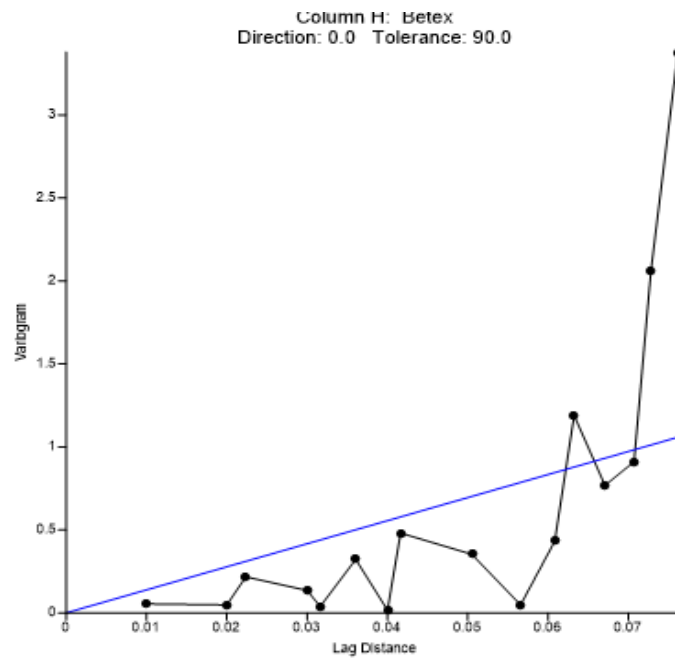


**Fig 4.35a: Station Variations of Betex for groundwater**

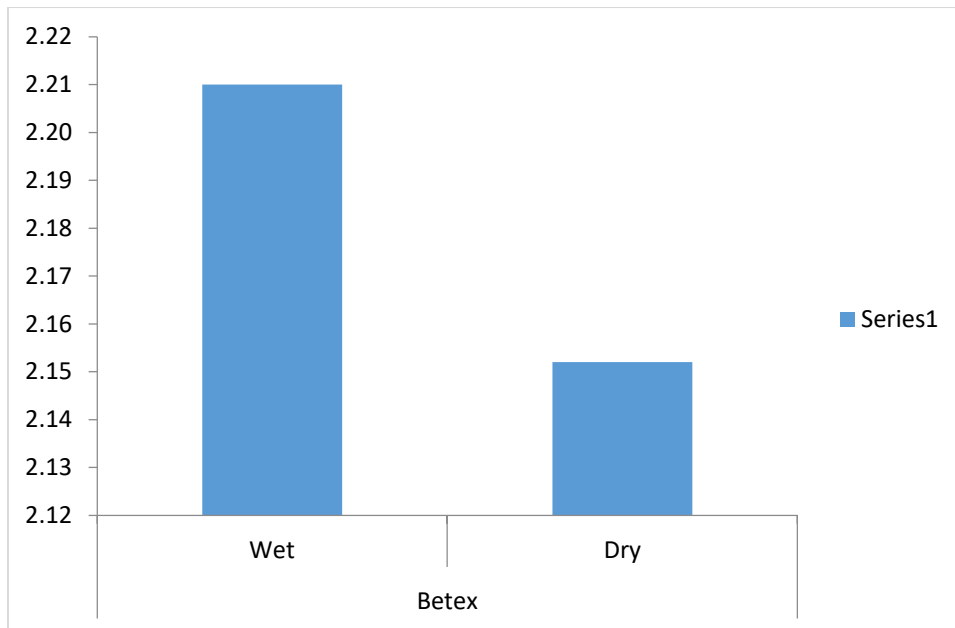


**Fig 4.35b: Seasonal Variations of Betex in groundwater**

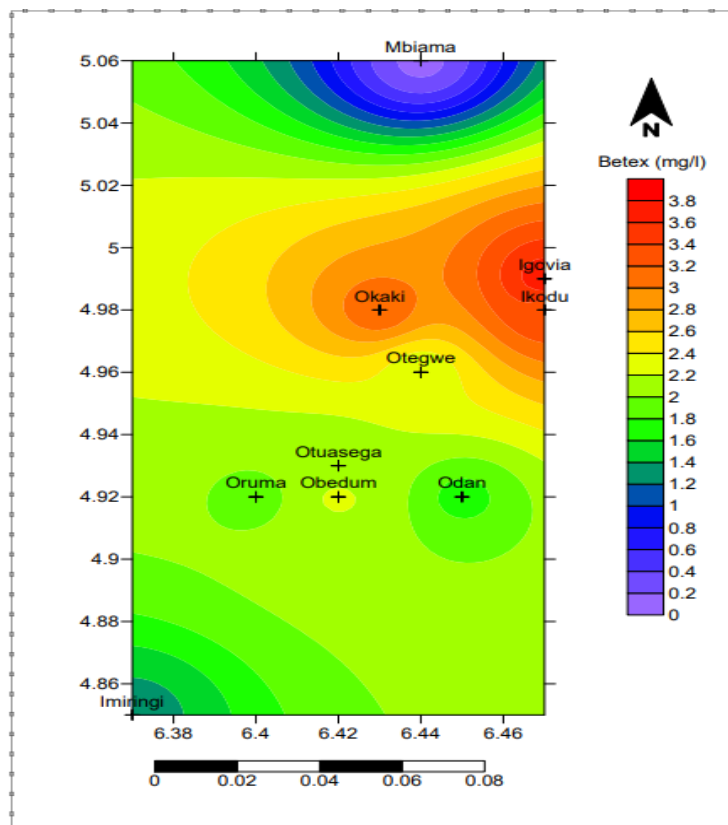


**Fig 4.35c: Spatial Distribution of Betex in Kolo Creek groundwater**

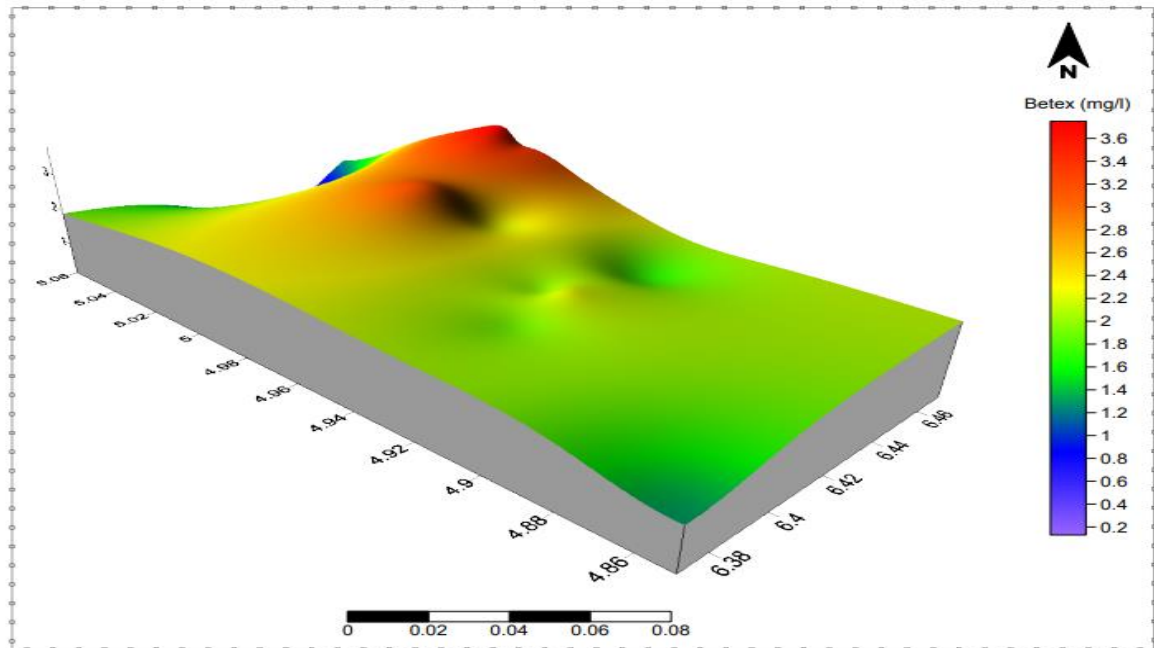


**Fig 4.35d: 3D view of Betex in Kolo Creek groundwater**

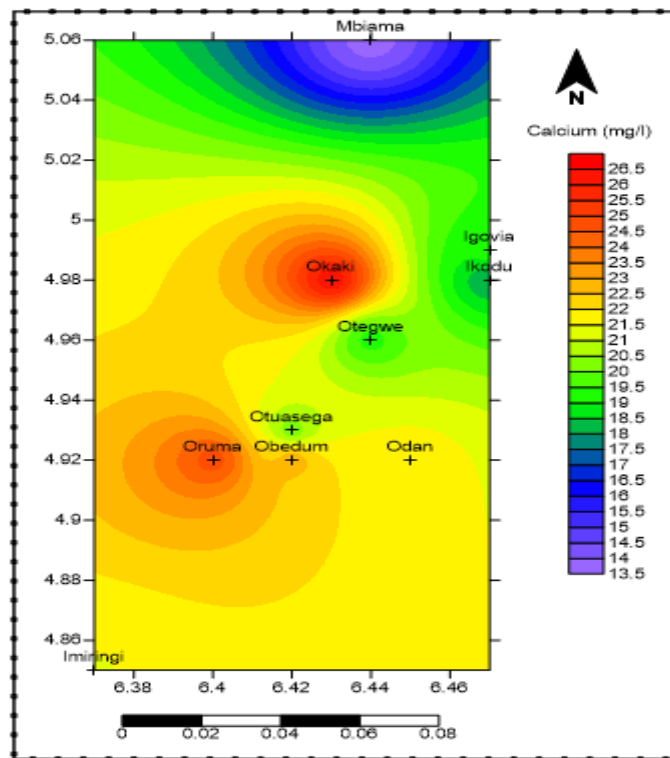


**Fig 4.36a: Spatial Distribution of Calcium in Kolo Creek groundwater**

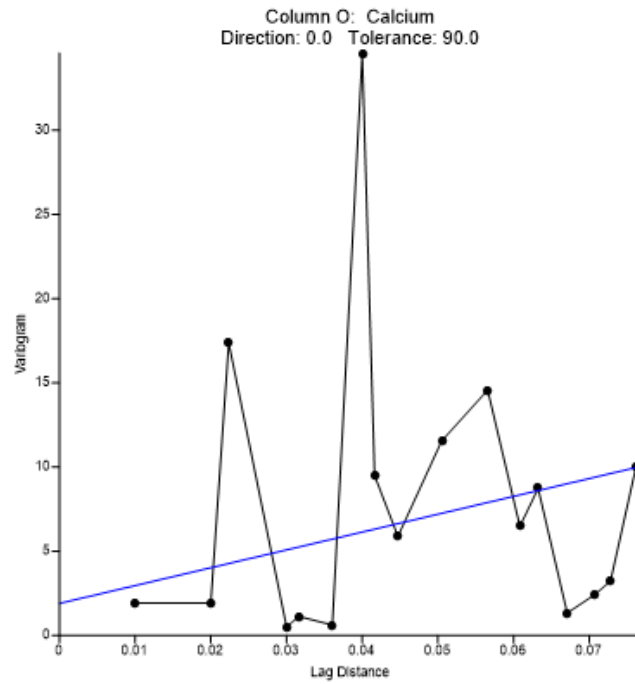


**Fig 4.36b: Station Variations of Calcium for groundwater**

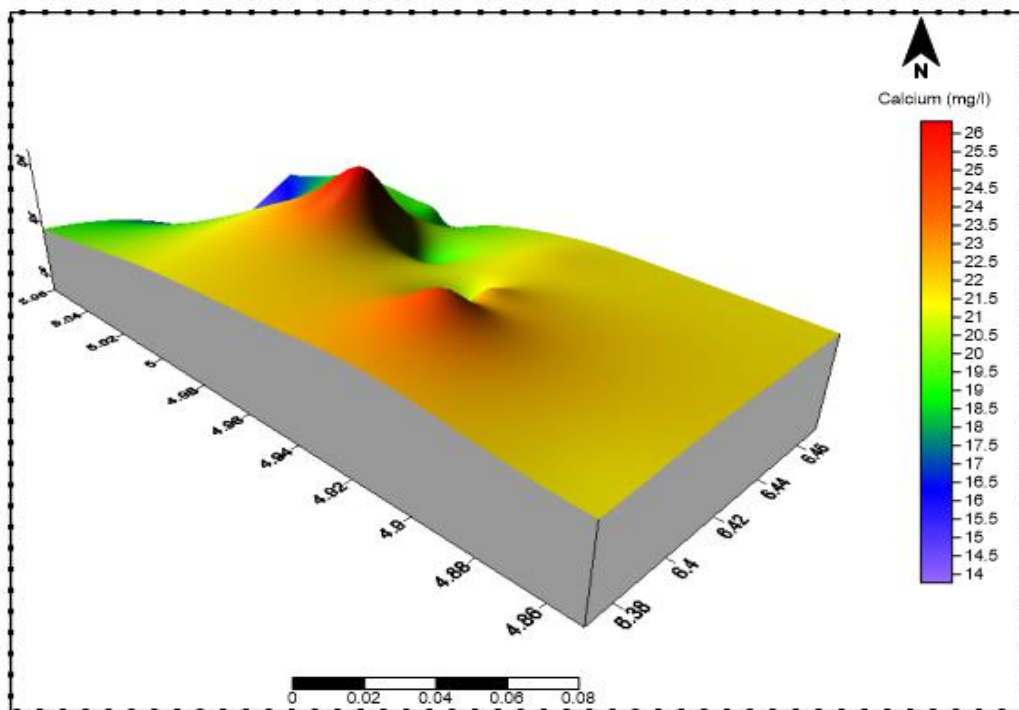


**Fig 4.36c: 3D view of Calcium in Kolo Creek groundwater**

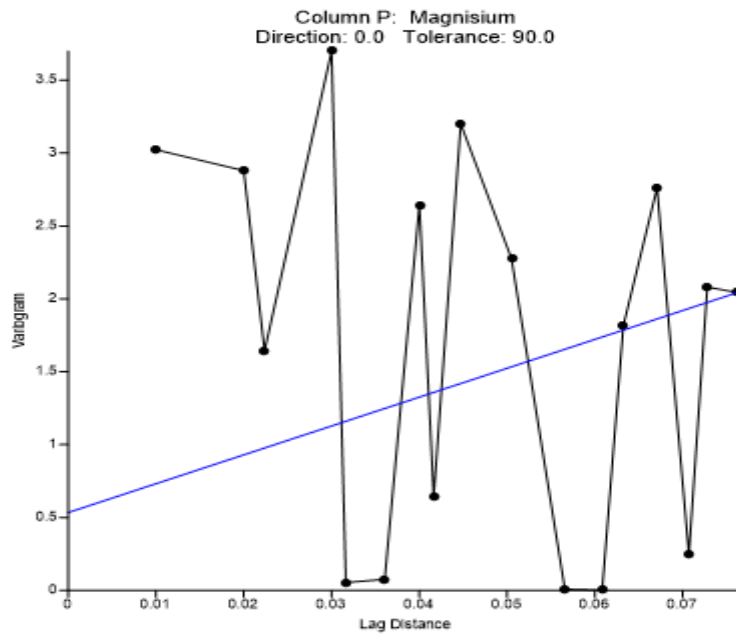


**Fig 4.37a: Variogram of Magnesium for groundwater**

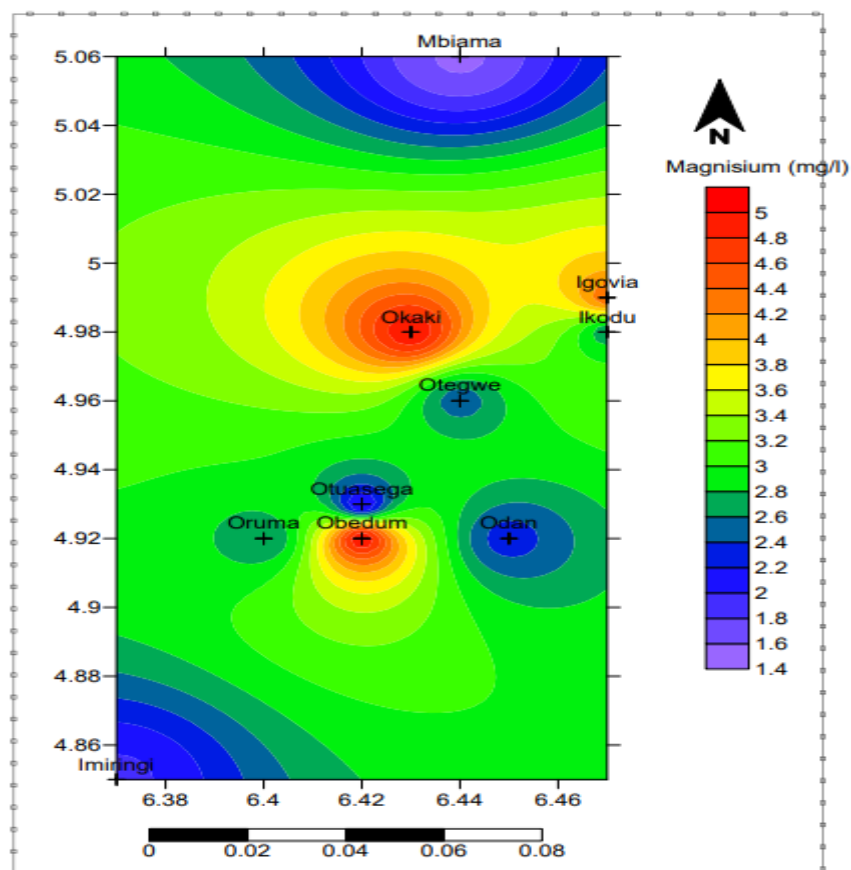


**Fig 4.37b: Spatial Distribution of Magnesium in Kolo Creek groundwater**

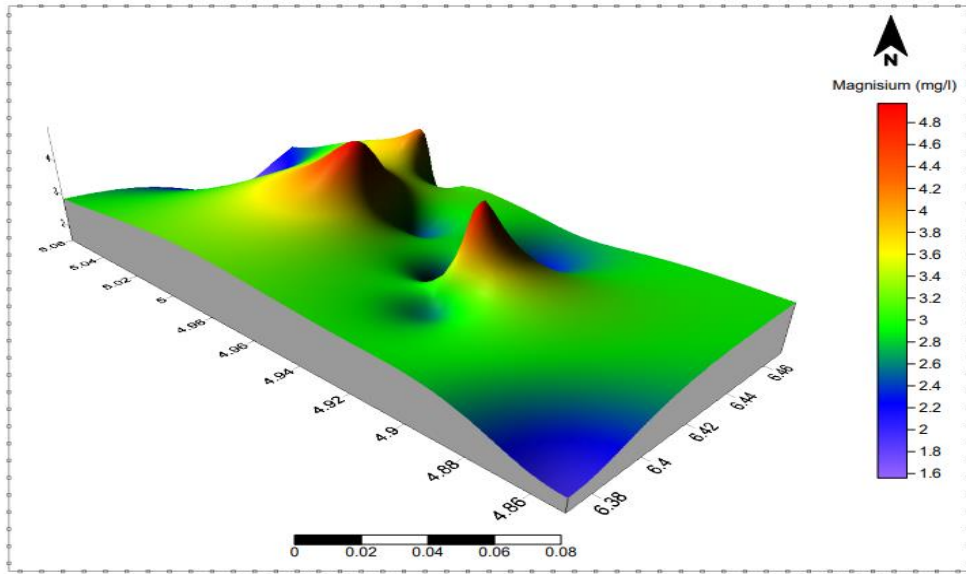


**Fig 4.37c: 3D view of Magnesium in Kolo Creek groundwater**

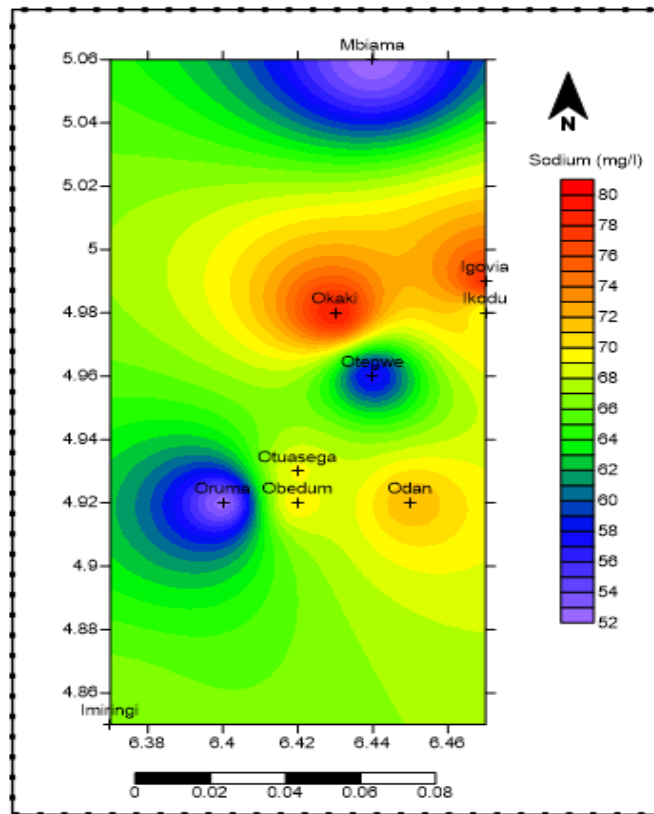


**Fig 4.38a: Spatial Distribution of Sodium in Kolo Creek groundwater**

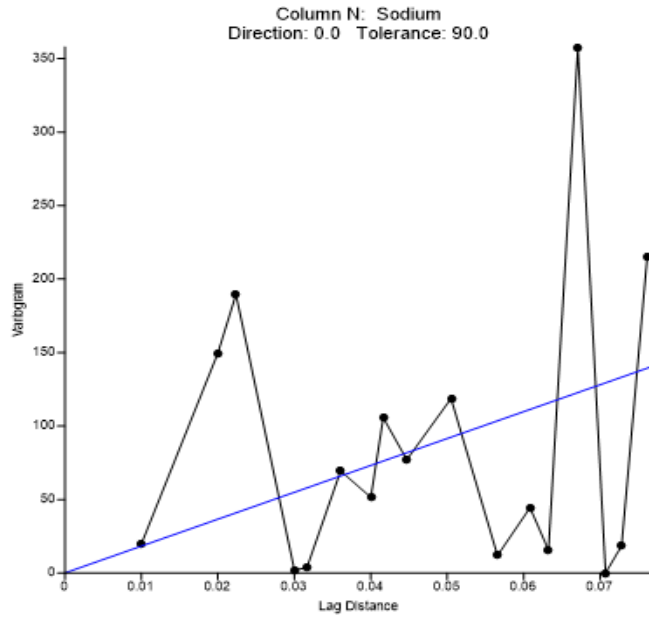


**Fig 4.38b: Variogram of Sodium for groundwater**

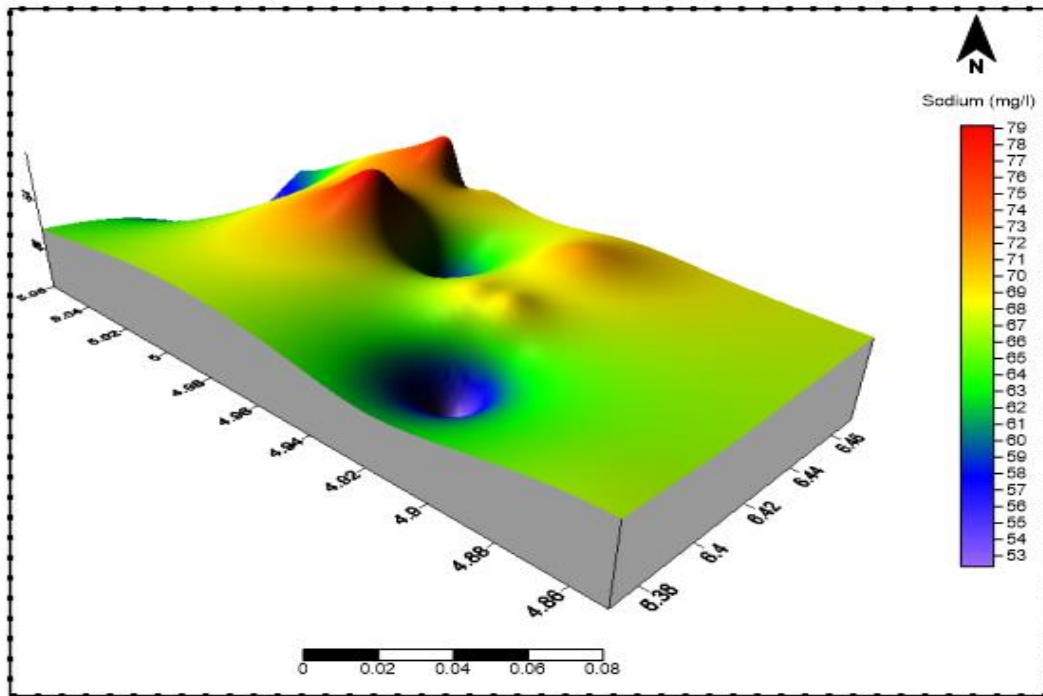


**Fig 4.38c: 3D view of Sodium in Kolo-Creek groundwater**

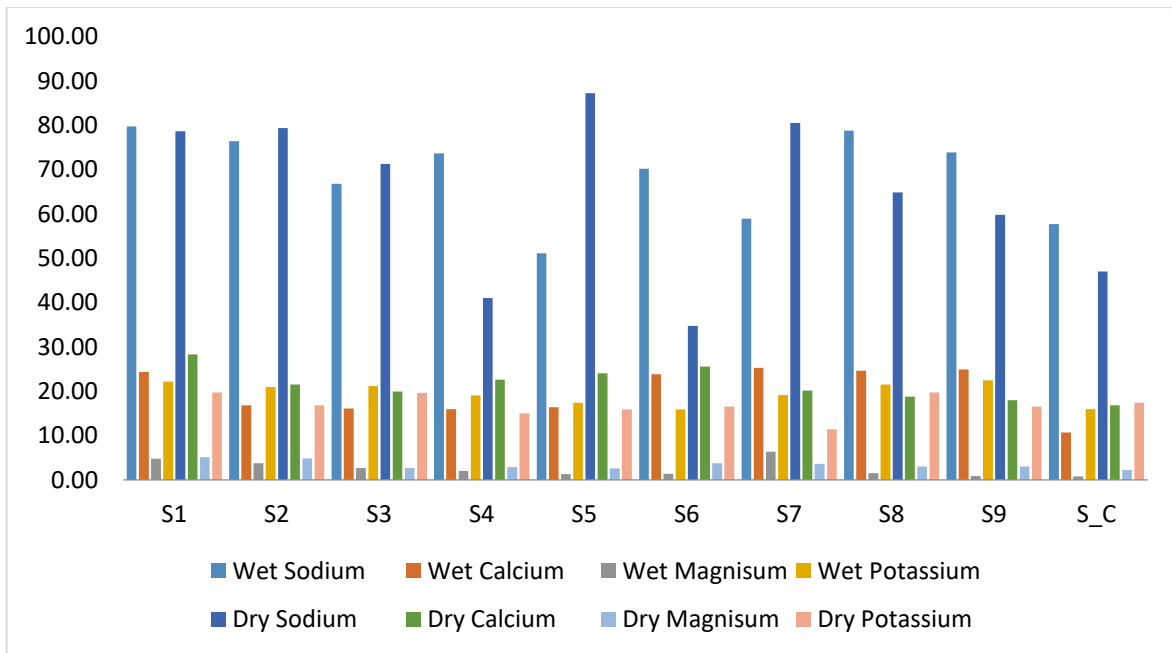


**Fig 4.39: Mean Variations of Major Cations for groundwater**

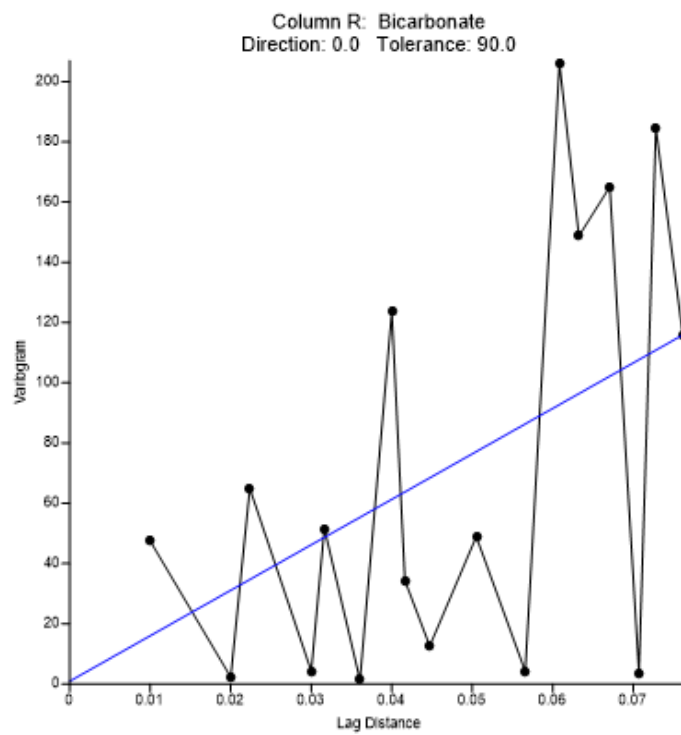


**Fig 4.40a: Variogram of Bicarbonate for groundwater**

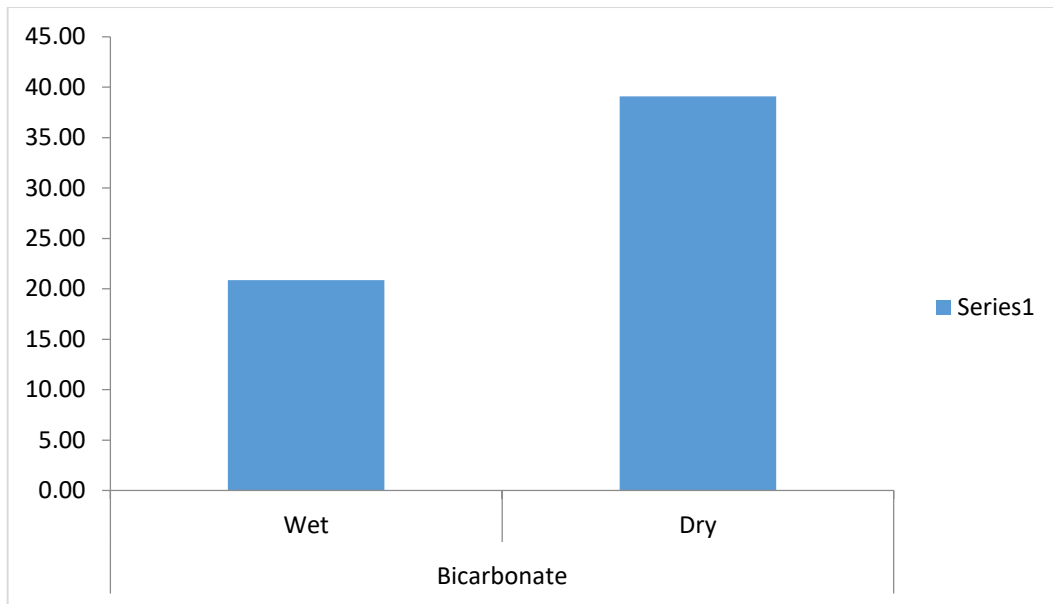


**Fig 4.40b: Seasonal Variations of Bicarbonate in Kolo Creek groundwater**

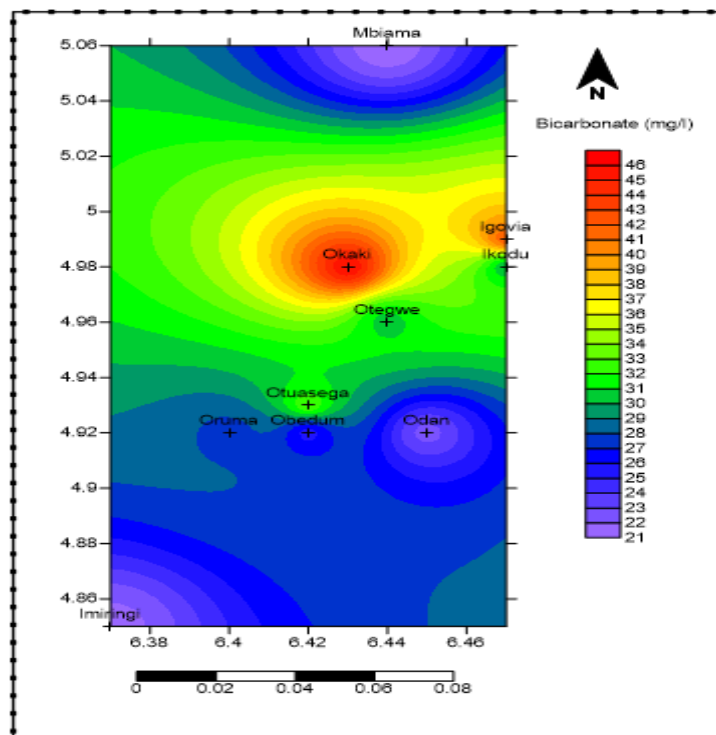


**Fig 4.40c: Spatial Distribution of Bicarbonate in Kolo Creek groundwater**

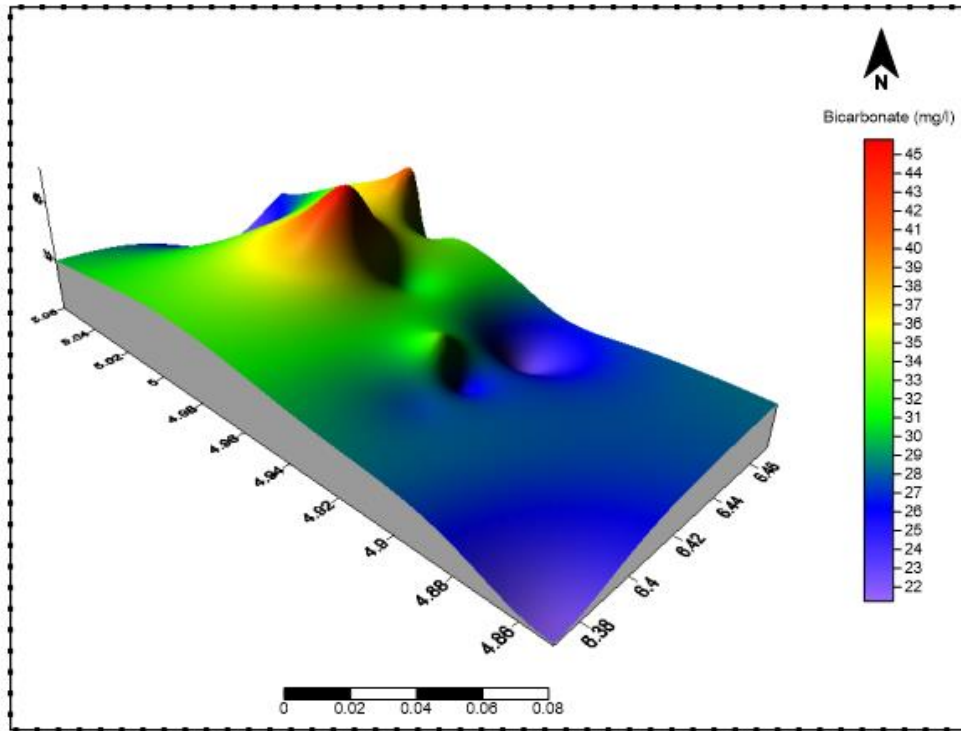


**Fig 4.40d: 3D view of Bicarbonate in Kolo Creek groundwater**

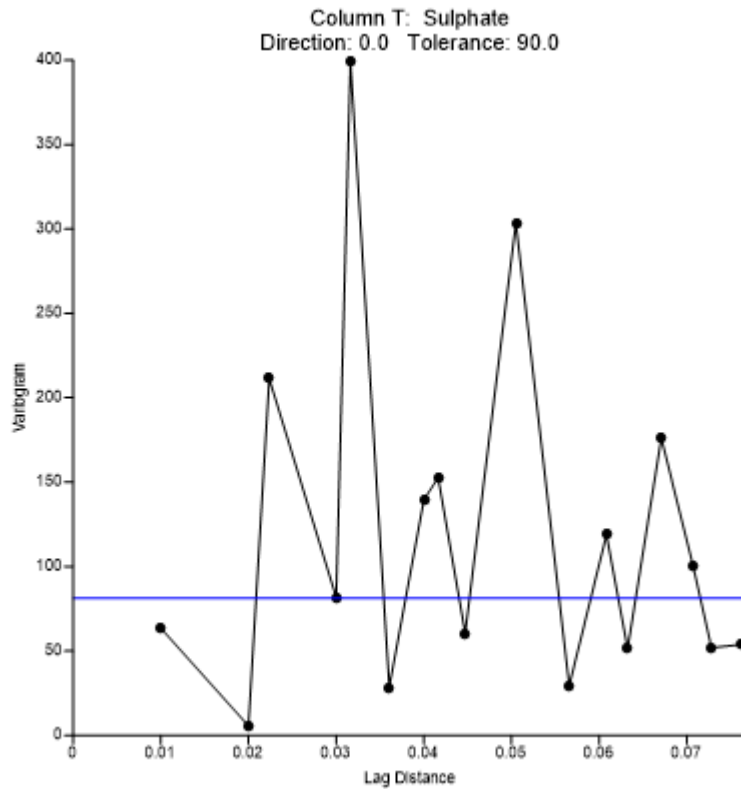


**Fig 4.41a: Mean Variations of Sulphate for groundwater**

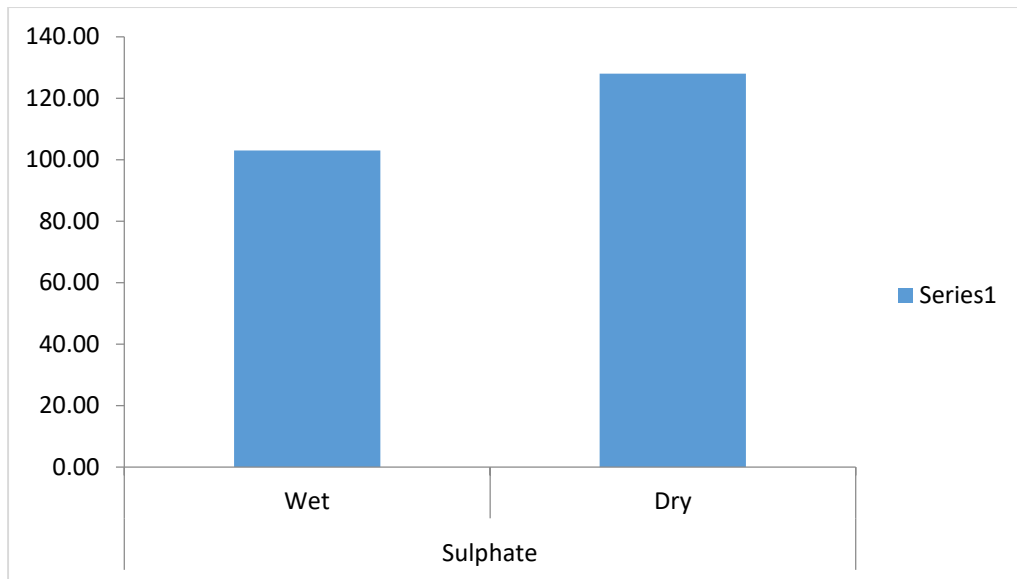


**Fig 4.41b: Seasonal Variations of Sulphate in Kolo Creek groundwater**

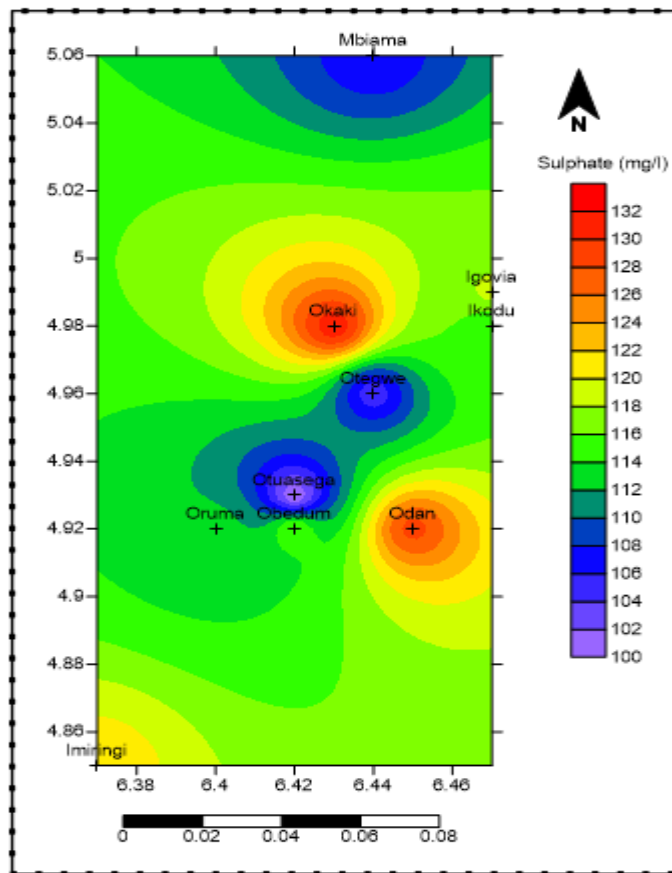


**Fig 4.41c: Spatial Distribution of Sulphate in Kolo Creek groundwater**

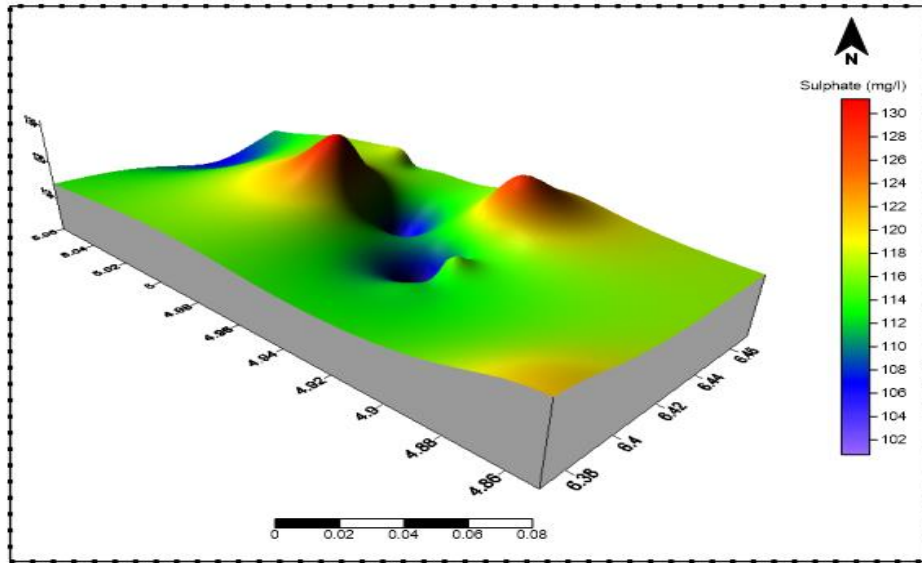


**Fig 4.41d: 3D view of Sulphate in Kolo Creek groundwater**

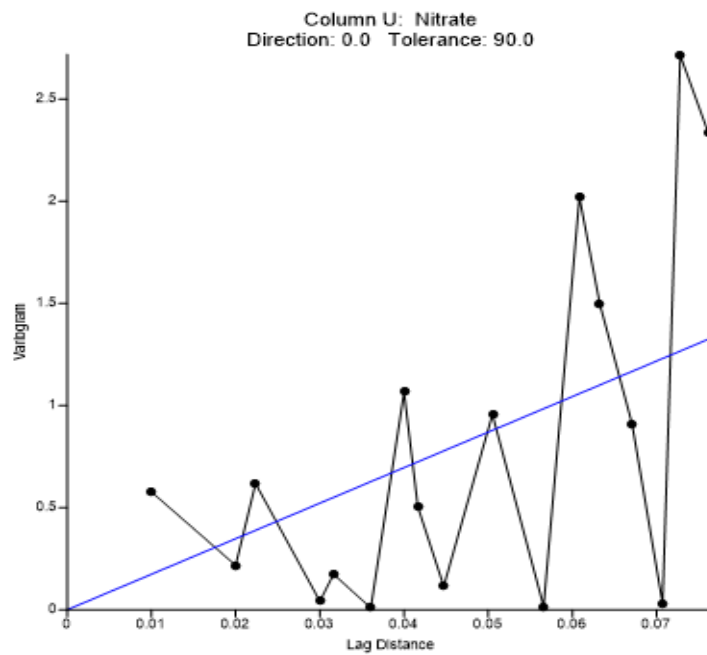


**Fig 4.42a: Variogram of Nitrate for groundwater**

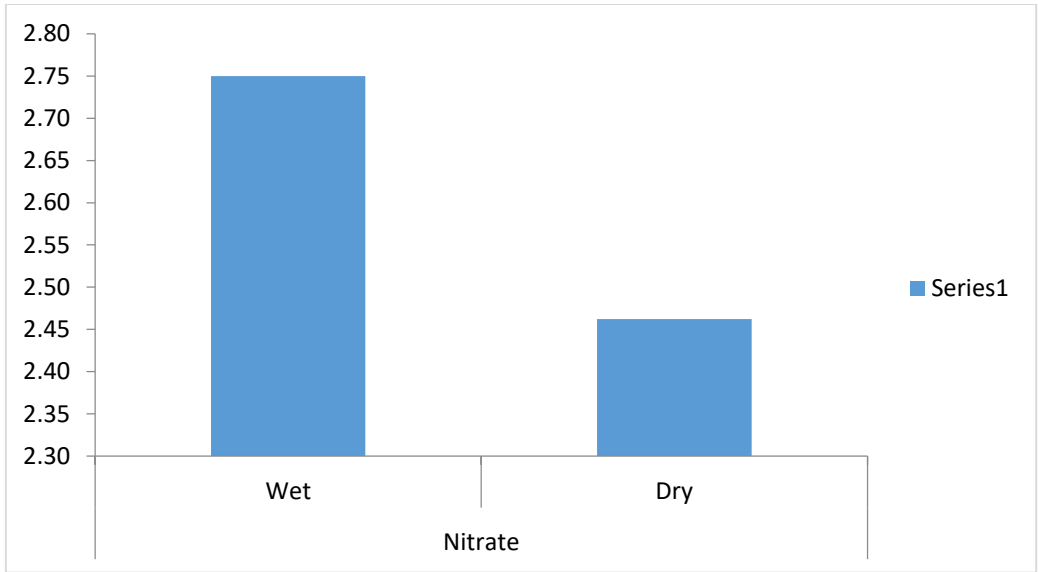


**Fig 4.42b: Seasonal Variations of Nitrate in Kolo Creek groundwater**

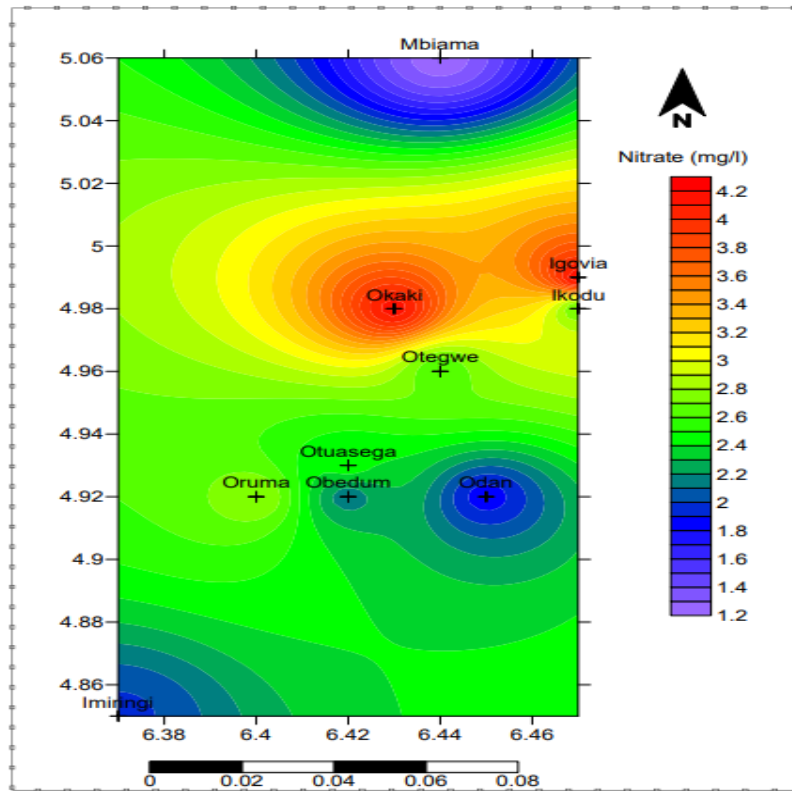


**Fig 4.42c: Spatial Distribution of Nitrate in Kolo Creek groundwater**

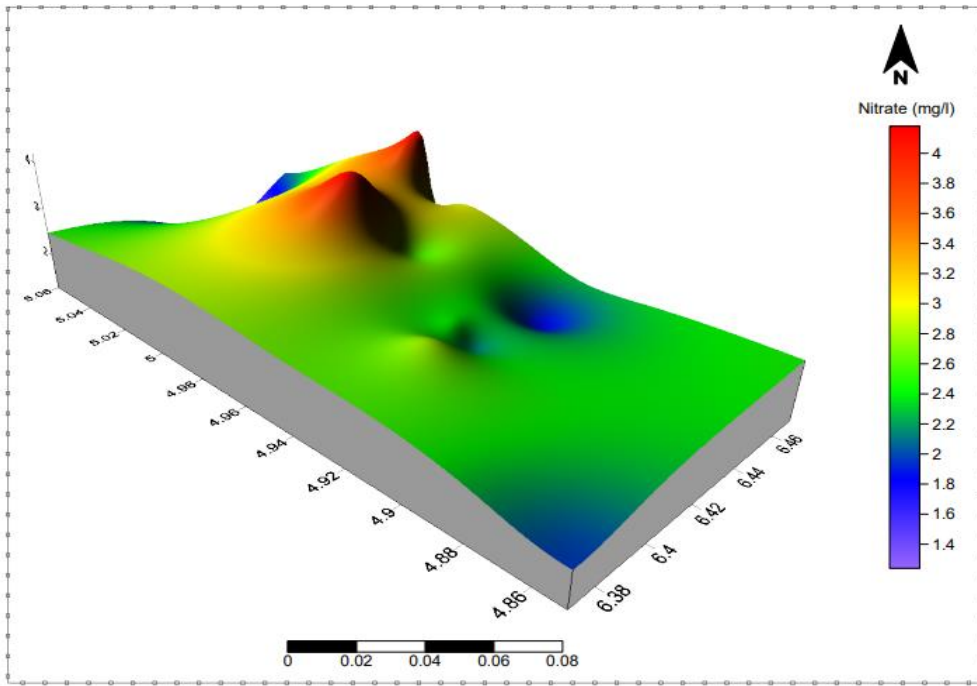


Fig 4.42d: 3D view of Nitrate in Kolo Creek groundwater

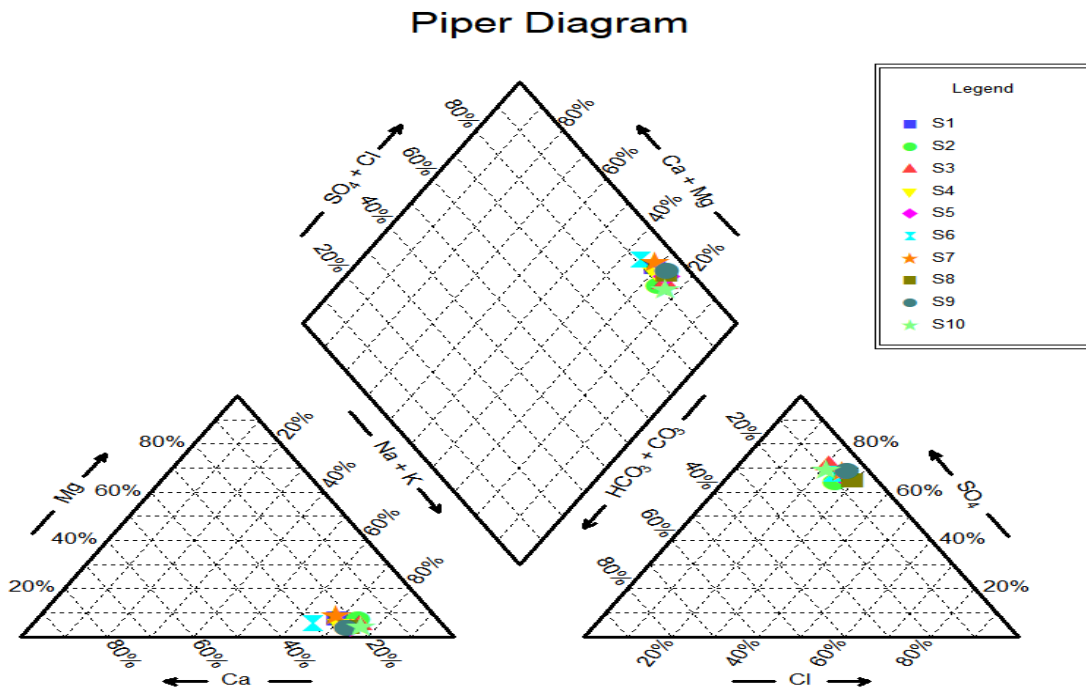
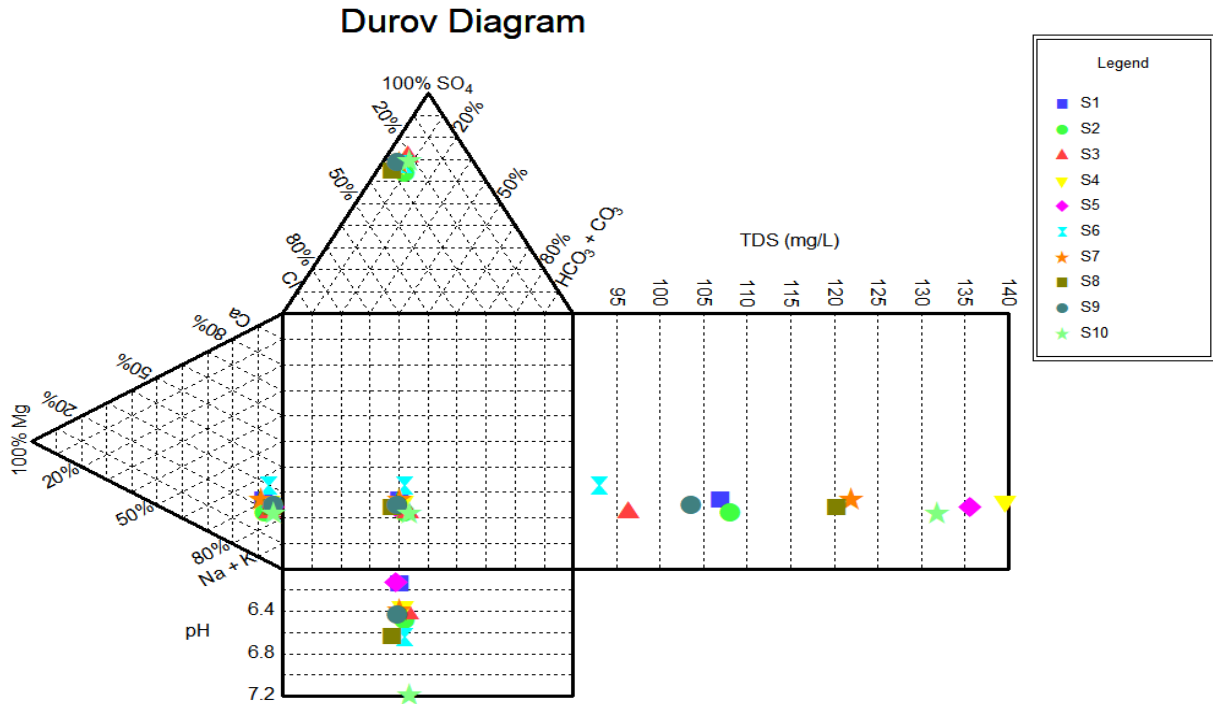
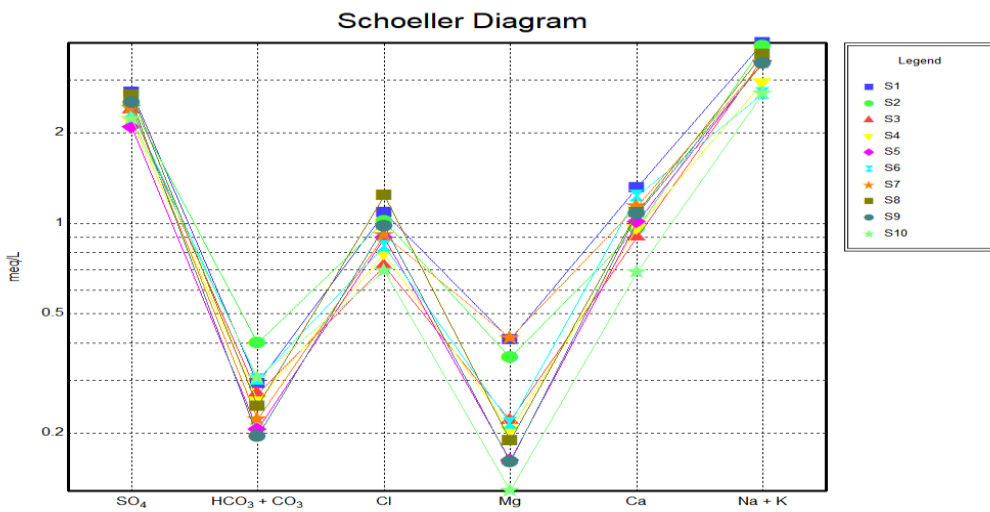


Fig 4.43 Piper Diagram Showing the major Cations and Anions



**Fig 4.44 Durov Diagram Showing the major Cations and Anions**



**Fig 4.45 Schoeller Diagram Showing the major Cations and Anions**

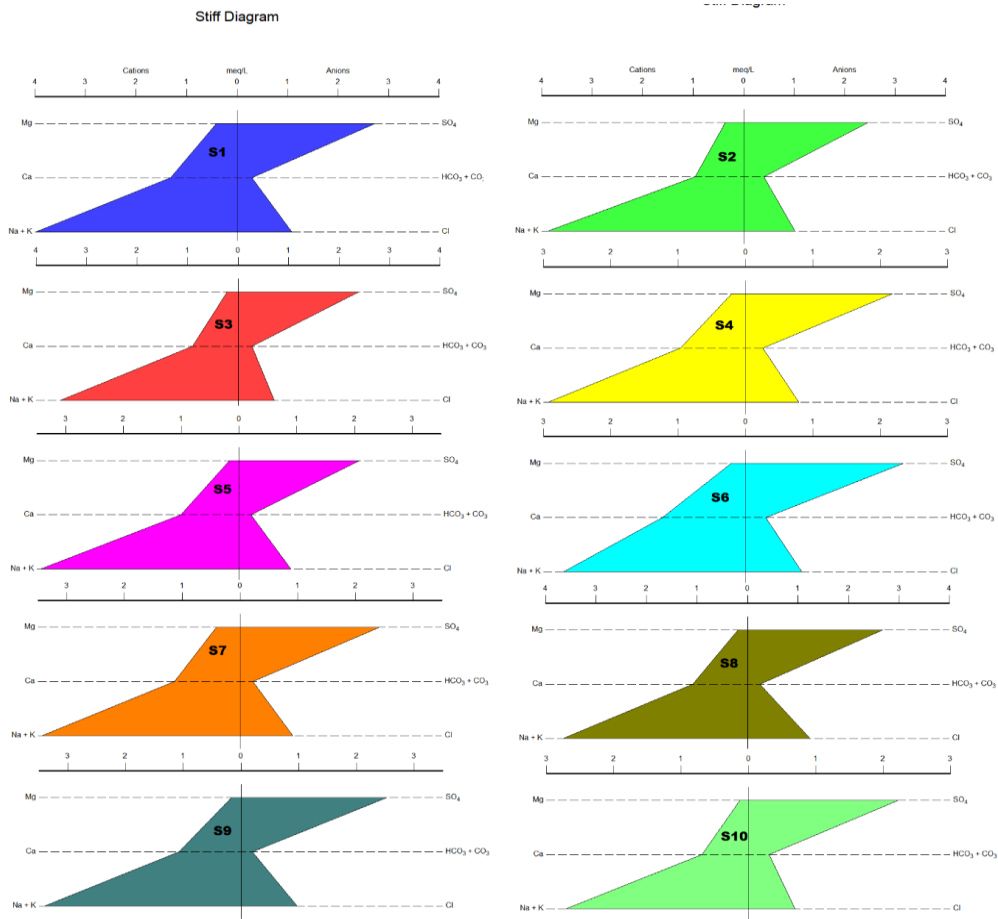


**Fig 4.46: Showing Piper Diagrams of Station S1-S10 for groundwater**

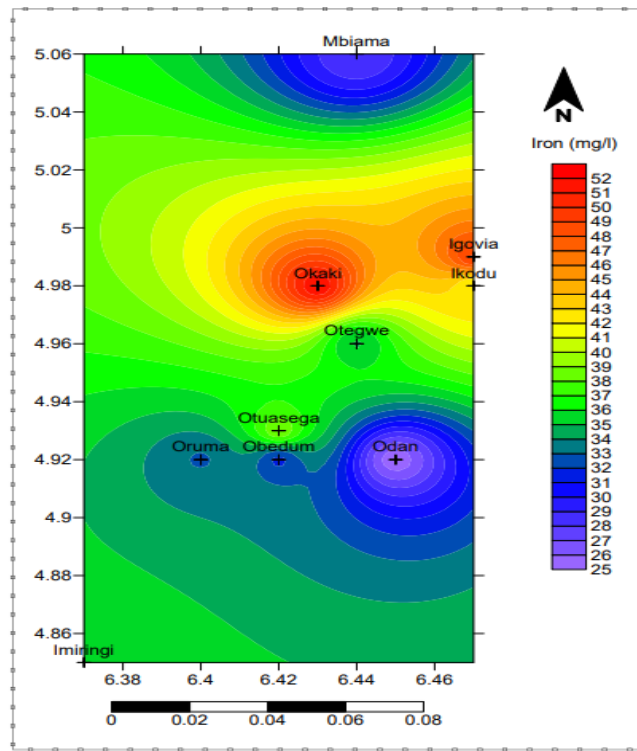


**Fig 4.47a: Spatial Distribution of Iron in Kolo Creek groundwater**

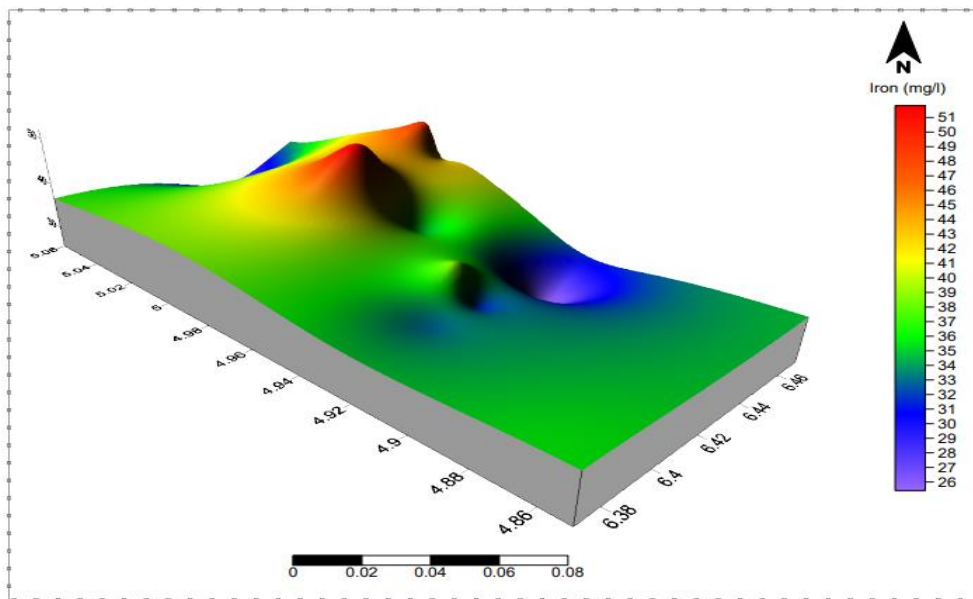


**Fig 4.47b: 3D view of Iron in Kolo Creek groundwater**

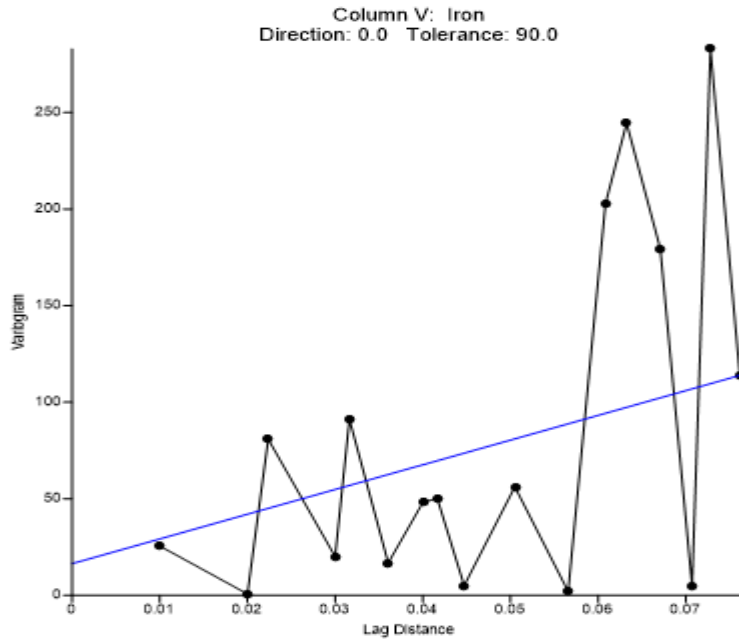


**Fig 4.47c: Variogram of Iron for groundwater**

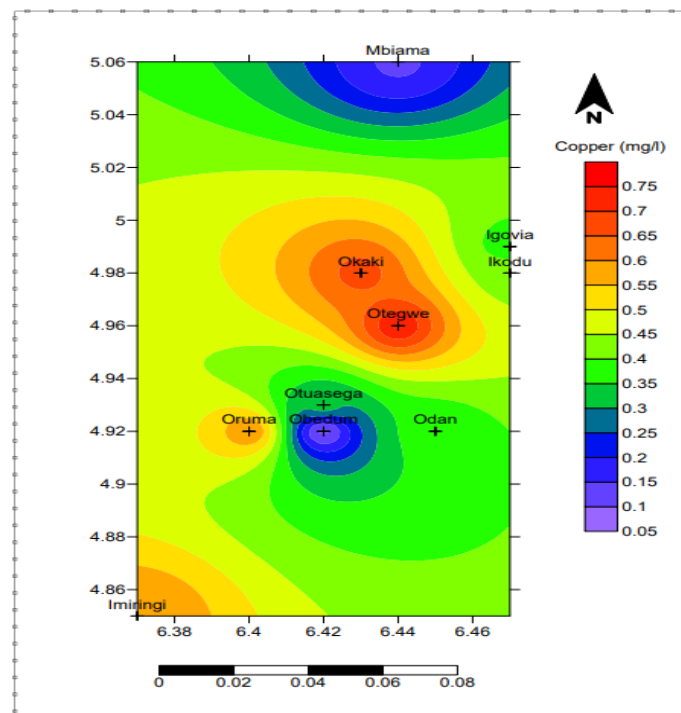


**Fig 4.48a: Spatial Distribution of Copper in Kolo Creek groundwater**

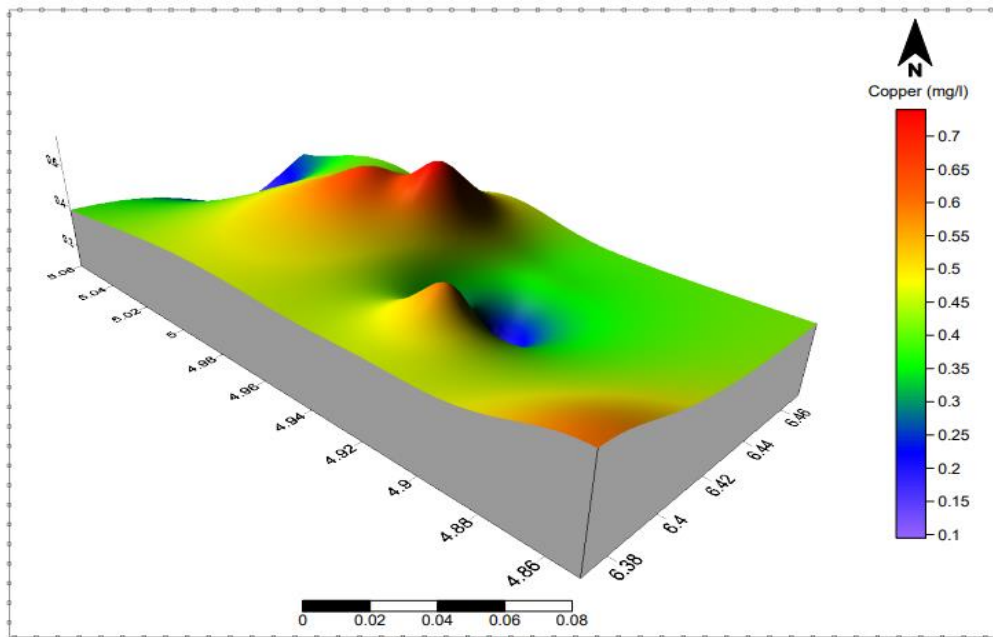


**Fig 4.48b: 3D view of Copper in Kolo Creek groundwater**

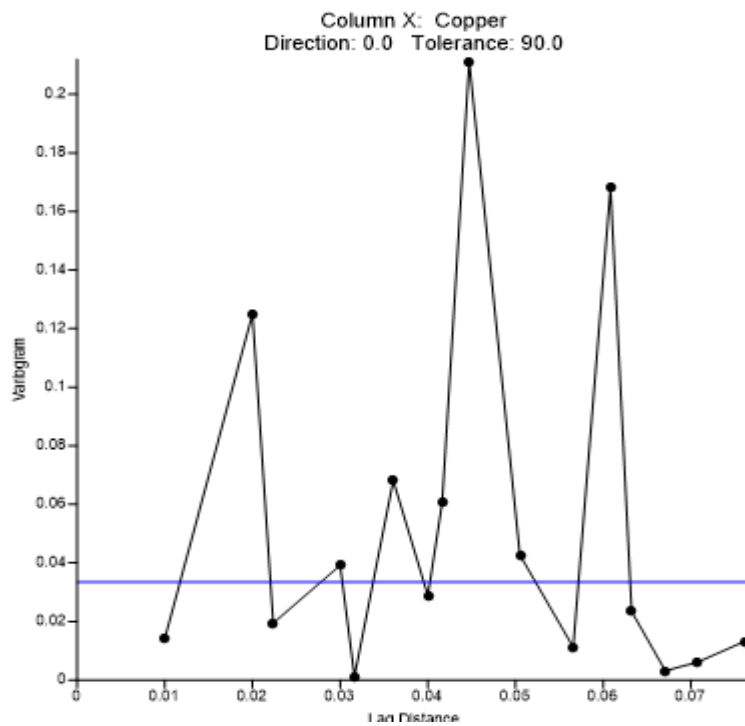


**Fig 4.48c: Variogram of Zinc for groundwater**

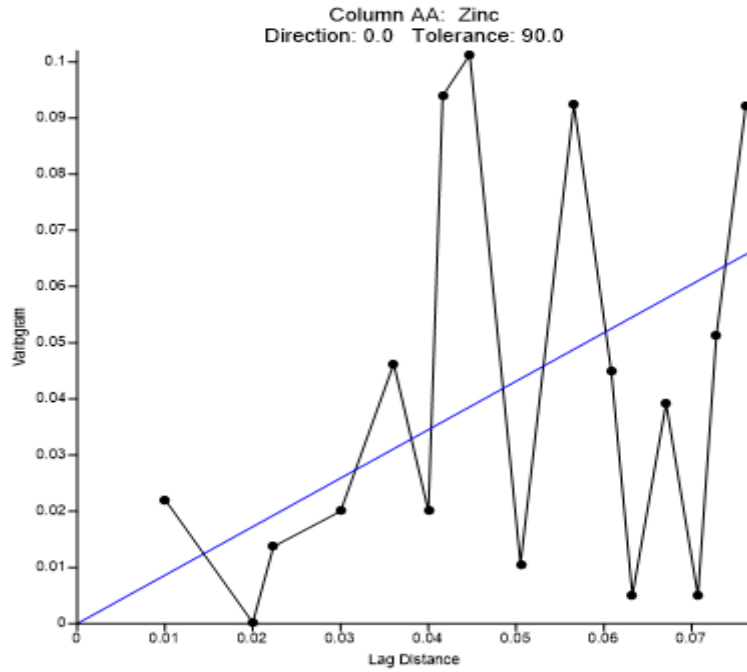


**Fig 4.49a: Variogram of Zinc for groundwater**

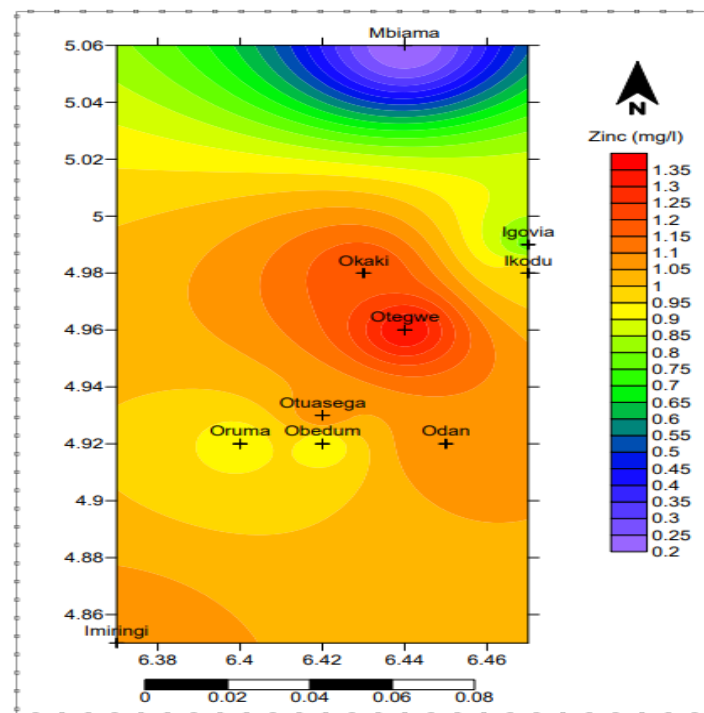


**Fig 4.49b: Spatial Distribution of Zinc in Kolo Creek groundwater**

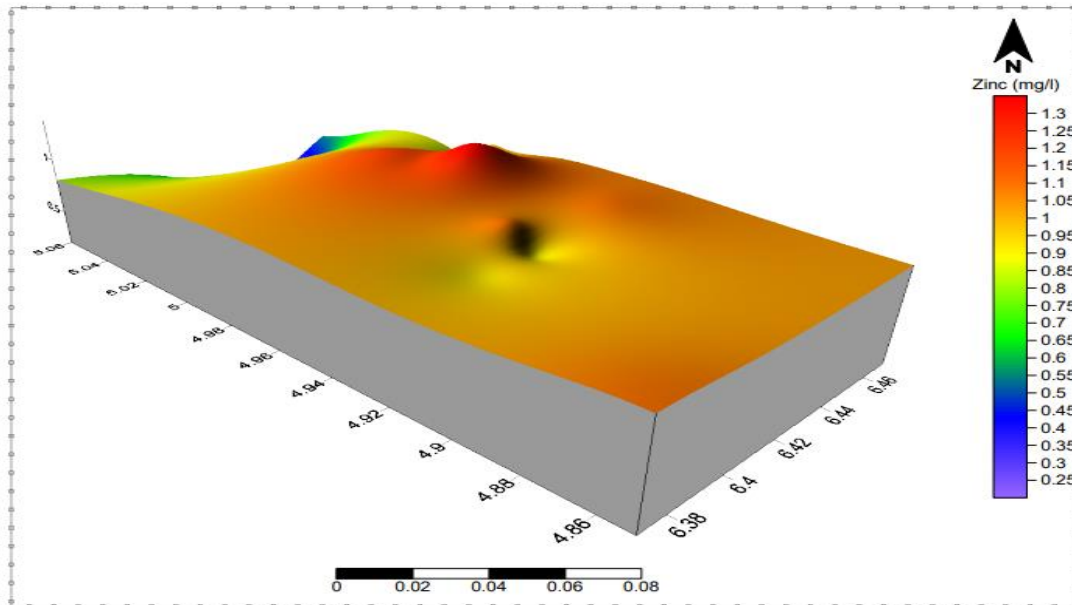


**Fig 4.49c: 3D view of Zinc in Kolo Creek groundwater**

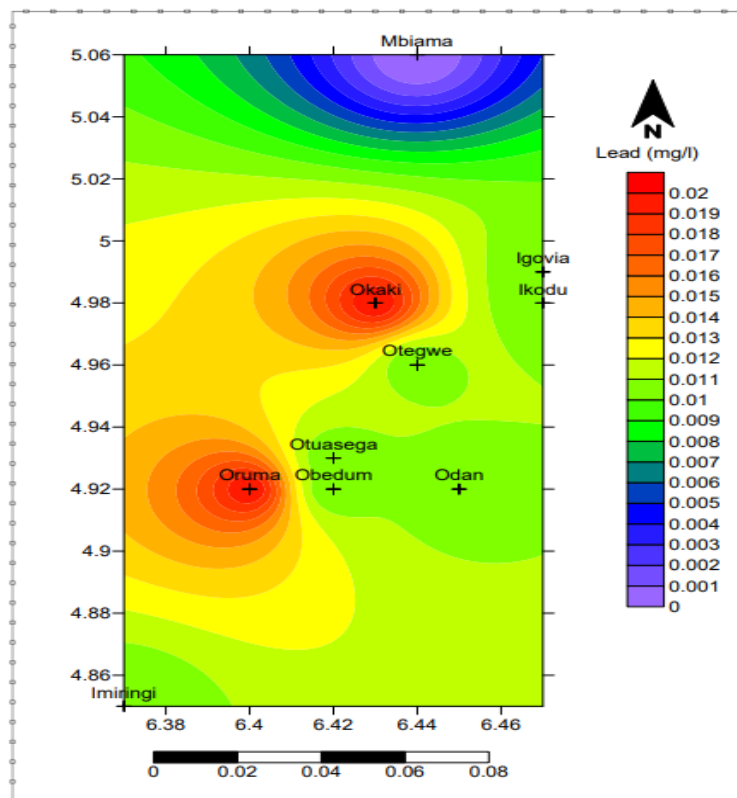


**Fig 4.50a: Spatial Distribution of Lead in Kolo Creek groundwater**

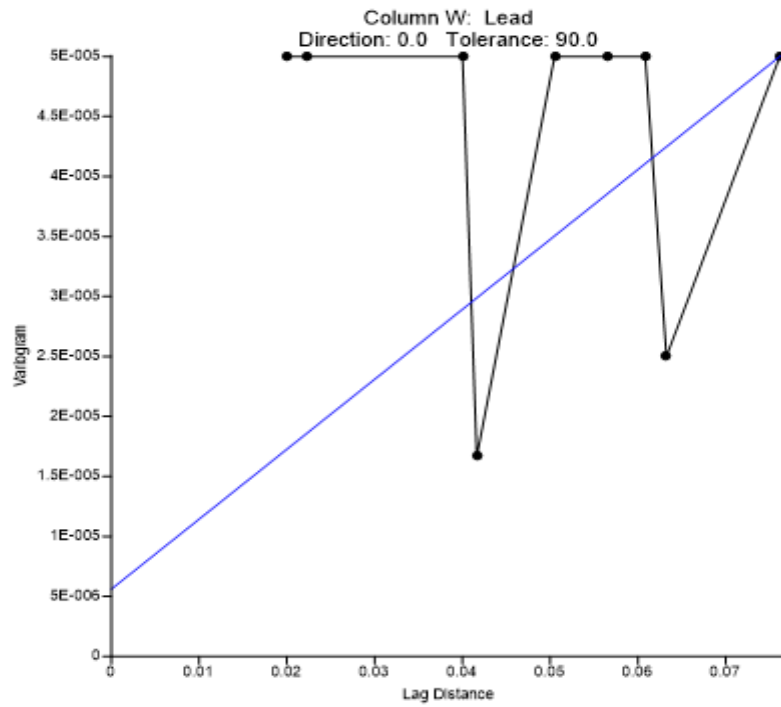


**Fig 4.50b: Variogram of Zinc for groundwater**

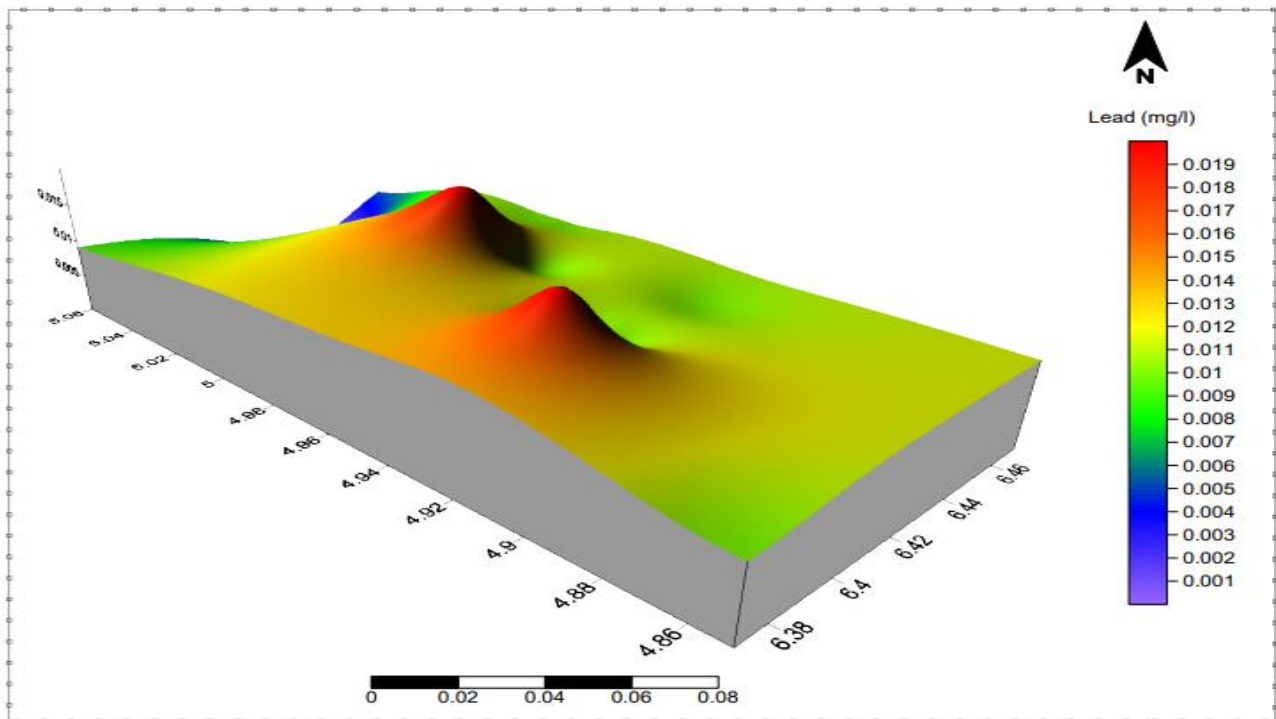


**Fig 4.50c: 3D view of Lead in Kolo Creek groundwater**

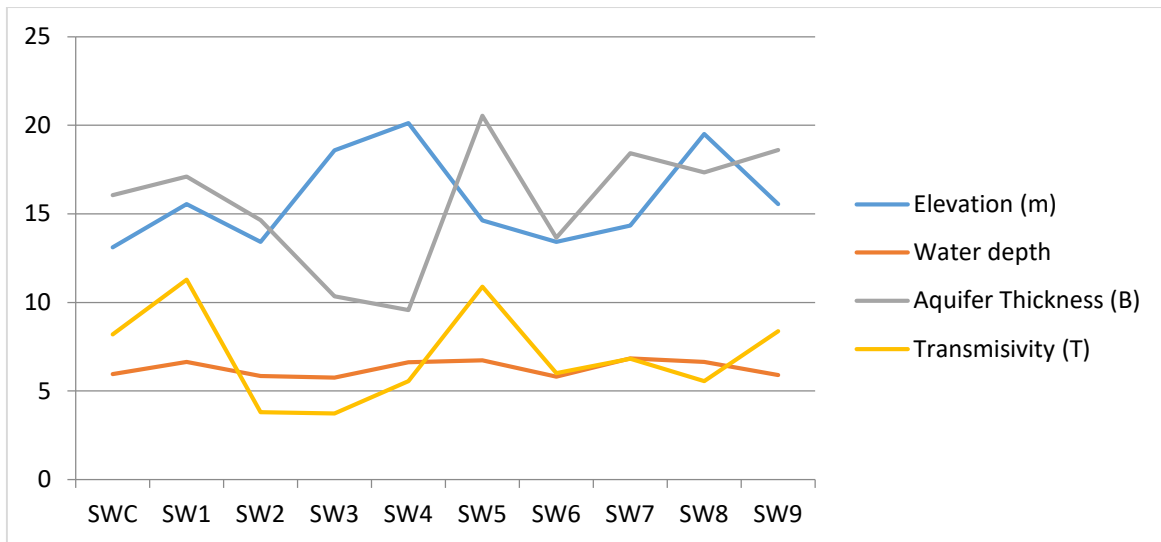


Fig 4.51: Elevation, water table, aquifer thickness and transmissivity variations

Fig 4.52: Elevation Plot Showing Groundwater Flow Direction.

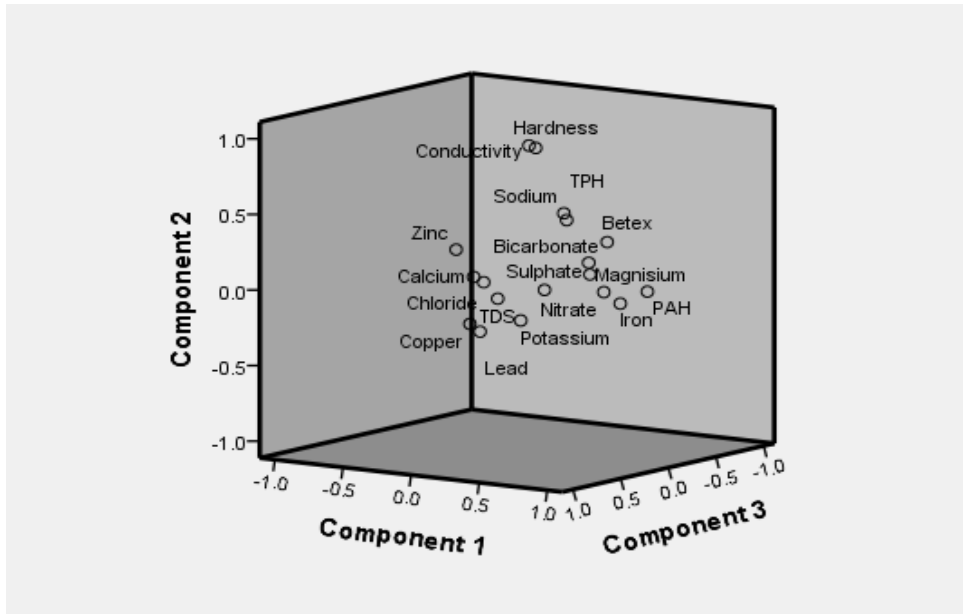


Fig. 4.53: Principal component plot in rotated space

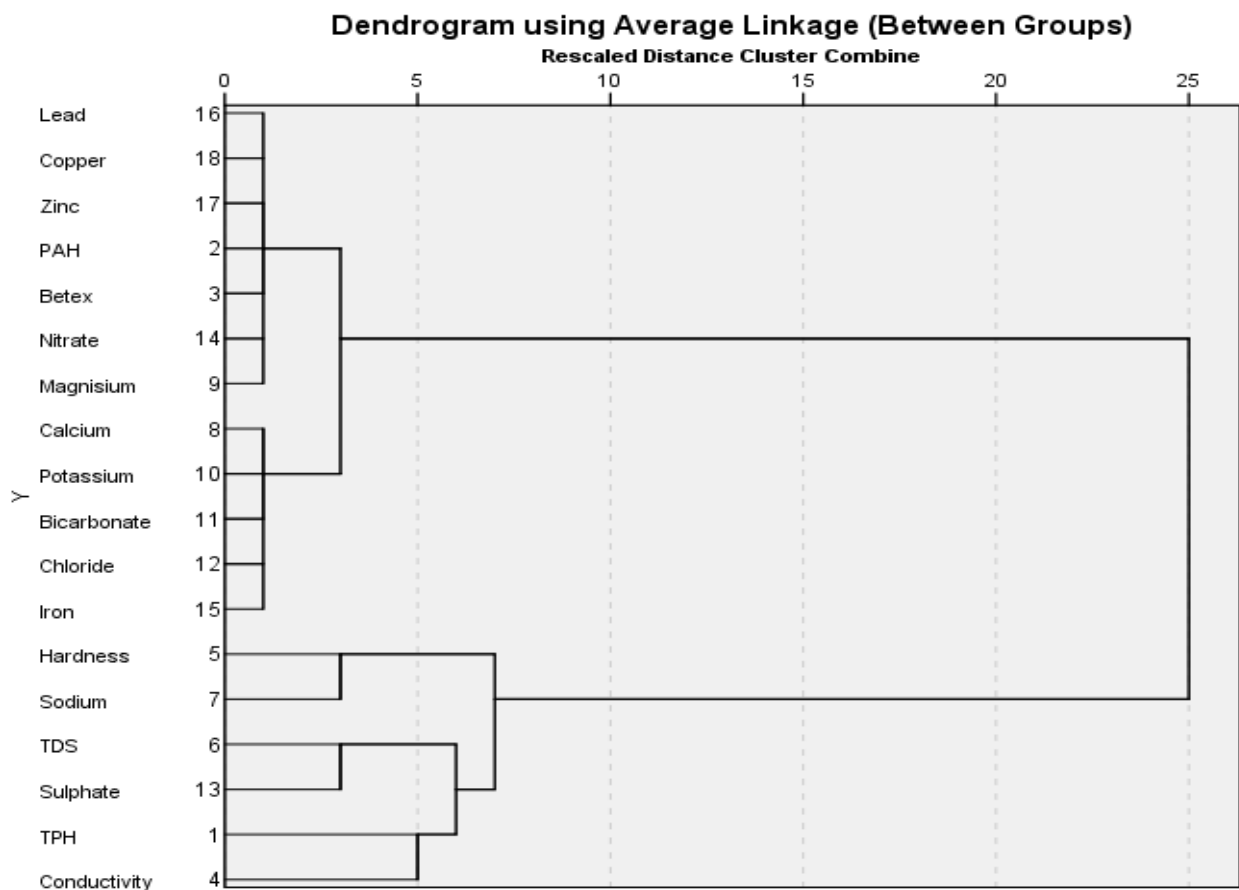


Fig 4.54: Dendrogram of ground water parameters of the study area

Wilcox Diagram in the Study Area (Ground Water)

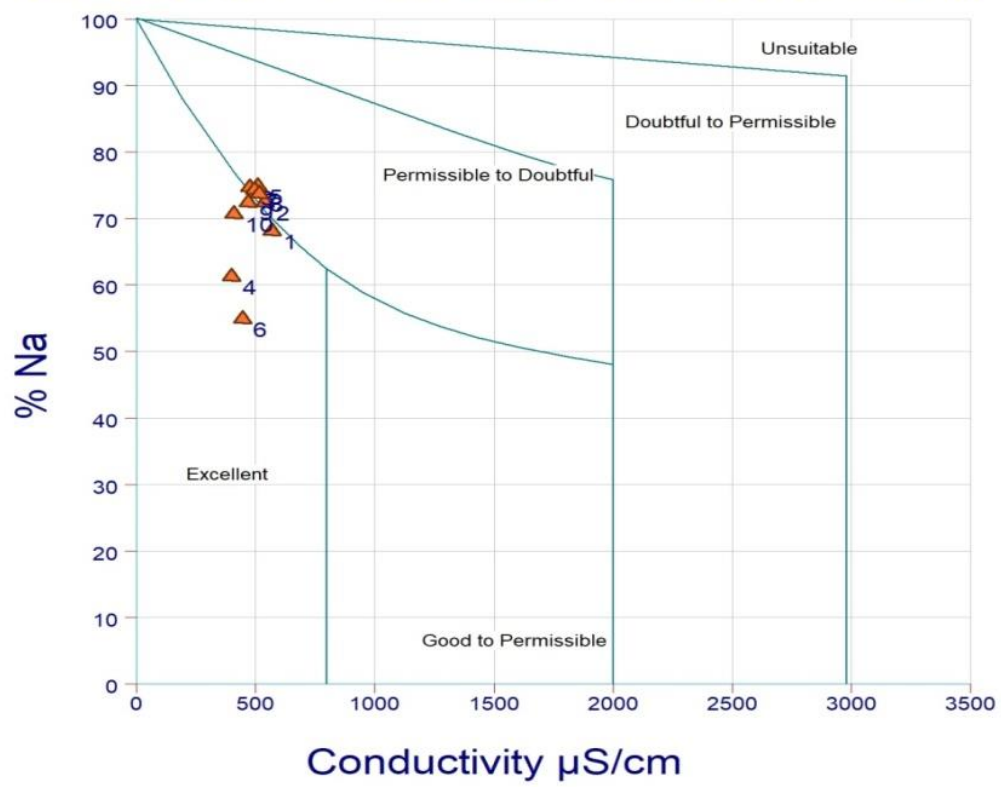


Fig 4.55: Wilcox diagram of ground water parameters of the study area

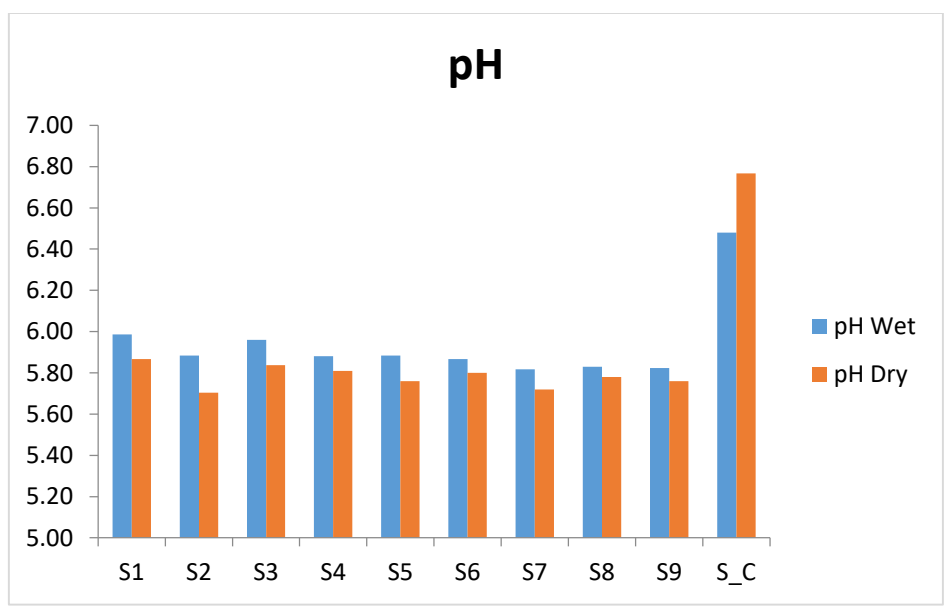


Fig 4.56a: Station Variations of pH in Kolo Creek soil

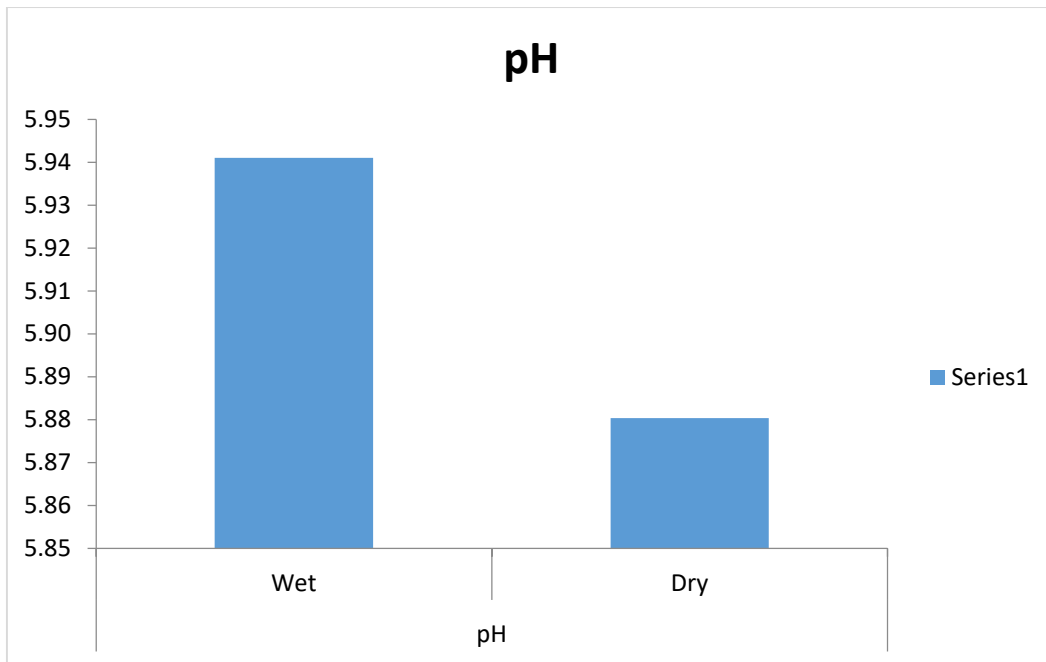


Fig 4.56b: Seasonal Variations of pH in Kolo Creek Soil

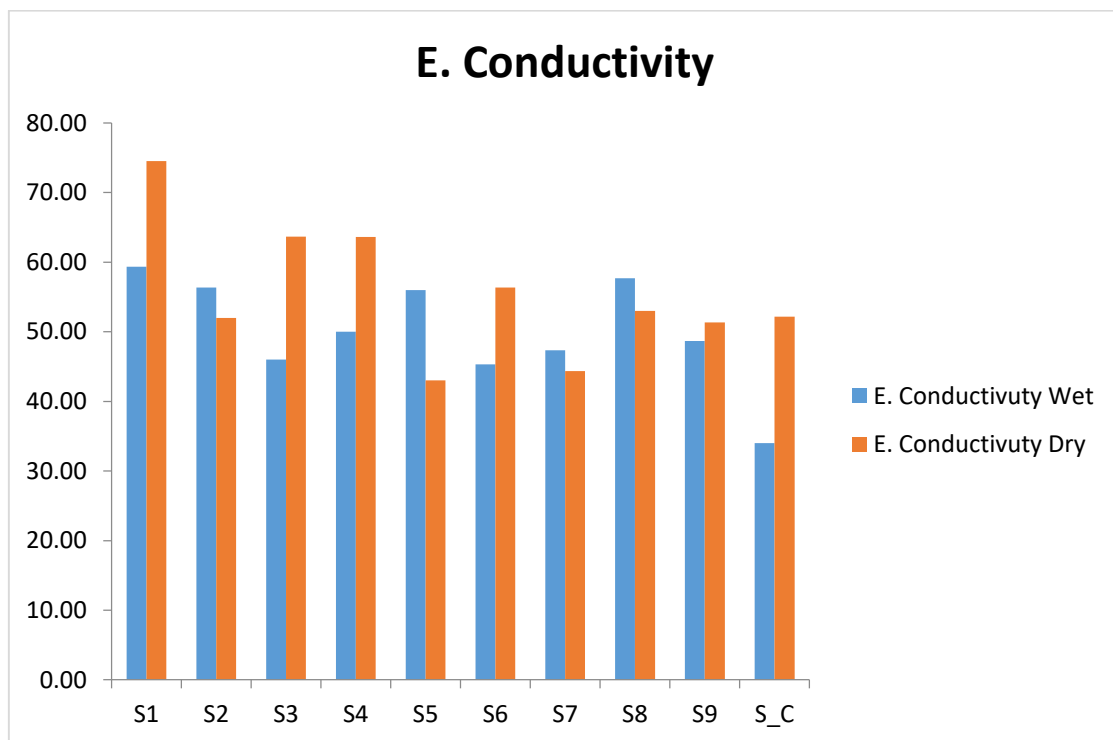


Fig 4.57a: Station Variations of E. Conductivity in Kolo Creek Soil

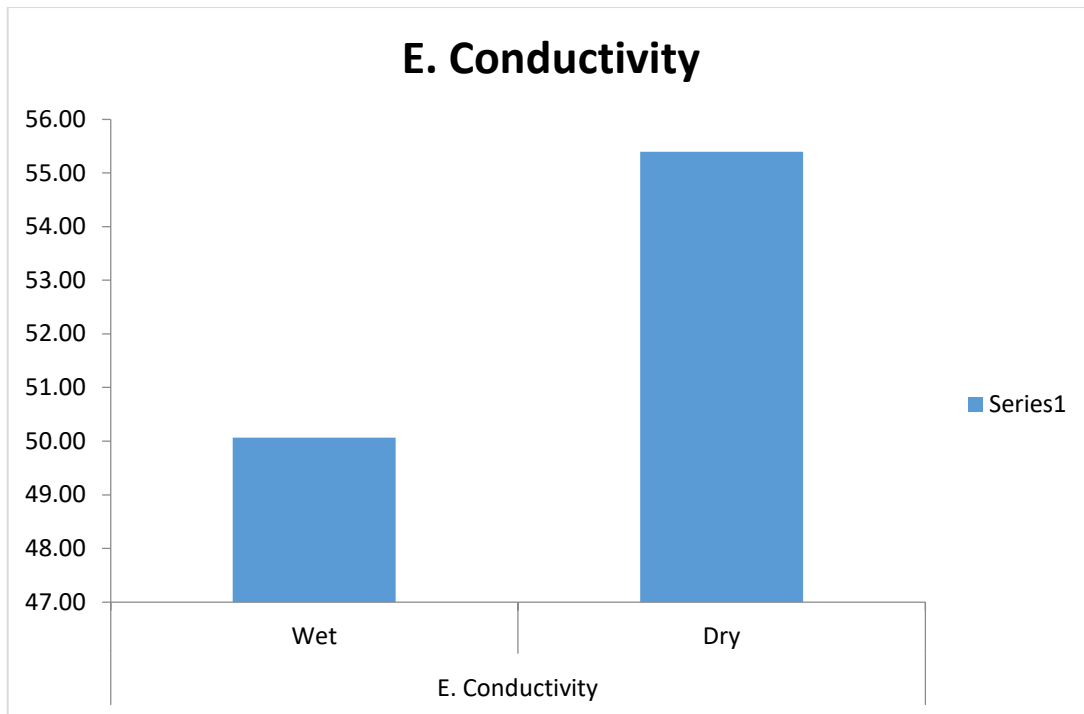


Fig 4.57b: Seasonal Variations of E. Conductivity in Kolo Creek Soil

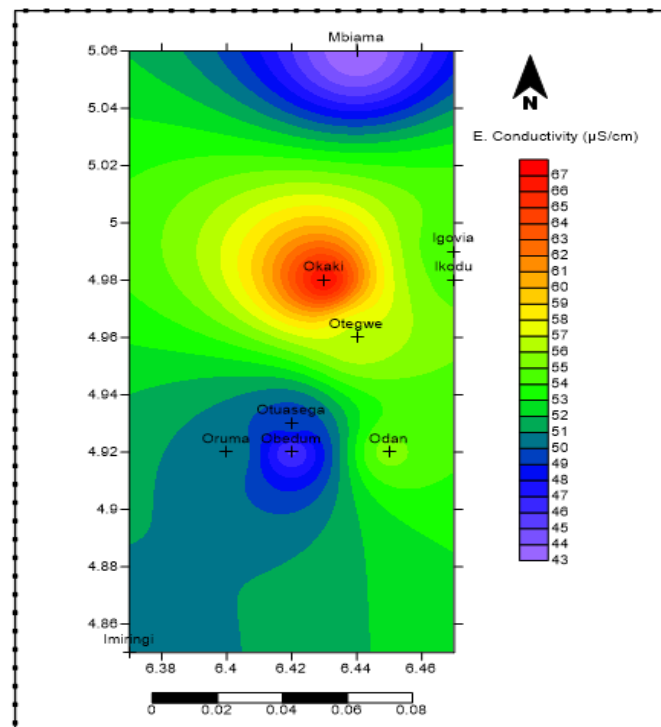


Fig 4.57c: Spatial Variations of E. Conductivity in Kolo Creek Soil

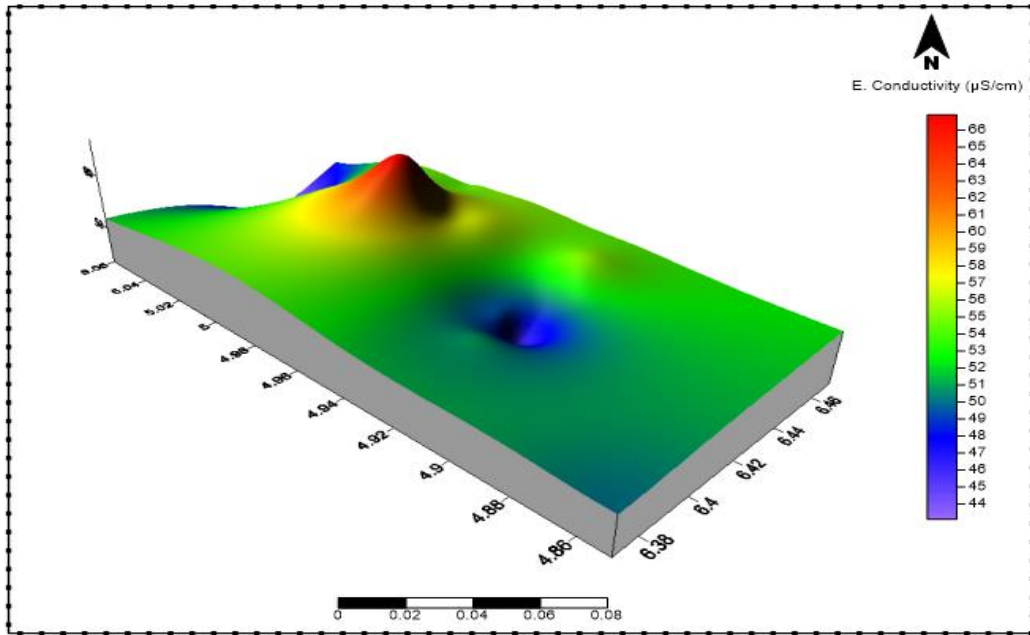


Fig 4.57d: 3D view of Electrical Conductivity in Kolo Creek Soils

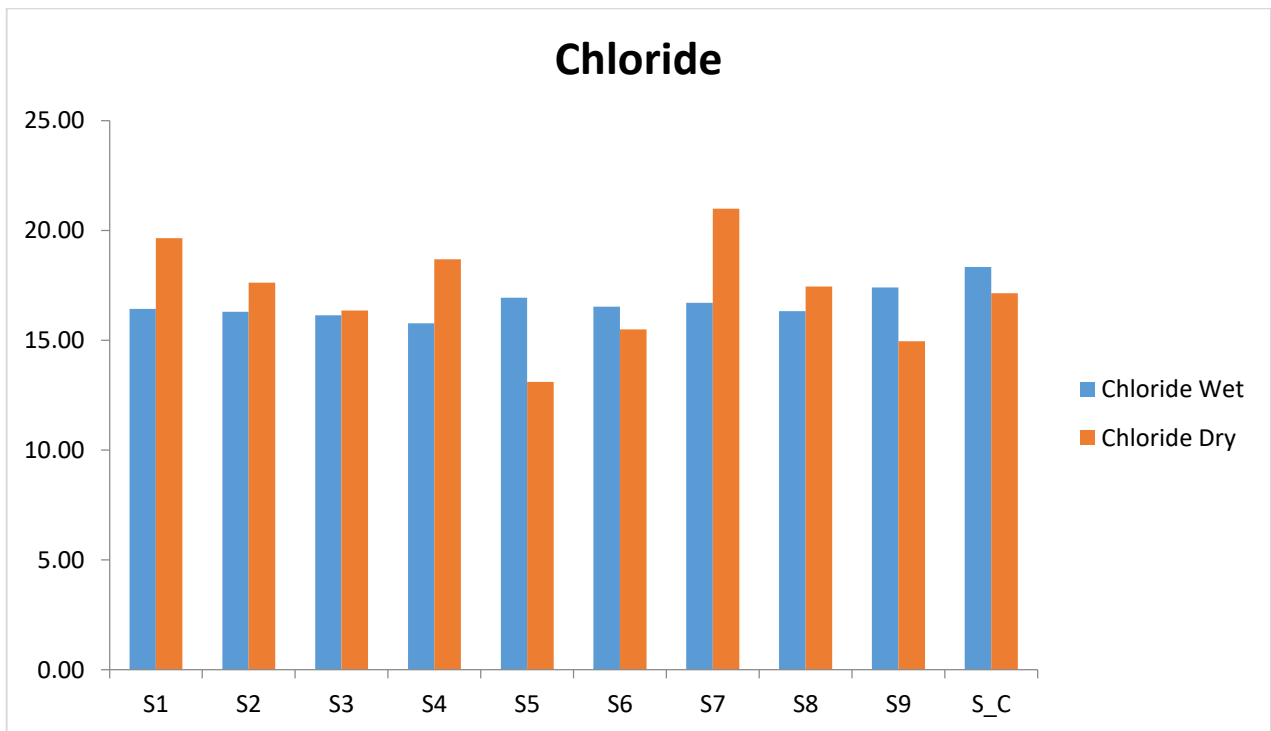


Fig 4.58a: Station Variations of Chloride in Kolo Creek Soil

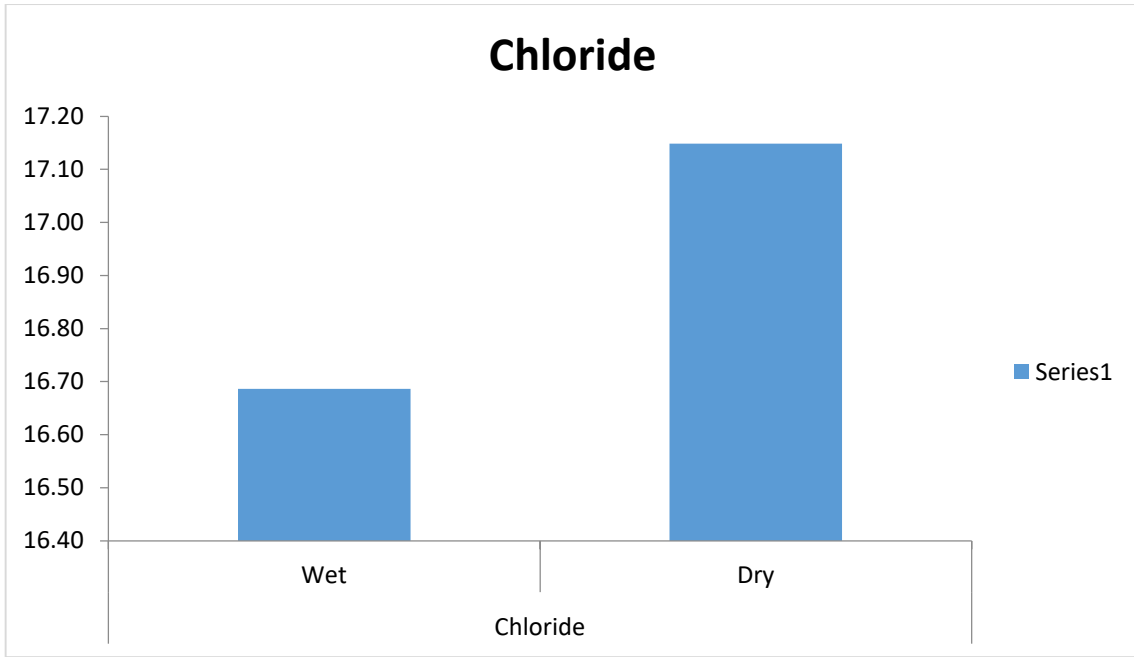


Fig 4.58b: Seasonal Variations of Chlorides in Kolo Creek Soils

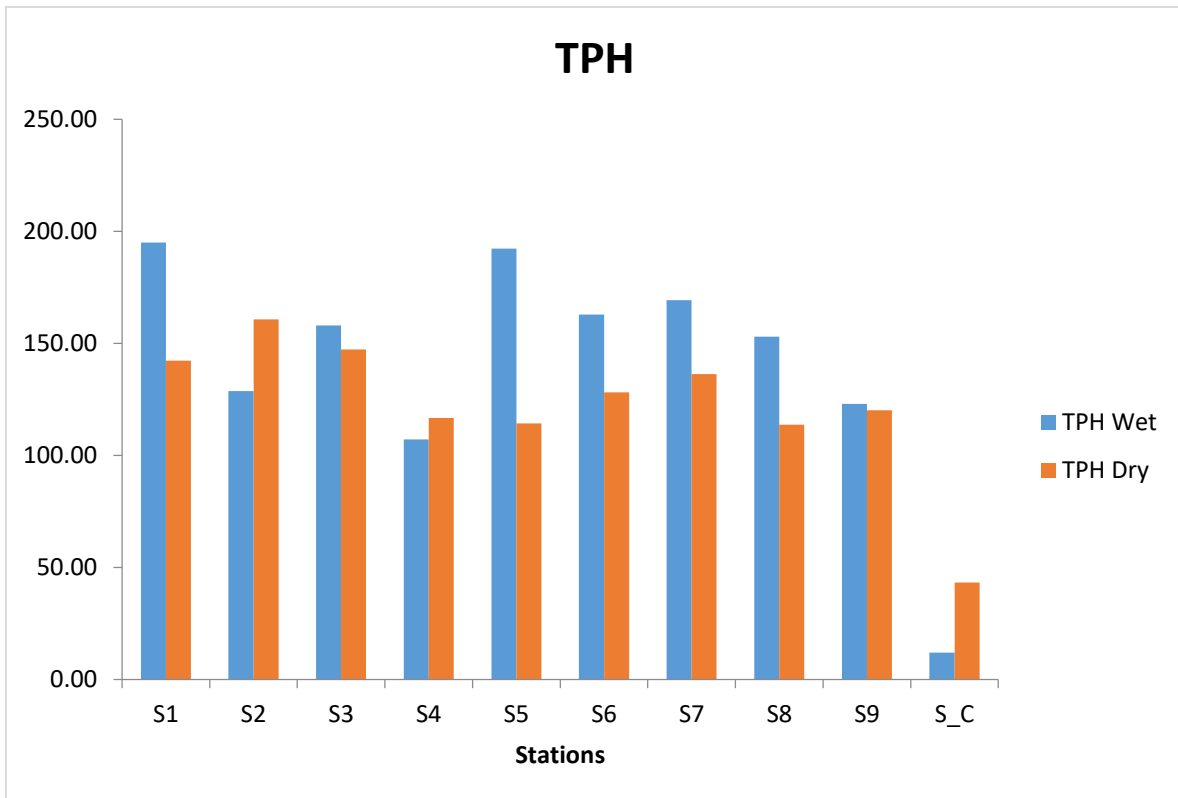


Fig 4.59a: Station Variations of TPH in Kolo Creek Soil

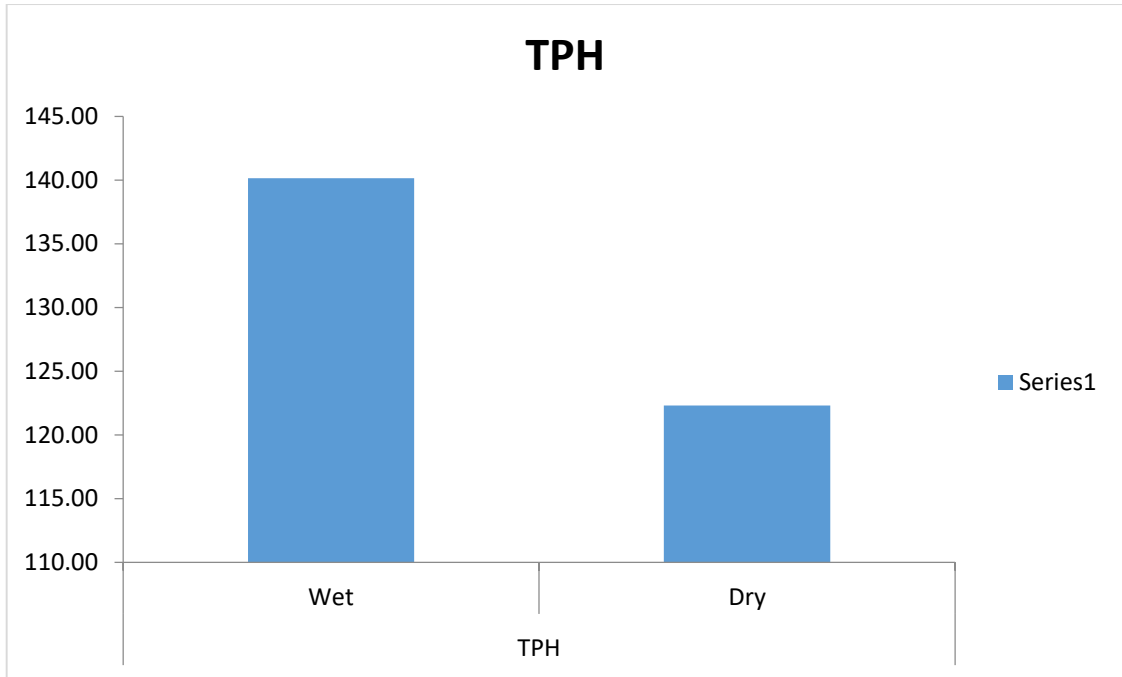


Fig 4.59b: Seasonal Variations of TPH in Kolo Creek Soil

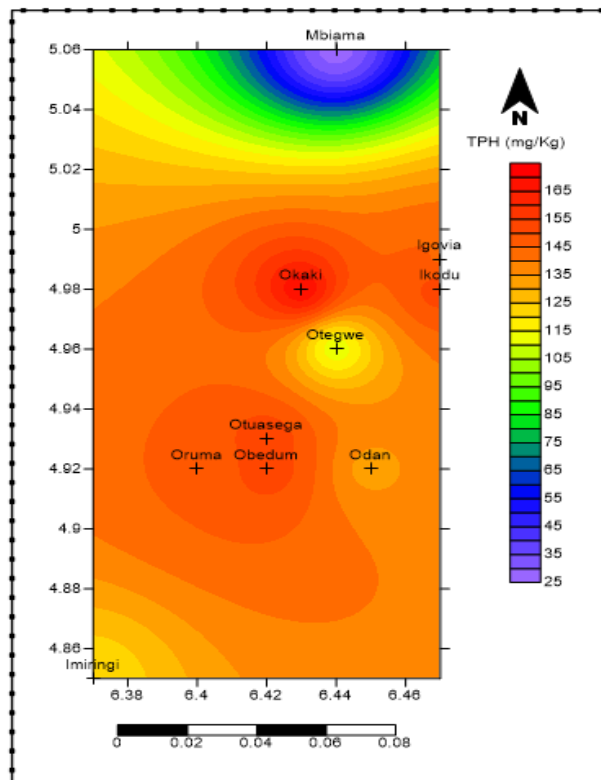


Fig 4.59c: Spatial Variations of TPH in Kolo Creek Soil

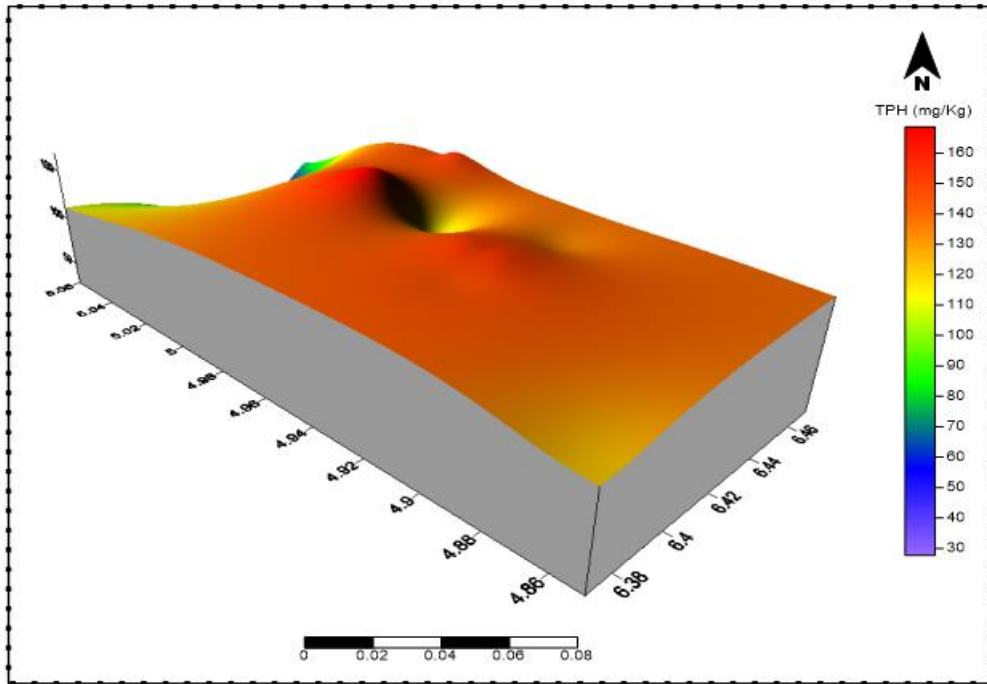


Fig 4.59d: 3D View of TPH in Kolo Creek Soils

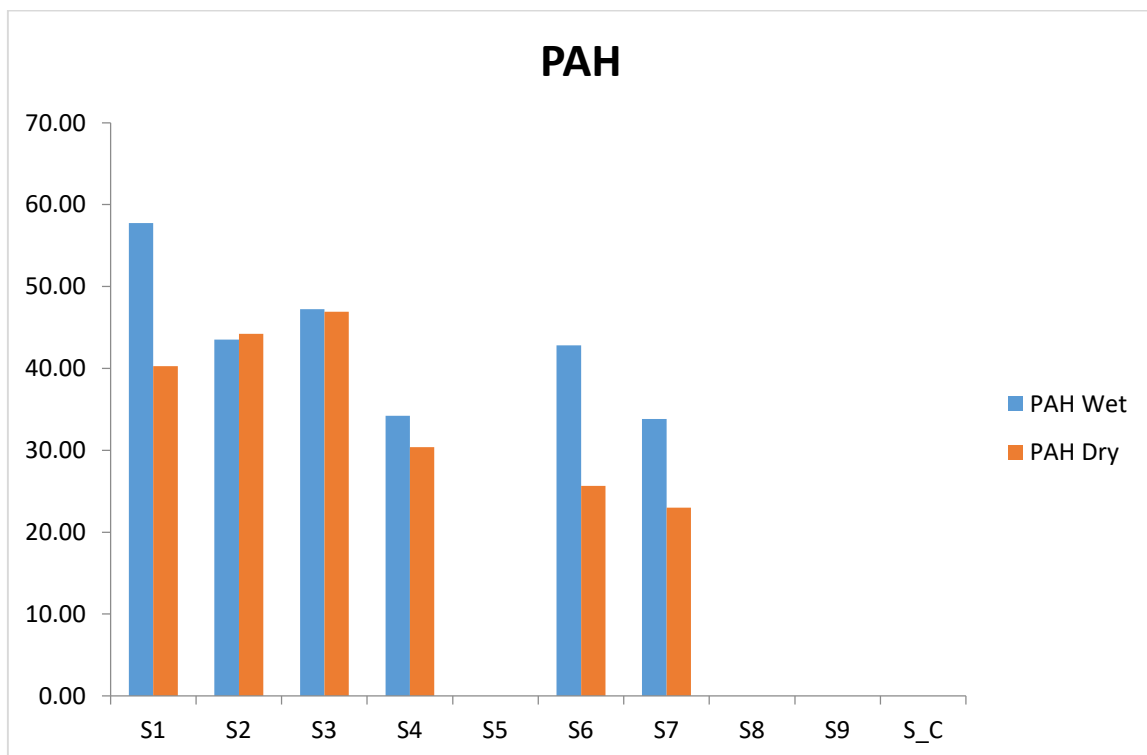


Fig 4.60a: Station Variations of PAH in Kolo Creek soil

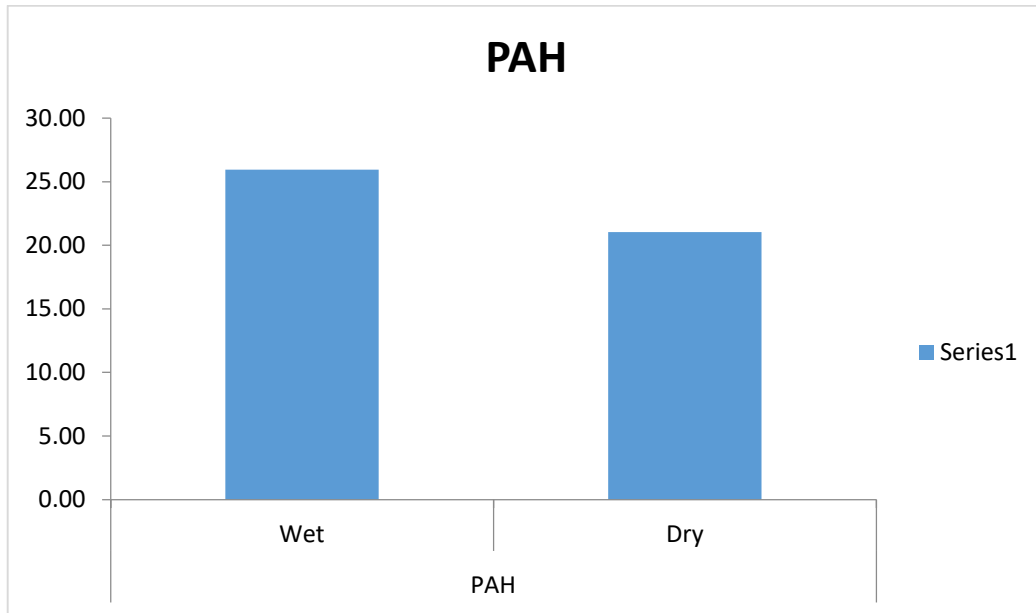


Fig 4.60b: Seasonal Variations of PAH in Kolo Creek Soil

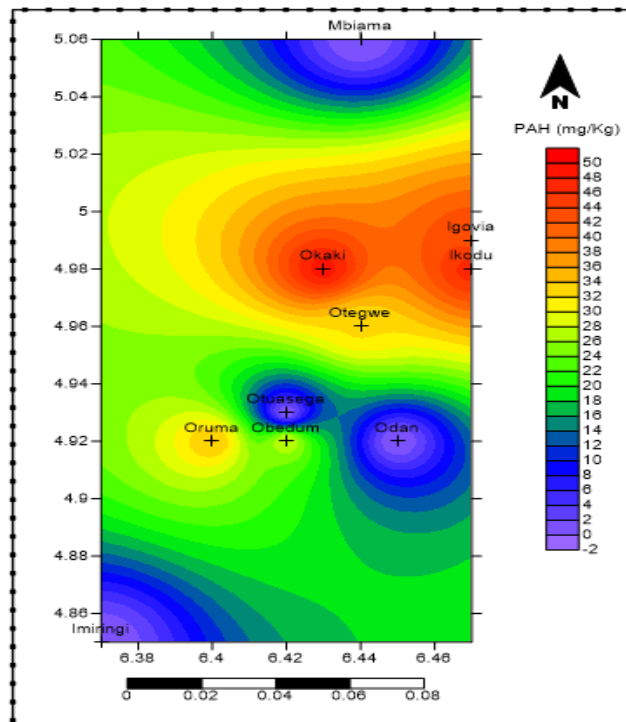


Fig 4.60c: Spatial Distribution of PAH in Kolo Creek Soil

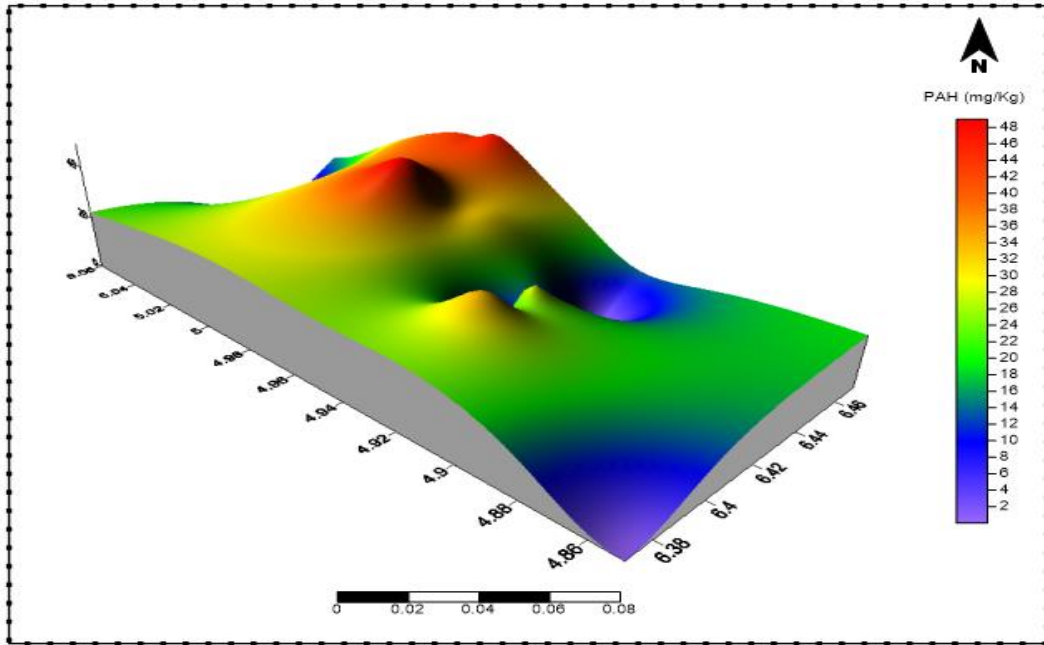


Fig 4.60d: 3D View of PAH in Kolo Creek Soils

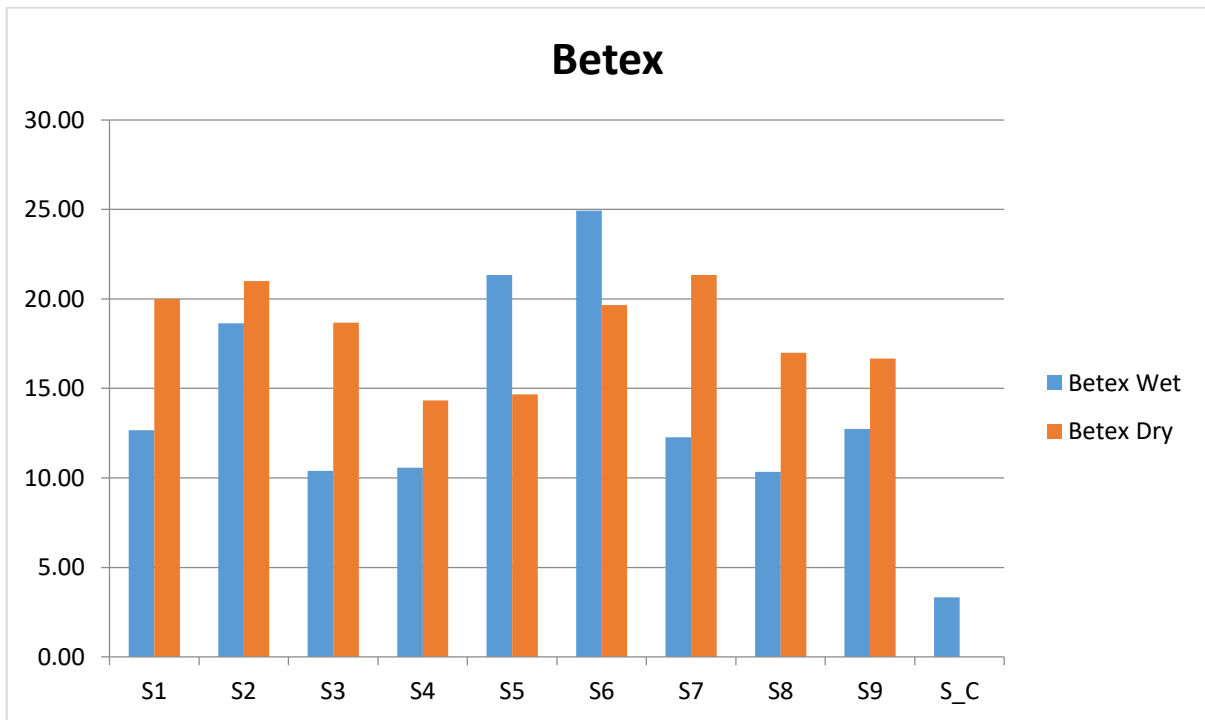


Fig 4.61a: Station Variations of Betex in Kolo Creek Soil

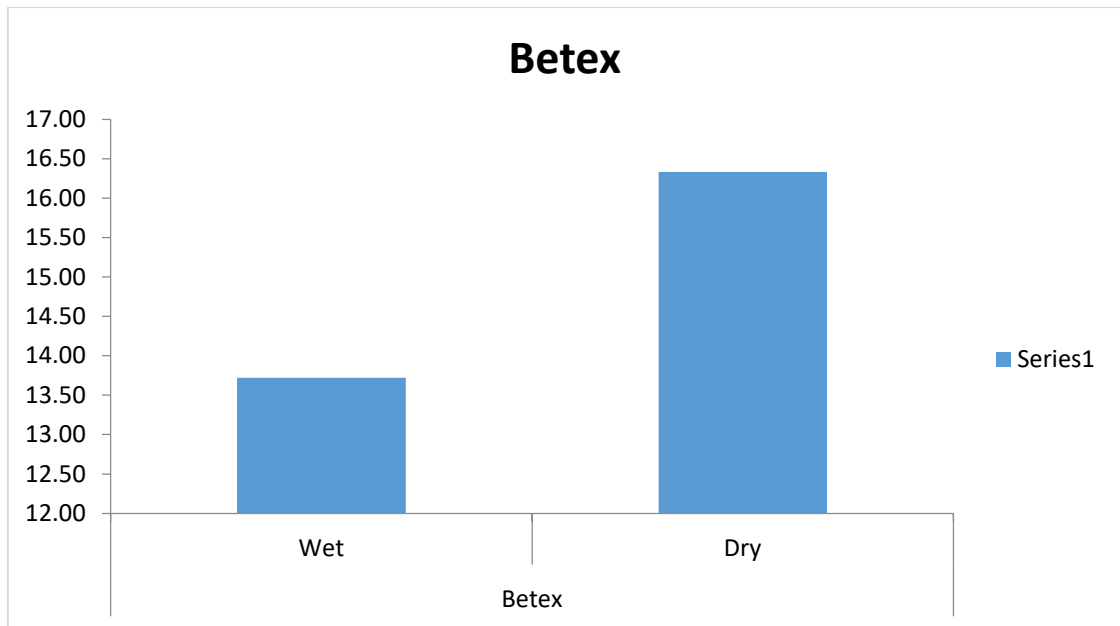


Fig 4.61b: Seasonal Variations of Betex in Kolo Creek Soils

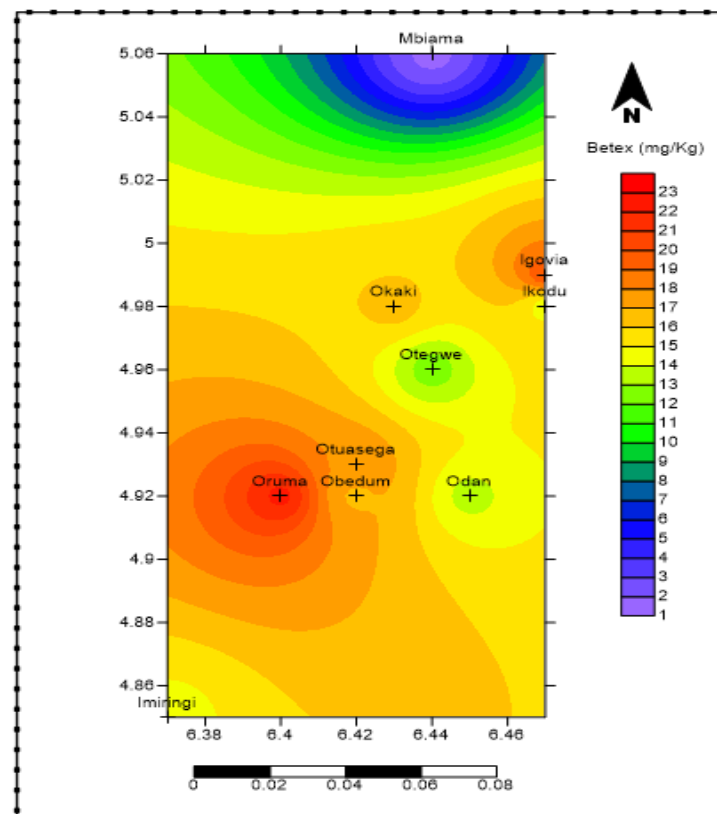


Fig 4.61c: Spatial Distribution of Betex in Kolo Creek Soil

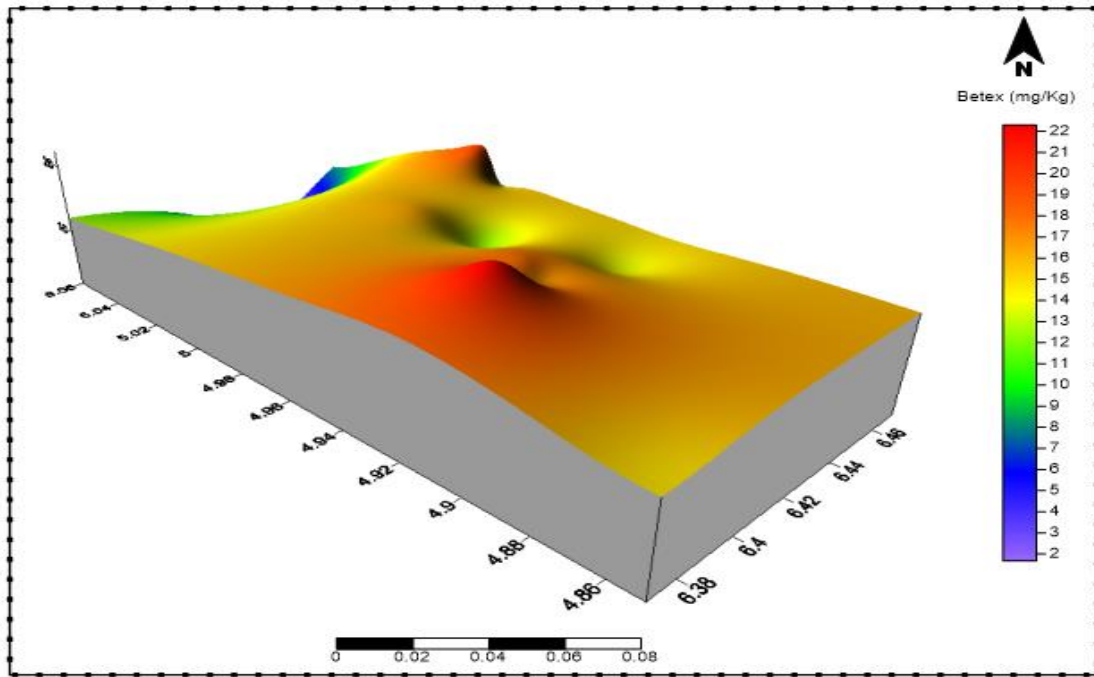


Fig 4.61d: 3D View of Betex in Kolo Creek Soil

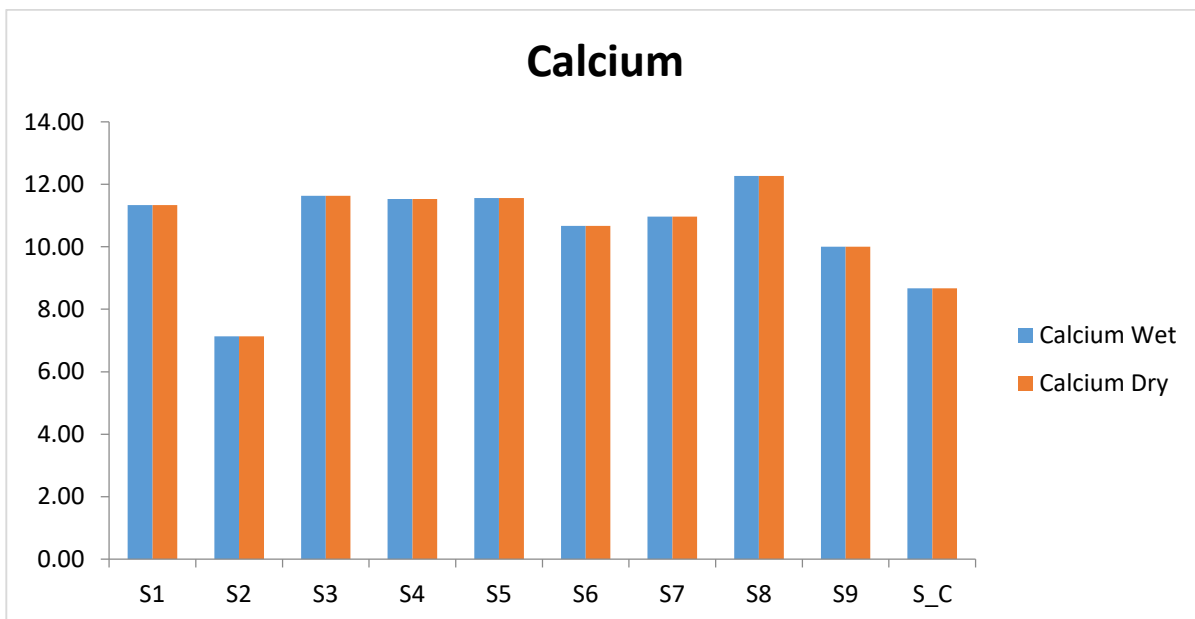


Fig 4.62a: Station Variations of Calcium in Kolo Creek Soil

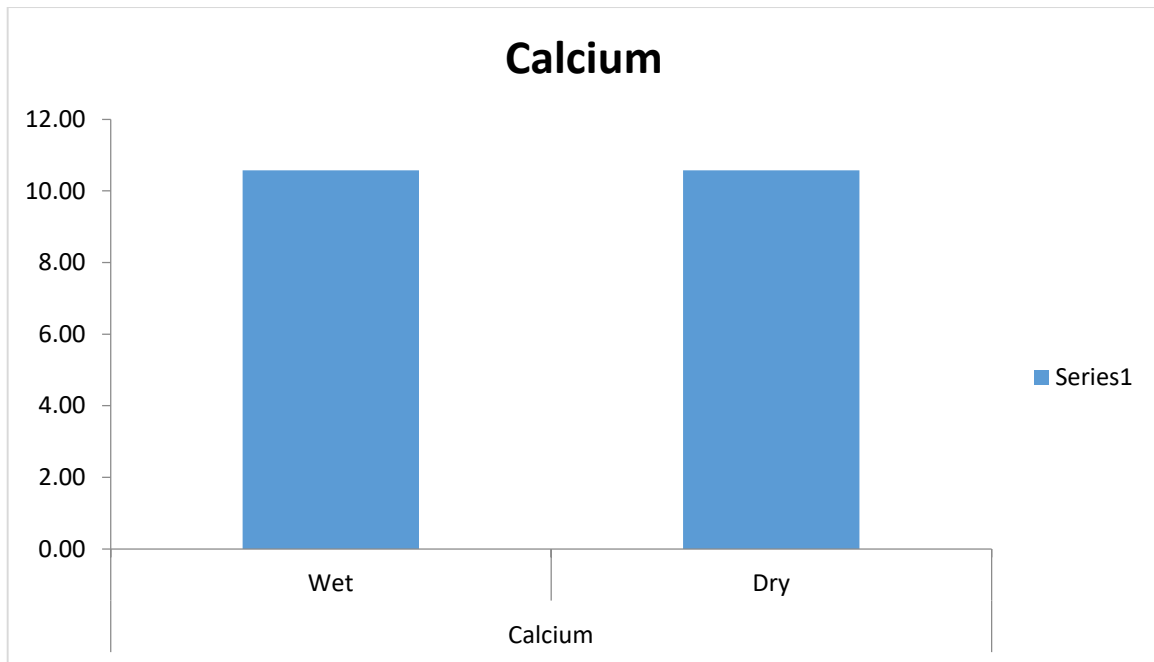


Fig 4.62b: Seasonal Variations of Calcium in Kolo Creek Soil

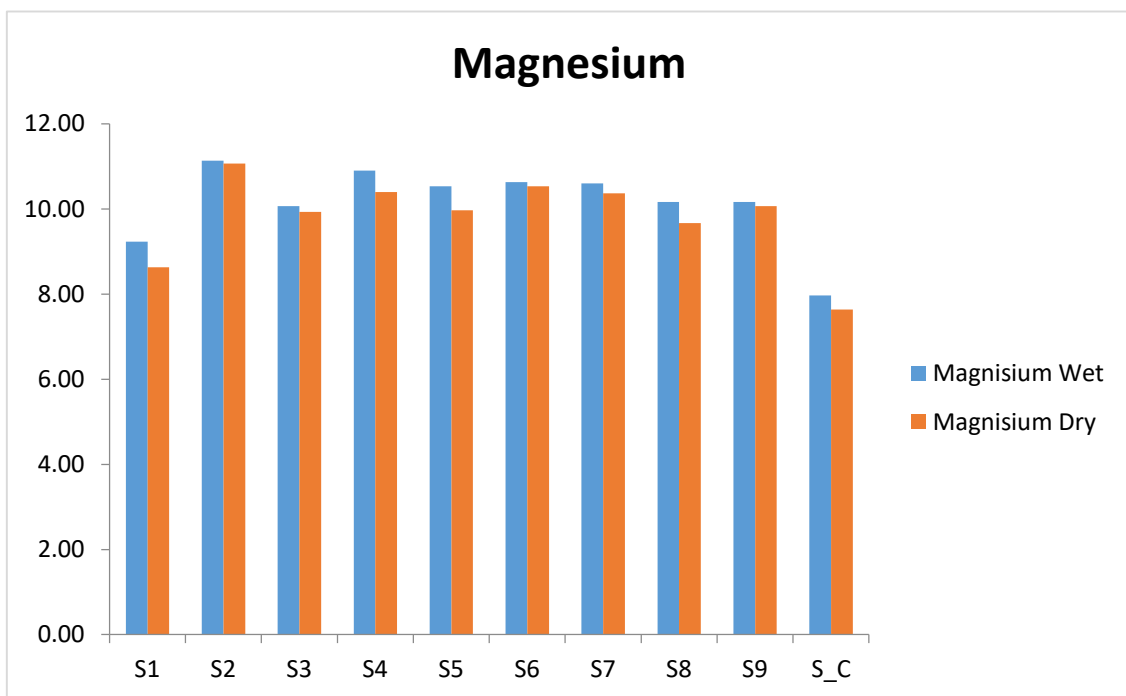


Fig 4.63a: Station Variations of Magnesium in Kolo Creek Soil

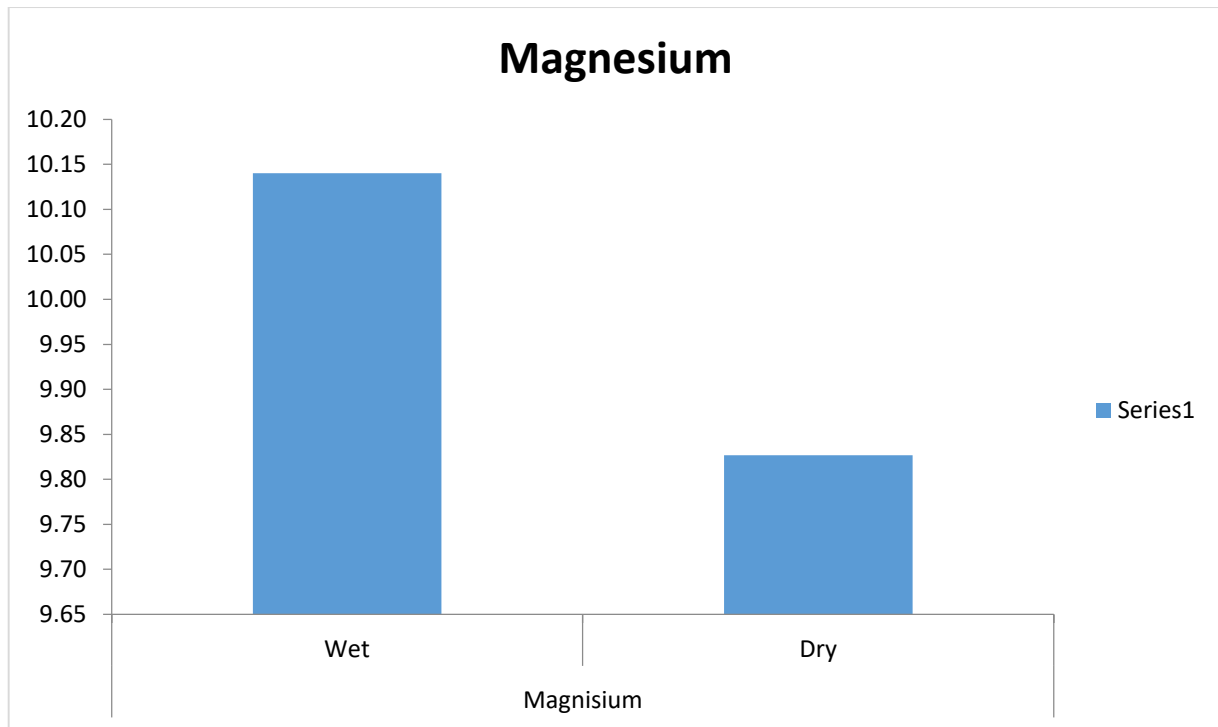


Fig 4.63b: Seasonal Variations of magnesium in Kolo Creek Soil

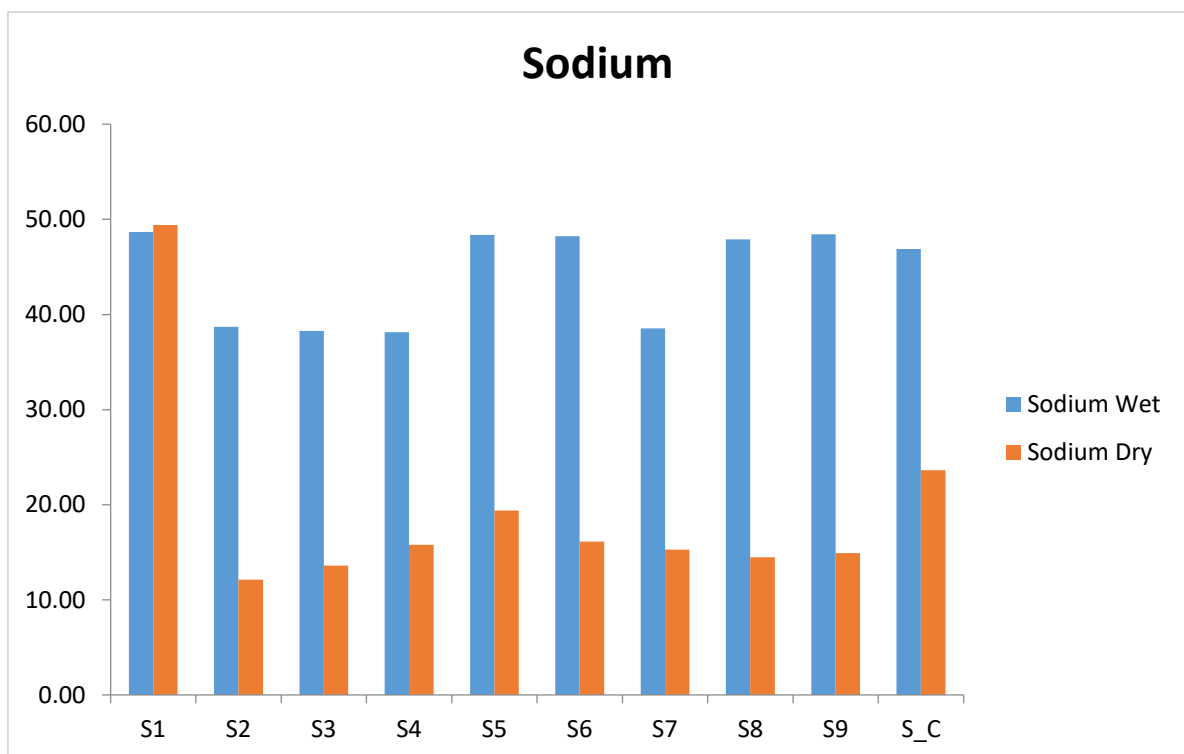


Fig 4.64a: Station Variations of Sodium in Kolo Creek Soil

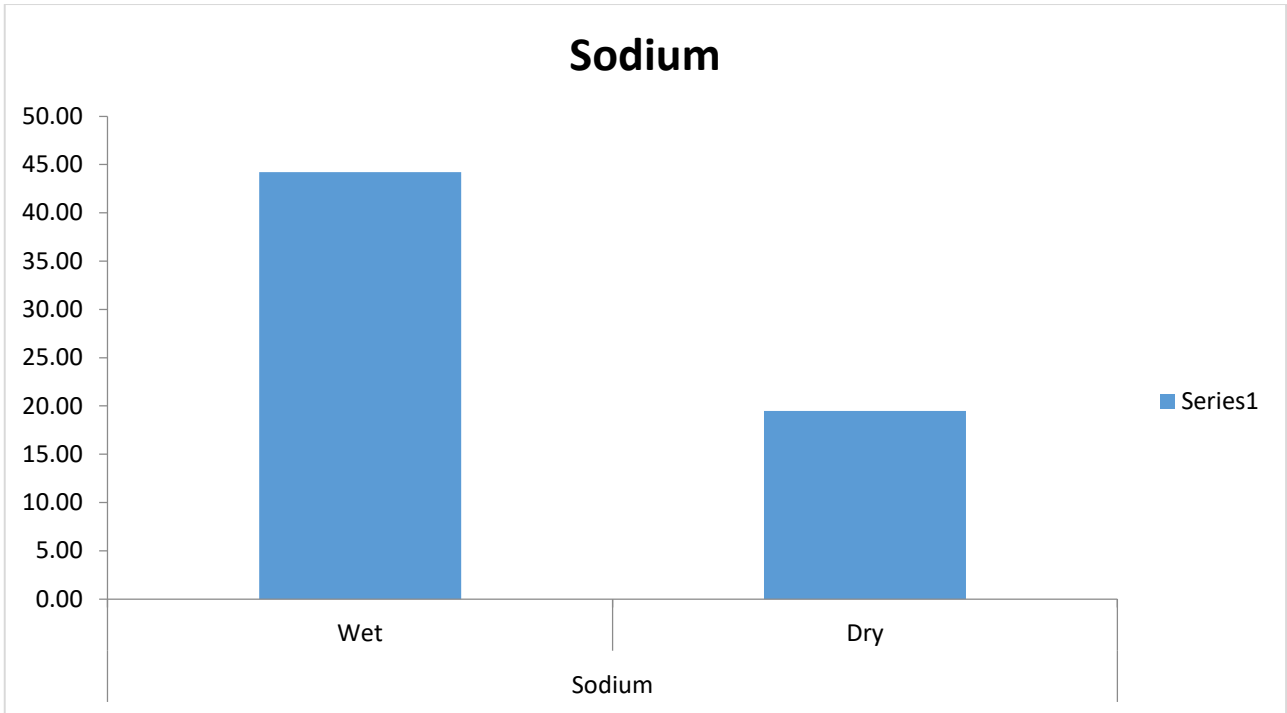


Fig 4.64b: Seasonal Variations of Sodium in Kolo Creek Soil

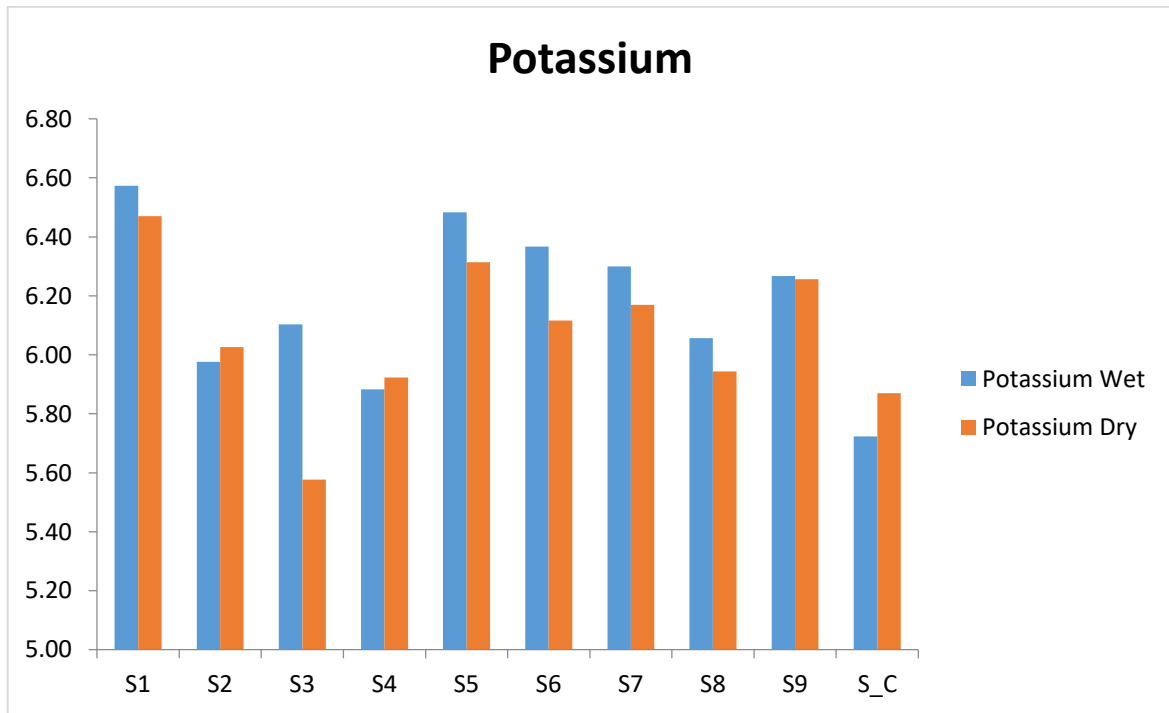


Fig 4.65a: Station Variations of Potassium in Kolo Creek Soil

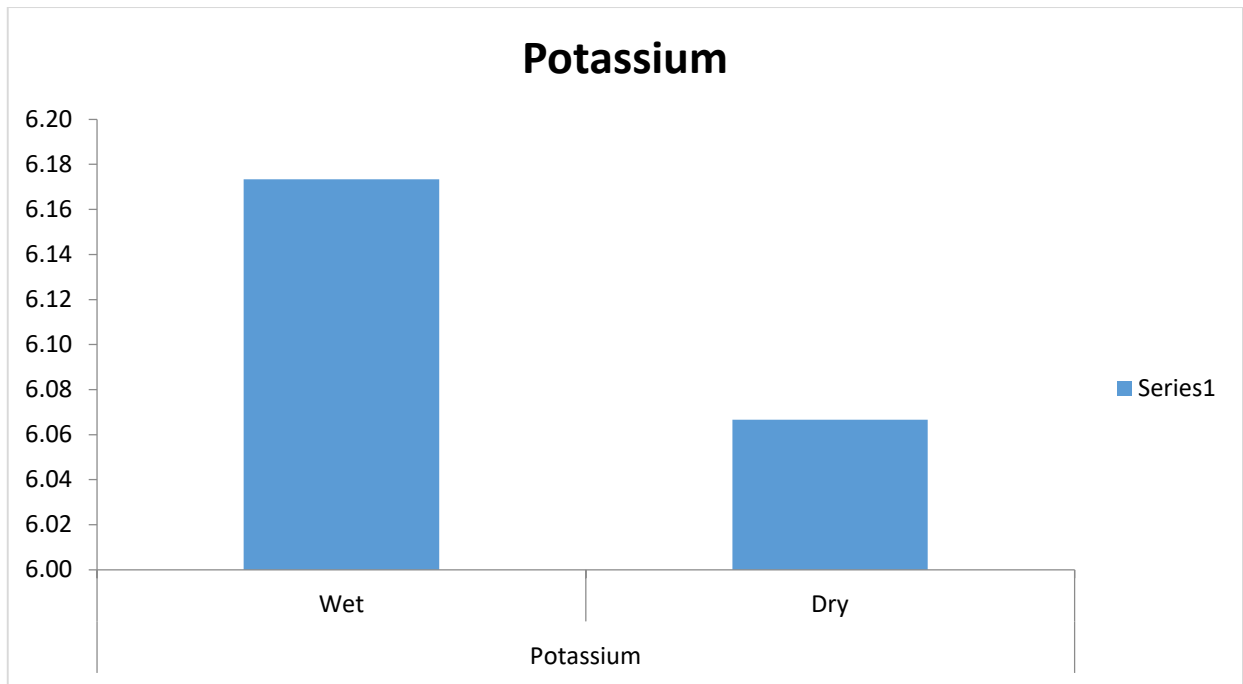


Fig 4.65b: Seasonal Variations of Potassium in Kolo Creek Soil

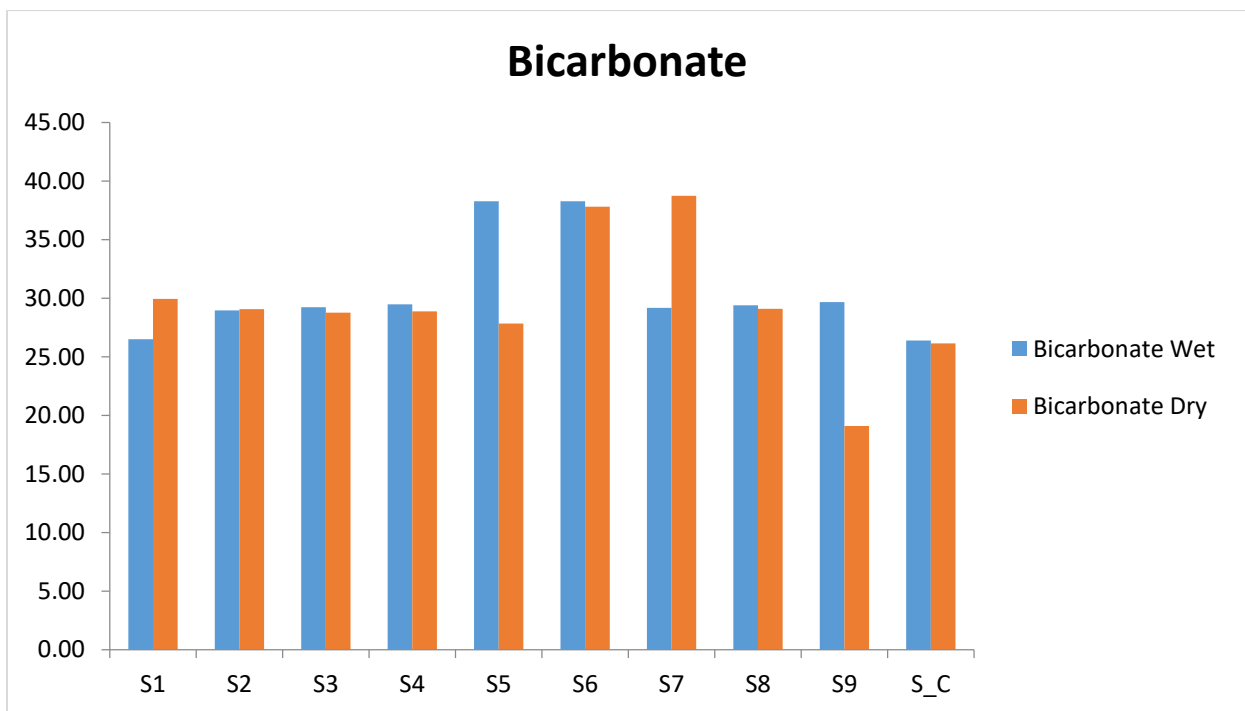


Fig 4.66a: Station Variations of Bicarbonate in Kolo Creek Soil

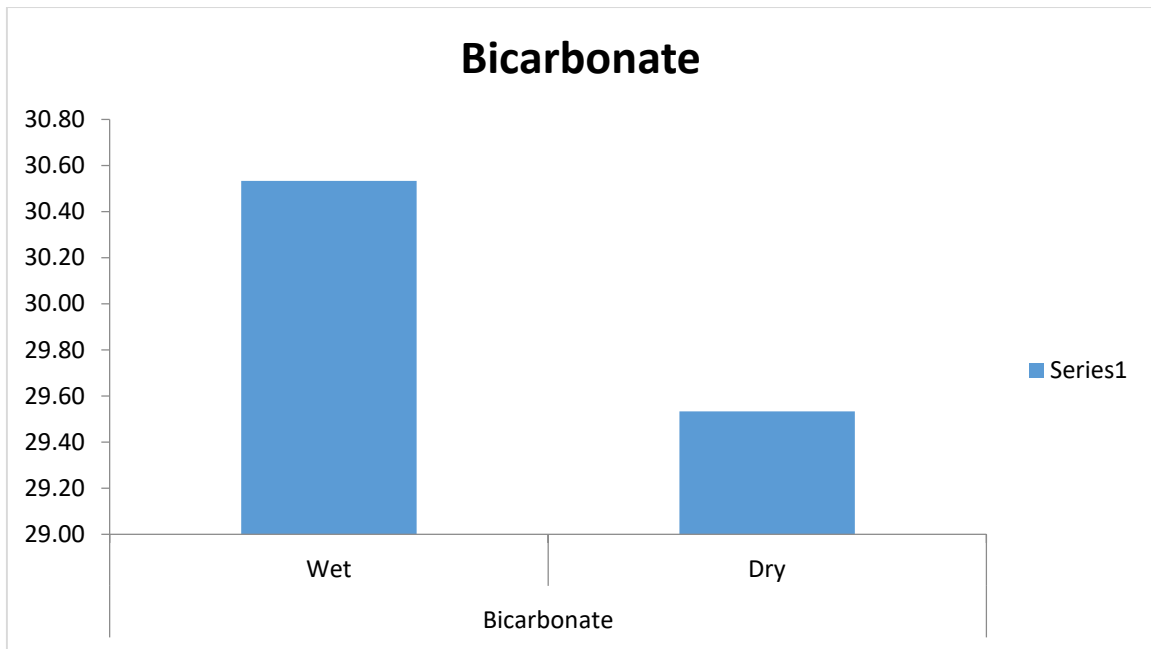


Fig 4.66b: Seasonal Variations of Bicarbonates in Kolo Creek Soils

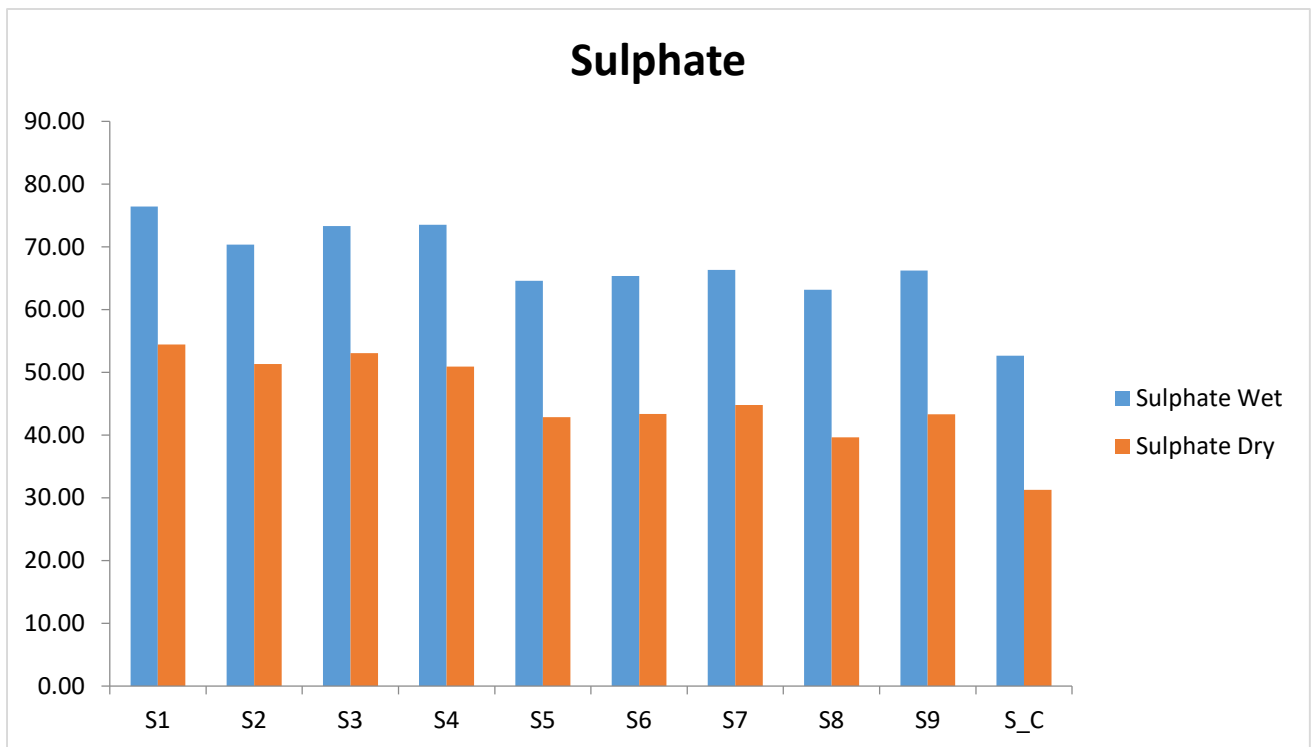


Fig 4.67a: Station Variations of Sulphate in Kolo Creek Soil

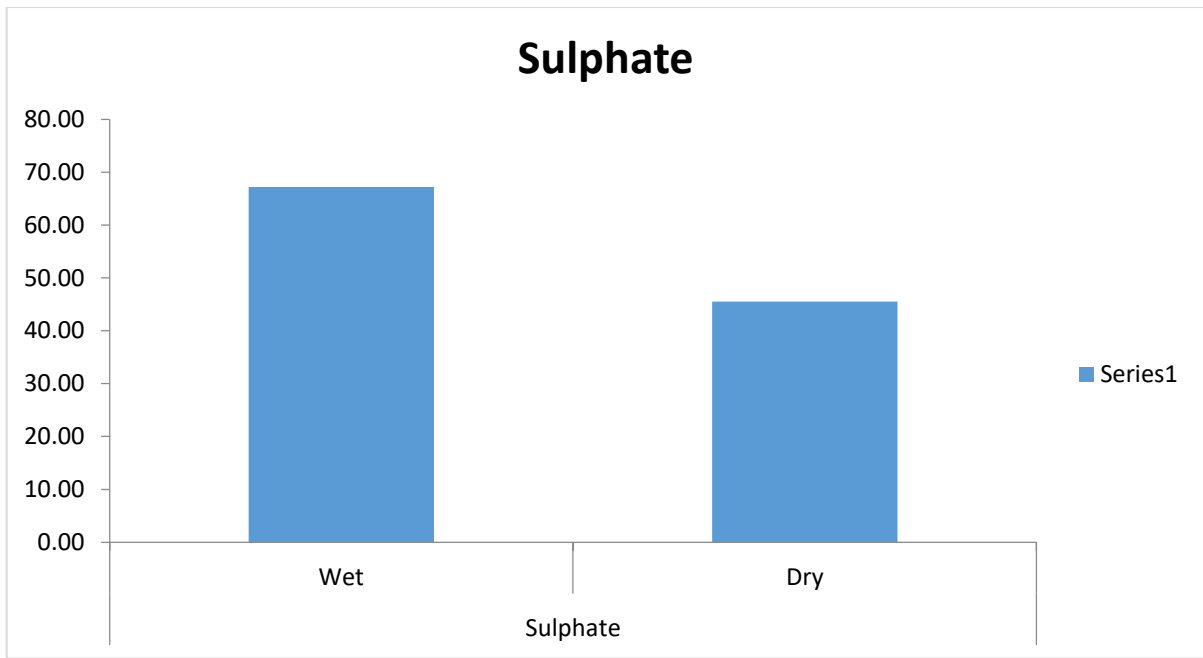


Fig 4.67b: Seasonal Variations of Sulphates in Kolo Creek Soils

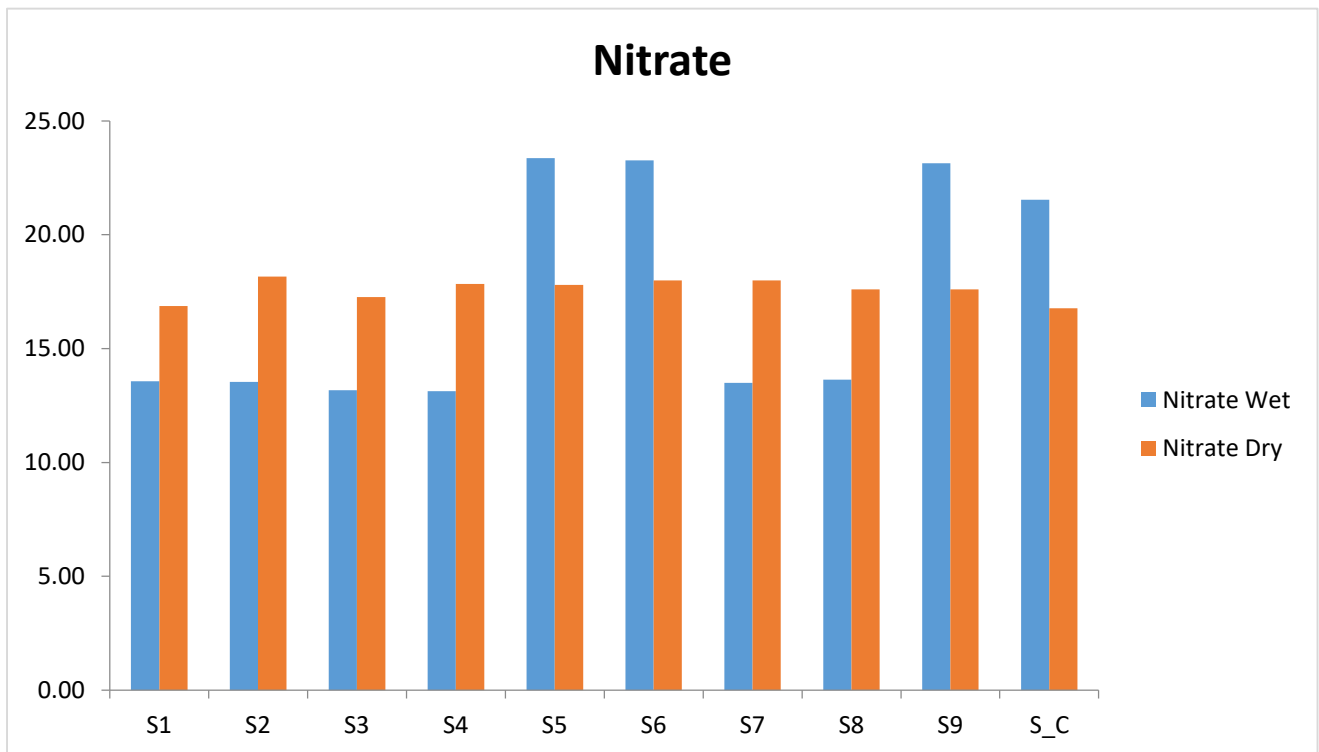


Fig 4.68a: Station Variations of Nitrate in Kolo Creek Soil

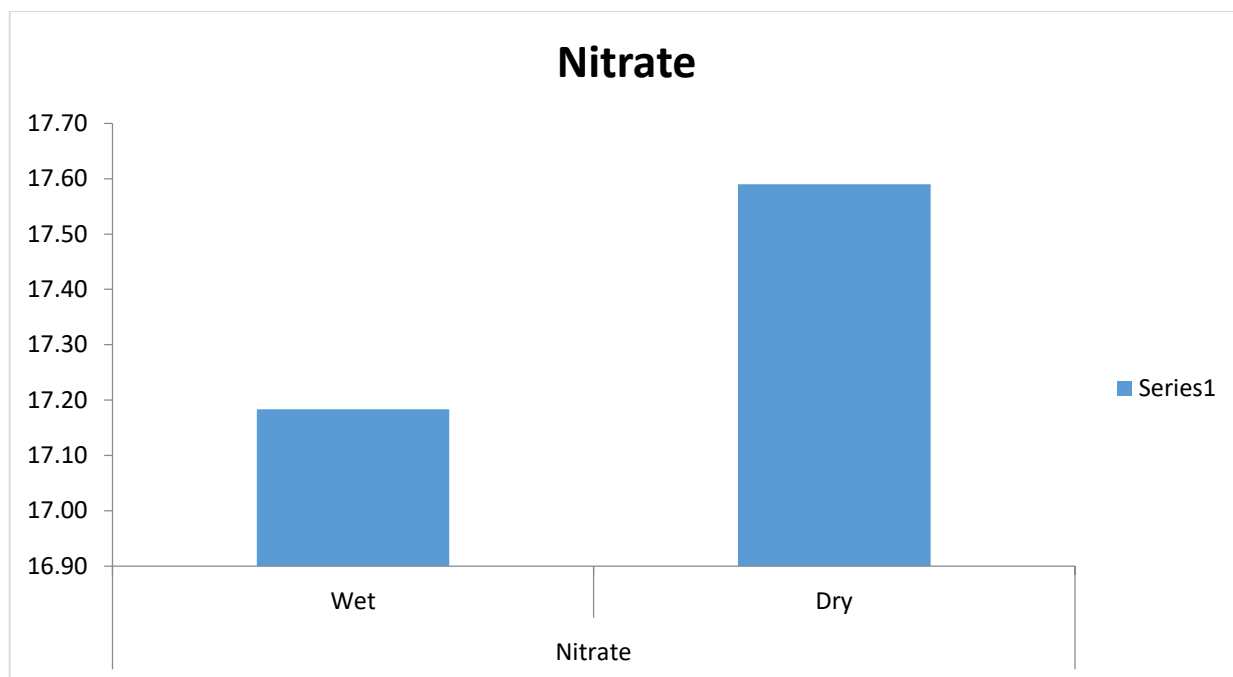


Fig 4.68b: Seasonal Variations of Nitrates in Kolo Creek Soils

Fig 4.69a: Spatial Distribution of Iron in Kolo Creek Soil

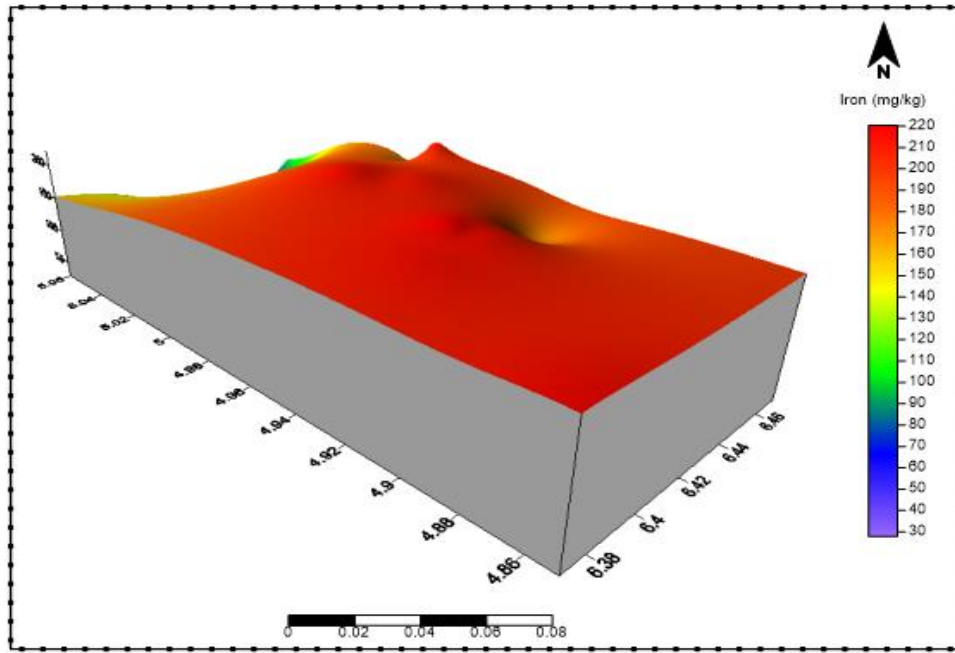


Fig 4.69b: 3D View of Calcium in Kolo Creek Soil

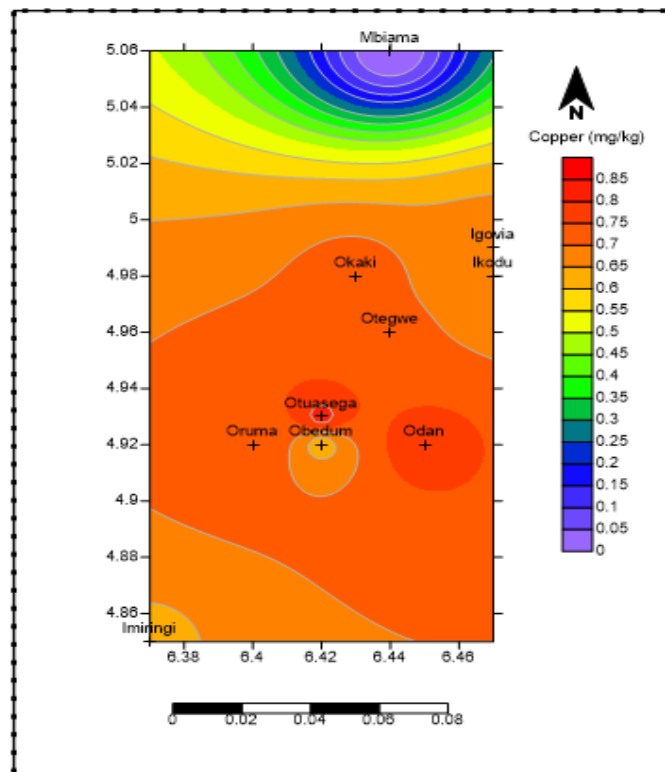


Fig 4.70a: Spatial Distribution Copper in Kolo Creek Soil

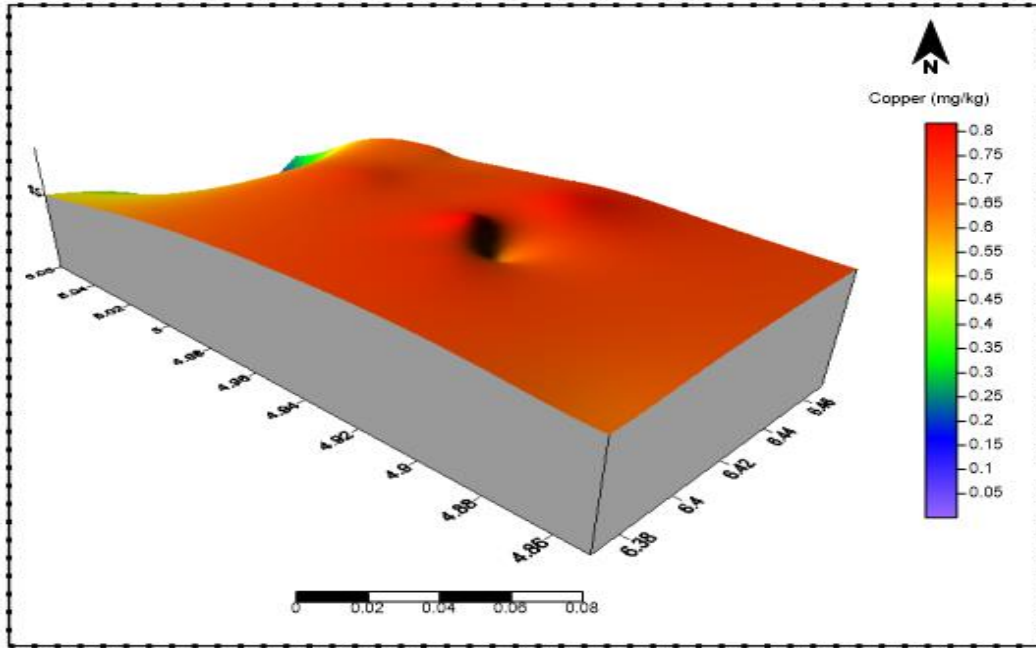


Fig 4.70b: 3D View of Copper in Kolo Creek Soil

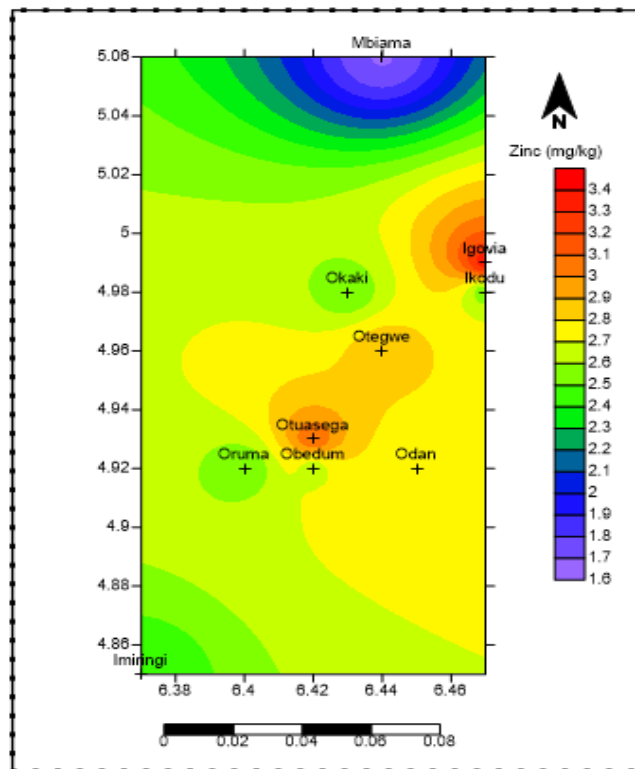


Fig 4.71a: Spatial Distribution map of Zinc in Kolo Creek Soil

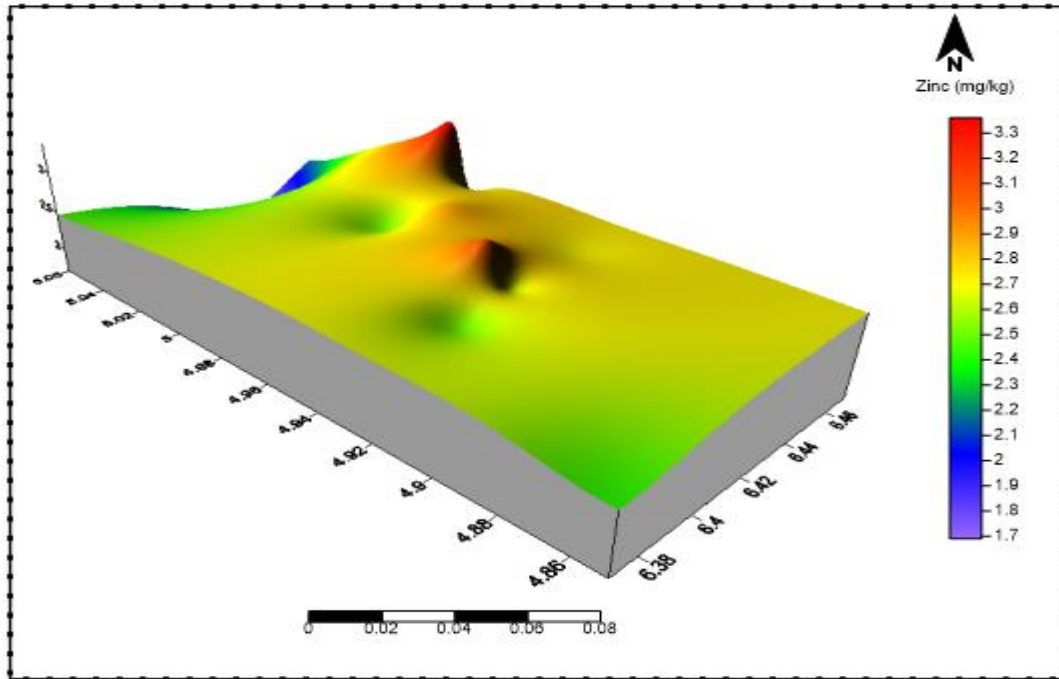


Fig 4.71b: 3D View map of Zinc in Kolo Creek Soil

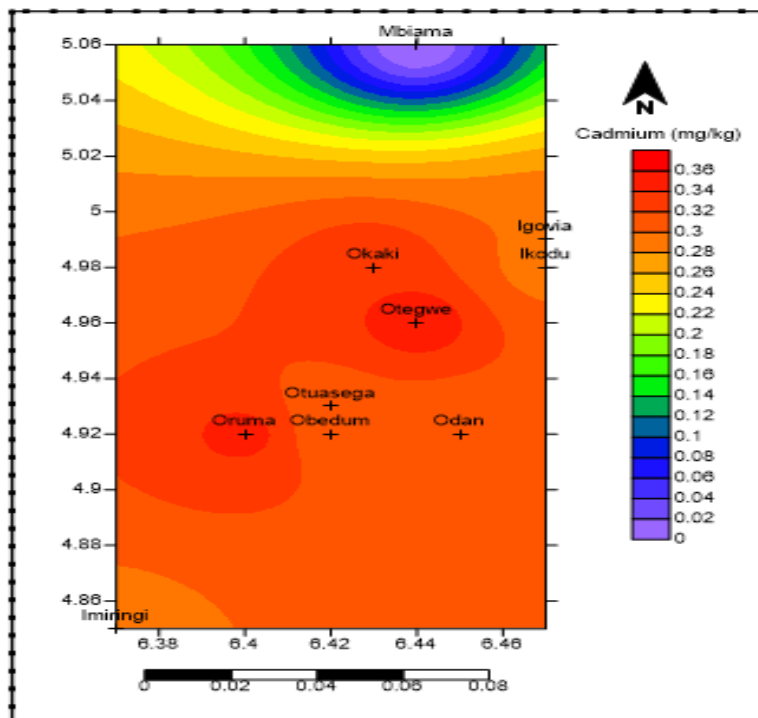


Fig 4.72a: Spatial Distribution map of Cadmium in Kolo Creek Soil

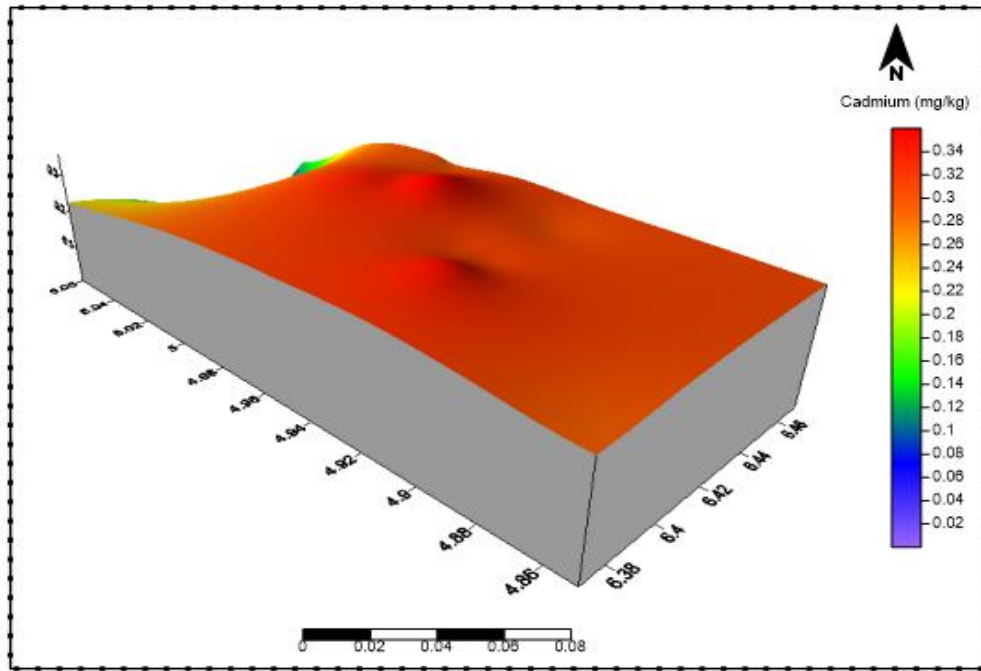


Fig 4.72b: 3D View map of Cadmium Kolo Creek Soil

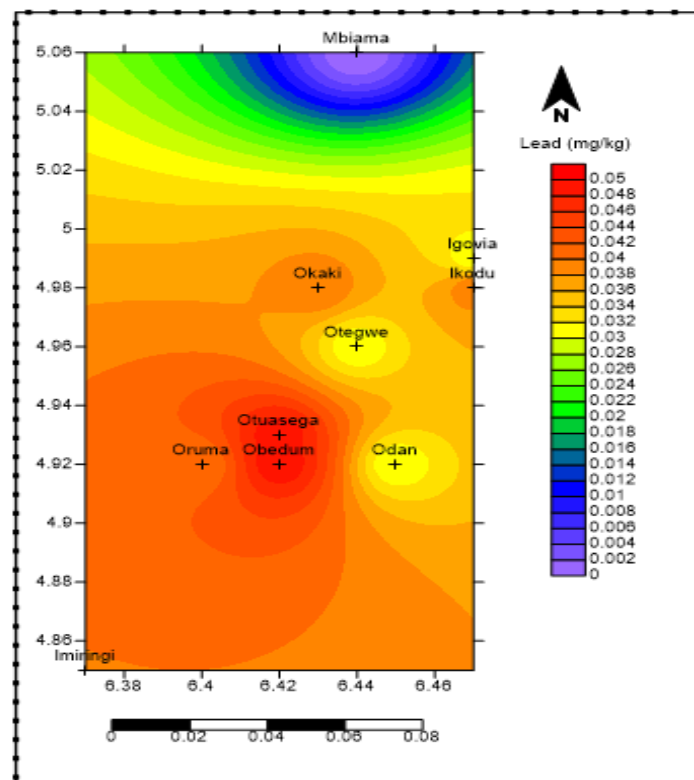


Fig 4.73a: Spatial Distribution map of Lead in Kolo Creek Soil

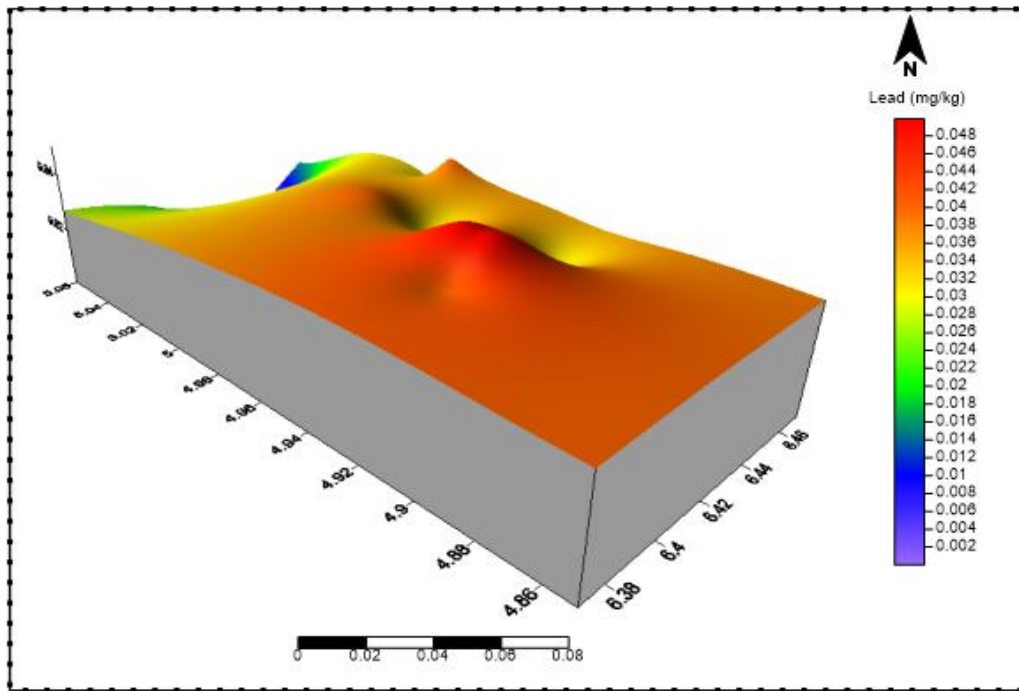


Fig 4.73b: 3D View map of Lead in Kolo Creek Soil

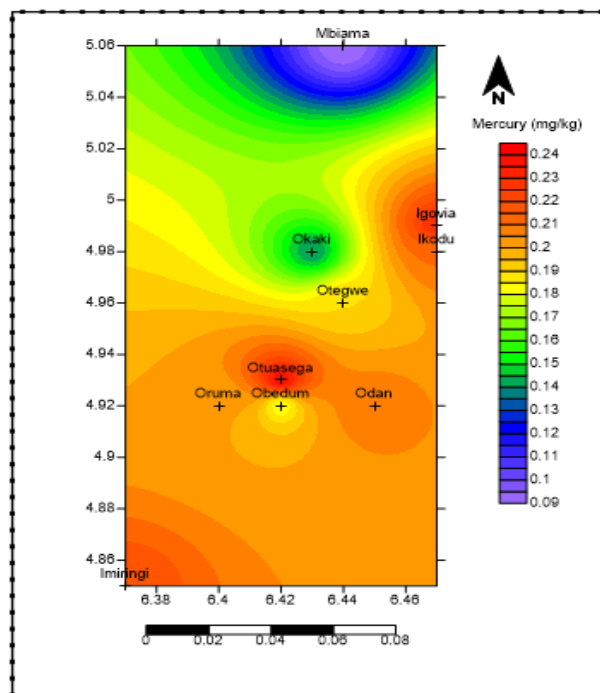


Fig 4.74a: Spatial Distribution map of Mercury in Kolo Creek Soil

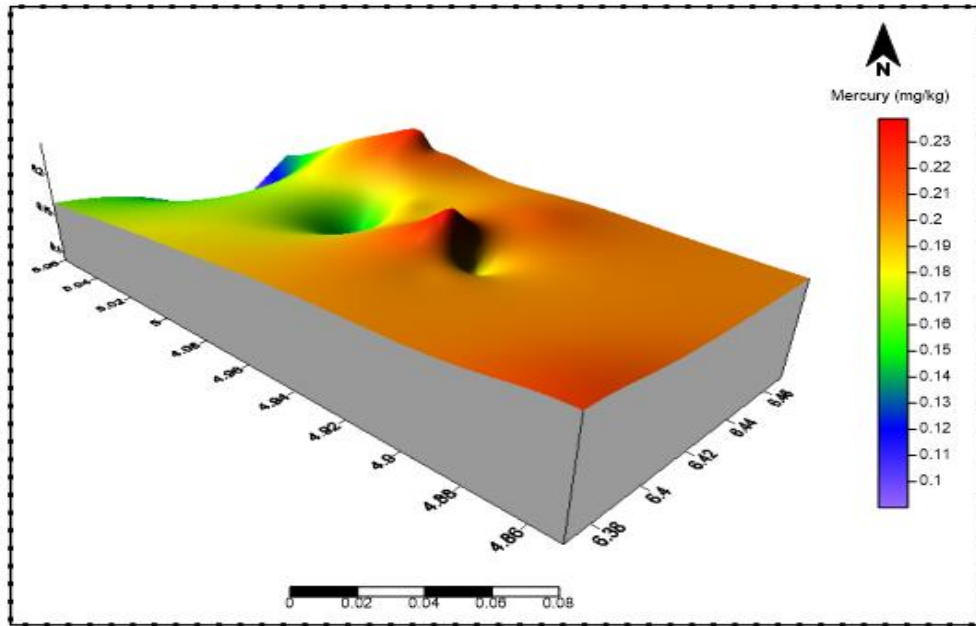


Fig 4.74b: 3D view map of Mercury in Kolo Creek Soil

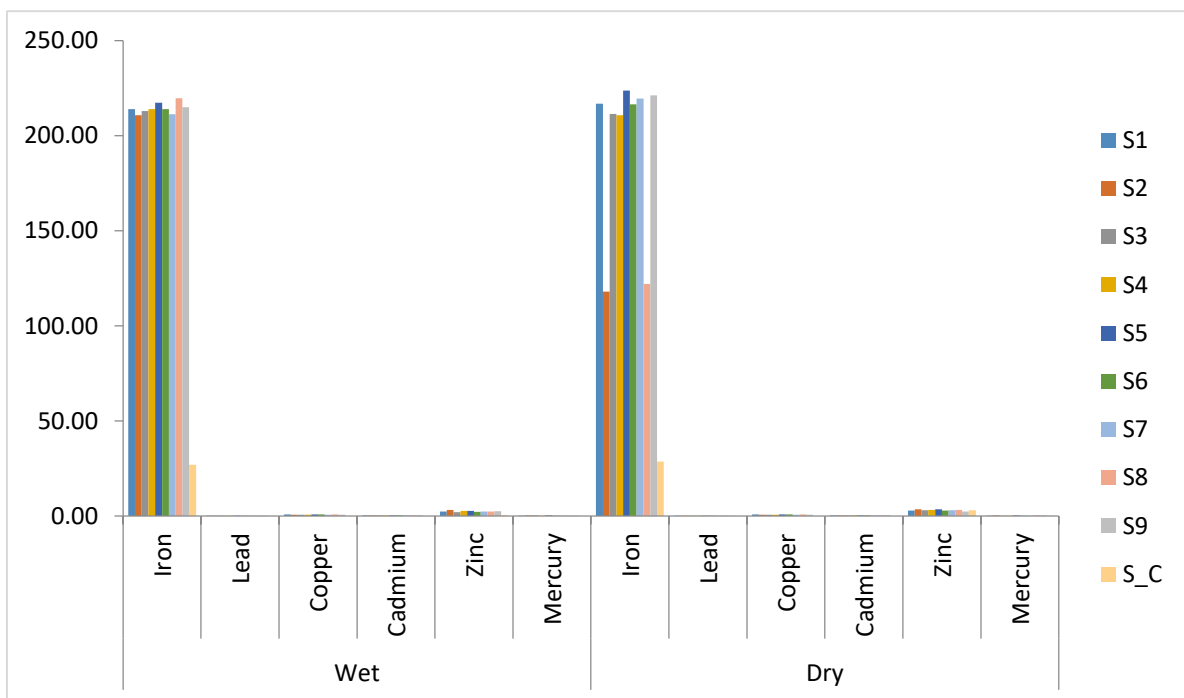


Fig 4.75: Seasonal Variations of Heavy Metals in Kolo Creek Soils

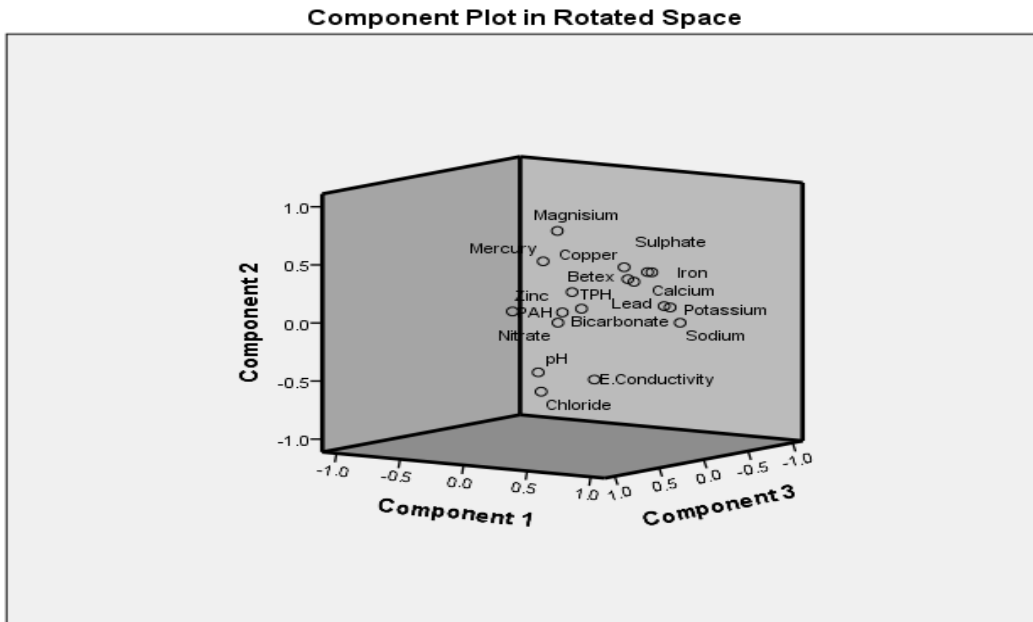


Fig.4.76: Principal component plot in rotated space soil Parameters

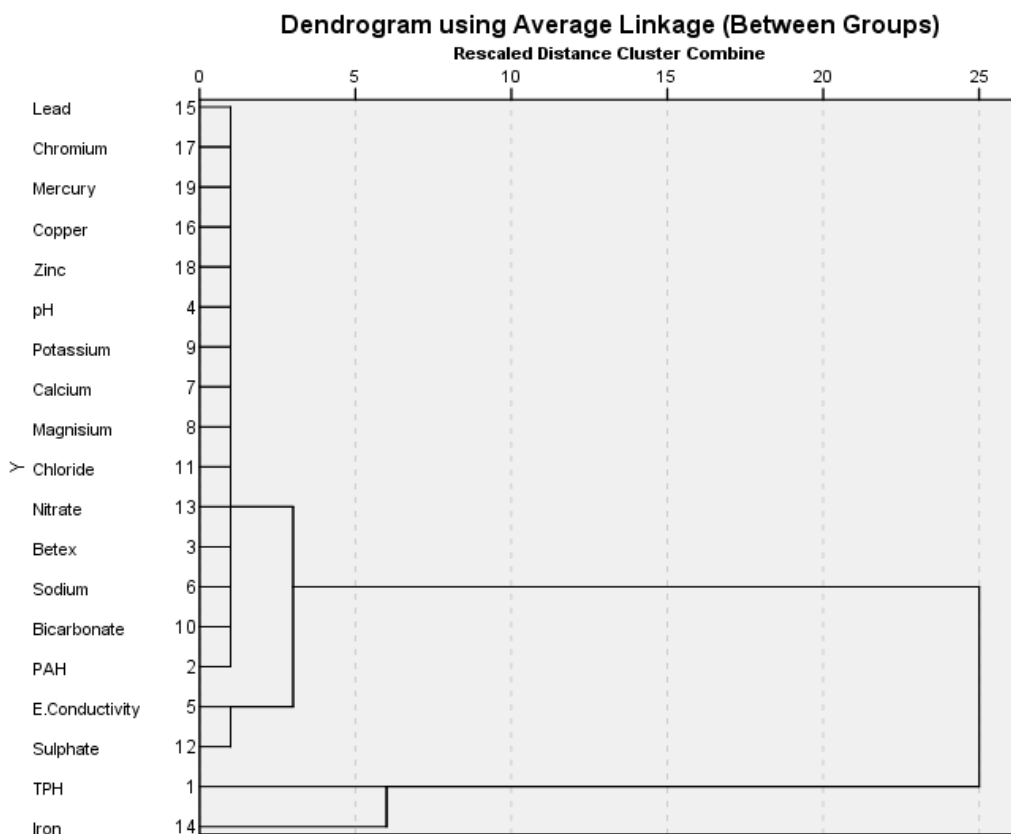


Fig 4.77: Dendrogram of soil parameters of the study area

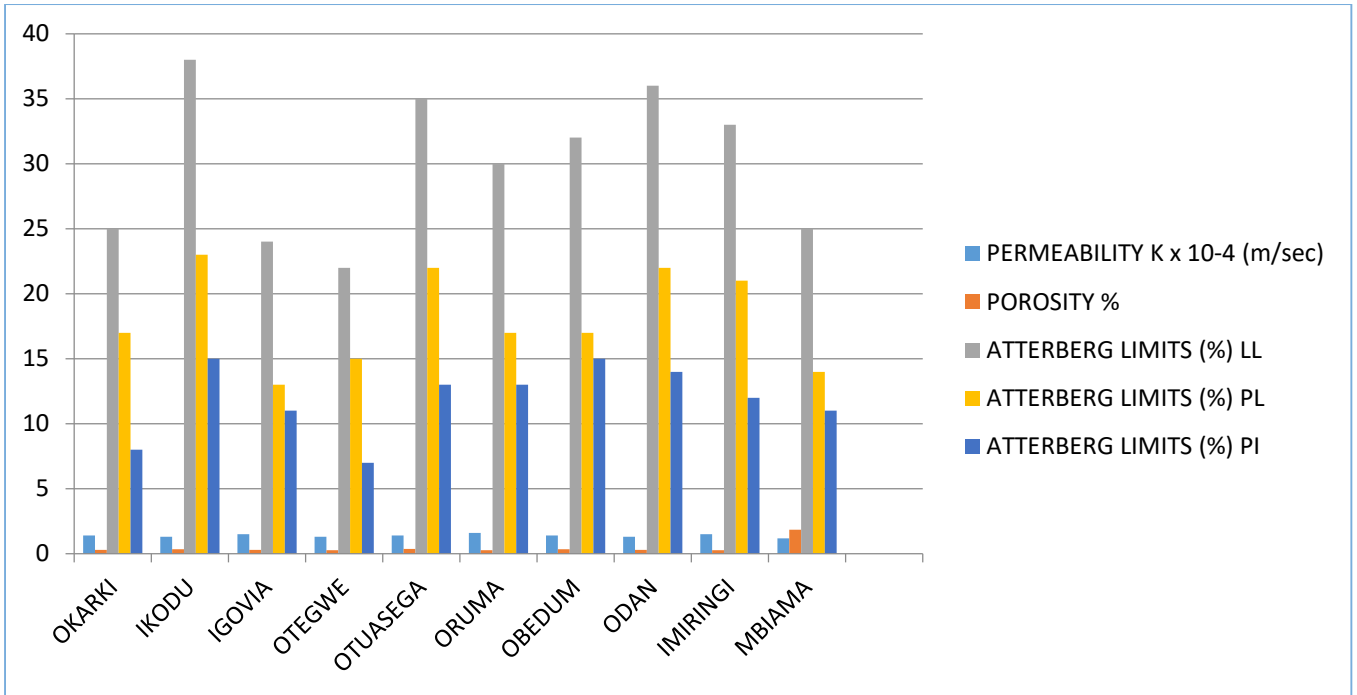


Fig 4.78: Soil Permeability, Porosity and Consistency Chart.

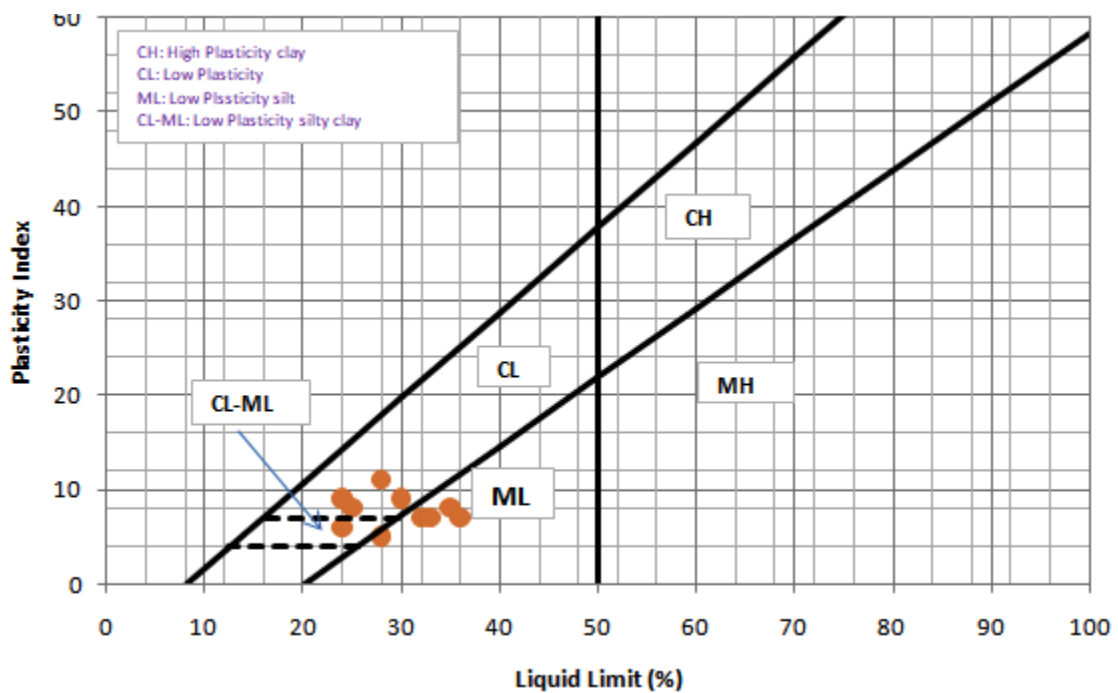
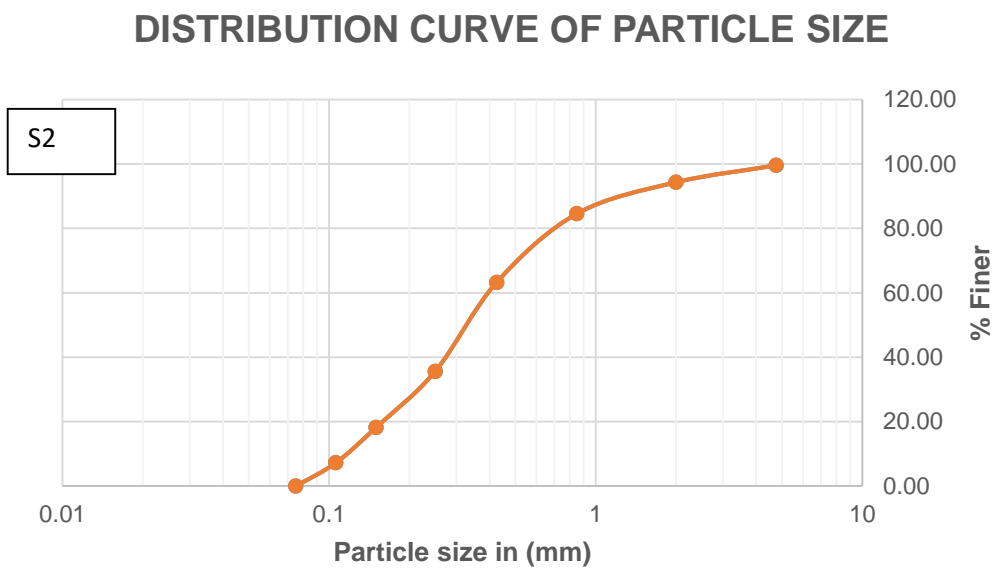
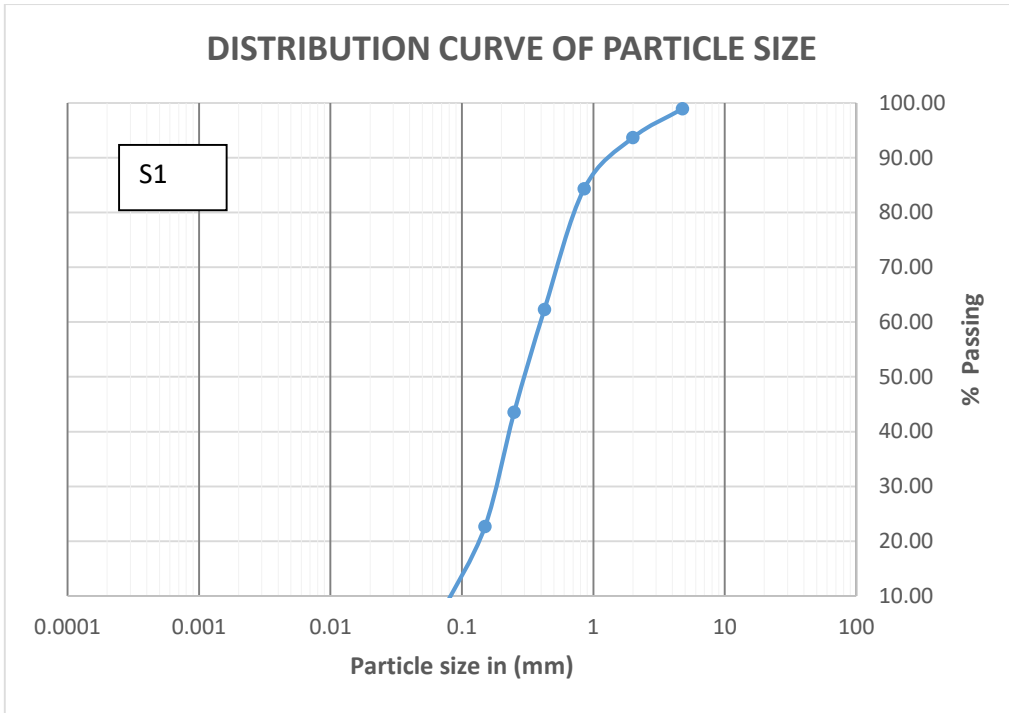
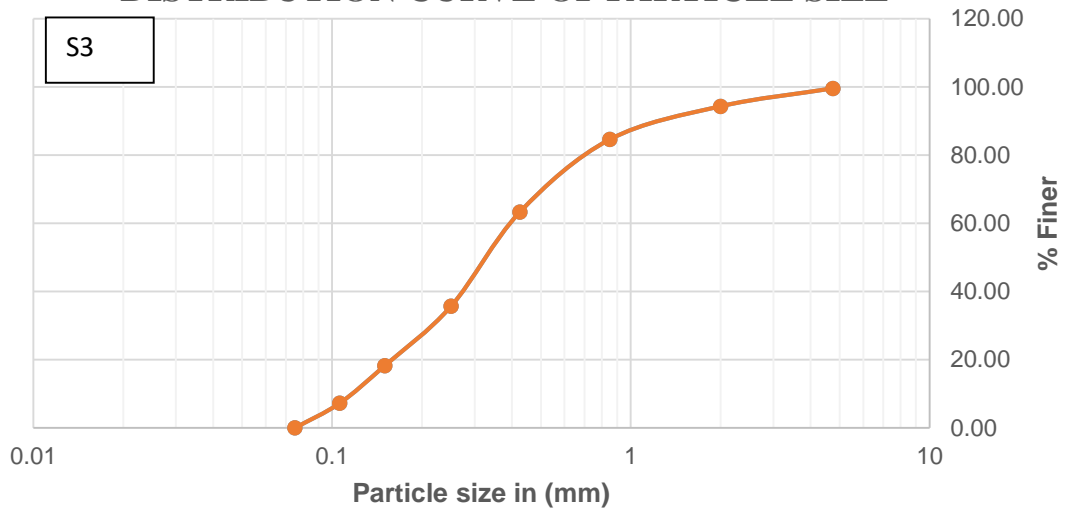


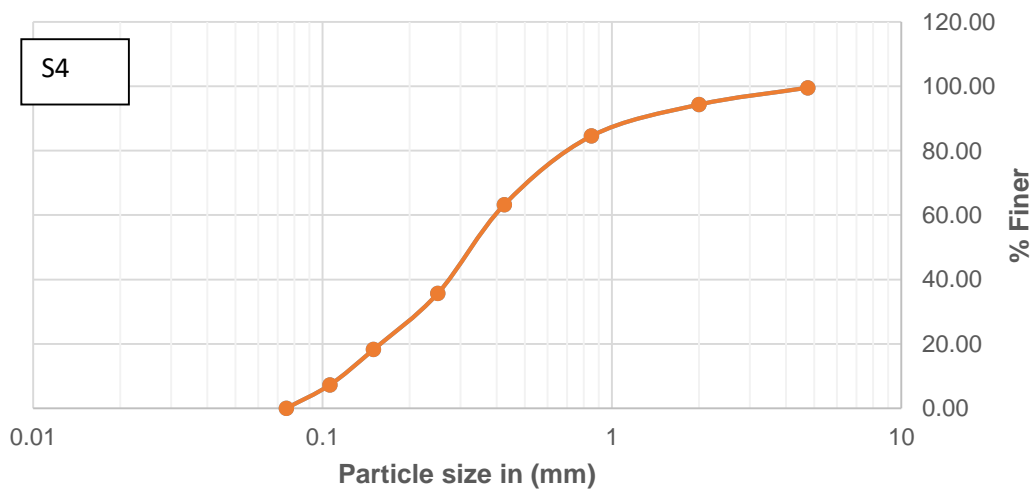
Fig 4.79: Plots of the 10 subsoil samples from Kolo-Creek and environs on modified Cassagrande Plasticity chart (ASTM D2487)



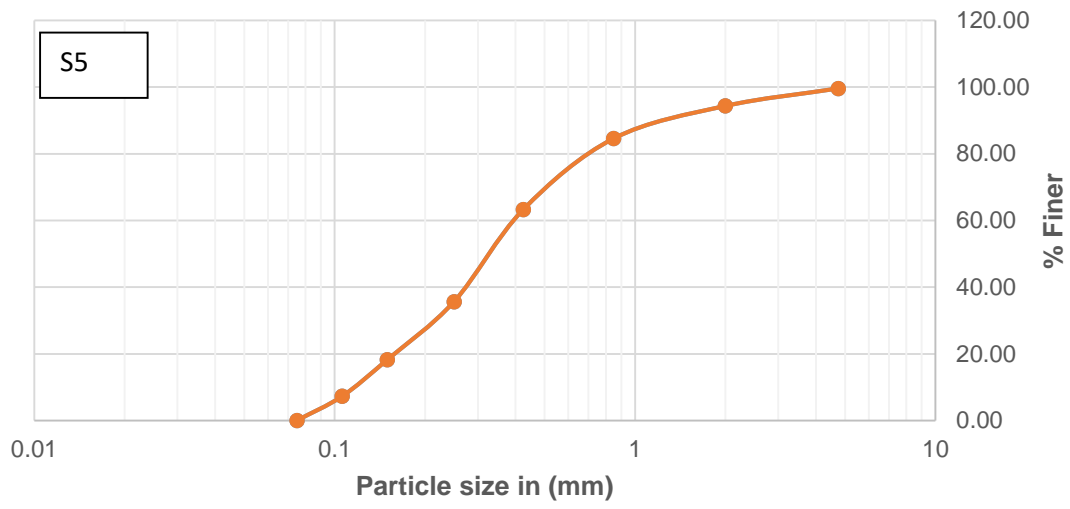
### DISTRIBUTION CURVE OF PARTICLE SIZE



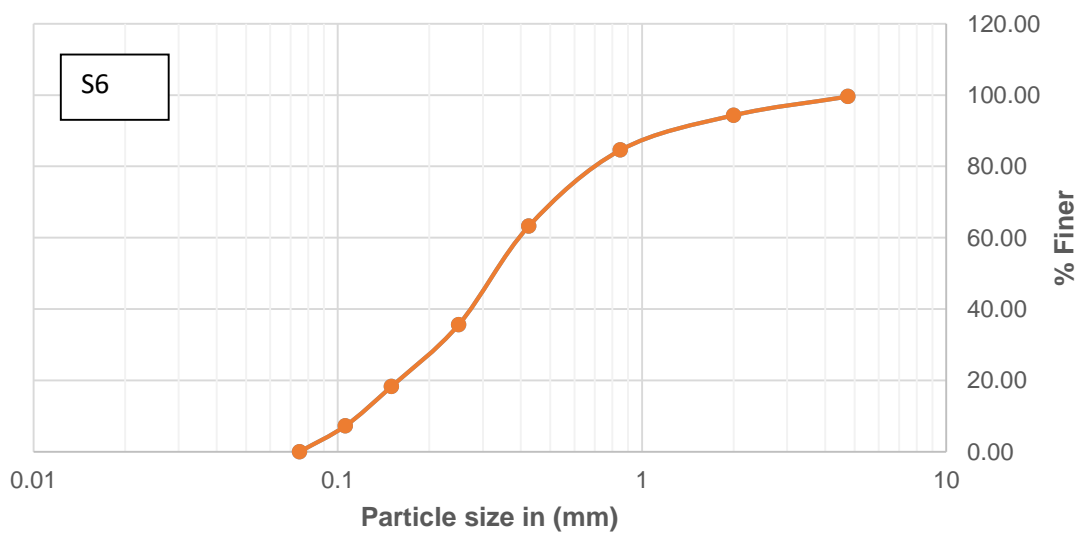
### DISTRIBUTION CURVE OF PARTICLE SIZE



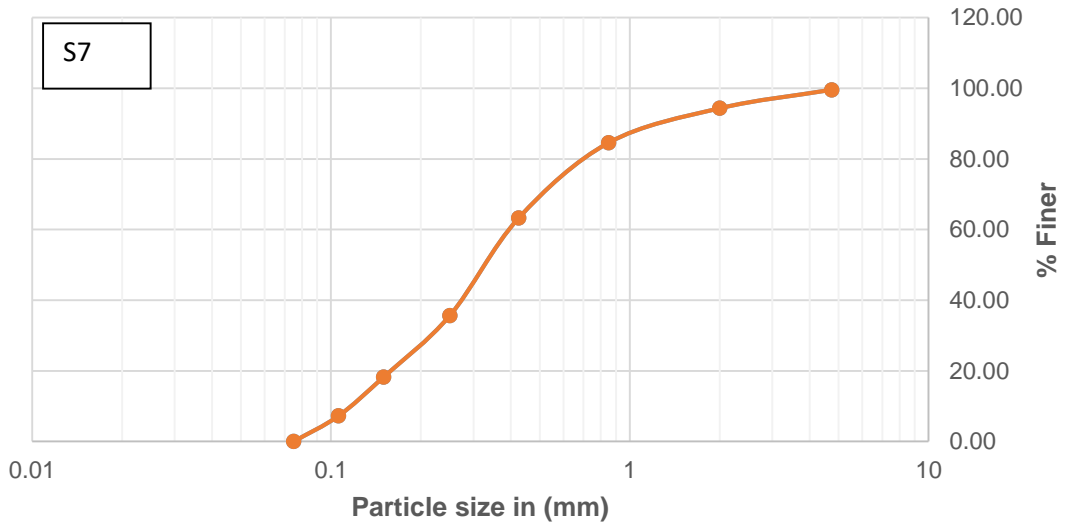
### DISTRIBUTION CURVE OF PARTICLE SIZE



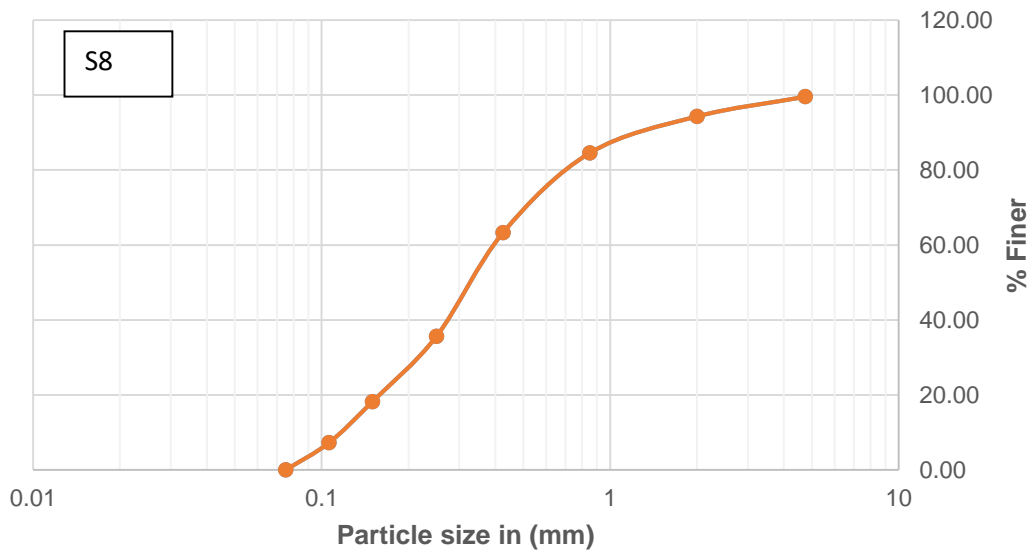
### DISTRIBUTION CURVE OF PARTICLE SIZE



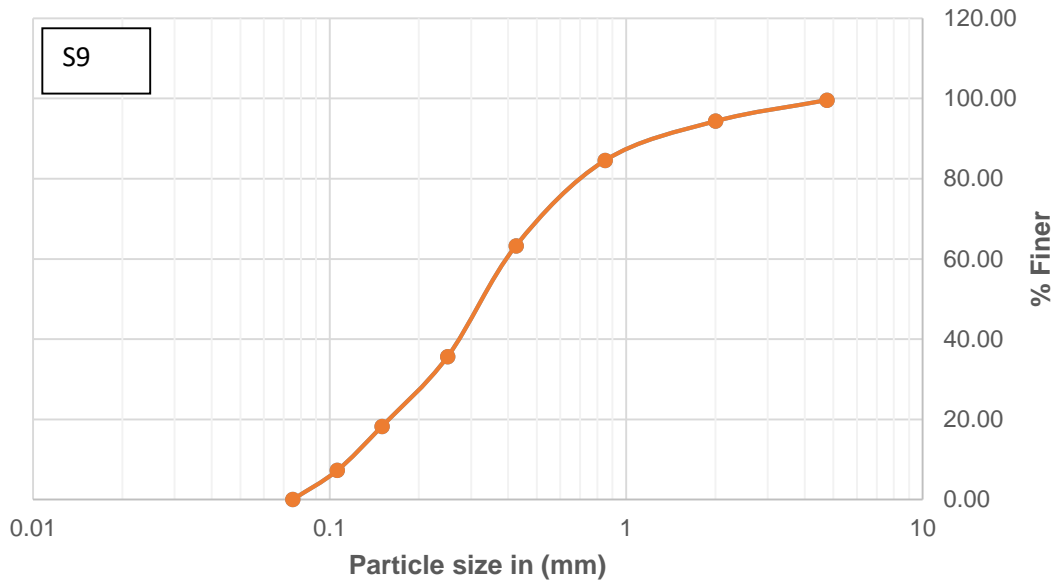
### DISTRIBUTION CURVE OF PARTICLE SIZE



### DISTRIBUTION CURVE OF PARTICLE SIZE



### DISTRIBUTION CURVE OF PARTICLE SIZE



### DISTRIBUTION CURVE OF PARTICLE SIZE

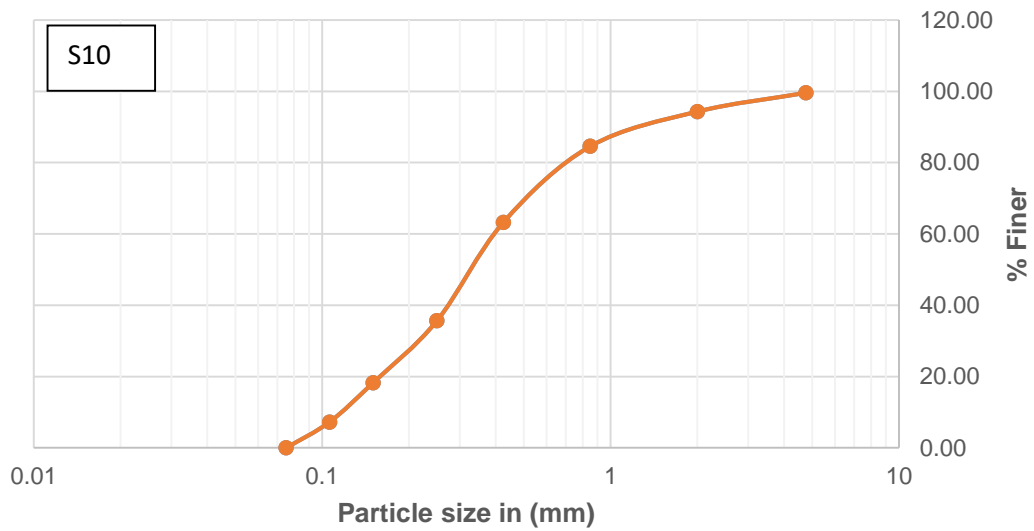


Figure 4.80: Typical soil particle size distribution of the Study area (S1-S10).

## **4.2 Discussion**

### **4.2.1 Dry and Wet Season Surface Water Samples' Physical and Biochemical Properties**

#### **PH**

The pH fluctuations along the Kolo-Creek surface water stretch or stations during the dry season are displayed in Tables 4.1a and 4.1b. The pH, which ranges from 5.77 to 6.49, has a control point value of 6.48 and a mean value of 6.48.

The pH range in the wet season is 5.59 to 6.90, with a control point value of 6.48 and a mean value of 6.77 (Table 4.1b). These numbers, however, fall short of the WHO (2017) safe water standard. The pH readings at Kolo-Creek indicate that the surface water is acidic. Reduced submerged aquatic vegetation and a lack of a basic food source for organisms are the results of surface water's increasing acidity (Ahiarakwem, 2013).

Freshwater shrimp cannot survive at pH values below 6.0; Unprocessed leaf litter and other organic debris fall to the bottom as bottom-dwelling bacterial decomposers begin to die at pH values of roughly 5.50 (Ahiarakwem, 2013). This results in the starvation death of plankton.

The ANOVA test reveals a statistically significant variation in the average pH levels among the sites ( $F = 14.11$ ,  $P < 0.05$ ). The mean seasonal pH readings along the creek's length do not significantly differ from one another ( $F = 0.26$ ,  $pr > 0.05$ ). The dry period has a more acidic pH than the season of rainfall due to Acidic pH in the dry season compared to the wet season occurs due to: concentration of acids from evaporation, reduced dilution without rainfall, decomposition of organic matter releasing acids, accumulation of acidic pollutants from the atmosphere, oxidation of Sulfide-Bearing Soils producing sulfuric acid and stagnation of water with minimal groundwater recharge. Figures 4.1(a-d) show the pH variogram, seasonal variation, pH spatial distribution and 3D perspective plots, respectively.

## **Electrical Conductivity and Total Dissolved Solids**

During the dry season, the total dissolved solids (TDS) in Kolo Creek range from 24.6 to 147.0 mg/l, with a mean value of 95.57 mg/l and a control point value of 68.60 mg/l (Tables 4.1a and 4.1b). The electrical conductivity (EC) during this period ranges from 9.0 to 27.0  $\mu\text{S}/\text{cm}$ , with a mean value of 14.0  $\mu\text{S}/\text{cm}$  and a control point value of 14.0  $\mu\text{S}/\text{cm}$ . The higher TDS and EC values in the dry season can be attributed to:

- Evaporation: Concentrates dissolved solids and ions.
- Reduced water flow: Stagnation leads to the accumulation of dissolved substances.
- Limited dilution: Absence of rainfall minimizes the dilution of dissolved solids.

### **Wet Season TDS and EC Values**

In the wet season, TDS concentrations range from 24.6 to 148.0 mg/l, with a mean value of 94.61 mg/l and a control point value of 68.60 mg/l (Tables 4.1a and 4.1b). The EC values during this period range from 11.3 to 16.5  $\mu\text{S}/\text{cm}$ , with a mean value of 13.36  $\mu\text{S}/\text{cm}$  and a control point value of 12.17  $\mu\text{S}/\text{cm}$ . The lower and more stable TDS and EC values in the wet season are influenced by:

- Increased dilution: Rainfall dilutes dissolved solids and ions.
- Enhanced water flow: Flushing of the system removes accumulated substances.
- Groundwater recharge: Contributes to lower concentrations of dissolved solids.

### **Compliance with WHO Guidelines**

Both TDS and EC concentrations in Kolo Creek meet the World Health Organization (2017) safe drinking water guidelines. As noted by Carol (1962), “While the electrical conductivity measurements do not indicate any salt dangers, the TDS values demonstrate that the river is fresh.” This indicates that the water in Kolo Creek is suitable for drinking and other domestic uses in terms of dissolved solids and ionic content.

### **Statistical Analysis of TDS and EC Variations**

- Electrical Conductivity (EC):

- The ANOVA test reveals a statistically significant difference in the mean EC values among the sampling stations ( $F = 94.14$ ,  $Pr < 0.05$ ).
- However, the mean seasonal EC values along the creek do not differ significantly ( $F = 0.03$ ,  $pr > 0.05$ ).
- EC values are generally higher in the dry season compared to the wet season due to the concentration of ions from evaporation and reduced dilution.
- Total Dissolved Solids (TDS):
  - The mean TDS readings among the stations are not significantly different ( $F = 0.51$ ;  $Pr > 0.05$ ).
  - However, the mean seasonal TDS values along the creek's length vary significantly ( $F = 6.34$ ,  $pr < 0.05$ ).
  - TDS values are typically higher in the dry season than in the wet season, reflecting the influence of evaporation and reduced water flow.

### **Total hardness**

With a control point value of 19.50 mg/l and mean values of 31.85 mg/l, the total hardness values for the dry season range from 19.0 to 38.0 mg/l. With a control point value of 19.50 mg/l and a mean value of 31.85 mg/l, the total hardness values for the wet season range from 19.0 to 37.0 mg/l (Figure 4.3 and Tables 4.1a and 4.1b). However, these values were less than 50 mg/l, indicating that the water is soft (Wilcork, 1993). These results were in line with the 2017 WHO recommendation of 150 mg/l for  $\text{CaCO}_3$  and  $\text{MgCO}_3$ . The ANOVA test indicates that there is a statistically significant variation in the stations' mean total hardness values ( $F = 17.40$ ,  $Pr < 0.05$ ). Total hardness is often higher during the dry season than during the wet season, even while there is no significant difference in the mean seasonal values of total hardness along the stream ( $F = 0.73$ ,  $pr > 0.05$ ).

## **Chloride**

Total chloride concentration means values during the dry season range from 8 to 18 mg/l, respectively, along the stations; a control point value of 8.33 mg/l and a mean value of 15.69 mg/l are found for the dry season, while a control point value of 8.33 mg/l and a mean value of 9.45 mg/l are found for the wet season (Tables 4.1a and 4.1b). These levels are in line with the 400 mg/l WHO guideline values from 2017. The results of the ANOVA test indicate that, on average, there is no significant variation in the mean chloride values along the station's length ( $F = 0.30$ ,  $Pr > 0.05$ ). The mean seasonal values of chlorine along the creek vary significantly ( $F = 49.42$ ,  $pr < 0.05$ ), but in general, the dry season has greater chloride levels than the rainy season.

## **Turbidity**

During the dry season, the mean concentration values of turbidity along the creek vary from 23 to 32 NTU, respectively. The control point value is 30.87 NTU, while the mean value is 26.94 NTU. Along the creek's length in the rainy season, the mean concentration values for turbidity also vary from 14.0 to 29.0 NTU, respectively (Table 4.1 and Figure 4.5), with a control point value of 14.3 NTU and a mean value of 23.81 NTU. The control point shows a slight turbidity, whereas the look of the river waters is murky. The cause of turbidity in water is the presence of extremely finely divided materials that are difficult for standard filtration techniques to remove.

The presence of turbidity in water will have an impact on how people perceive it and how useful it is for specific businesses. There is a chance that pathogenic organisms could be covered by the turbidity particles and evade the disinfectant's action since sewage materials can generate turbidity in water. The results of the ANOVA test indicate that the mean turbidity values of the stations differ in a generally significant way ( $F = 487.18$ ,  $Pr < 0.05$ ). Although the mean seasonal turbidity values along the stream vary significantly ( $F = 0.01$ ,  $pr < 0.05$ ), the turbidity value is often higher in the dry season than in the wet season.

## **Major Cations and Anions**

### **Calcium**

With a control point value of 8.60 mg/l and a mean value of 11.08 mg/l, the calcium values in the dry season range from 8.6 to 12.03 mg/l along the stations, respectively (Tables 4.1a and 4.1b). The calcium values in the wet season range from 7.13 to 12.27 mg/l along the stations, respectively, with a control point value of 8.67 mg/l and a mean value of 10.58 mg/l. According to the results of the ANOVA test, the mean calcium levels along the stations and the mean seasonal values along the creek stretch do not differ significantly ( $F = 3.79$ ,  $Pr > 0.05$  and  $F = 0.73$ ,  $Pr > 0.05$ , respectively). In general, the dry season has a higher calcium value than the wet season. These values meet the WHO's 2017 recommended values.

### **Magnesium**

Throughout the dry season, magnesium concentrations range from 7.97 to 11.13 mg/l along the stations, with a mean of 10.14 mg/l and a control point value of 7.97 mg/l (Tables 4.1a and 4.1b). Magnesium concentrations vary from 7.63 to 11.07 mg/l throughout the stations throughout the rainy season, with a mean value of 9.83 mg/l and a control point value of 7.63 mg/l (Tables 4.1a and 4.1b).

The results of the ANOVA test indicate that the mean magnesium values at the stations differ significantly ( $F = 26.53$ ,  $Pr < 0.05$ ). The mean seasonal magnesium values along the stream do not significantly differ from one another ( $F = 0.53$ ;  $pr > 0.05$ ); nonetheless, the magnesium value is often higher in the dry season compared to the wet season. These values meet the WHO's 2017 recommended values.

### **Sodium**

With a control point value of 6.90 mg/l (Table 4.1 and Figure 4.14) and a mean value of 8.21 mg/l, the sodium value in the dry season varies from 6.90 to 8.70 mg/l along the stations, respectively. With a control point value of 23.63 mg/l (Table 4.1a and Figure 4.14) and a mean value of 8.21 mg/l, the sodium value in the wet season varies along

the stations from 9.40 to 23.63 mg/l, respectively. These values correspond to the 2017 World Health Organization standards. The mean sodium values among the stations do not differ significantly, according to the ANOVA test ( $F = 0.17$ ,  $Pr > 0.05$ ).

Sodium readings are normally higher during the rainy season than during the dry season, yet there is a significant variation in the mean seasonal values of sodium along the creek ( $F = 34.40$ ,  $pr < 0.05$ ).

### **Potassium**

A control point value of 5.72 mg/l and mean values of 6.17 mg/l are found for potassium during the dry season, which varies from 5.72 to 6.57 mg/l along stations. While the mean values of 6.07 mg/l and the control point value of 5.87 mg/l indicate that potassium values during the wet season range from 5.58 to 6.47 mg/l along the stations (Tables 4.1a and 4.1b).

The mean potassium values among the stations do not differ significantly, according to the ANOVA test ( $F = 5.6$ ,  $Pr > 0.05$ ). The mean seasonal potassium readings over the creek's length do not change significantly ( $F = 0.81$ ,  $pr > 0.05$ ). In general, the dry season has a higher potassium value than the wet season.

The main constituent cations' concentrations are typically low and meet the WHO's (2017) criteria for safe drinking water. The main constituent cations' relative abundances follow the following order:  $Na^+ > Ca^{2+} > Mg^{2+} > K^+$ .

### **Bicarbonate**

Bicarbonate concentrations in the dry season vary along the stations from 6.40 to 9.67 mg/l, with a mean value of 6.40 mg/l and a control point value of 6.40 mg/l. According to Table 4.1 and Figure 4.16, the bicarbonate concentration during the rainy season varies between 6.13 and 9.93 mg/l along the stations, with a mean value of 8.53 mg/l and a control point value of 6.13 mg/l.

These values meet the WHO's 2017 recommended values. Although there is no significant difference in the mean seasonal values of bicarbonate over the creek's length ( $F = 0.00$ ,  $Pr > 0.05$ ), the ANOVA test indicates that there is generally no significant difference in the mean bicarbonate values of the stations ( $F = 2.65$ ,  $Pr > 0.05$ ). Generally speaking, the bicarbonate values are the same in both seasons.

### **Sulphates**

Between 52.63 and 76.43 mg/l, respectively, is the concentration of  $\text{SO}_4^{2-}$  during the dry season. The mean value is 67.19 mg/l, and the control point is 52.63 mg/l. In contrast, the concentration of  $\text{SO}_4^{2-}$  varies from 31.26 to 54.43 mg/l throughout the wet season (Table 4.1 and Figure 4.10), with a mean value of 45.49 mg/l and a control point value of 31.26 mg/l.

The WHO (2017) guideline values are met by these values. The ANOVA test reveals that, on average, there is no discernible variation in the mean sulfate values along the stations ( $F = 0.41$ ,  $Pr > 0.05$ ). While the mean seasonal sulfate values along the creek's length fluctuate significantly ( $F = 48.83$ ,  $pr < 0.05$ ). The dry season often has a greater sulfate value than the wet season.

### **Nitrates**

During the dry season, the concentration of  $\text{NO}_3$  varies between 1.53 and 3.63 mg/l, with a mean value of 3.18 mg/l and a control point value of 1.53 mg/l. Although the concentration of  $\text{NO}_3$  during the wet season varies between 6.77 and 8.17 mg/l, with a mean value of 7.59 mg/l and a control point value of 6.77 mg/l (Table 4.1 and Figure 4.11). These values meet the WHO's 2017 recommended values. According to the ANOVA test, the mean nitrate values at the stations generally don't differ significantly ( $F = 0.05$ ,  $Pr > 0.05$ ). Although the mean seasonal nitrate values along the creek's length vary significantly ( $F = 322.7$ ,  $pr < 0.05$ ). In general, the wet season has a higher nitrate value than the dry season. The trend  $\text{SO}_4^{2-} > \text{Cl}^- > \text{HCO}_3^- > \text{NO}_3^-$  is followed by the relative abundance of main anions.

### **Total Petroleum Hydrocarbon (TPH)**

During the dry season, the total petroleum hydrocarbons (TPH) in Kolo Creek range from 12.0 to 395.0 mg/l, with a control point value of 12.0 mg/l and a mean value of 260.14 mg/l. These elevated TPH levels indicate significant contamination from petroleum-related activities, such as oil spills, illegal refining, and industrial discharges. In the wet season, the TPH levels range from 43.0 to 543.0 mg/l, with a control point value of 43.27 mg/l and a mean value of 320.29 mg/l (Tables 4.1a and 4.1b). The higher TPH values during the wet season can be attributed to:

- **Runoff:** Increased rainfall washes petroleum residues from surrounding areas into the creek.
- **Flooding:** Transport of contaminated sediments and debris into the waterway.
- **Dilution effects:** While rainfall may dilute some pollutants, it can also mobilize and redistribute petroleum hydrocarbons.

The ANOVA test reveals a statistically significant difference in the mean TPH values among the sampling stations ( $F = 12.13$ ,  $Pr < 0.05$ ). However, there is no significant difference in the mean seasonal TPH values along the creek's length ( $F = 0.79$ ,  $pr > 0.05$ ). Generally, TPH values are higher during the wet season compared to the dry season, reflecting the influence of runoff and flooding.

The TPH values in Kolo Creek significantly exceed the World Health Organization (4th Edition) recommendations, indicating that the water is heavily contaminated with petroleum hydrocarbons. This poses serious risks to aquatic ecosystems, human health, and the overall water quality of the creek.

### **Pyrolytic Aromatic Hydrocarbon (PAH)**

During the dry season, the PAH fluctuates along the stations from 0.0 to 58.0 mg/l, with a mean value of 32.91 mg/l and a control point value of 0.0 mg/l. While the PAH in the wet season has a mean value of 21.38 mg/l and a control point value of 0.0 mg/l, it ranges along the stations from 0.0 to 84.0 mg/l, respectively.

The results of the ANOVA test indicate that, on average, there is no significant difference in the mean PAH values at the stations ( $F = 4.09$ ,  $Pr > 0.05$ ) or in the mean seasonal values of PAH over the creek's length ( $F = 0.83$ ,  $Pr > 0.05$ ). In general, the dry season has a greater PAH value than the wet season. The WHO (4th Edition) recommendations are not followed by these values.

### **Betex**

During the dry season, the Betex values along the stations range from 3.0 to 30.0 mg/l, with a land value of 18.94 mg/l and a control point value of 3.33 mg/l. With a control point value of 0.0 mg/l and a mean value of 18.94 mg/l, the Betex values during the wet season range from 0.0 to 55.0 mg/l along the stations, respectively. These results greatly surpass the WHO (2017) recommended values.

According to the results of the Anova test, there is often no discernible difference in the mean Betex values at the stations ( $F = 0.88$ ,  $Pr > 0.05$ ) or in the mean seasonal values of Betex along the creek's length ( $F = 8.29$ ,  $Pr > 0.05$ ). In general, the wet season has a greater Betex value than the dry season.

## **Heavy Metals and Other Metals in Surface Water**

### **Iron Fe<sup>2+</sup>**

During the dry season, the iron concentrations in the stream fluctuate from 134 to 277.40 mg/l, with a mean value of 194.07 mg/l and a control point value of 236.93 mg/l. Iron concentrations in the wet season range from 161.47 to 226.77 mg/l over the creek's length, with a mean value of 207.26 mg/l and a control point value of 220.60 mg/l (Table 4.1 and Figure 4.15). The ANOVA test reveals that, on average, there is no discernible variation in the stations' mean iron readings ( $F = 0.76$ ,  $Pr > 0.05$ ). The mean seasonal values of iron over the creek's length do not change significantly ( $F = 0.62$ ,  $pr > 0.05$ ). Generally speaking, the wet season has a larger iron value than the dry season. Every area has iron levels that are significantly higher than the WHO (2017) drinking water norm.

### **Copper Cu<sup>2+</sup>**

During the dry season, copper concentrations range from 0.0 to 0.82 mg/l without detection at the control point, with an average value of 0.64 mg/l. Conversely, during the wet season, copper concentrations range from 0.2 to 0.89 mg/l, with an average value of 0.63 mg/l and 0.02 mg/l at the control point (Table 4.1 and Figure 4.16).

The ANOVA test indicates that there is a statistically significant variation in the stations' mean copper levels ( $F = 128.18$ ,  $Pr < 0.05$ ). The mean seasonal copper readings over the creek's length do not differ significantly ( $F = 0.001$ ,  $pr > 0.05$ ). During the dry season, the value of copper is marginally higher.

### **Zinc Zn<sup>2+</sup>**

During the dry season, the average zinc concentrations in the creek range from 0.40 to 3.19 mg/l, with a mean of 2.24 mg/l and a control point value of 0.40 mg/l. The mean zinc content during the wet season is 3.02 mg/l, although it varies along the creek from 2.37 to 2.57 mg/l with a control point value of 2.97 mg/l (Table 4.1 and Figure 4.17).

The results of the ANOVA test indicate that, on average, there is no significant difference between the stations' mean zinc values ( $F = 0.75$ ,  $Pr > 0.05$ ). The mean seasonal values of zinc do not significantly differ along the creek's length ( $F = 9.31$ ,  $pr < 0.05$ ). In general, the wet season has a higher concentration of zinc than the dry season.

### **Cadmium Cd<sup>2+</sup>**

Cadmium concentrations during the dry season range from 0.1 to 0.37 mg/l on average along the creek's length, with a mean value of 0.29 mg/l and no detection at the control site. While the mean cadmium concentrations during the rainy season range from 0.1 to 0.34 mg/l along the creek's length, with a mean value of 0.27 mg/l at the control point showing no detection (Table 4.1 and Figure 4.18),

The ANOVA test reveals that the mean Cadmium values of the stations differ in a generally significant way ( $F = 54.41$ ,  $Pr < 0.05$ ). The mean seasonal values of zinc do

not significantly differ over the creek's length ( $F = 0.21$ ,  $pr > 0.05$ ). The dry season often has a higher concentration of cadmium than the wet season.

### **Lead $Pb^{2+}$**

Lead concentrations in the dry and rainy seasons range from 0.00 to 0.05 mg/l, respectively, over the creek's length, with a mean value of 0.03 mg/l and no detection at the control location (Table 4.1 and Figure 4.19). According to the ANOVA test, there is a statistically significant difference between the stations' mean Lead values ( $F=14.78$ ,  $Pr < 0.05$ ). The mean seasonal lead readings along the creek's length do not differ significantly ( $F = 0.23$ ,  $pr > 0.05$ ). Between the two seasons, the lead value is essentially the same.

### **Mercury $Hg^+$**

Throughout the dry season, the concentrations of mercury in the creek range from 0.10 to 0.24 mg/l, with a mean value of 0.18 mg/l and a control point value of 0.10 mg/l. Mercury concentrations in the wet season range from 0.11 to 0.27 mg/l over the creek's length, with a mean value of 0.20 mg/l and a control point value of 0.18 mg/l (Table 4.1 and Figure 4.20). The results of the ANOVA test indicate that, on average, there is no significant difference between the stations' mean Mercury readings ( $F = 1.43$ ,  $Pr > 0.05$ ). The mean seasonal values of Mercury do not significantly differ along the creek's length ( $F = 0.94$ ,  $pr > 0.05$ ). Generally speaking, the dry season has a higher concentration of mercury than the wet season.

### **Aluminum $Al^+$**

Throughout the creek's length, no concentration of aluminum was found during either the rainy or dry seasons. Kolo Creek's surface water is at risk because the amounts of iron-measured heavy metals ( $Fe^{2+}$ ), with the exception of  $Cu^{2+}$  and  $Zn^{2+}$ , were higher than the WHO (2017) criterion for safe drinking water.  $Pb^{2+}$  concentrations, however, were highly substantial and would soon surpass the allowable limit. The trend of the detected heavy metal relative abundance in Kolo Creek surface water is

$\text{Fe}^+ > \text{Zn}^{2+} > \text{Cu}^{2+} > \text{Pb}^{2+} > \text{Cd}^+ > \text{Hg}^+ > \text{Al}^+$ . The reason for this is that garbage gets washed into surface water from the river drainage, which is closer to the municipal and hydrocarbon waste sites.

Nonetheless, it is advised to treat river water before usage. While other heavy metals can be handled with ascorbic acid, ion exchange techniques, chemical precipitation, or any other conventional approach iron can only be treated with aeration or ozonation techniques.

### **Multivariate Statistical Analyses of hydro geochemical data for surface water**

“Principal Component Analysis (PCA) is a major tool in identifying designs, investigating the fluctuation of sets of connected factors, and furthermore separating the Eigen values and Eigenvectors (loadings) for head parts from their related change” (Akakuru *et al.*, 2022). “It explains the relationship that exists between the parameters to identify the likely wellsprings of groundwater or surface water contamination in the review region” (Akakuru *et al.*, 2022). Five significant principal components were identified. All loadings that are greater than 0.4 (+ or –) are considered in the analysis interpretation as a significant contributor. From the result as presented in Table 4.4, in PC1, 63.64% had loadings that were all positive (Cu, Cr, pH, Pb, Mg, TPH, HC03, Betex, Hg, Ca, Fe, Zn, DS, and K). This is an attribute of the factors that are contributing to the expanded pollution of the surface water in the review region. This is due to anthropogenic activities as a result of industrial activities in the study area. For PC2, 36.36% of the variables had loadings; Betex, N03, Na, Al, Fe, and Zn are positive (22.72%), while S04, Cl, and EC had negative loadings (13.64%). PC3, 13.64% of the variables had loading, and all the variables had positive load-ings for TPH, DS, and PAH. PC4, 9.09% of the variables had loading, 4.5% of the variables had positive loadings for PAH, and K had a negative loading of 4.5%. PC5: 4.5% of the variables had loadings; all of the variables had positive loadings (Akakuru *et al.*, 2022; Edori & Odoemelum, 2022; Ajayi & Okeke, 2024). Figure 4.22 presents a component plot in rotated space.

The PCA results underscore the significant role of anthropogenic activities, particularly industrial operations, in driving water pollution in Kolo Creek. The identification of key pollutants such as TPH, PAH, and heavy metals (e.g., Cu, Cr, Pb, Hg, Fe, Zn) highlights the need for targeted mitigation strategies to address these contamination sources.

### **Correlation matrix analysis**

“When evaluating the relationship and source of hydro-geochemical parameters for groundwater quality, correlation matrix analysis is a trustworthy method” (Akakuru *et al.*, 2022; Akakuru *et al.*, 2021). “A strong correlation between the two boundaries is indicated by correlation coefficients greater than 0.7; a weak correlation is suggested by correlation coefficients falling between 0.5 and 0.7” (Akakuru, *et al.*, 2021; Gaagai *et al.*, 2023). Betex and NO<sub>3</sub>, Cr, Zn, Hg, Al, pH, Cu, Fe; PAH and Dissolved Solid, S04, TPH; TPH and Dissolved solid, Cr, Zn, pH, Cu, Pb; Fe and NO<sub>3</sub>, Zn, Al, pH, Pb; Pb and Ca, mg, K, HCO<sub>3</sub>, Cr, Hg, pH, Cu; Cu and Dissolved Solid, Ca, mg, K, HCO<sub>3</sub>, Cr, Zn, Hg, pH; Zn and Na, NO<sub>3</sub>; Cr and Dissolved solid, Ca, Mg, K, HCO<sub>3</sub>, Cl, S04; NO<sub>3</sub> and EC, Na, Cl; S04 and EC, Na, Cl; Cl and EC, Na, Mg, K; HCO<sub>3</sub> and EC, Mg. The majority of the parameters show strong correlations, indicating that surface water contamination in the study area is primarily driven by anthropogenic activities, such as industrial operations, agricultural practices, and improper waste disposal. These findings underscore the need for targeted mitigation strategies to address the identified sources of pollution and protect water quality.

### **Cluster analysis**

The result of hierarchical cluster analysis (HCA) for the surface water sample is respectively shown in Fig.4.24 as dendrogram. “The HCA was intended to arrange the pollutants into different groups which could suggest the similarity or dissimilarity in their source of occurrence in the surface water samples, the analysis was carried out in line with Ward’s Method, where the distance apart reflects the level of association between the metallic pollutants” (Akakuru *et al.*, 2022; Ajayi & Okeke, 2024). The dendrogram in Fig. 4.24 indicates that there are four groups with only three clusters. In

the first group Pb, Al, Cr, Hg, Cd, Cu, Fe, Zn, EC, Cl, Ca, Mg, HC03, pH, K, N03, Na, Hardness, Turbidity, Betex and PAH formed a coherent cluster, Na and dissolved solid formed second group, dissolved solid and S04 formed third group and TPH is alone. This suggests that the presence of these metals in the surface water is influenced by similar anthropogenic activities in the study area. The result of hierarchical cluster analysis (HCA) for the surface water sample is shown in Fig. 4.24 as a dendrogram. The dendrogram in Fig. 4.24 indicates that there are four groups with only three clusters. In the first group,  $Pb^{2+}$ ,  $Al^{3+}$ ,  $Cr^{3+}$ ,  $Hg^{2+}$ ,  $Cd^{2+}$ ,  $Cu^{2+}$ ,  $Fe^{2+}/Fe^{3+}$ ,  $Zn^{2+}$ , EC,  $Cl^{-}$ ,  $Ca^{2+}$ ,  $Mg^{2+}$ ,  $HCO_3^{-}$ , pH,  $K^{+}$ ,  $NO_3^{-}$ ,  $Na^{+}$ , Hardness, Turbidity, BTEX, and PAH formed a coherent cluster;  $Na^{+}$  and dissolved solids formed the second group; dissolved solids and  $SO_4^{2-}$  formed the third group; and TPH was alone. This suggests that the presence of these metals in the surface water is influenced by similar anthropogenic activities in the study area.

### **Contamination factor (CF) and Pollution Index (PI)**

From Table 4.6a & 4.6b, CF for surface investigation shows that the concentrations of  $HCO_3^{-}$ ,  $NO_3^{-}$ ,  $Na^{+}$ ,  $Mg^{2+}$ ,  $SO_4^{2-}$ ,  $Ca^{2+}$ , and  $Cl^{-}$  were comparatively low, all with values less than 1, while  $Fe^{2+}/Fe^{3+}$  has 9.1, respectively. Hence, the surface water is highly contaminated with iron This finding indicates that anthropogenic activities are the main source of pollution in the study area. The high CF value for iron highlights the need for targeted mitigation measures to address industrial and mining-related pollution. While most parameters show low contamination levels, the overall pollution index indicates that the surface water is moderately polluted, necessitating ongoing monitoring and management efforts. The dominance of anthropogenic activities as pollution sources underscores the importance of stricter regulations and sustainable practices to reduce environmental impacts.

### **Water quality index**

WQI is a ranking system that makes it simple and effective to classify water into different groups. The acceptability of water for drinking uses depends critically on the

quality of the groundwater (Akakuru *et al.*, 2022; Gopinath *et al.*, 2019). The whole sample's WQI showed that all samples (100%) are unsuitable for use in industry, irrigation, or drinking; prior to use, they must be properly treated (Table 4.41). See table 4.43 below for WQI classification of the study area.

### **Quality assessment for irrigation**

#### **SAR**

The surface water throughout the region is classified as wonderful (Z1) in Table 4.9, SAR arrangement (Akakuru *et al.*, 2022). This is suggestive that the region's groundwater is excellent for irrigation purposes.

#### **Sodium percentage (%Na<sup>+</sup>)**

% Na<sup>+</sup> values (percent) have a mean of 75.92 and a standard deviation of 5.52, and they range from 68.7 to 80.1. The total samples are within 60-80, which indicate that the surface water in the research region is doubtful for irrigation, according to the surface water quality requirements (Table 4.10).

#### **Magnesium hazard**

Overly high levels of magnesium in water cause pungency, which slows down plant growth and yield (Mokoena *et al.*, 2020; Gaagai *et al.*, 2023; Talib *et al.*, 2019). The MH esteems in the review region increased from 11.3 to 18.5, with a mean of 13.54 and a standard deviation of 2.51, as Table 4.7 demonstrates. Furthermore, the results indicate that all 100 full instances fall below the 50-point threshold, indicating that the examples are suitable and suitable for use in water systems.

#### **Kelly ratio**

Kelly's ratio (KR) is efficient in assessing the irrigation suitability of water (Eyankware *et al.*, 2020; Mokoena *et al.*, 2020). A KR value greater than one indicates that Na in surface water is high whereas any value less than one is suitable for irrigation. Table 4.7

shows that KR values range from 1.18 to 3.3, with a mean of 2.62 and a standard deviation of 0.73. This result also shows that 100% of the surface water sample is unsuitable for irrigation (Table 4.12).

### **Soluble sodium percentage**

SSP has been utilized by scholars in the assessment of the suitability of surface water for irrigation purposes. It assesses the percentage of soluble sodium in surface water. SSP values exceeding 50 are deemed inappropriate for irrigation, whereas those below 50 are okay. The result from Table 4.7 shows that SSP values range between 0.50 and 0.65 with a mean of 0.60 and a standard deviation of 0.08. Table 4.13 shows that the entire samples are safe and suitable for irrigation. SSP result aligns with other irrigation assessment tools.

### **Wilcox Plot**

The Wilcox plot (Wilcox, 1955) is used to link EC to %Na. According to (fig. 4.15), 100% of the sample as a whole in the research area is excellent or very good for irrigation. This finding suggests that all of the study area's surface water is safe and acceptable for irrigation. With the exception of the Kelly ratio and Na%, all of the irrigation assessment instruments used in this study concur that the water is acceptable for irrigation, therefore supporting its validity.

### **Evaluation of health risk of the surface water samples**

Using Usepa (2011) health risk assessment models, the health risk associated with metallic pollutants in surface water samples was assessed using the hazard quotient (HQ). The amount of surface water that a person consumes, their age, and their body weight all affect the risk that contaminated surface water poses to their health. Using Eqs. (17)– (20), this was calculated using the measured concentrations of metallic pollutants as indicated in Tables 4.14 and 4.15. All of the metallic elements in the area have HQ values lower than one ( $\text{Cu}^{2+} > \text{Zn}^{2+} > \text{Pb}^{2+} > \text{Fe}^{2+}/\text{Fe}^{3+} > \text{Cd}^{2+} > \text{Hg}^{2+} > \text{Cr}^{3+}$ )

for both adults and children. The HQ values of the metals for adults and children are shown in Tables 4.15 and 4.16, respectively. The range of HI readings for adults is 0.155002 to 0.719632, whereas the range for children is 0.051585-0.169783. The samples' Hi values were less than 1. But since sample site S5 (adult) is leaning toward 1, appropriate action from the appropriate authorities is needed to prevent the emergence of cancer in this research region.

The likelihood that an individual may get cancer during their lifetime due to exposure to pollutants through certain channels, such as drinking tainted water, is known as their carcinogenic risk (CR) (Akakuru *et al.*, 2022). CR was computed using Equation (17–20). Due to the lack of SF values for other metals in the literature, the CR result is displayed in Table 4.17 with values for only Cd<sup>2+</sup>, Cr<sup>3+</sup>, and Pb<sup>2+</sup> (Akakuru *et al.*, 2022). The findings showed that the CR values for Cd<sup>2+</sup>, Cr<sup>3+</sup>, and Pb<sup>2+</sup> in all samples (Table 4.16) for both adults and children were above 10<sup>-6</sup> (> 10<sup>-6</sup>), suggesting a potential carcinogenic risk from surface water intake for both groups in the research area.

## **GEOCHEMICAL MODELS**

The following parameters were employed for interpretation utilizing geochemical models: HCO<sub>3</sub><sup>-</sup>, NO<sub>3</sub><sup>-</sup>, Cl<sup>-</sup>, and SO<sub>4</sub><sup>2-</sup> were the anions, and Na<sup>+</sup>, Ca<sup>2+</sup>, K<sup>+</sup>, and Mg<sup>2+</sup> were the cations. After being translated from milligrams per liter to milli-equivalents per liter, Piper's trilinear, Durov, Stiff, and Scholler diagrams were produced.

### **Piper Diagram**

“Anion and cation triangles combined on a common baseline diamond shape between them form Piper diagrams” (Piper, 1944). Ajayi & Okeke 2024 argued that “these diagrams can be used to define various water types and arrive at a preliminary conclusion on the origin of the water represented by the analysis”. Based on where the waters were located in relation to the diamond's four corners, Piper classified the waters into four fundamental categories. An area of persistent hardness is caused by the water that plots at the top of the diamond because it has high concentrations of Ca<sup>2+</sup>, Mg<sup>2+</sup>,

and  $\text{Cl}^- + \text{SO}_4^{2-}$ . The area of temporarily hard water is the water that plots close to the left corner and is rich in  $\text{Ca}^{2+}$ ,  $\text{Mg}^{2+}$ , and  $\text{HCO}_3^-$ .

All ten of the stations are located close to the left corner of the diamond in the plot (Figure 4.26), suggesting that they are Ca- $\text{HCO}_3$  (typical of shallow, fresh surface waters) and Mg- $\text{HCO}_3$  (typical of shallow, fresh surface waters).

### **Durov Diagram**

“This graphic was introduced by and helps to distinguish the different types of water and can show some potential geochemical processes that could be useful in evaluating and understanding groundwater quality” (Durov, 1948; Ajayi & Okeke, 2024). It also helps to provide more information about the hydrochemical facies. The two ternary diagrams that make up the composite plot show the concentrations of the cations and anions of interest, with the sides forming a binary plot of total cation vs. total anion. The expanded version of the diagram adds pH and electrical conductivity ( $\mu\text{S}/\text{cm}$ ) data to the binary plot's sides to enable more comparisons.

The plot's pH section indicates that the river's water is acidic, making it unsafe to drink. The river's electrical conductivity falls within the WHO (2017) drinking water standard range (Figure 4.26).

### **Scholler Diagram**

For each of the ten sites, the average chemical composition of Kolo-Creek water is displayed using a Schoeller (1977) diagram. The relative ion tendency in mg/L is as follows:  $\text{Cl}^- > \text{HCO}_3^- = \text{NO}_3^- = \text{SO}_4^{2-}$  and  $\text{Na}^+ > \text{K}^+ > \text{Mg}^{2+} > \text{Ca}^{2+}$ . The plotted Schoeller diagram below (Figure 4.27) illustrates the predominant water type,  $\text{Na}^+ + \text{K}^+ - \text{SO}_4^{2-}$  hydro-geochemical facies, found in the research area.

### **Stiff Diagrams**

Diagrams show the various water ions graphically (Stiff, 1951; Ajayi & Okeke, 2024).  $\text{Na}^+ + \text{K}^+$  and  $\text{Mg}^{2+}$  are dominant, although  $\text{SO}_4^{2-} + \text{HCO}_3^-$  are almost equal in

proportion, according to the average ionic composition analysis by the Stiff diagram displayed in Figure 4.29. Based on their unique forms, the hydro geochemical water

### **4.3 Physical and Bio-Chemical Characteristics of Ground Water Samples**

#### **pH**

The pH range along the stations or stretch of Kolo-Creek groundwater in the dry season is 6.0 to 7.20 (Table 4.1a), with a control point value of 7.20 and a mean value of 6.42, and the pH range along the stations or stretch of Kolo-Creek groundwater in the wet season is 6.27 to 7.20 (Table 4.1b), with a control point value of 7.20 and a mean value of 6.55; these values do not conform to the WHO (2017) standard for safe water. Figure 4.18 depicts how the pH varies between stations. The pH measurements indicate that Kolo Creek's groundwater is acidic. The Anova test indicates a significant variation in mean pH values between stations ( $F = 7.15$ ,  $Pr < 0.05$ ). There is no significant difference in seasonal mean pH values along the creek ( $F = 0.88$ ,  $P > 0.05$ ). The mean pH is somewhat higher in the wet season than in the dry season.

#### **Temperature**

In the dry season, the temperature range along the stations or stretch of Kolo Creek groundwater is 25.9 to 27.43 (Table 4.1a), with a control point value of 27.43 and a mean value of 26.49, and in the wet season, the temperature range is 25.60 to 27.30 (Table 4.1b), with a control point value of 27.30 and a mean value of 26.19. These values are consistent with the WHO (2017) criteria for safe drinking water. Figure 4.18 depicts the variation in temperature between stations. The Anova test indicates a significant difference in mean temperature values between stations ( $F = 6.22$ ,  $Pr < 0.05$ ). While there is a substantial fluctuation in mean seasonal temperature values along the creek's length ( $F = 1.55$ ,  $pr > 0.05$ ), temperature concentrations are generally consistent between seasons.

## Electrical Conductivity and TDS

The mean concentrations of electrical conductivity in the groundwater of Kolo Creek in the **dry season** range from 77.0 to 186.37  $\mu\text{S}/\text{cm}$ , respectively, with a control point value of 94.40  $\mu\text{S}/\text{cm}$  and mean values of 128.4  $\mu\text{S}/\text{cm}$ , while the mean concentrations of total dissolved solids (TDS) range from 46.27 to 175.03 mg/l, respectively (Tables 4.1a and 4.1b), with a control point value of 46.27 mg/l and a mean value of 101.04 mg/l, while the mean concentrations of electrical conductivity in the groundwater of Kolo Creek in the **wet season** range from 31.17 to 177.43  $\mu\text{S}/\text{cm}$ , respectively, with a control point value of 31.17  $\mu\text{S}/\text{cm}$  and a mean value of 123.5  $\mu\text{S}/\text{cm}$ .

The mean concentrations of total dissolved solids (TDS) in the **dry season** range from 110.87 to 119.07 mg/l, respectively (Tables 4.1a and 4.1b), with a control point value of 117.47 mg/l and a mean value of 115.51 mg/l, while the mean concentrations of total dissolved solids (TDS) in the **wet season** range from 68.37 to 166.73 mg/l, respectively (Tables 4.1a and 4.1b), with a control point value of 146.27 mg/l and a mean value of 116.04 mg/l. The concentrations of TDS and electrical conductivity conformed to the WHO (2017) standard for safe drinking water. The TDS values indicate that the river is fresh (Carol, 1962), while the electrical conductivity values show no salinity hazards (Todd, 1980).

The Anova test shows that there is generally no significant difference in the mean electrical conductivity values of the stations ( $F = 2.23$ ,  $Pr > 0.05$ ). While there is no significant difference in the mean seasonal values of electrical conductivity along the stretch of the creek ( $F = 0.07$ ,  $pr > 0.05$ ), the electrical conductivity value is generally higher during the dry season than during the wet season.

The Anova test shows that there is generally no significant difference in the mean TDS values of the stations ( $F = 0.94$ ,  $Pr > 0.05$ ). There is also no significant difference in the mean seasonal values of TDS along the stretch of the creek ( $F = 1.2$ ,  $pr > 0.05$ ). The TDS value is generally higher during the dry season than during the wet season.

## **Hardness**

The total hardness values for the dry **season** range from 56.0 to 118.40 mg/l, with a control point value of 78.83 mg/l and mean values of 92.53 mg/l. While the total hardness values for the wet **season** range from 30.67 to 100.70 mg/l (Figure 4.3 and Tables 4.1a and 4.1b), with a control point value of 30.67 mg/l and a mean value of 79.90 mg/l. These values were less than 50 mg/l and thus indicate that the water is soft (Wilcork, 1993). These values conformed to the WHO (2011) guideline of 150 mg/l of  $\text{CaCO}_3$  and  $\text{MgCO}_3$ . The Anova test shows that there is generally no significant difference in the mean total hardness values of the stations ( $F = 2.40$ ,  $Pr > 0.05$ ). While there is no significant difference in the mean seasonal values of total hardness along the stretch of the creek ( $F = 1.66$ ,  $pr > 0.05$ ). The total hardness value is generally higher during the dry season than during the wet season.

## **Total Chloride**

The mean concentration values for total chloride in the dry **season** range from 32.4 to 44.40 mg/l, respectively, along the stretch of the stations with a control point value of 33.90 mg/l and a mean value of 36.47 mg/l, while the mean concentration values for total chloride in the wet **season** range from 15.03 to 43.40 mg/l, respectively, along the stretch of the stations with a control point value of 15.17 mg/l and a mean value of 28.49 mg/l (Tables 4.1a and 4.1b). These values conform to the WHO (2017) guideline values, which are 250 mg/l. The Anova test shows that there is generally no significant difference in the mean chloride values at the stations ( $F = 0.83$ ,  $Pr > 0.05$ ). While there is no significant difference in the mean seasonal values of chlorine along the stretch of the creek ( $F = 4.83$ ,  $pr > 0.05$ ). The chloride value is generally higher during the dry season than during the wet season.

## **Total Petroleum Hydrocarbon (TPH)**

TPH levels in the dry season range from 15.33 to 137.67 mg/l among the stations, with a control point of 15.33 mg/l and a mean of 106.10 mg/l. During the wet season, TPH levels range from 15.00 to 156.80 mg/l among the stations (Tables 4.1a and 4.1b), with

a control point of 15.0 mg/l and a mean value of 107.25 mg/l. The Anova test indicates a significant difference in mean TPH values between stations ( $F = 49.98$ ,  $Pr < 0.05$ ) while there is no significant difference in the mean seasonal values of TPH along the stretch of the creek. These values do not conform to the WHO 2017 guidelines.

### **Pyrolytic Aromatic Hydrocarbon**

The PAH in the **dry season** varies from 0.0 to 4.27 mg/l at the stations, respectively, with a control point value of 0.0 mg/l and a mean value of 1.13 mg/l. While the PAH in the **wet season** varies from 0.0 to 3.23 mg/l at the stations, respectively, with a control point value of 0.0 mg/l and mean value of 0.99 mg/l. The Anova test shows that there is a generally significant difference in the mean PAH values of the stations ( $F = 28.73$ ,  $Pr < 0.05$ ), while there is no significant difference in the mean seasonal values of PAH along the stretch of the creek ( $F = 0.24$ ,  $Pr . > 0.05$ ). The PAH value is generally higher during the dry season than during the wet season. These values do not conform to the WHO 2017 guidelines.

### **Betex**

The Betex values in the **dry season** vary from 0.0 to 3.83 mg/l at the stations, respectively, with a control point value of 0.00 mg/l and a mean value of 2.15 mg/l. While the Betex values in the **wet season** vary from 0.26 to 3.67 mg/l at the stations, respectively, with a control point value of 0.26 mg/l and a mean value of 2.21 mg/l, these values far exceed the WHO (2017) guideline values. The Anova test shows that there is generally a significant difference in the mean Betex values at the stations ( $F = 27.53$ ,  $Pr < 0.05$ ), and there is no significant difference in the mean seasonal values of Betex along the stretch of the creek ( $F = 0.014$ ,  $Pr > 0.05$ ). The Betex value is generally higher during the wet season than during the dry season.

## Major Cations and Anions

### Calcium

The calcium values in the **dry season** vary from 16.83 to 28.33 mg/l along the stations, respectively, with a control point value of 16.83 mg/l and a mean value of 21.60 mg/l. While the calcium values in the **wet season** vary from 10.70 to 25.30 mg/l along the stations, respectively (Tables 4.1a and 4.1b), with a control point value of 10.70 mg/l and a mean value of 19.92 mg/l. The Anova test shows that there is generally no significant difference in the mean calcium values along the stations ( $F = 1.65$ ,  $Pr > 0.05$ ), and there is no significant difference in the mean seasonal values of calcium along the stretch of the creek ( $F = 0.69$ ,  $Pr > 0.05$ ). The calcium value is generally higher during the dry season than during the wet season. These values conform to the WHO (2017) guideline values.

### Magnesium

Magnesium values in the **dry season vary** from 2.30 to 5.13 mg/l along the stations, respectively, with a control point value of 2.30 mg/l (Tables 4.1a and 4.1b) and a mean value of 3.40 mg/l. While magnesium values in the **wet season vary** from 0.82 to 6.37 mg/l along the stations, respectively, with a control point value of 0.82 mg/l (Tables 4.1a and 4.1b) and a mean value of 2.57 mg/l, The ANOVA test shows that there is generally no significant difference in the mean magnesium values at the stations ( $F = 2.59$ ,  $Pr > 0.05$ ) while there is no significant difference in the mean seasonal values of magnesium along the stretch of the creek ( $F = 0.69$ ,  $pr > 0.05$ ), The magnesium value is generally higher during the dry season than during the wet season. These values conform to the WHO (2017) guideline values.

### Sodium

The sodium value in the **dry season** varies from 34.73 to 87.27 mg/l along the stations, respectively, with a control point value of 47.0 mg/l (Table 4.1 and Figure 4.38) and a mean value of 64.46 mg/l. While the sodium value in the **wet season** varies from 51.17

to 79.77 mg/l along the stations, respectively, with a control point value of 57.70 mg/l (Table 4.1a and Figure 4.14) and a mean value of 68.74 mg/l. These values conform to the WHO (2017) guideline values. The Anova test shows that there is generally no significant difference in the mean sodium values at the stations ( $F = 0.79$ ,  $Pr > 0.05$ ). While there is no significant difference in the mean seasonal values of sodium along the stretch of the creek ( $F = 0.43$ ,  $pr > 0.05$ ), the sodium value is generally higher during the **wet season** than during the **dry season**.

### **Potassium**

Potassium values in the **dry season** vary from 11.47 to 19.77 mg/l along the stations, with a control point value of 17.43 mg/l and mean values of 16.89 mg/l. While potassium values in the **wet season** vary from 15.90 to 22.47 mg/l along the stations, with a control point value of 16.0 mg/l and mean values of 19.59 mg/l (Tables 4.1a and 4.1b), The Anova test shows that there is generally no significant difference in the mean potassium values at the stations ( $F = 1.21$ ,  $Pr > 0.05$ ). While there is no significant difference in the mean seasonal values of potassium along the stretch of the creek ( $F = 5.79$ ,  $pr > 0.05$ ), the potassium value is generally higher during the wet season than during the dry season.

The concentrations of the major constituent cations are generally low and conform to the WHO (2017) standard for safe drinking water. The relative abundance of the major constituent cations follows the trend  $Na^+ > Ca^{2+} > K^+ > Mg^{2+}$ .

### **Bicarbonates**

The concentration of bicarbonate in the **dry season** ranges from 31.57 to 45.87 mg/l along the stations, respectively, with a control point value of 31.57 mg/l and a mean value of 39.09 mg/l while the concentration of bicarbonate in the **wet season** ranges from 10.75 to 46.00 mg/l along the stations, respectively, with a control point value of 10.90 mg/l and a mean value of 20.88 mg/l (Table 4.1 and Figure 4.40), these values conform to the WHO (2017) guideline values. The ANOVA test shows that there is generally no significant difference in the mean bicarbonate values of the stations ( $F =$

0.68,  $Pr > 0.05$ ) while there is a significant difference in the mean seasonal values of bicarbonate along the stretch of the creek ( $F = 17.96$ ,  $pr < 0.05$ ), the bicarbonate values are generally higher during the dry season than the wet season.

### Sulphates

The concentration of  $SO_4^{2-}$  in the dry season ranges from 105.40 to 156.57 mg/l, with a control point value of 111.0 mg/l and a mean value of 127.97 mg/l. Meanwhile, the concentration of  $SO_4^{2-}$  in the wet season ranges from 85.83 to 114.70 mg/L, with a control point value of 102.33 mg/l and a mean value of 102.96 mg/l (Table 4.1 and Figure 4.41). These values conform to the WHO (2017) guideline values. The Anova test shows that there is generally no significant difference in the mean sulfate values along the stations ( $F = 0.44$ ,  $Pr > 0.05$ ), while there is a significant difference in the mean seasonal values of sulfate along the stretch of the creek ( $F = 17.62$ ,  $Pr < 0.05$ ). The sulfate value is generally higher during the dry season than during the wet season.

### Nitrates

The concentration of  $NO_3$  in the **dry season** ranges from 1.24 to 4.57 mg/l, respectively, with a control point value of 1.24 mg/l and a mean value of 2.46 mg/l. While the concentration of  $NO_3$  in the **wet season** ranges from 1.23 to 3.83 mg/l, respectively, with a control point value of 1.23 mg/l (Table 4.1 and Figure 4.42) and a mean value of 2.75 mg/l. These values conform to the WHO (2017) guideline values. The Anova test shows that there is generally no significant difference in the mean nitrate values at the stations ( $F = 5.94$ ,  $Pr > 0.05$ ) while there is no significant difference in the mean seasonal values of nitrate along the stretch of the creek ( $F = 322.7$ ,  $pr > 0.05$ ), the nitrate value is generally higher during the wet season than the dry season.

The relative abundance of major anions follows the trend  $SO_4^{2+} > Cl^- > HCO_3^- > NO_3^-$ . The water type is sodium bicarbonate ( $NaHCO_3$ ).

### 4.3.1 GEOCHEMICAL MODELS

The following parameters were employed for interpretation utilizing geochemical models:  $\text{HCO}_3^-$ ,  $\text{NO}_3^-$ ,  $\text{Cl}^-$  and  $\text{SO}_4^{2-}$  were the anions, and  $\text{Na}^+$ ,  $\text{Ca}^{2+}$ ,  $\text{K}^+$ , and  $\text{Mg}^{2+}$  were the cations. After being translated from milligrams per liter to milli-equivalents per liter, Piper's trilinear, Durov, Stiff, and Scholler diagrams were produced.

#### **Piper Diagram**

Anion and cation triangles combined on a common baseline diamond shape between them form Piper diagrams (Piper, 1944). These diagrams can be used to define various water types and arrive at a preliminary conclusion on the origin of the water represented by the analysis. Based on where the waters were located in relation to the diamond's four corners, Piper classified the waters into four fundamental categories. There is a permanent hardness zone in the water that plots at the top of the diamond because it has high levels of  $\text{Ca}^{2+} + \text{Mg}^{2+}$  and  $\text{Cl}^- + \text{SO}_4^{2-}$ . The area of temporarily hard water is the water that plots close to the left corner and is rich in  $\text{Ca}^{2+}$ ,  $\text{Mg}^{2+}$ , and  $\text{HCO}_3^-$ . The majority of the water plotted at the diamond's lower corner is made up of alkali carbonates, specifically  $\text{Na}+\text{K}$ ,  $\text{HCO}_3^+$ , and  $\text{CO}_3^{2+}$ . Water that is close to the diamond's right side ( $\text{Na}^+ + \text{K}^+$  and  $\text{Cl}^- + \text{SO}_4^{2-}$ ) may be saline. All ten of the stations are located close to the left corner of the diamond in the plot (Figure 4.43), suggesting that they are  $\text{Ca}^{2+} \text{HCO}_3^-$  (typical of shallow, fresh surface waters) and  $\text{Mg}^{2+} \text{HCO}_3^-$  (typical of shallow, fresh surface waters).

#### **Durov Diagram**

This graphic was introduced by (Durov, 1948). It helps distinguish the different types of water and can show some potential geochemical processes that could be useful in evaluating and understanding groundwater quality. The diagram also offers further information on the hydro-chemical facies. Comprising two ternary diagrams, the diagram displays the concentrations of the cations and anions of interest. The sides of the binary plot show the total concentrations of the cations and anions, and an expanded version of the diagram allows for additional comparisons by adding pH and electrical

conductivity ( $\mu\text{S}/\text{cm}$ ) data to the binary plot. The plot's pH section indicates that the groundwater is suitable for drinking because it is normal. The river's electrical conductivity falls within the WHO (2017) drinking water standard range (Figure 4.44).

### **Scholler Diagram**

At each of the ten locations, the average chemical composition of Kolo Creek groundwater is also displayed using the Schoeller (1977) graphic. The relative tendency of ions in mg/l is as follows:  $\text{SO}_4^{2-} > \text{NO}_3^- > \text{Cl}^- > \text{HCO}_3^-$  and  $\text{Na}^+ > \text{K}^+ > \text{Ca}^{2+} > \text{Mg}^{2+}$ . According to the plotted Scholler diagram below (Figure 4.45), the hydro-geochemical facies discovered in the study area are primarily the water type  $\text{Na}^+ + \text{K}^+ - \text{SO}_4^{2-}$ .

### **Stiff Diagrams**

One way to visualize the various water ions is with a diagram. As can be shown in Figure 4.46, the study of the average ionic composition using the stiff diagram indicates that  $\text{Na}^+$ ,  $\text{K}^+$ , and  $\text{SO}_4^{2-}$  predominate, with  $\text{Mg}^{2+}$  and  $\text{Cl}^-$  having almost equal shares. Based on the differences in form between the several stiff graphs, the hydro-geochemical water types are interpreted (Stiff, 1951).

### **Heavy Metals and Other Metals in Groundwater**

#### **Iron $\text{Fe}^{2+}$**

During the dry season, the iron concentrations in the creek fluctuate from 24.87 to 53.46 mg/l, respectively, with a mean value of 37.75 mg/l and a control point value of 29.04 mg/l. While the iron concentrations in the wet season range from 25.88 to 53.17 mg/l along the creek's run, with a mean value of 36.40 mg/l and a control point value of 27.06 mg/l (Table 4.1 and Figure 4.47). According to the results of the Anova test, the mean iron values of the stations differ significantly ( $F = 7.16$ ,  $\text{Pr} < 0.05$ ) whereas the mean seasonal values of iron along the creek do not differ significantly ( $F = 0.11$ ,  $\text{Pr} > 0.05$ ). In general, the dry season has higher iron values than the wet season. Every area has iron levels that are significantly higher than the WHO (2017) drinking water norm.

### **Copper Cu<sup>2+</sup>**

Along the creek, copper concentrations during the dry season range from 0.10 to 0.67 mg/l, with a mean of 0.43 mg/l and a control point at 0.17 mg/l. The creek's copper concentrations range from 0.7 to 0.80 mg/l, with a mean value of 0.10 mg/l and a control point of 0.43 mg/l (Table 4.1 and Figure 4.48). The results of the Anova test indicate that there is a significant difference in the stations' mean copper values ( $F = 14.14$ ,  $Pr < 0.05$ ), but not in the mean seasonal values of copper along the creek ( $F = 0.00$ ,  $Pr > 0.05$ ). During the dry season, the value of copper is marginally higher.

### **Zinc (Zn<sup>2+</sup>)**

During the dry season, the average zinc concentrations in the creek range from 0.20 to 1.3 mg/l, with a mean of 0.97 mg/l and a control point value of 0.20 mg/l. The mean zinc content during the rainy season is 0.95 mg/l, although it varies along the stream from 0.24 to 1.40 mg/l with a control point value of 0.20 mg/l (Table 4.1 and Figure 4.49). The results of the Anova test indicate that the mean zinc levels of the stations differ in a way that is generally significant ( $F = 69.90$ ,  $Pr < 0.05$ ) while there is no significant difference in the mean seasonal values of zinc along the stretch of the creek ( $F = 0.02$ ,  $pr > 0.05$ ), the zinc concentration is generally higher in the wet season than in the in the dry season.

### **Lead (Pb<sup>2+</sup>)**

Lead concentrations in the dry and rainy seasons range from 0.00 to 0.05 mg/l, respectively, along the creek's length, with a mean value of 0.03 mg/l and no detection at the control location (Table 4.1 and Figure 4.50). According to the results of the ANOVA test, there is typically no discernible difference between the mean lead values of the stations ( $F = 1.7$ ,  $Pr > 0.05$ ) and the mean seasonal values of lead along the creek ( $F = 0.1$ ,  $Pr > 0.05$ ). In other words, the lead value remains relatively constant between the two seasons.

### **Aquifer geometric and hydraulic properties of the study location**

“The discharge of groundwater  $Q$  through a porous media is related to the product of saturated hydraulic conductivity  $k_f$ , the cross-sectional area of flow  $A$ , and the hydraulic gradient  $J$  normal to that area:  $Q = k_f A J$ ” (Knodel *et al.*, 2007). This is computed using Darcy's law (Whitaker, 1986). In cases where  $T = k_f b$  (Niwas & Singhal, 1985) is used to express transmissivity.

### **Elevation**

The research area's elevation ranged from 91.3m to 163.7m, with a mean elevation of 126.4m and a standard deviation of 26.4m. Fig. 4.51 shows a graph of the height and water depth in the research area, illustrating the close relationship between elevation and water table fluctuation. The elevation is trending NE-SW, according to the map (Fig. 4.51).

### **Water depth**

The water depth values in the area range from 28.0m to 75.6m, with a mean value of 52.6m and a standard deviation of 16.5 m. Aquifer thickness ( $B$ ) is the vertical thickness of the hydro-geologically defined aquifer, measured after water has filled (saturated) the pore spaces of the rock that forms the aquifer. The  $B$  values (m) from Table 4.17 show that it has a mean value of 106.6m, a minimum value of 76.95m, a maximum value of 126.8m, and a standard deviation of 17.72m. The research area's aquiferous materials are both quite shallow and very permeable.

### **Hydraulic conductivity (K)**

“To comprehend the transport of pollution, hydraulic conductivity is yet another crucial aquifer parameter; this corresponds to a quantification of the saturated soil's hydraulic gradient-induced water-transfer capacity” (Omoko *et al.*, 2023). A standard deviation of 0.11, a minimum and maximum value of 0.32 and 0.66, respectively, and a mean value of 0.468 are found for  $K$  in Table 4.17  $K$  values (m/day). The hydraulic

conductivity flows from southeast to northwest, as can be seen on the map. The groundwater potential of the area is moderately high (1980) according to the Todd scale. “It is also indicated that the contaminants and liquids can pass through cracks in the rock and pores; the primary cause of significant hydraulic conductivity in the study area is the extremely permeable soils based on geology” (Omoko *et al.*, 2023, p.23). In order to ascertain whether the water quality in the region has declined, it is advised that water samples drawn from boreholes be sporadically examined for pollutant loading (Omoko *et al.*, 2023).

### **Transmissivity (T)**

"Transmissivity describes the ability of an aquifer to transfer groundwater over its entire saturated thickness" (Omoko *et al.*, 2023). Table 4.17, T values, shows that the mean and standard deviation were 2.64 and 7.02, respectively, and that the range of values was 3.73 to 11.29. The research area's transmissivity indicates that it is traveling in a NW-SW direction. The high T value that was found in the research area could be related to the level of pollution in that area.

“Because of the aquifer transmissivities and protective qualities of the local overburden rock types, the relative proximity of these aquiferous layers to the surface has a significant effect on the groundwater quality” (Omoko *et al.*, 2023). “The surrounding overburden rock materials offer very little in the way of protection. The absence of substantial overburden impermeable rock material (shale or clay), which can prevent pollutant infiltration, is the cause of the poor protective capacity ratings” (Omoko *et al.*, 2023). Because surface pollutants will descend faster, enter the aquifer more readily, and eventually, it is implied that surface pollutants will have an unparalleled effect on groundwater quality. Transmissivity in an unconfined aquifer varies with changes in its saturated thickness. The equation  $T = kf b$ , where  $b$  is the thickness of the saturated portion of the aquifer, relates  $T$  to the average hydraulic conductivity ( $kf$ ) of the saturated portion of the aquifer.

### **Multivariate Statistical Analyses of hydro geochemical data for groundwater**

Six significant principal components were identified. All loadings that are greater than 0.4 (+ or -) are considered in the analysis interpretation as a significant contributor. From the result as presented in Table 4.31, in PC1, 61.11% had loadings that were all positive (Betex, TPH, Nitrate, Iron, PAH, Mg, HC03, Ca, Na, Pb, Cu, and Zinc). This is an attribute of the factors that are contributing to the expanded pollution of the groundwater in the review region; this could be due to anthropogenic activities as a result of industrial activities in the study area. For PC2, 22.22% of the variables had loadings; Pb and Cu are positive (11.11%), while Hardness and CEC had negative loadings (11.11%). This implies that they are of geogenic origin (rock-water-environment interactions). PC3: 27.78% of the variables had loading; 22.22% of the variables had positive loadings for Mg, HC03, S04, and Cl; and K had a negative loading of 5.56%. PC4, 11.11% of the variables had loading, 5.56% of the variables had positive loadings for Zn, and PAH had a negative loading of 5.56%. PC5: 11.11% of the variables had loadings, and all of the variables had positive loadings for K and Na. PC6 5.56% of the variables had loading; it has positive loadings for Mg and TDS. Figure 4.53 presents a component plot in rotated space.

### **Correlation matrix analysis**

From Table 4.20, there is a correlation between  $\text{NO}_3^-$  and  $\text{Pb}^{2+}$ ,  $\text{Fe}^{2+}/\text{Fe}^{3+}$ , TPH, PAH, BTEX, EC,  $\text{Na}^+$ , and  $\text{Mg}^{2+}$ ; EC and salinity,  $\text{SO}_4^{2-}$ ,  $\text{K}^+$ ,  $\text{Ca}^{2+}$ , and  $\text{Mg}^{2+}$ ; TDS and  $\text{SO}_4^{2-}$ ,  $\text{K}^+$ ,  $\text{Mg}^{2+}$ , and  $\text{Fe}^{2+}/\text{Fe}^{3+}$ ;  $\text{SO}_4^{2-}$  and  $\text{Mg}^{2+}$ ,  $\text{HCO}_3^-$ , and  $\text{Cl}^-$ ;  $\text{Cl}^-$  and  $\text{Ca}^{2+}$ ,  $\text{HCO}_3^-$ ;  $\text{HCO}_3^-$  and  $\text{Fe}^{2+}/\text{Fe}^{3+}$ , PAH, and  $\text{K}^+$ ;  $\text{Mg}^{2+}$  and  $\text{Fe}^{2+}/\text{Fe}^{3+}$ , TPH, PAH, BTEX, and  $\text{Ca}^{2+}$ ;  $\text{Ca}^{2+}$  and  $\text{Zn}^{2+}$ ,  $\text{Pb}^{2+}$ ; hardness and TPH, EC; EC and TPH, BTEX; BTEX and  $\text{Fe}^{2+}/\text{Fe}^{3+}$ , TPH, PAH; PAH and  $\text{Fe}^{2+}/\text{Fe}^{3+}$ , TPH; TPH and  $\text{Zn}^{2+}$ ,  $\text{Fe}^{2+}/\text{Fe}^{3+}$ ;  $\text{Cu}^{2+}$  and  $\text{Zn}^{2+}$ . Strong correlations observed in the majority of the parameters imply that the groundwater contamination emanated from the same source and could be a result of anthropogenic activities in the study area. This further means that contaminants percolate into the groundwater of the study area.

## Cluster analysis

The results of hierarchical cluster analysis (HCA) for the groundwater samples are shown in Fig. 4.54 as a dendrogram. A hierarchical cluster analysis of the metallic pollutants was carried out to separate the constituents of the different sources in the samples. The HCA was intended to arrange the metallic pollutants into different groups, which could suggest a similarity or dissimilarity in their source of occurrence in the groundwater samples. The dendrogram in Fig. 4.54 indicates that there are six groups with four clusters. In the first group,  $Pb^{2+}$ ,  $Cu^{2+}$ ,  $Zn^{2+}$ , PAH, BTEX,  $NO_3^-$ , and  $Mg^{2+}$  formed a coherent cluster; PAH and  $K^+$  formed the second group;  $Ca^{2+}$ ,  $K^+$ ,  $HCO_3^-$ ,  $Cl^-$ , and  $Fe^{2+}/Fe^{3+}$  formed the third group; hardness and  $Na^+$  formed the fourth cluster; TDS and  $SO_4^{2-}$  formed the fifth group; and TPH and EC formed the sixth group. This suggests that the presence of these metals in the groundwater is influenced by similar anthropogenic activities, possibly due to hydrocarbon exploration and related activities in the area.

## Contamination factor (CF)

Table 4.21 CF for groundwater investigation shows that the concentrations of  $HCO_3^-$ ,  $NO_3^-$ ,  $Na^+$ ,  $Mg^{2+}$ ,  $SO_4^{2-}$ , and  $Cl^-$  were comparatively low, all with values less than 1, while  $Ca^{2+}$  has 2.880 and  $Fe^{2+}/Fe^{3+}$  has 125.82, respectively. This finding indicates that anthropogenic activities are the main source of pollution in the study area.

## Pollution load index

“For assessing the degree of toxicity of heavy metals in representative samples, PLI is a useful method” (Yang *et al.*, 2011). “PLI is often divided into four categories: very heavy pollution ( $3 > PLI$ ), heavy pollution ( $2 > PLI > 3$ ), moderate pollution ( $PLI > 2$ ), and no pollution ( $PLI = 1$ )” (Akakuru *et al.*, 2022). The results from table 4.21 showed that the groundwater in the research region had a concentration value of less than one at the following stations (S3-S10), whereas the values at S1 and S2 (1.785 and 1.363,

respectively) were larger than 1. This suggests that station S1–S2 is polluted, while station S3–S10 does not appear to be significantly polluted.

### **Correlation matrix analysis**

From Table 4.20, there is a correlation between  $\text{NO}_3^-$  and  $\text{Pb}^{2+}$ ,  $\text{Fe}^{2+}/\text{Fe}^{3+}$ , TPH, PAH, BTEX, EC,  $\text{Na}^+$ , and  $\text{Mg}^{2+}$ ; EC and salinity,  $\text{SO}_4^{2-}$ ,  $\text{K}^+$ ,  $\text{Ca}^{2+}$ ,  $\text{Mg}^{2+}$ ; TDS and  $\text{SO}_4^{2-}$ ,  $\text{K}^+$ ,  $\text{Mg}^{2+}$ ,  $\text{Fe}^{2+}/\text{Fe}^{3+}$ ;  $\text{SO}_4^{2-}$  and  $\text{Mg}^{2+}$ ,  $\text{HCO}_3^-$ ,  $\text{Cl}^-$ ;  $\text{Cl}^-$  and  $\text{Ca}^{2+}$ ,  $\text{HCO}_3^-$ ;  $\text{HCO}_3^-$  and  $\text{Fe}^{2+}/\text{Fe}^{3+}$ , PAH,  $\text{K}^+$ ;  $\text{Mg}^{2+}$  and  $\text{Fe}^{2+}/\text{Fe}^{3+}$ , TPH, PAH, BTEX, and  $\text{Ca}^{2+}$ ;  $\text{Ca}^{2+}$  and  $\text{Zn}^{2+}$ ,  $\text{Pb}^{2+}$ ; hardness and TPH, EC; EC and TPH, BTEX; BTEX and  $\text{Fe}^{2+}/\text{Fe}^{3+}$ , TPH, PAH; PAH and  $\text{Fe}^{2+}/\text{Fe}^{3+}$ , TPH; TPH and  $\text{Zn}^{2+}$ ,  $\text{Fe}^{2+}/\text{Fe}^{3+}$ ;  $\text{Cu}^{2+}$  and  $\text{Zn}^{2+}$ . Strong correlations observed in the majority of the parameters imply that the groundwater contamination emanated from the same source and could be a result of anthropogenic activities in the study area. This further means that contaminants percolate into the groundwater.

### **Water quality index**

The whole sample's WQI showed that all samples (100%) are unsuitable for use in industry, irrigation, or drinking; prior to use, they must be properly treated (Table 4.21). See table 4.23 below for the WQI classification of the study area.

### **Groundwater pollution index (PIG)**

Akakuru *et al.* (2022) and Subba *et al.* (2012) stated “that an  $O_w$  larger than 0.1 indicates that the sample contributes 10% of the PIG's 1.0 value, this gives clear information on the parameter's influence on the groundwater body contamination”. According to the PIG result, the main causes of groundwater contamination were  $\text{Fe}^{2+}$  which had  $O_w$  value larger than 0.1 (Table 4.20). PIG values in the research region varied from 9.264 to 17.587. Drinking water pollution is divided into five categories: less than 1 denotes negligible contamination, between 1 and 1.5 denotes low pollution, 1.5–2.0 denotes moderate pollution, 2.0–2.5 denotes high pollution, and more than 2.5 denotes

extremely high pollution (Table 4.23). According to the study's findings, all of the samples have values over 2.5, which indicate extremely high pollution levels in the area.

### **Quality assessment for irrigation**

Table 4.24 displays the findings of the irrigation quality assessment that was computed.

#### **SAR**

The groundwater throughout the region is classified as wonderful (Z1) in Table 4.24 SAR arrangement. This suggests that the region's groundwater is excellent for the water system as a whole.

#### **Sodium percentage (%Na<sup>+</sup>)**

“Although the increase in %Na<sup>+</sup> is believed to be unqualified for the water system, it does demonstrate a cation exchange with the calcium and magnesium in the soil” (Richards, 1954; Akakuru *et al.*, 2022). This exchange reduces the waste and porosity of the dirt. “The soil is rather severe in dry conditions, and dampness on the dirt reduces air and water dissemination” (Akakuru & Akudinobi, 2018; Akakuru *et al.*, 2022). “Alkaline soils are created when inorganic carbon is present along with sodium chloride; these soils eventually become saline; thus, a crucial factor in assessing whether groundwater is suitable for irrigation is the amount of sodium present in agricultural goods” (Akakuru *et al.*, 2022). Table 4.25 % Na<sup>+</sup> values (percent) have a mean of 40.46 and a standard deviation of 1.48, and they range from 38.2 to 43.2. 40% of the total sample is within 20-40 (S2, S3, S4 & S5) while 60% of the sample is within 40-60(S1, S6, S7, S8, S9& S10) which indicates that the groundwater in the research region is 40% good and 60% permissible for irrigation, according to the groundwater quality requirements (Table 4.25). This confirms the SAR finding, which indicated that all of the groundwater examined is very appropriate for irrigation.

### **Magnesium hazard**

“Magnesium hazard is a crucial device in deciding the water reasonableness limit with regards to water system purposes; a MH proportion of more than 50 is unsatisfactory and considered unsafe/unsuitable for water system purposes while MH less than 50 is considered appropriate for water system” (Akakuru *et al.*, 2022). Table 4.22 shows that the MH esteems in the review region went from 43.97 to 50.53, with a mean of 47.78 and a standard deviation of 1.96. Besides, the outcomes show that 90% of the complete examples are below 50 while 10% is slightly above 50, suggesting that they are fit and truly appropriate for water system purposes.

### **Kelly's ratio**

“KR has been a veritable tool based on its efficacy in assessing the irrigation suitability of groundwater” (Eyankware *et al.*, 2020; Mokoena *et al.*, 2020; Akakuru *et al.*, 2022; Ajayi & Okeke, 2024). “A KR value greater than one indicates that Na in groundwater is high, whereas any value less than one is suitable for irrigation” (Akakuru *et al.*, 2022; Ajayi & Okeke, 2024). Table 4.22 shows that KR values range from 0.35 to 0.41, with a mean of 0.39 and a standard deviation of 0.02. This result also shows that 100% of the groundwater sample is suitable for irrigation (Table 4.27).

### **Soluble sodium percentage**

“SSP has been utilized by scholars in the assessment of the suitability of groundwater for irrigation purposes; it assesses the percentage of soluble sodium in groundwater” (Akakuru *et al.*, 2022). “SSP less than 50 is suitable for irrigation, while SSP above 50 is considered unsuitable” (Akakuru *et al.*, 2022). The result from Table 4.22 shows that SSP values range between 0.21 and 0.24, with a mean of 0.23 and a standard deviation of 0.007. Table 4.28 shows that the entire sample is safe and suitable for irrigation. SSP aligns with other irrigation assessment tools.

## **Wilcox**

This study also used Wilcox's (1955) plot to relate EC to %Na. The diagram shows that 40% of the entire study area sample falls into the excellent category and is very good to be used for irrigation, while 60% falls into the good to permissible category (Fig. 4.55). “This suggests that the groundwater throughout the study area is suitable and free of hazards for irrigation, further validating the other irrigation assessment tools used in this study” (Akakuru *et al.*, 2022)

## **Evaluation of the health risk of the groundwater samples**

The HQ results of the metals in adults and children are presented in Tables 4.29 and 4.30, respectively. The average HQ value of all the metallic elements ( $\text{Fe}^{2+}/\text{Fe}^{3+} > \text{Cu}^{2+} > \text{Pb}^{2+} > \text{Zn}^{2+}$ ) and ( $\text{Cr}^{3+} = \text{Cd}^{2+} = \text{Al}^{3+} = \text{Hg}^{2+}$ ) for children in the studied area is higher than one. The average HI (non-carcinogenic risk) value for adults is higher than 1. This also suggests that there would be health problems resulting from the consumption of the metallically contaminated groundwater samples by the children.

Also, the HI (non-carcinogenic risk) values for children range from 2.175 to 5.481 and the HI values of all the locations (S1–S10) are higher than 1, suggesting health problems resulting from the consumption of heavy metals from the groundwater samples due to the presence of the investigated metallic contaminants by the children. The result revealed that the average CR (carcinogenic risk) values for  $\text{Pb}^{2+}$  in adults in all locations are  $3.36\text{E}^{-06}$ , which far exceeds  $1 \times 10^{-6}$  ( $> 10^{-6}$ ) as opined by (Adeyemi and Ojekunle 2021) suggesting the possibility of carcinogenic risk due to prolonged intake of the contaminated groundwater system in all the study areas. The result also revealed that the average CR (carcinogenic risk) values of  $\text{Pb}^{2+}$  in children are  $7.96\text{E}^{-06}$ , exceed  $1 \times 10^{-6}$  ( $> 10^{-6}$ ), and were higher than those of adults (Table 4.30), indicating the possibility of carcinogenic risk due to the prolonged intake of groundwater in the study area. The cancer risk involved in the children of the study areas is three times higher than that of adults.

## 4.4 Physicochemical Characteristics of Soil

### pH

The pH range along the stations or stretch of Kolo-Creek soil in the wet season is 5.82 to 6.48 (Table 4.1b), with a control point value of 6.48 and a mean value of 5.94. These values do not meet the FME standard for safe water. The pH range along the stations or stretch of Kolo-Creek soil in the dry season is 5.70 to 6.77 (Table 4.1a). Figure 4.18 displays the variation in pH along the stations. The Kolo-Creek soil's pH measurements show that it is acidic. The results of the Anova test indicate that there is a statistically significant variation in the average pH levels among the stations ( $F = 14.11$ ,  $Pr < 0.05$ ). The seasonal mean pH values along the creek's length do not significantly differ from one another ( $F = 0.26$ ,  $pr > 0.05$ ). Figures 4.56a, 4.56b, 4.56c, and 4.56d show that the average mean pH value is marginally higher during the wet season than it is during the dry season.

### Electrical Conductivity

The electrical conductivity of Kolo Creek soil varies from 43.0 to 74.5  $\mu\text{S}/\text{cm}$  during the dry season, with mean values of 55.19  $\mu\text{S}/\text{cm}$  and a control point value of 52.17  $\mu\text{S}/\text{cm}$ . Similarly, during the wet season, the soil exhibits mean concentrations of electrical conductivity ranging from 34.00 to 59.33  $\mu\text{S}/\text{cm}$  with a control point value of 34  $\mu\text{S}/\text{cm}$  and a mean value of 50.07  $\mu\text{S}/\text{cm}$ . The results of the Anova test indicate that, on average, there is no significant difference between the stations' mean soil values ( $F = 1.24$ ,  $Pr > 0.05$ ). The seasonal mean values of steam soil do not significantly differ over the creek's length ( $F = 1.90$ ,  $pr > 0.05$ ). The average mean pH value is higher in the dry season than the wet season (Fig. 4.57a, 4.57b, 4.57c, and 4.57d).

### Chloride

During the dry season, the average chloride concentrations in Kolo Creek soil range from 13.10 to 21.0 mg/kg, with a control point value of 17.15  $\mu\text{S}/\text{cm}$  and mean values of 17.15  $\mu\text{S}/\text{cm}$ . During the wet season, the average chloride concentrations in Kolo

Creek soil range from 15.77 to 18.33 mg/kg, with a control point value of 18.33 and a mean value of 16.69 mg/kg. According to the Anova test, the mean chloride values at the stations are typically not significantly different from one another ( $F = 0.78$ ,  $Pr > 0.05$ ), and the mean seasonal values of chloride over the creek's length are not significantly different from one another ( $F = 0.36$ ,  $Pr > 0.05$ ) (Figs. 4.58a and 4.58b).

### **Total Petroleum Hydrocarbon (TPH)**

Kolo Creek soil contains mean TPH concentrations ranging from 43.27 to 160.67 mg/kg during the dry season, with a control point value of 43.27 mg/kg and mean values of 122.29 mg/kg. Conversely, during the wet season, mean TPH concentrations in Kolo Creek soil range from 12.0 to 195.00 mg/kg, with a control point value of 12 mg/kg and a mean value of 140.14 mg/kg. The results of the Anova test indicate that there is no statistically significant variation in the stations' mean TPH values ( $F = 4.3$ ,  $Pr > 0.05$ ). The mean seasonal levels of TPH along the creek's length do not significantly differ from one another ( $F = 0.83$ ,  $pr > 0.05$ ). The TPH value is generally higher during the wet season than during the dry season (Figs. 4.59a, 4.59b, 4.59c, and 4.59d).

### **Pyrolytic Aromatic Hydrocarbon**

Kolo Creek soil has mean PAH concentrations ranging from 0.001 to 57.77 mg/kg during the wet season, with no detection at the control point and mean values of 25.94 mg/kg; in the dry season, the mean PAH concentrations range from 0.01 to 43.96 mg/kg, with no detection at the control point and a mean value of 21.05 mg/kg. The results of the Anova test indicate that the mean seasonal PAH values along the creek's length do not differ significantly from one another ( $F = 0.26$ ,  $Pr > 0.05$ ), while the mean PAH values of the stations do differ significantly ( $F = 24.54$ ,  $Pr < 0.05$ ). The PAH value is generally higher during the wet season than during the dry season (Fig. 4.60a, 4.60b, 4.60c, and 4.60d).

## **Betex**

During the dry season, the Betex readings range from 0.0 to 21.33 mg/kg along the stations, with a mean value of 16.33 mg/kg and a control point value of 0.00 mg/kg. With a control point value of 3.3 mg/kg and a mean value of 13.72 mg/kg, the Betex values during the wet season range from 3.33 to 24.93 mg/kg along the stations, respectively. These values are significantly higher than the FME guidelines. According to the results of the Anova test, there is often no discernible difference in the mean Betex values at the stations ( $F = 3.35$ ,  $Pr > 0.05$ ) or in the mean seasonal values of Betex along the creek's length ( $F = 0.88$ ,  $Pr > 0.05$ ). The Betex value is generally higher during the dry season than during the wet season (Fig. 4.61a, 4.61b, 4.61c, and 4.61d).

## **Major Cations and Anions**

### **Calcium**

With a control point value of 8.67 mg/l and a mean value of 10.58 mg/kg, the calcium levels during the dry season range from 7.13 to 12.27 mg/kg along the stations, respectively. With a control point value of 8.60 mg/kg and a mean value of 11.08 mg/kg, the calcium levels in the wet season range from 8.60 to 12.0 mg/kg along the stations, respectively (Tables 4.1a and 4.1b). Based on the results of the Anova test, it can be concluded that there is no significant difference in the mean calcium values along the stations ( $F = 3.79$ ,  $Pr > 0.05$ ) or in the mean seasonal values of calcium along the creek ( $F = 0.73$ ,  $Pr > 0.05$ ). In general, the wet season has a higher calcium value than the dry season. The FME guideline values (Figs. 4.62a and 4.62b) are met by these values.

### **Magnesium**

Throughout the stations, the magnesium values during the dry season range from 7.63 to 11.07 mg/kg, with a mean value of 9.83 mg/kg and a control point value of 7.63 mg/kg. While the mean value of magnesium during the wet season is 10.14 mg/kg, the control point value is 7.97 mg/kg, and the values along the stations range from 7.97 to 11.13 mg/kg, respectively (Tables 4.1a and 4.1b). The results of the Anova test indicate

that there is no significant difference in the mean seasonal values of magnesium along the stretch of the creek ( $F = 0.53$ ,  $Pr > 0.05$ ), but there is a generally significant difference in the mean magnesium values along the stations ( $F = 26.53$ ,  $Pr < 0.05$ ). In general, the wet season has a higher magnesium value than the dry season. The FME guideline values (Figs. 4.63a and 4.63b) are met by these values.

### **Sodium**

Although the sodium values in the wet season (Tables 4.1a and 4.1b) vary from 38.13 to 48.67 mg/kg along the stations, respectively, with a control point value of 46.90 mg/kg and a mean value of 44.21 mg/kg, the dry season values range from 12.13 to 49.40 mg/kg along the stations, with a control point value of 23.63 mg/l and a mean value of 19.47 mg/kg. According to the results of the Anova test, there is a significant difference in the mean seasonal values of sodium along the stretch of the creek ( $F = 41.84$ ,  $Pr < 0.05$ ) but not in the mean values along the stations ( $F = 0.28$ ,  $Pr > 0.05$ ). In general, the wet season has a higher salt value than the dry season. The FME guideline values (Figs. 4.64a and 4.64b) are met by these values.

### **Potassium**

The potassium values in the wet season vary from 5.72 to 6.57 mg/kg along the stations, respectively (Tables 4.1a and 4.1b), with a control point value of 5.72 mg/kg and a mean value of 6.17 mg/kg. The ANOVA test indicates that there is generally no significant difference in the mean potassium values along the stations ( $F = 5.60$ ,  $Pr > 0.05$ ) and no significant difference in the mean seasonal values of potassium along the creek ( $F = 0.81$ ,  $Pr > 0.05$ ). In general, the wet season has a higher potassium value than the dry season. The FME guideline values (Figs. 4.65a and 4.65b) are met by these values. Major constituent cation concentrations are generally modest and in accordance with the FME Standard (2006). The main constituent cations' relative abundances follow the following order:  $Na^+ > Ca^{2+} > Mg^{2+} > K^+$ .

## **Bicarbonates**

In the wet season, bicarbonate values vary from 26.40 to 38.27 mg/kg along the stations, respectively (Tables 4.1a and 4.1b), with a control point value of 26.40 mg/kg and a mean value of 30.53 mg/kg. In the dry season, bicarbonate values vary from 19.10 to 38.73 mg/kg along the stations, respectively, with a control point value of 26.13 mg/kg and a mean value of 29.53 mg/kg. Generally speaking, there is no significant difference in the mean bicarbonate values along the stations ( $F = 1.90$ ,  $Pr > 0.05$ ) or in the mean seasonal values of bicarbonate along the creek's length ( $F = 0.21$ ,  $Pr > 0.05$ ), according to the results of the ANOVA test. In general, the wet season has a greater bicarbonate value than the dry season. The FME guideline values (Figs. 4.66a and 4.66b) are met by these values.

## **Sulphates**

With a control point value of 31.26 mg/kg and a mean value of 45.49 mg/kg, the sulfate values in the dry season range from 31.26 to 54.43 mg/kg along the stations, respectively. With a control point value of 52.63 mg/kg and a mean value of 67.17 mg/kg, the sulfate values in the wet season vary from 52.63 to 76.43 mg/kg along the stations, respectively (Tables 4.1a and 4.1b). According to the results of the Anova test, there isn't much of a difference in the average sulfate values along the stations ( $F = 0.41$ ,  $Pr > 0.05$ ) or in the average seasonal sulfate values along the creek ( $F = 48.83$ ,  $Pr < 0.05$ ). In general, the rainy season has a greater sulfate value than the dry season. The FME guideline values (Figs. 4.67a and 4.67b) are met by these values. These values meet the WHO's 2017 recommended values. Although there is no significant difference in the mean seasonal values of bicarbonate over the creek's length ( $F = 0.00$ ,  $Pr > 0.05$ ), the ANOVA test indicates that there is generally no significant difference in the mean bicarbonate values of the stations ( $F = 2.65$ ,  $Pr > 0.05$ ). Generally speaking, the bicarbonate values are the same in both seasons.

## **Nitrates**

Tables 4.1a and 4.1b show that the nitrate values in the wet season vary from 13.13 to 23.37 mg/kg along the stations, respectively. The nitrate values in the dry season vary from 16.77 to 18.17 mg/kg along the stations, respectively, with a control point value of 16.77 mg/kg and a mean value of 17.59 mg/kg. According to the results of the ANOVA test, there is often no discernible variation in the mean nitrate levels along the stations ( $F = 1.10$ ,  $Pr > 0.05$ ) or in the mean seasonal values of nitrate over the creek's length ( $F = 0.07$ ,  $Pr > 0.05$ ). In general, the dry season has a greater nitrate value than the wet season, the FME guideline values (Figs. 4.68a and 4.68b) are met by these values. The trend is reflected in the relative abundance of major anions  $SO_4^{2+} > HCO_3^- > NO_3^- > Cl^-$

## **Heavy Metals and Other Metals in Soils**

### **Iron (Fe<sup>+</sup>)**

A control point value of 28.60 mg/kg and a mean value of 178.86 mg/kg are found for the iron values along the stations in the dry season, which vary from 28.60 to 223.73 mg/kg along the stations in the wet season (Tables 4.1a and 4.1b), with a control point value of 26.93 mg/kg and a mean value of 195.57 mg/kg. According to the results of the ANOVA test, there is no significant difference in the mean seasonal values of iron along the creek's length ( $F = 0.35$ ,  $Pr > 0.05$ ) and a significant difference in the mean iron values along the stations ( $F = 7.74$ ,  $Pr < 0.05$ ). Generally speaking, the wet season has a larger iron value than the dry season. These values (Figs. 4.69a and 4.69b) are in accordance with the FME guideline values.

### **Copper (Cu<sup>2+</sup>)**

ANOVA test results indicate that there is generally a significant difference in the mean seasonal values of copper along the stretch of the creek ( $F = 0.007$ ,  $Pr > 0.05$ ) and no significant difference in the mean seasonal values of copper along the stations ( $F = 379.18$ ,  $Pr < 0.05$ ). The copper value is generally the same for both the wet season and

the dry season. The dry season values range from 0.00 to 0.82 mg/kg along the stations, respectively, with no detection at the control point and a mean value of 0.63 mg/kg. These values conform to the FME guideline values (Figs. 4.70a and 4.70b).

### **Zinc (Zn<sup>2+</sup>)**

The zinc values in the **dry season** vary from 2.37 to 3.57 mg/kg along the stations, respectively, with a control point value of 2.97 mg/kg and a mean value of 3.02 mg/kg, while the zinc values in the **wet season** vary from 0.40 to 3.19 mg/kg along the stations, respectively (Tables 4.1a and 4.1b), with a control point value of 0.43 mg/kg and a mean value of 2.24 mg/kg. According to the results of the Anova test, the mean zinc values along the stations ( $F = 0.75$ ,  $Pr > 0.05$ ) and the mean seasonal values of zinc along the creek's stretch ( $F = 9.31$ ,  $Pr > 0.05$ ) are not significantly different from one another. The zinc value is higher in the dry season than it is in the wet season. These values are in line with the FME guideline values (Figs. 4.71a and 4.71b).

### **Cadmium Cd<sup>2+</sup>**

There is no detection at the control point and a mean value of 0.27 mg/kg for the cadmium values in the dry season, which range from 0.00 to 0.34 mg/kg along the stations (Tables 4.1a and 4.1b). There is no detection at the control point and a mean value of 0.29 mg/kg for the cadmium values in the wet season.

The ANOVA test shows that there is generally a significant difference in the mean cadmium values along the stations ( $F = 54.41$ ,  $Pr < 0.05$ ) and no significant difference in the mean seasonal values of cadmium along the stretch of the creek ( $F = 0.21$ ,  $Pr > 0.05$ ). The cadmium value is generally higher during the **wet season** than during the **dry season**. These values conform to the FME guideline values (Figs. 4.72a and 4.72b).

### **Lead Pb<sup>2+</sup>**

With no detection at the control point and a mean value of 0.03 mg/kg, the lead values in the wet and dry seasons vary from 0.00 to 0.05 mg/kg along the stations, respectively;

the lead value is roughly the same for both the wet and dry seasons, and the Anova test indicates that there is a generally significant difference in the mean lead values along the stations ( $F = 14.78$ ,  $Pr < 0.05$ ) and no significant difference in the mean seasonal values of lead along the stretch of the creek ( $F = 0.23$ ,  $Pr > 0.05$ ). These values are in accordance with the FME guideline values (Figs. 4.73a and 4.73b).

### **Mercury Hg<sup>+</sup>**

While the mercury values in the wet season (Tables 4.1a and 4.1b) vary from 0.00 to 0.24 mg/kg along the stations, respectively, with no detection at the control point and a mean value of 0.18 mg/kg, the dry season values range from 0.11 to 0.27 mg/kg along the stations, with a control point value of 0.18 mg/kg and a mean value of 0.20 mg/kg. According to the results of the ANOVA test, there isn't a significant difference in the mean mercury values along the stations ( $F = 1.43$ ,  $Pr > 0.05$ ) or in the mean seasonal values of mercury along the stream ( $F = 0.94$ ,  $Pr > 0.05$ ) in general. Generally speaking, the dry season has a greater mercury value than the wet season. These values (Figs. 4.74a and 4.74b) are in accordance with the FME guideline values.

### **Aluminum Al<sup>+</sup>**

No aluminum is found in any season. Kolo Creek soils are at risk due to the concentrations of observed heavy metals (Hg<sup>+</sup>, Cd<sup>2+</sup>, Fe<sup>2+</sup>, and Pb<sup>2+</sup>) being higher than the FME ST standards, with the exception of Cu<sup>2+</sup> and Zn<sup>2+</sup>. Al<sup>3+</sup> concentrations, however, were not found. Kolo-Creek Soil's measured heavy metal relative abundances follow the following trend Fe<sup>+</sup> > Zn<sup>2+</sup> > Cu<sup>2+</sup> > Cd<sup>+</sup> > Hg<sup>+</sup> > Pb<sup>+</sup> > Al<sup>+</sup>.

### **Evaluation of Heavy Metal Pollution**

Table 4.33 shows that the CF values varied from 0.83 to 18.97. The order of the mean CF values across all sampled locations is as follows: Fe<sup>2+</sup>/Fe<sup>3+</sup> = (18.971), Pb<sup>2+</sup> = (0.92), Cu<sup>2+</sup> = (0.83), Zn<sup>2+</sup> = (0.93), Cd<sup>2+</sup> = (1.128), Hg<sup>2+</sup> = (1.049), Al<sup>3+</sup> = (1.002). A low contamination factor is indicated by values less than one (<1). According to Hakanson

(1980), CF values higher than 1.5 imply that the sources are more likely to be human, whereas values between 0.5 and 1.5 indicate that the metal is entirely produced from crustal elements or natural processes. Kolo Creek soil is tainted with aluminum, mercury, cadmium, and iron. Zinc, lead, and copper values are also trending in the direction of 1.

Table 4.33 displays the calculated values for the soil sample geo-accumulation index in the research area. The average Igeo readings showed the following declining trend:  $\text{Hg}^{2+}$  (6.94) >  $\text{Cd}^{2+}$  (0.95) >  $\text{Al}^{3+}$  (-1.94) >  $\text{Cu}^{2+}$  (-1.88) >  $\text{Zn}^{2+}$  (-1.53) >  $\text{Pb}^{2+}$  (-0.99) is less than  $\text{Fe}^{2+}/\text{Fe}^{3+}$  (7.05). The findings indicate that all of the heavy metal geo-accumulation index values ( $\text{Pb}^{2+}$ ,  $\text{Cu}^{2+}$ ,  $\text{Zn}^{2+}$ , and  $\text{Al}^{3+}$ ) in all of the soil samples that were taken were less than zero (0), indicating that the soils were contaminated by  $\text{Fe}^{2+}/\text{Fe}^{3+}$ , Cadmium, and  $\text{Hg}^{2+}$  with values higher than zero instead of heavy metals ( $\text{Pb}^{2+}$ ,  $\text{Cu}^{2+}$ ,  $\text{Zn}^{2+}$ , and  $\text{Al}^{3+}$ ).

### **Multivariate statistical analyses of geochemical data for soil**

Akakuru *et al.*, (2022) opined that “PCA is a crucial tool for discovering designs, examining the variation of collections of related factors, and also isolating the Eigen values and Eigen vectors (loadings) for head parts from the associated change; it describes the connection between the parameters to determine the likelihood of soil contamination in the review area”. Akakuru *et al.* (2022) mentioned that “any loading larger than 0.4 (+ or –) is regarded as a major contributor. According to Table 4.31, there were five noteworthy major components found. 61.11% of the loadings in PC1 (TPH, BTEX, pH,  $\text{NO}_3^-$ ,  $\text{Ca}^{2+}$ ,  $\text{Mg}^{2+}$ ,  $\text{K}^+$ ,  $\text{Fe}^{2+}/\text{Fe}^{3+}$ ,  $\text{Pb}^{2+}$ ,  $\text{Cu}^{2+}$ ,  $\text{Zn}^{2+}$ , and  $\text{Hg}^{2+}$ ) were all positive. This is a characteristic of the elements that are causing the soil pollution in the review region to spread; anthropogenic activities resulting from industrial operations in the study area may be the cause of this. In PC2, loadings were found for 22.22% of the variables; loadings for  $\text{Na}^+$  and  $\text{SO}_4^{2-}$  were positive (11.11%), while loadings for  $\text{Zn}^{2+}$  and  $\text{Hg}^{2+}$  were negative (11.11%). This implies that geological processes are their source. PC3:  $\text{Mg}^{2+}$ ,  $\text{HCO}_3^-$ , and  $\text{NO}_3^-$  all exhibited positive loadings, making up 11.11%

of the variables with loadings. PAH, EC, and  $\text{Cl}^-$  all showed positive loadings; loadings were present in 16.67% of the variables in PC4. PC5: Of the variables, 5.56% displayed negative loading for magnesium and 5.56% displayed positive loading for EC. 11.11% of the variables had loading. A rotated space component plot is shown in Figure 4.77.

### **Correlation matrix analysis**

When evaluating soil, “correlation matrix analysis is a dependable method for determining the origin and relationship of geochemical data” (Akakuru *et al.*, 2021a, 2021b). “A strong correlation between the two limits is indicated by correlation coefficients greater than 0.7; a weak correlation is suggested by correlation coefficients falling between 0.5 and 0.7” (Akakuru *et al.*, 2021b; Gaagai *et al.*, 2023).

TPH and PAH are correlated, as shown in Table 4.35: BTEX,  $\text{Ca}^{2+}$ ,  $\text{Mg}^{2+}$ ,  $\text{K}^+$ ,  $\text{SO}_4^{2-}$ ,  $\text{Fe}^{2+}/\text{Fe}^{3+}$ ,  $\text{Pb}^{2+}$ ,  $\text{Cu}^{2+}$ ,  $\text{Hg}^{2+}$ ; PAH and  $\text{SO}_4^{2-}$ ; BTEX and pH,  $\text{Mg}^{2+}$ ,  $\text{HCO}_3^-$ ,  $\text{Fe}^{2+}/\text{Fe}^{3+}$ ,  $\text{Pb}^{2+}$ ,  $\text{Cu}^{2+}$ ,  $\text{Hg}^{2+}$ ; pH and  $\text{Mg}^{2+}$ ,  $\text{Fe}^{2+}/\text{Fe}^{3+}$ ,  $\text{Pb}^{2+}$ ,  $\text{Cu}^{2+}$ ,  $\text{Hg}^{2+}$ ; EC and  $\text{Zn}^{2+}$ ;  $\text{Na}^+$  and  $\text{SO}_4^{2-}$ ,  $\text{Zn}^{2+}$ ;  $\text{Ca}^{2+}$  and  $\text{Fe}^{2+}/\text{Fe}^{3+}$ ,  $\text{Pb}^{2+}$ ,  $\text{Cu}^{2+}$ ;  $\text{Mg}^{2+}$  and  $\text{Fe}^{2+}/\text{Fe}^{3+}$ ,  $\text{Pb}^{2+}$ ,  $\text{Cu}^{2+}$ ,  $\text{Hg}^{2+}$ ;  $\text{K}^+$  and  $\text{Fe}^{2+}/\text{Fe}^{3+}$ ,  $\text{Pb}^{2+}$ ,  $\text{Cu}^{2+}$ ;  $\text{NO}_3^-$  and  $\text{Fe}^{2+}/\text{Fe}^{3+}$ ;  $\text{Fe}^{2+}/\text{Fe}^{3+}$  and  $\text{Pb}^{2+}$ ,  $\text{Cu}^{2+}$ ;  $\text{Pb}^{2+}$  and  $\text{Cu}^{2+}$ ,  $\text{Hg}^{2+}$ ;  $\text{Cu}^{2+}$  and  $\text{Zn}^{2+}$ ,  $\text{Hg}^{2+}$ ;  $\text{Zn}^{2+}$  and  $\text{Hg}^{2+}$ . Robust associations detected across most of the criteria suggest that comparable human activities within the research region are the cause of the soil contamination

### **Cluster analysis**

A dendrogram representing the soil sample findings from hierarchical cluster analysis (HCA) is displayed in Fig. 4.77. The goal of the HCA was to categorize the metal contaminants into groups that would indicate how similar or dissimilar the sources of the pollutants' prevalence in the soil and groundwater samples were. The research was conducted using Ward's technique, which uses distance as a measure of how closely related the metallic contaminants are to one another. There are four groups in Fig. 4.77 with only three clusters, according to the dendrogram. First group:  $\text{NO}_3^-$  and EC; second group:  $\text{NO}_3^-$  and  $\text{SO}_4^{2-}$ ; third group: EC and  $\text{SO}_4^{2-}$ ; fourth group: TPH and  $\text{Fe}^{2+}/\text{Fe}^{3+}$ ;

Pb<sup>2+</sup>, Cr<sup>3+</sup>, Hg<sup>2+</sup>, Cu<sup>2+</sup>, Zn<sup>2+</sup>, pH, K<sup>+</sup>, Ca<sup>2+</sup>, Mg<sup>2+</sup>, Cl<sup>-</sup>, NO<sub>3</sub><sup>-</sup>, BTEX, Na<sup>+</sup>, HCO<sub>3</sub><sup>-</sup>, and PAH formed a cohesive cluster. “This implies that comparable anthropogenic activities, perhaps as a result of nearby industrial operations and related activities have an impact on the presence of these metals in the soil” (Ajayi & Okeke, 2024).

### **Evaluation of the health risk of the soil samples**

This was ascertained by applying Eqs (17) through (20) to the measured concentrations of metallic pollutants. Tables 4.37, 4.38, 4.39, and 4.40 give the HQ of the metals for dermal and ingestion by adults and children, respectively. For every metallic element under investigation, the HQ values were all less than one (Cu<sup>2+</sup> > Zn<sup>2+</sup> > Pb<sup>2+</sup> > Fe<sup>2+</sup>/Fe<sup>3+</sup> > Cd<sup>2+</sup> > Hg<sup>2+</sup> > Cr<sup>3+</sup>). The samples' HQ values were less than 1. However, sample location 5 (children) is trending in the direction of 1, and pertinent agencies should take appropriate measures to prevent the occurrence of cancer in this research area. Children's HI readings fall between 0.155002 and 0.719632, whereas adult HI values fall between 0.051585-0.169783. Hence, in every sample, the HI for both adults and children was less than 1. “The likelihood that an individual may get cancer during their lifetime due to specific exposure to pollutants, such as drinking tainted water, is known as the carcinogenic risk (CR)” (Akakuru *et al.*, 2022). CR was computed using Equations (17–20). The CR result is presented in tables 4.37 and 4.40, respectively. The findings showed that the CR values for Cd<sup>2+</sup>, Cr<sup>3+</sup>, and Pb<sup>2+</sup> in all the samples exceeded 10<sup>-6</sup> (> 10<sup>-6</sup>) for both adults and children, suggesting a potential carcinogenic risk from soil intake and skin exposure for both groups in the study area.

#### **4.4.1 Geotechnical Characteristics of soil Samples**

##### **Composition of Soil Moisture**

Table 4.4 shows that throughout the rainfall season, the soil's humidity varies from 21% to 33%, with an average humidity level of 22.8% as the reference point. The value for the dry season ranges from 12% to 30%, with a control point moisture content value of 14.4%. During the period of drought, the humidity content readings are significantly

lower than during the period of rainfall. The variations also suggest a higher water retention potential of contaminated soils compared to normal clean soils, which enhances the contaminant persistence of the soil.

#### **4.4.2. Porosity and Permeability**

The range of soil porosity values is 1.27% to 1.9%, with a control point value of 1.8%. Similarly, the range of permeability values is  $1.2 \times 10^{-4}$  (m/sec) to  $2.5 \times 10^{-4}$  (m/sec), with a control point value of  $2.2 \times 10^{-4}$  (m/sec). “Porosities and permeability values at impacted sites are generally lower than at control sites, the impacted sections of the site have suffered some distortions; these reductions are attributed to the effects of the hydrocarbon contamination” (Nwankwoala & Mzaga, 2017). Compared to the affected locations, the baseline site had greater values for porosity and permeability. “These changes in soil characteristics have the capacity to determine the behavior of contaminants in the soil hence the downward mobilization of contaminants” (Nwankwoala & Mzaga, 2017). “This considers the fact that the transport of contaminants in groundwater is dependent on the solubility of the substance in water and the advective flow, retardation, and mechanical dispersion of the solute, which are dependent on the geophysical properties of the soil in a specific location” (Nwankwoala & Mzaga, 2017). The high levels of infiltrating and percolating water in the area increase the risk of groundwater contamination.

#### **4.4.3 Distribution of Soil Particle Sizes/Consistency Limits**

The soils have uneven dimensions of grains, ranging from extremely fine sand with a 0.10 mm mesh size to fine gravel with a 0.6 mm mesh size (fig: 4.79). The Unified Soil Classification System (ASTM, 2017) shows that 100% of the tested soils varies amongst the sites, ranging from fine silty sands to fine gravel sands (figure 4.78 & table 4.4). This type of soil will not be able to block the circulation of contaminated water through it, nor will it be able to stop the penetration of liquid petrochemical products.

At the affected sites, the boundaries established by Atterberg are higher. The baseline site value is 25%, while the affected soils have maximum liquid percentages ranging from 22% to 38%. The plastic limit is 15%–29% for impacted soils and 17% for control soils. The affected samples' plasticity rating figures, which vary from 5% to 11%, show alterations brought on by the presence of pollutants. Ersoy *et al.*, 2013 opined “that consistency is an important property and is a useful measure for the processing of very fine clayey soils”. “In addition to significantly increasing the safety factor against overturning and sliding, the presence of cohesiveness in the soil lowers the consequence of active soil pressure. Cohesion also reflects the soil's consistency and workability” (Ersoy *et al.*,2013). These soil characteristics, however, are crucial for many engineering projects. For example, they are needed to build an earth fill dam's clay core, cover a polluted material deposit with a low-permeability layer, design slab bridges, retaining walls, and foundations, and assess the stability of the soil. Prakash (1979) mentioned that “atterberg soil plasticity classification chart (table: 4.7), the plasticity index of the impacted sites falls within the range of 5%-9% and are categorized as low plastic and partly cohesive silt soil, while the control point (11%) fall within medium plastic and cohesive silt clay soil”. Hence, the soils at the impacted sites can be reused for engineering construction due to their low plastic nature as a result of hydrocarbon pollution. It can then be inferred that the hydrocarbon products within Kolo-Creek have soil improvement characteristics.

## CHAPTER FIVE

### 5.0 CONCLUSION AND RECOMMENDATIONS

#### 5.1 Conclusion

From this research, the following conclusions can be drawn:

##### 1. Water and Soil Contamination:

- Most measured values for surface water, groundwater, and soil fall within WHO drinking water standards, except for pH (acidic),  $\text{Fe}^{2+}/\text{Fe}^{3+}$ ,  $\text{Hg}^{2+}$ , PAH, and BTEX, which significantly exceed recommended limits
- The low pH and elevated levels of TPH, PAH, and BTEX are primarily due to anthropogenic activities, including petroleum exploration, illegal bunkering, and refining.

##### 2. Contamination Factor Analysis:

- Surface Water:  $\text{Fe}^{2+}$  contamination factor is 9.1 (high contamination).
- Groundwater: Contaminated by  $\text{Ca}^{2+}$  (2.88 - moderate contamination) and  $\text{Fe}^{2+}$  (125.82 - very high contamination).
- Soil: Heavy metal contamination observed for  $\text{Fe}^{2+}/\text{Fe}^{3+}$  (18.97),  $\text{Al}^{3+}$  (1.02),  $\text{Hg}^{2+}$  (1.05), and  $\text{Cd}^{2+}$  (1.28).  $\text{Pb}^{2+}$ ,  $\text{Cu}^{2+}$ , and  $\text{Zn}^{2+}$  values are slightly below 1, indicating minor contamination.

The geo-accumulation index classifies soil samples as heavily polluted by  $\text{Fe}^{2+}$  and  $\text{Hg}^{2+}$  and moderately polluted by  $\text{Cd}^{2+}$ .

##### 3. Pollution Index (PI) and Water Quality Index (WQI):

- Surface water PI values approach 1, indicating slight pollution.
- Groundwater PI values exceed 2.5, indicating severe contamination.
- WQI analysis confirms that 100% of surface and groundwater samples are unsuitable for drinking, irrigation, or industrial use without proper treatment.

##### 4. Principal Component Analysis (PCA) and Multivariate Analysis:

- Surface Water: Five (5) principal components identified. PC1 accounts for 63.64% of variance, with all parameters positively loaded.

- Groundwater: Six (6) principal components identified.
- Soil Samples: Five (5) principal components identified.
- Strong correlations between most parameters indicate that groundwater, surface water, and soils share a common contamination source.

#### 5. Irrigation Suitability Analysis:

- Surface Water: 100% of samples are suitable based on SAR, SSP, and MH, but 100% are unsuitable based on Na and KR.
- Groundwater:
  - SAR, KR, and SSP: 100% of samples are suitable.
  - Na suitability: 40% good, 60% permissible, 10% unsafe.
  - Wilcox Plot: 60% of samples fall within the good-to-permissible category, 40% in the excellent category.

#### 6. Carcinogenic Risk (CR) Analysis:

- CR values for both adults and children exceed  $10^{-6}$  ( $>10^{-6}$ ), indicating potential carcinogenic risk from using surface and groundwater.
- Children face a threefold higher cancer risk than adults.
- Soil CR values also exceed  $10^{-6}$ , suggesting potential health risks.

#### 7. Geotechnical Properties:

- Permeability and porosity values show a slight reduction in contaminated sites compared to control sites.
- Atterberg limit values are higher in contaminated sites, resulting in lower plasticity indices.
- Affected soils exhibit a plasticity index of 5-9% (low plasticity, partially cohesive silt), while control soils have 11% (medium plasticity, cohesive silt-clay).
- Hydrocarbon contamination appears to modify soil properties, but affected soils may still be suitable for certain engineering applications.

## 5.2 Recommendations

### Pollution Control and Environmental Monitoring:

- The state government should integrate pollution control measures into its developmental action plan to reduce contamination of water and soil resources.
- Strict regulations should be enforced to prohibit solid waste dumping, untreated wastewater discharge, and illegal hydrocarbon waste disposal into Kolo Creek and its surroundings.
- Regular monitoring of water and soil quality is essential to track pollution levels and implement timely remediation.
- Before using creek water for residential purposes, proper treatment methods must be applied to ensure safety.

### 2. Water Resource Management and Public Health:

- Kolo Creek oil facility operators and the government must conduct routine water and soil quality assessments to safeguard environmental and public health.
- The government should ensure the lawful and beneficial use of the creek, particularly for irrigation, based on Sodium Absorption Ratio (SAR) values.
- Recommended safety measures for water usage:
  - Boiling and chlorination before drinking.
  - pH correction using sodium bicarbonate to neutralize acidity.
- Proper waste management infrastructure, including sanitary landfills and designated disposal sites, should be established outside the Kolo Creek watershed to prevent further contamination.

### 3. Geotechnical Considerations for Engineering Projects:

- The geotechnical properties of the soil in Kolo Creek are crucial for various engineering applications, including:

- Clay core construction in earth-fill dams
- Low-permeability barriers over contaminated sites
- Slab bridge and retaining wall designs
- Foundation stability and slope assessments
- Before any construction projects in the Kolo Creek area, comprehensive laboratory tests should be conducted on soil samples to ensure structural stability and prevent future engineering failures.

#### 4. Pollution Control and Environmental Monitoring:

- The state government should integrate pollution control measures into its developmental action plan to reduce contamination of water and soil resources.
- Strict regulations should be enforced to prohibit solid waste dumping, untreated wastewater discharge, and illegal hydrocarbon waste disposal into Kolo Creek and its surroundings.
- Regular monitoring of water and soil quality is essential to track pollution levels and implement timely remediation.
- Before using creek water for residential purposes, proper treatment methods must be applied to ensure safety.

#### 5. Water Resource Management and Public Health:

- Kolo Creek oil facility operators and the government must conduct routine water and soil quality assessments to safeguard environmental and public health.
- The government should ensure the lawful and beneficial use of the creek, particularly for irrigation, based on Sodium Absorption Ratio (SAR) values.
- Recommended safety measures for water usage:
  - Boiling and chlorination before drinking.
  - pH correction using sodium bicarbonate to neutralize acidity.

- Proper waste management infrastructure, including sanitary landfills and designated disposal sites, should be established outside the Kolo Creek watershed to prevent further contamination.

#### 6. Geotechnical Considerations for Engineering Projects:

- The geotechnical properties of the soil in Kolo Creek are crucial for various engineering applications, including:
  - Clay core construction in earth-fill dams
  - Low-permeability barriers over contaminated sites
  - Slab bridge and retaining wall designs
  - Foundation stability and slope assessments
- Before any construction projects in the Kolo Creek area, comprehensive laboratory tests should be conducted on soil samples to ensure structural stability and prevent future engineering failures.

#### 7. Pollution Control and Environmental Monitoring:

- The state government should integrate pollution control measures into its developmental action plan to reduce contamination of water and soil resources.
- Strict regulations should be enforced to prohibit solid waste dumping, untreated wastewater discharge, and illegal hydrocarbon waste disposal into Kolo Creek and its surroundings.
- Regular monitoring of water and soil quality is essential to track pollution levels and implement timely remediation.
- Before using creek water for residential purposes, proper treatment methods must be applied to ensure safety.

#### 8. Water Resource Management and Public Health:

- Kolo Creek oil facility operators and the government must conduct routine water and soil quality assessments to safeguard environmental and public health.

- The government should ensure the lawful and beneficial use of the creek, particularly for irrigation, based on Sodium Absorption Ratio (SAR) values.
- Recommended safety measures for water usage:
  - Boiling and chlorination before drinking.
  - pH correction using sodium bicarbonate to neutralize acidity.
- Proper waste management infrastructure, including sanitary landfills and designated disposal sites, should be established outside the Kolo Creek watershed to prevent further contamination.

#### 9. Geotechnical Considerations for Engineering Projects:

- The geotechnical properties of the soil in Kolo Creek are crucial for various engineering applications, including:
  - Clay core construction in earth-fill dams
  - Low-permeability barriers over contaminated sites
  - Slab bridge and retaining wall designs
  - Foundation stability and slope assessments
- Before any construction projects in the Kolo Creek area, comprehensive laboratory tests should be conducted on soil samples to ensure structural stability and prevent future engineering failures.

### **5.3 Contribution to Knowledge**

This study provides significant insights into the environmental impact of hydrocarbon pollution on soil and water resources in Kolo Creek. The key contributions to knowledge include:

#### 1. Carcinogenic Risk Assessment:

- The Carcinogenic Risk (CR) values for adults exceed  $1 \times 10^{-6}$  ( $> 10^{-6}$ ), indicating a potential cancer risk due to heavy metal contamination in soil, surface water, and groundwater.

- Children face an even higher risk, with CR values three times greater than those of adults, significantly surpassing the  $1 \times 10^{-6}$  ( $> 10^{-6}$ ) threshold.

## 2. Geotechnical Properties and Engineering Applications:

- The study reveals that contaminated soils in Kolo Creek exhibit soil improvement characteristics, making them suitable for reuse in engineering construction.
- The reduction in plasticity index (5%–9%) classifies the soil as low plastic and partially cohesive silt soil, which can be beneficial for construction projects.

## 3. Water Resource Utilization:

- Despite pollution concerns, water resources in Kolo Creek remain suitable for agricultural use, particularly irrigation. However, strict treatment measures are required before any domestic or industrial use.

## 4. Heavy Metal Contamination and Hydrocarbon Influence:

- Hydrocarbon activities, including oil exploration and illegal refining, have significantly contributed to heavy metal contamination, particularly iron ( $\text{Fe}^{2+}$ ).
- The increasing  $\text{Fe}^{2+}$  concentration is attributed to:
  - Longer rainfall duration and deeper percolation, leading to the leaching of  $\text{Fe}^{2+}$  into water bodies.
  - Dissolution of  $\text{Fe}^{2+}$  from metallic scraps, hydrocarbon waste, and lateritic soil particles, further exacerbating pollution levels.

## REFERENCES

- Adebayo, A. R., & Tawabini, B. (2012). Hydrocarbon exploration and production-a balance between benefits to the society and impact on the environment. *J. Pet Environ. Biotechnol*, 3, 1-9.
- Adeyemi, A. A., & Ojekunle, Z. O. (2021). Concentrations and health risk assessment of industrial heavy metals pollution in groundwater in Ogun state, Nigeria. *Scientific African*, 11, e00666.
- Ahiarakwem, C. A. (2013). The impacts of Njoku sawmill landfill on the water quality of the Otamiri River, Owerri metropolis, Niger Delta Basin, Southeastern Nigeria. *International Journal of Engineering Inventions*, 2(2), 26–34.
- Ajayi, O., & Okeke, O. C. (2024). Assessment of Quality of Surface Water Resources of Kolo Creek and Environs, Niger Delta, Nigeria, using Water Quality index and Multivariate Statistical Analysis. *Scholarly Journal of Science and Technology Research and Development*, 3(1), 101-138.
- Akakuru, O. C., & Akudinobi, B. E. B. (2018). Determination of water quality index and irrigation suitability of groundwater sources in parts of coastal aquifers of Eastern Niger Delta, Nigeria. *International Journal of Applied and Natural Sciences (IJANS)*, 7(1), 1–6.
- Akakuru, O. C., Akudinobi, B. E., Nwankwoala, H. O., Akakuru, O. U., & Onyekuru, S. O. (2021). Compendious evaluation of groundwater in parts of Asaba, Nigeria for agricultural sustainability. *Geosciences Journal*, 25(6), 915–927.
- Akakuru, O. C., Akudinobi, B., Opara, A. I., Onyekuru, S. O., & Akakuru, O. U. (2021). Hydrogeochemical facies and pollution status of groundwater resources of Owerri and environs, Southeastern Nigeria. *Environmental Monitoring and Assessment*, 193, 1–26.

- Akakuru, O. C., Eze, C. U., Okeke, O. C., Opara, A. I., Usman, A. O., Iheme, O., Ibeneme, S. I., & Iwuoha, P. O. (2022). Hydrogeochemical evolution, water quality indices, irrigation suitability and pollution index of groundwater (PIG) around Eastern Niger Delta, Nigeria. *International Journal of Energy and Water Resources*, 1–23
- Akinwumi, I. I., Diwa, D., & Obianigwe, N. (2014). Effects of crude oil contamination on the index properties, strength and permeability of lateritic clay. *International Journal of Applied Sciences and Engineering Research*, 3(4), 816-824.
- American Society for Testing and Materials. (2017). ASTM D4318-17: Standard Test Methods for Liquid Limit, Plastic Limit, and Plasticity Index of Soils. ASTM international.
- ASTM D 4318-17. Standard test Methods for liquid limit, plastic limit, and plasticity index of soils. West Conshohocken: ASTM International; 2017
- Ayotunde, O., & Bariweni, P. A. (2018). Impact of Urban runoff on the Heavy metals concentrations of the Epic Creek, Niger Delta. *Wilberforce Journal of Social Sciences (WJSS)* Vol, 3, 12–19.
- BS 1377, B. S. (1990). Methods of test for soils for civil engineering purposes. British Standards Institution. London. UK.
- Canora, F., & Sdao, F. (2022). Groundwater Vulnerability to Pollution Assessment. *Water*, 14(14), 2205.
- Carol, D. (1962). Rain water as a chemical agent of geological process. A review. *US Geological Survey Water Supply Papers*, 15, 336–338.
- Chinemelu, & Okeke, O. C. (2019). Evaluation of Heavy Metal Pollution in Soils of Warri and Environs, Southwestern Nigeria, Using Contamination Indexes.

- Doust, H., Omatsola, E., Edwards, J. D., & Santogrossi, P. A. (1990). Divergent/passive margin basins. *AAPG Memoir*, 48, 239–248.
- Dupuis, A., & Ucan-Marin, F. (2015). A literature review on the aquatic toxicology of petroleum oil: An overview of oil properties and effects to aquatic biota. Canadian Science Advisory Secretariat Vancouver, BC, USA.
- Durov, S. A. (1948). Natural waters and graphic representation of their composition. *Dokl Akad Nauk SSSR*, 59(3), 87–90.
- Ebueke, A. W., & Bariweni, P. A. (2019). Water Quality Index of Kolo Creek, Bayelsa State, Nigeria. *Journal of Applied Sciences and Environmental Management*, 23(11), 1923-1927.
- Edori, O. S., & Odoemelam, S. (2022). Concentration, source apportionment and ring size analysis of Polycyclic Aromatic Hydrocarbons (PAHs) in water from Kolo Creek, Niger Delta, Nigeria. *International Journal of Chemical Research*, 4, 36-41.
- Egaspin, D. P. R. (2002). Environmental Guidelines and Standards for the Petroleum Industry in Nigeria (EGASPIN). Department of Petroleum Resources, Lagos, Nigeria.
- Eli, H. D. (2012). Analysis of flooding on farmlands along the Kolo Creek of Bayelsa State, Nigeria. Unpublished Ph. D. Thesis, University of Calabar, Nigeria.
- Enaregha EB, Omotete TR, Izah SC, Odubo TC (2022). Comparison of total viable bacteria counts and in situ characteristics in drinking water sources in Sagbama town, Bayelsa state, Nigeria. *International Journal of Pathogen Research*, 11(3-4), 79-87.
- Ersoy, H., Karsli, M. B., Cellek, S., Kul, B., Baykan, I., & Parsons, R. L. (2013). Estimation of the soil strength parameters in Tertiary volcanic regolith (NE Turkey) using analytical hierarchy process. *Journal of Earth System Science*, 122,

1545–1555.

- Etu-Efeotor, J. O., & Akpokodje, E. G. (1990). Aquifer systems of the Niger Delta. *Journal of Mining and Geology*, 26(2), 279-284.
- Eyankware, M. O., Obasi, P. N., Omo-Irabor, O. O., & Akakuru, O. C. (2020). Hydrochemical characterization of abandoned quarry and mine water for domestic and irrigation uses in Abakaliki, southeast Nigeria. *Modeling Earth Systems and Environment*, 6, 2465–2485.
- Ezekwe, C. I., & Utong, I. C. (2017). Hydrocarbon Pollution and Potential Ecological Risk of Heavy Metals in the Sediments of the Oturuba Creek, Niger Delta, Nigeria. *Journal of Environmental Geography*, 10(1–2), 1–10.
- Cherry, J. A., & Freeze, R. A. (1979). *Groundwater* (p. 370). Englewood Cliffs, NJ: Prentice-Hall.
- Gaagai, A., Aouissi, H. A., Bencedira, S., Hinge, G., Athamena, A., Heddami, S., ... & Ibrahim, H. (2023). Application of water quality indices, machine learning approaches, and GIS to identify groundwater quality for irrigation purposes: A case study of Sahara Aquifer, Doucen Plain, Algeria. *Water*, 15(2), 289.
- George, D. S., Hart, A. I., & Osuji, L. C. (2021). Concentration of heavy metals and petroleum hydrocarbons in previously remediated sites in Niger Delta, Nigeria. *Scientia Africana*, 20(3), 53-72.
- Gobo, A. E., Amangabara, G. T., & Etiga, G. E. (2013). Estimating macrophyte load for water hyacinth in the Kolo Creek, Niger Delta. *International Journal of Ecosystem*, 3(1), 7–11.
- Gopinath, S., Srinivasamoorthy, K., Saravanan, K., Prakash, R., & Karunanidhi, D. (2019). Characterizing groundwater quality and seawater intrusion in coastal aquifers of Nagapattinam and Karaikal, South India using hydrogeochemistry and

modeling techniques. *Human and Ecological Risk Assessment: An International Journal*, 25(1–2), 314–334.

Hakanson, L. (1980). An ecological risk index for aquatic pollution control. A sedimentological approach. *Water Research*, 14(8), 975–1001.

Horton, R. K. (1965). An index number system for rating water quality. p 300–305. *Water Quality Criteria-Stream vs. Effluent Standards. J Wat Pollut Contr Fed*, 37(3), 292–315.

Hospers, J. (1965). Gravity field and structure of the Niger delta, Nigeria, West Africa. *Geological Society of America Bulletin*, 76(4), 407–422.

Hussein, E. E. (2021). A GIS-Based Groundwater Contamination Assessment Using Modified DRASTIC Geospatial Technique. *Water*, 13(20), 2868.

Inengite, A. K., Oforka, N. C., & Osuji, L. C. (2010). Survey of heavy metals in sediments of Kolo creek in the Niger Delta, Nigeria. *African Journal of Environmental Science and Technology*, 4(9), 558–566.

Izonfuo, L. W. A., & Bariweni, A. P. (2001). The effect of urban runoff water and human activities on some physico-chemical parameters of the Epie Creek in the Niger Delta. *Journal of Applied Sciences and Environmental Management*, 5(1).

Kaçmaz, Hülya, and M. Eran Nakoman. "Shallow Groundwater and Cultivated Soil Suitability Assessments with Respect to Heavy Metal Content in the Köprübaşı U Mineralization Area (Manisa, Turkey)." *Bulletin of environmental contamination and toxicology* 85 (2010): 37-41.

Kazakis, N., et al. (2021). Groundwater Quality and Groundwater Vulnerability Assessment. *Environments*, 8(10), 100.

Kelley, W. P. (1963). Use of saline irrigation water. *Soil Science*, 95(6), 385–391.

- Knödel, K., Lange, G., Voigt, H. J., Beims, U., Jenn, F., Knödel, K., ... & Voigt, H. J. (2007). Methods for Characterizing the Hydrologic and Hydraulic Conditions. *Environmental Geology: Handbook of Field Methods and Case Studies*, 567-748.
- Koepfinger, J. L., Sherr, S. I., & Cook, W. H. (1976). 268-1976-IEEE/ASTM Standard Metric Practice. IEEE Std 268-1976 (Supersedes ASTM E380-1974 IEEE Std 268-1973 IEEE Std 322-1971), 1-48.
- Mokoena, P., Kanyerere, T., & van Bever Donker, J. (2020). Hydrogeochemical characteristics and evaluation of groundwater quality for domestic and irrigation purposes: A case study of the Heuningnes Catchment, Western Cape Province, South Africa. *SN Applied Sciences*, 2(9), 1548.
- Muller, G. (1969). Index of geoaccumulation in sediments of the Rhine River. *Geojournal*, 2, 108–118.
- Niwas, S., & Singhal, D. C. (1985). Aquifer transmissivity of porous media from resistivity data. *Journal of Hydrology*, 82(1–2), 143–153.
- Nwankwo, I. L., Ekeocha, N. E., & Ikoro, D. O. (2015). Evaluation of Deviation of Some Soil Contamination Indicators Due to Oil Spillage in Akinima, Rivers State.
- Nwankwoala, H. O., & Mzaga, T. M. (2017). Geo-environmental assessment of hydrocarbon contaminated sites in parts of central swamp depobelt, Eastern Niger Delta. *MOJ Eco Environ Sci*, 2(3), 23.
- Nwankwoala, H. O., & Omofuophu, E. (2020). Investigation of hydrocarbon contaminant levels and groundwater quality assessment in parts of Bonny Island, Rivers State of Nigeria. *Central Asian Journal of Environmental Science and Technology Innovation*, 1(1), 61–70.
- Obeta, I. N., & Eze-Uzomaka, O. J. (2013). Geotechnical properties of waste engine

oil contaminated laterites. *Nigerian Journal of Technology*, 32(2), 203-210.

Ogamba, E. N., Ebere, N., & Izah, S. C. (2017). Heavy metal concentration in water, sediment and tissues of *Eichhornia crassipes* from Kolo Creek, Niger Delta.

*Greener J. Environ. Manage. Public Safety*, 6(1), 1–5.

Okafor, V. N., Omokpariola, D. O., Igbokwe, E. C., Theodore, C. M., & Chukwu, N. G. (2022). Determination and human health risk assessment of polycyclic aromatic hydrocarbons (PAHs) in surface and ground waters from Ifite Ogwari, Anambra State, Nigeria. *International Journal of Environmental Analytical Chemistry*, 1–23.

Okonofua, E. S., Babatola, J. O., & Ojuri, O. O. (2019). Geo-environmental Assessment of Total Petroleum Hydrocarbon Content in Ologbo Field, Niger Delta, Nigeria. *FULa a Journal of Science and Technology*, Federal University, La A, 5(1), 16–22.

Okoroh, D. O., & Ibuot, J. C. (2022). Hydrogeochemical assessment of groundwater quality: A case study of Federal College of Education (Technical), Omoku, Rivers State. *Water Practice & Technology*, 17(7), 1458-1469.

Olobaniyi, S. B., & Owoyemi, F. B. (2004). Quality of groundwater in the Deltaic Plain Sands aquifer of Warri and environs, Delta State, Nigeria. *Water Resour*, 15, 38–44.

Omoko, E. N., Opara, A. I., Onyekuru, S. O., Ibeneme, S. I., Akakuru, O. C., & Fagorite, V. I. (2023). Pollution status and hydrogeochemical characterization of water resources in Onne industrial layout and environs, Rivers state, Nigeria. *Sustainable Water Resources Management*, 9(4), 116.

Osman, A. I., Chen, L., Yang, M., Msigwa, G., Farghali, M., Fawzy, S., ... & Yap, P. S. (2023). Cost, environmental impact, and resilience of renewable energy under a

changing climate: a review. *Environmental chemistry letters*, 21(2), 741-764.

Oteze, G. E. (1981). Water resources in Nigeria. *Environmental Geology*, 3(4), 177–184.

Peng, X., Jiang, Y., Chen, Z., Osman, A. I., Farghali, M., Rooney, D. W., & Yap, P. S. (2023). Recycling municipal, agricultural and industrial waste into energy, fertilizers, food and construction materials, and economic feasibility: a review. *Environmental Chemistry Letters*, 21(2), 765-801.

Piper, A. M. (1944). A graphic procedure in the geochemical interpretation of water-analyses. *Eos, Transactions American Geophysical Union*, 25(6), 914–928.

Reijers, T. J. A. (2011). Stratigraphy and sedimentology of the Niger Delta.

Richards, L. A. (1954). Diagnosis and improvement of saline and alkali soils (Issue 60). US Government Printing Office.

Schoeller, H. (1977). Geochemistry of groundwater. *Groundwater Studies, an International Guide for Research and Practice*, UNESCO, Paris, 1–18.

Seiyaboh, E., & Jackson, F. (2017). Level and impact of hydrocarbon in sediment characteristics of Imiringi oil and gas field facilities in the Niger Delta. 15th International Conference on Environmental Science and Technology. Rhodes, Greece, 1370.

Sherrard, J. H., Moore, D. R., & Dillaha, T. A. (1987). Total dissolved solids: Determination, sources, effects, and removal. *The Journal of Environmental Education*, 18(2), 19–24.

Short, K. C., & Stäuble, A. J. (1967). Outline of geology of Niger Delta. *AAPG Bulletin*, 51(5), 761–779.

Sikakwe, G. U., B. E. Ephraim, T. N. Nganje, E. E. U. Ntekim, and E. A. Amah.

"Geoenvironmental impact of Okpara coal mine, Enugu, Southeastern Nigeria." *Adv. Appl. Sci. Res* 6, no. 4 (2015): 5-16.

Stiff Jr, H. A. (1951). The interpretation of chemical water analysis by means of patterns. *Journal of Petroleum Technology*, 3(10), 13–15.

Subba Rao, N., Subrahmanyam, A., Ravi Kumar, S., Srinivasulu, N., Babu Rao, G., Rao, P. S., & Reddy, G. V. (2012). Geochemistry and quality of groundwater of Gummanampadu sub-basin, Guntur District, Andhra Pradesh, India. *Environmental Earth Sciences*, 67, 1451–1471.

Szabolcs, I. (1964). The influence of irrigation water of high sodium carbonate content on soils. *Agrokémia És Talajtan*, 13(sup), 237–246.

Talib, M. A., Tang, Z., Shahab, A., Siddique, J., Faheem, M., & Fatima, M. (2019). Hydrogeochemical characterization and suitability assessment of groundwater: a case study in Central Sindh, Pakistan. *International Journal of Environmental Research and Public Health*, 16(5), 886.

Todd, D. K. (1980). *Groundwater Hydrogeology* ed. 2nd. John Willey and Sons, New York, 537.

Usepa, I. (2011). US Environmental Protection Agency's integrated risk information system Environmental protection agency region I. Washington DC, 20460.

Whitaker, S. (1986). Flow in porous media I: A theoretical derivation of Darcy's law. *Transport in Porous Media*, 1, 3–25.

Whiteman, A. J. (2012). *Nigeria: Its Petroleum Geology, Resources and Potential: Volume 1 (Vol. 1)*. Springer Science & Business Media.

World Health Organization. (2017). Guidelines for drinking-water quality: first addendum to the fourth edition. In *Guidelines for drinking-water quality: first*

*addendum to the fourth edition.*

Wilcork, A. B. (1993). Acceptable Levels of Chemicals. Drinking Water Engineering Handbook, USA, 121–140.

Wilcox, Lv. (1955). Classification and use of irrigation waters (Issue 969). US Department of Agriculture.

World Health Organization. (2017). Guidelines for drinking-water quality: first addendum to the fourth edition.

Yang, Q., Xu, Y., Liu, S., He, J., & Long, F. (2011). Concentration and potential health risk of heavy metals in market vegetables in Chongqing, China. *Ecotoxicology and Environmental Safety*, 74(6), 1664–1669.

Zessner, M. (2021). Monitoring, Modelling and Management of Water Quality. *Water*, 13(11), 1523.